REFERENCE ONLY

UNIVERSITY OF LONDON THESIS

Degree PhD Year 2006 Name of Author NAYAR, S.N

Bone Cell Responses to Ion-Implanted Titanium

Saima Naveed Nayab, B.Sc (Hons)

A thesis submitted for the degree of Doctor of Philosophy

Biomaterials and Tissue Engineering Division,

University College London Eastman Dental Institute, UK.

2005

ProQuest LLC
789 East Eisenhower Parkway
P.O. Box 1346
Ann Arbor, MI 48106-1346

Acknowledgements

First and foremost, I would like to express my humble gratitude to God Almighty for giving me the strength and the knowledge to undertake this project. It would have been merely a dream without the excellent supervision and kind support of Professor Irwin Olsen and Dr. Frances Jones of University College London Eastman Dental Institute (UCL EDI), for which I am extremely thankful.

I would like to acknowledge the help I received from the staff of UCL EDI especially Ms N Morden, and also Mr T. Tate of Imperial College of Science, for producing the ion-implanted titanium surfaces. Financial assistance for this project was kindly provided by the Biotechnology and Biological Sciences Research Council (BBSRC) and via UCL EDI's EFFORT grants.

Last but not least, I am grateful to my friends and family, especially my beloved husband and our wonderful children for their patience, understanding and constant support. I also owe a debt of gratitude to our parents for the belief they showed in me and for their sincere and endless prayers.

Abstract

Among the various surface modification techniques developed to improve the biocompatibility of titanium (Ti), ion-implantation is a method which can alter Ti surface chemistry in a relatively controlled manner. Although implantation of Ti surfaces with calcium (Ca) ions has previously been shown to enhance osseointegration *in vivo*, the underlying mechanisms responsible for such responses still remain unclear. The aim of the current study was, therefore, to examine the precise effects of ion-implanted Ti on human bone cells by assessing a range of biological activities *in vitro*.

Ca, potassium (K) and argon (Ar) ions were selected to be implanted. Although similar in mass, chemically they are quite different, which was reflected in the differential response of bone cells. Thus, Ti surfaces implanted with 1 x 10^{17} cm^{-2} Ca ions reduced cell adhesion at 4 h, but, nevertheless, significantly increased cell spreading and subsequent growth compared with the (non-implanted) Ti control. In contrast, cells on K-Ti responded in a very similar manner as the control, whereas cells on the Ar-implanted Ti appeared less flattened and did not grow well.

The effects of Ca ion-implantation were further examined by implanting Ti discs with different levels of this ion. However, surfaces implanted with medium (1 x 10^{16} ions cm^{-2}) and low (1 x 10^{15} ions cm^{-2}) levels of Ca ions had no significant effects on cell adhesion. Results showed that the number of cells attaching to Ca (high) (1 x 10^{17} ions cm^{-2})-Ti was increased following prolonged incubation of 24 h. Moreover, an enhanced cell spreading and an elevated expression of important cell adhesion proteins

such as vinculin and $\alpha 5\beta 1$ integrin by cells cultured on Ca (high)-Ti was also measured at this time point. In addition, compared with the control, Ca (high)-Ti surfaces increased cell proliferation, whereas Ca (med)-Ti and Ca (low)-Ti had no significant effects. The current study also showed, for the first time, that controlled alteration of the surface chemistry of Ti by implantation of high doses of Ca ions substantially modulated the progression of the bone cell cycle and up-regulated the expression of vital bone-specific markers such as bone morphogenetic receptor 1B, bone sialoprotein and most significantly osteopontin. Surface modification by Ca ion-implantation could thus prove a valuable tool for improving the clinical efficacy of Ti implants.

Contents

Posters:

1. **Nayab SN**, Jones FH and Olsen I (2002) "Bone Cell Response to Novel Ion-implanted Titanium" *4th Annual Conference of Tissue and Cell Engineering Society (TCS),* University of Glasgow.
2. Jones FH, Olsen I, **Nayab SN**, Brett P, Harle J, Shinawi L, Mihoc R and Armitage D (2004) "Ion Implantation for Model Biomedical Implant Surfaces" *Surface Science of Biologically Important Interfaces XI,* University of Sheffield.

List of Figures

List of Tables

Chapter 1

Background

The strength of all sciences, which consists in their harmony, each supporting the other.....

Francis Bacon (1561-1626)

1.0 Introduction

Due to an increase in human life expectancy (80 + years), the majority of people in developed countries now outlive the quality of their connective tissues. Apart from the normal ageing process, 90% of the population over the age of 40 suffer from degenerative or inflammatory diseases affecting their joints, such as osteoarthrosis, rheumatoid arthritis and chondromalacia (runner's knee) [Long and Rack 1998]. Replacement of diseased tissues with implants has led to a remarkable increase in the quality of life of millions of patients. Each year around 300,000 hip and knee implants, and approximately 100,000 dental implants, are used in the United States [Puleo and Nanci 1999]. The survivability of current implant materials is only about 15 years. However, due to longer human life expectancy and the need for implantation in younger patients, biomaterials with at least 20-30 year survivability are currently required [Hench1998; Hench and Polak 2002].

During the last 30 years, considerable attention has been directed towards research and development of implant materials. Several different ceramics, polymeric materials and metals have been developed to replace, repair, or augment more than 40 different parts of the body. The properties of metals and metal alloys, such as high corrosion resistance, strength, rigidity, ease of shaping, machining and suitability for a wide range of sterilization techniques have made them highly valuable biomaterials for replacing hard tissues [Ratner et al., 1996]. The most common metals / metal alloys used for bone and tooth tissue reconstruction are stainless steel, cobalt-based alloys, Ti alloys and commercially pure (cp) Ti [Brunette et al. 2001].

Many strategies have been developed in the past for modifying existing implant materials in order to improve their clinical efficacy. This thesis is concerned with one particular material, "cpTi", and one particular type of modification technique, "ion-implantation". The aim of this introductory chapter is to give an overview of Ti as an implant material, and to briefly discuss the different surface treatments which have previously been applied to it. Specific details of literature similar to the current study, pertinent to each section of this investigation, will be covered in detail in the Introduction of each later chapter.

1.1 Titanium as an implant material

Ti, a transition metal, belongs to group 4B in the periodic table of elements. It is the ninth most abundant metal on earth. It occurs in the minerals rutile, ilmenite and sphene, and is present in titanates and many iron ores. Ti was first identified by W. Gregor in 1791 in Creed, Cornwall, who called it "menachite". It was rediscovered by M. Klaproth in 1795 in Berlin and became known as "titanium", deriving its name from the Greek mythology of Titans. Although J. Berzelius isolated this metal in 1825, it was not characterised in its pure form until 1910 by Hunter. In 1938 the first commercial scale production of pure Ti was carried out by Kroll [Brown1997].

CpTi is a well-characterised oral implant material. It is used to replace teeth for partial or fully edentulous patients, and also to fabricate maxillofacial reconstruction. CpTi is available in four grades, which vary in their strength. Contamination by other elements such as oxygen (O), nitrogen (N), hydrogen (H), carbon (C) and iron (Fe) is lowest in grade 1 and highest in grade 4 cpTi.

Despite its widespread use in dentistry Ti is, nevertheless, not considered strong enough to be used in orthopaedics. Aluminium (Al) and vanadium (V) are generally added to create Ti-6Al-4V alloy in order to achieve better strength and a lower elastic modulus (measure of the stiffness of a given material, defined as the ratio of stress (force per unit area) to corresponding strain (deformation) in a material under tension or compression) [Brunette et al. 2001]. Previous studies reported only slight differences in the clinical responses to cpTi and Ti alloys [Doundoulakis1987; Hernàndez de Gatica et al. 1993], while Maetzu et al observed no significant differences between the use of either cpTi or Ti-6Al-4V alloy as dental implants [Maeztu et al. 2003].

The ideal implant material should exhibit the following properties: a biocompatible chemical composition to avoid adverse tissue reaction, a high resistance to degradation (corrosion) in the human body environment; acceptable strength to endure stress; a low modulus to minimise bone resorption; and a high wear resistance to minimise debris generation [Long and Rack 1998]. Ti combines the strength of iron and steel and the light weight of Al, which accounts for its widespread use in aviation, marine industry, sports equipment and, more relevantly, medical and dental bone replacement devices. Moreover, the first scientifically documented clinical successes of Brånemark and his co-workers showed that Ti is capable of being a highly osseointegrated bone implant material [Brånmark1983]. Brånemark defined "osseointegration" as "a direct structural and functional connection between ordered and living bone and the surface of a load bearing implant" [Brånmark1985]. Albrektsson et al proposed six factors as especially important for successful osseointegration of an implant: implant

material; implant design; surface conditions; status of the bone; the surgical technique; and the implant loading conditions [Albrektsson and Johansson 1991].

Ti, despite its generally successful clinical application, has also produced some undesirable responses. For example, a failure rate of nearly 5% has been reported for Ti plates following jaw and skull surgery. Lack of sufficient stiffness and high friction rates have also reduced the use of Ti implants for femoral head replacement [Esposito et al. 1998; Arys et al. 1998; Donley and Gillete 1991; Long and Rack 1998]. In addition, an increased bacterial adhesion and colonisation at the supra and sub-gingival sites of Ti dental implants causing infection, have also raised concerns regarding the biocompatibility of Ti implants [Yoshinari et al. 2001].

Ti derives its biocompatibility from a strong and tightly bound 2-5 nm thick native passivating oxide layer which is formed over its surface within a millisecond of exposure to air. It has been previously proposed that because of this layer Ti is capable of withstanding the physiological environment without disintegration [Kasemo and Lausmaa 1986]. However, this protective oxide layer is not entirely stable and can grow in thickness, allowing ion-exchange with the surrounding tissue. Local adverse effects which elicit allergic reactions are known to originate from the release of metal ions from implant materials. Ions leaching out over long periods of time into the implant interface could interfere with the localised mineralization and remodeling processes of bone, possibly resulting in subsequent loosening of the implant [Albrektsson and Johansson 1991]. Although this is not a major problem for cpTi, impaired bone formation on Ti alloy has been shown to be related to the

release of Al ions, which can be detrimental to bone cell differentiation [Albrektsson and Johansson 1991; LeGeros et al. 1991; Thompson and Puleo 1996]. Arys et al measured the composition and thickness of non-osseointegrated cpTi dental implants [Arys et al. 1998]. They observed partial dissolution or complete disappearance of the protective titanium dioxide layer and also ion-exchange through the surrounding tissues [Arys et al. 1998]. Ti implants have also been shown to undergo corrosion and biodegradation [Estessabi et al. 1996; Lucas and Lemons 1992; Arys et al. 1998]. Wear debris around Ti oral implants has been shown to activate macrophages (a main part of the immune response to a foreign body) which, in turn, triggered bone resorption [Esposito et al. 1998]. Such undesirable reactions have ultimately contributed to the failure of Ti implants, especially in high risk patients such as postmenopausal women suffering from osteoporosis [Mackie2003]. As a result of these and other disadvantages, a number of techniques have been developed in order to improve the biocompatibility of Ti implants, as discussed below.

1.2 Modification of titanium surfaces to enhance biological responses

Physiochemical surface characteristics such as surface energy, roughness, topography and chemistry are known to play important roles in mediating interactions between the implant and the host tissue. Surface characteristics of implants are particularly vital to the biological response as cells interact with the outermost atomic layers, approximately 0.1-1 nm thick [Kasemo and Lausmaa 1986]. Since events occurring at the cell-material

interface are likely to play an important role in the clinical success of an implant, an optimum surface compatibility with the surrounding tissue is essential for successful integration of the Ti implants [Anselme2000].

Following surgical insertion of an implant into bone a complicated cascade of events take place at the cell-material interface [Puleo and Nanci 1999]. As illustrated below (Figure 1.1), it involves protein adsorption onto the implant surface, recruitment of inflammatory and osteoblast precursor cells at the site of the wound, attachment of cells to implant surfaces, proliferation and differentiation of the undifferentiated mesenchymal cells into osteoblasts, secretion of bone extracellular matrix (ECM) by osteoblasts, and finally deposition and remodelling (restructuring) of new bone on the implant surface (Figure 1.1) [Davies1998; Masuda et al. 1997; Schwartz et al. 1997].

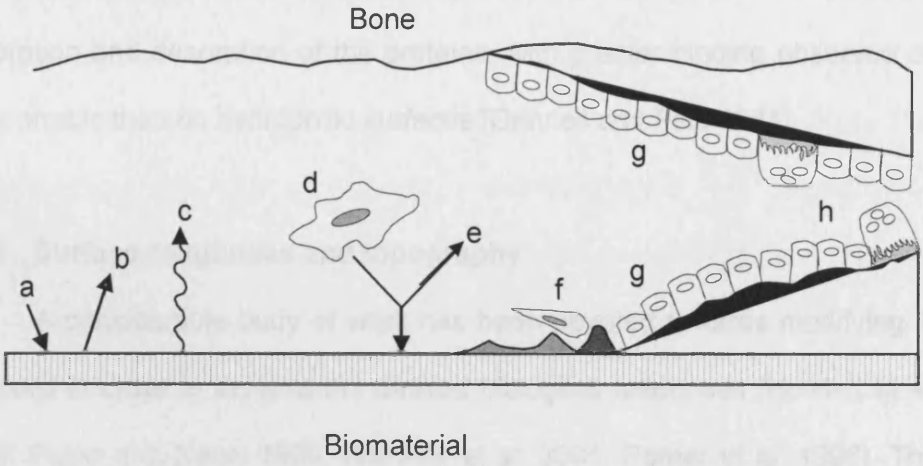

Figure 1.1: Representation of events at bone-implant interface. (a) Protein adsorption from blood and tissue fluids (b) protein desorption (c) surface changes and material release (d) Inflammatory and connective tissue cells approach the implant (e) possible targeted release and selected adsorption of ECM proteins (f) formation of *lamina limitans* and adhesion of osteogenic cells (g) bone deposition on both the exposed bone and the implant surface (h) remodelling of newly formed bone, adapted from [Puleo and Nanci 1999].

The initial binding of blood and tissue fluid proteins to the implant surfaces is via long range, weak van der Waal's interactions and short range, strong ionic and covalent chemical bond formation. Once on the surface, proteins (in native conformation, denatured, intact or fragmented) can desorb or remain adsorbed and possibly mediate tissue-implant interactions (Figure 1.1) [Puleo and Nanci 1999]. This protein conditioning layer may determine, in part, how various cell types might become adherent to the surface [Anselme2000]. In addition, differences in the amount and conformation of proteins adsorbed onto the Ti surfaces have also been shown to affect the adhesion of the bone-forming osteoblasts [Yang et al. 2003]. The surface chemical, morphological and electrical features of Ti are known to affect the nature of this adsorbed protein layer [Anselme2000; Schwartz et al. 1997]. For example, the surface wettability has been reported to influence adsorption and desorption of the proteins, with greater binding observed on hydrophobic than on hydrophilic surfaces [Grinnell and Feld 1981].

1.2.1 Surface roughness and topography

A considerable body of work has been devoted towards modifying Ti surfaces in order to achieve the desired biological responses [Howlett et al. 1999; Puleo and Nanci 1999; Brunette et al. 2001; Ratner et al. 1996]. The following sections present a brief discussion of some of the techniques which were previously employed to change the roughness, topography and the chemistry of the Ti surfaces in order to enhance their biocompatibility.

Alterations in surface roughness and topography have been used in the past to influence cell and tissue responses to implants [Boyan et al. 1995;

Lincks et al. 1998; Schwartz et al. 1996; Anselme et al. 2000; Brett et al. 2004; Degasne et al. 1999]. Surface roughness can be achieved by a number of methods including abrading, polishing, acid etching, and grit blasting [Kasemo and Lausmaa 1988]. While, surface topography can be altered by introducing pores in the range of 100–500 μm in dimension. Such porous coatings are used since they have been shown to improve the mechanical interlocking of bone with the Ti. Similarly, pits and grooves within the nano-scale range have been introduced to regulate orientation and migration of individual cells for improved osseointegration [Ellingsen1998; Ungerbock and Rahn 1994].

It has been suggested that roughened surfaces elicit more favourable cellular responses due to increased surface area. Previous studies have analysed the behaviour of MG-63 osteosarcoma cells cultured on Ti surfaces with five different surface roughnessess [Boyan et al. 1995; Lincks et al. 1998; Schwartz et al. 1996]. Their results demonstrated that when these cells were cultured on rougher surfaces, there were lower cell numbers and decreased rates of cell proliferation, but increased alkaline phosphatase (ALP) activity compared to those on smoother Ti surfaces and control polystyrene surfaces. However, the growth of cells on Ti surfaces of intermediate roughness did not differ significantly from the controls. It was reported that cell morphology and spreading were also affected by altering surface roughness. Thus, cells grown on the roughest Ti plasma-sprayed surfaces were more rounded in appearance than those grown on smooth electro-polished surfaces, which showed a flattened morphology similar to the control polystyrene surfaces [Boyan et al. 1995; Lincks et al. 1998;

Schwartz et al. 1996]. In another study, Ong et al demonstrated a possible influence of Ti surface roughness on the synthesis of proteins. They showed that after six days of cell culture, protein production by cells grown on the Ti surfaces roughened by grinding was greater than those on the polished surfaces [Ong et al. 1996].

Schneider et al demonstrated that osteoblast gene expression and mineralization were affected by roughened implant surface microtopographies during osseointegration of the dental implants [Schneider et al. 2003]. These authors cultured primary rat calvarial osteoblast (RCOB) and an osteoblastic cell line (UMR 106-01 BSP) on 600-grit (grooved) or sandblasted (roughened) cpTi discs. Mineralization was evaluated by Alizarin Red-S staining, while Real Time PCR was used for quantitative analysis of Cbfa1 and BSPII gene expression, markers of osteogenesis [Schneider et al. 2003]. They found enhanced mineralization of osteoblasts cultured on roughened implant surfaces compared with those on the tissue culture plastic. In addition, a significantly increased Cbfa1 and BSPII genes expression by cells grown on roughened as compared with grooved implant surfaces was found. These authors concluded that osteoblast gene expression and mineralization appear to be affected by roughened implant surface microtopographies during osseointegration of dental implants *in vivo* [Schneider et al. 2003]. Although increasing surface roughness reduces implant failure by distributing load bearing, it has been implicated as a cause of recurrent bone infections [Ellingsen1998]. Porous implants were also found to promote early infections, probably due to the sheltering of bacteria in

these cavities and thus resistant to host immune mechanisms [Esposito et al. 1998].

More recently, Brett et al showed that the surface roughness of Ti has a profound effect on the profile of genes expressed by bone cells. They examined the effects of a moderately rough (sand-blasted, acid-etched; SLA) Ti surface, a highly rough (plasma-sprayed; TPS) surface and a smooth surface (SMO) on bone cells *in vitro*. The number of cells was shown to be less on SLA surfaces compared with SMO, whereas the TPS surface elicited the greatest increase in both adhesion and growth of bone cells. In addition, based on the data generated by gene expression profiling, a technique used to simultaneously evaluate thousands of genes, they identified a number of 'roughness response genes' of the osteoblasts including, for example, caspases, intermediate filament proteins, stress response molecules and most specifically the axl/UFO receptor (a tyrosine kinase) [Brett et al. 2004].

1.2.2 Surface chemistry

Formation of a calcium phosphate-rich apatite layer, whose structure is similar to human bone mineral, is generally considered to be a major factor influencing the integration of an implant with the bone [Puleo and Nanci 1999]. Ti itself is not readily able to promote calcium phosphate precipitation on its surface. A previous study showed that upon immersion in simulated body fluid (SBF) (an inorganic solution containing ionic species in concentrations similar to those present in natural body fluids), calcium phosphate deposited on Ti surface. The ratio of calcium (Ca) and phosphorous (P) in the Ca/P layer formed was 1.63, which is close to that of

hydroxyapatite (HA) (1.67) [Hanawa1991]. HA ($Ca_5(PO_4)_3OH$) is a crystalline form of calcium phosphate which has an inorganic surface with physicochemical characteristics similar to those of bone, thus encouraging osseointegration [Brunette et al., 2001]. However, the Ca/P layer formed was very thin (less than 8 nm on the cpTi and Ti alloy plates studied), which indicated that it was not a true apatite layer and was deposited due to transfer and adsorption of Ca and P from SBF [Hanawa1991]. In a similar investigation, Li and Ducheyne measured the ratio of Ca and P deposited on a Ti surface. They found it to be equal to only 1.44 which is lower than HA. They termed this layer a quasi-biological apatite, formed on the surface of cpTi following binding of ions from SBF [Li and Ducheyne 1997].

Interest in the chemical modification of Ti surfaces has been stimulated by the successful use of HA coatings on Ti implants in order to enhance osseointegration [Ong and Chan 2000]. The force required to detach HA coated Ti from bone was found to be higher than that for uncoated Ti after 12 weeks of implant insertion [Tangvall and Lundström 1992]. HA coatings have been produced using plasma spraying, ion-plating, pulse laser deposition, various modes of sputtering, electrophoreses and immersion deposition techniques. Despite frequent use of HA coatings, there are certain problems associated with them such as weak adhesion of the coatings, causing fracture within the apatite and/or at HA-Ti interface, delamination and separation as well as dissolution and resorption. In addition to these mechanical drawbacks, formation of fragmented particles derived from the coatings into the joint space and susceptibility of HA coatings to bacterial colonisation, indicate a need for alternative surface modification techniques

to improve the biocompatibility of Ti [Ong and Chan 2000; Ellingsen1998; Peraire et al. 2006; Meng et al. 2005; Chen et al. 2005; Oh et al. 2005; Rohanizadeh et al. 2005].

Direct chemical treatments of Ti surfaces have been carried out to promote apatite formation from body fluids, thus creating the bone-like surface chemistry considered to be beneficial for osseointegration. Treatments include H_2O_2 with [Pan et al. 1998] or without [Ohtsuki et al. 1997] chloride ions, alkali solutions, with or without heat treatment [Kim et al. 1996], Ca ion containing solutions [Hanawa et al. 1997; Nishiguchi et al. 1999] and etching with HCl and H_2SO_4 [Wen et al. 1997; Kim et al. 1999]. Moreover, in an attempt to create an organic surface chemistry favourable for the interaction of target cells, immobilization of biomolecules on Ti surface has also been carried out. For example, by direct biocoating of Ti with bone morphogenetic protein 2 (BMP-2) [Jennissen2002], or by using plasma surface modification strategy to enable immobilization of bioactive molecules lysozyme and BMP-4 on the aminated Ti surfaces [Puleo et al. 2002]. Another study used silanisation (covalent attachment of an organic monolayer anchored by a siloxane network) of the Ti surface, where biological responses may depend on the terminal group or the use of cross-linking molecules to attach biologically active mediators [Sukenik et al. 1990].

1.3 Modification of surfaces chemistry by ion-implantation

This high energy technique, which forms the basis of the current investigation, offers several advantages over the above-mentioned methods including the ability to control implantation energy, selection of ionic species

and species purity, while allowing accurate dose and depth control. In addition to speed, it makes it possible to control dopant mass as well as homogeneity and reproducibility of the surface modified layer. Ion-implantation has been reported to alter only the surface characteristics of the material, the bulk mechanical properties usually remain unchanged. It also allows for multiple implantation of variant species into the substrate, and overcomes some of the common problems associated with HA coatings, such as, delamination and fracture, as mentioned above [Ziegler1988; Ryssel and Ruge 1986; Sze1981].

The ion-implantation process involves acceleration of ions, atoms or molecules through an electrostatic field and into the surface, the ions becoming physically embedded [Brunette et al. 2001; Ratner et al. 2004; Sze1981]. The theory of ion-implantation was proposed in 1913 by Niels Bohr. However, the technique was developed much later and the first patent for ion-implantation was obtained in 1957 by Shockley [Ziegler1988]. Ion-implantation is well known as a useful technique for the surface modification of metals in the fields of electronics and nuclear engineering. It was originally developed for semiconductor applications, and later, for improving wear properties of metallic machine tools and for generating electrical conductivity in polymers [Ryssel and Ruge 1986].

Various advantages of the ion-implanted surfaces have been reported. For example, mechanical benefits include increased resistance to wear and friction and increased surface hardness [Alonso et al. 1995; Feller et al. 1985; Hohmutz et al. 1985; Mucha and Braun 1992]. In addition, chemical (increased resistance to corrosion, less lixiviation) [Williams and Buchanan

1985; Buchanan et al. 1987a] and biological (enhanced osseointegration) benefits derived from such surfaces, make ion-implnatation a potentially useful surface modification technique [Hanawa et al. 1997; Ichikawa et al. 2000; Jinno et al. 2004; Krupa et al. 2001; Krupa et al. 2002; Krupa et al. 2005].

The following section describes some of the previous ion-implantation studies aimed at improving performance, longevity and biocompatibility of Ti implants. Implantation of nitrogen (N) and carbon (C) ions not only increased wear resistance and surface hardness of Ti but also improved its fatigue properties [Tangvall and Lundström 1992; Buchanan et al. 1987b]. Similarly, iridium (Ir) ion implantation of Ti significantly improved corrosion resistance by altering electrochemical properties of the Ti alloy, which approached those of Ir [Buchanan et al. 1990; Rieu et al. 1991]. High dose Al ion-implantation into Ti enhanced corrosion resistance and surface hardening, although this effect was measured only after exposure of ion-implanted surfaces to hydrochloric acid (5 M HCl) [Tsyganov et al. 2000]. Furthermore, Krupa et al demonstrated that P ion-implantation into cpTi enhanced corrosion resistance following short and long periods of exposure to SBF at 37°C [Krupa et al. 2002]. Wieser et al carried out double implantation of Ca and P ions into Ti and found enhanced nucleation and growth of HA in SBF on ion-implanted surfaces relative to that on the control cpTi [Wieser et al. 1999]. Similarly, sodium (Na) ion-implantation with subsequent thermal treatment of Ti surfaces has also been observed to promote HA nucleation and growth in SBF [Pham et al. 2000].

Ion-implantation studies examining biological responses have primarily used ions such as manganese (Mn), magnesium (Mg), O, N , P and Ca [Leitao and Barbosa1998; Howlett et al. 1993; Howlett et al. 1994; Hanawa et al. 1997]. When Mg ions were implanted into Al, an enhanced attachment and spreading of bone cells was observed, although the Mg ions were leached within 48 h when implanted on cpTi or Ti alloy [Howlett et al. 1994]. In contrast, Howlett et al demonstrated that implantation with Mg and Mn in addition to N and P had no preferential effect on human bone cell attachment [Howlett et al. 1993], whereas a mineralised ECM was observed to be formed by rat bone-marrow cells on N-implanted Ti surfaces after 3 weeks of cell culture [Leitao and Barbosa, 1998].

In another study, adhesion and spreading of the osteoblast cell line MC3T3-E1 on Ti surfaces which were plasma sprayed prior to implantation with amino (NH_2^+) group, was examined. Their findings supported the biocompatibility of such modified Ti surfaces [Yang et al. 2002]. A more recent *in vivo* study modified Ti dental implants via C, carbon oxide (CO), N and Ne ion-implantation attempting to obtain an intimate and lasting integration with the surrounding bone [Maeztu et al. 2003]. After 3 months of insertion in the rabbit tibiae, histomorphometric analyses of the retrieved implants were carried out and the percentage bone-implant contact was measured. Their results showed significantly enhanced osseointegration of only C and CO implanted Ti-6Al-4V and cpTi implants, respectively [Maeztu et al. 2003].

1.4 Calcium ion-implantation of titanium

Ca, first isolated by Sir Humphrey Davy in 1808 in London, is the fifth most abundant metal in the Earth's crust. It is an essential constituent of cells, teeth and bones. The normal amount found in an adult is over one kilogram, found mostly in teeth and bones as apatite [Anghileri2000; Lodish et al. 1996] The importance of Ca in cell biology was recognized as early as 1882 when Sidney Ringer demonstrated that minute amounts of this divalent ion were necessary to maintain heart muscle contractility. About a century later, physiologists described Ca as a second messenger. Calcium ions play a vital role in controlling cell functions by acting as transducers of intracellular messages [Lackie and Dow 2000].

Ca ions have previously been implanted on the surface of Ti in order to improve its biocompatibility and clinical efficacy [Hanawa et al. 1997; Howlett et al. 1999a; Ikeyama et al. 2000; Jinno et al. 2004; Krupa et al. 2001a; Wieser et al. 1999]. However, very few studies examined the in depth biological responses of Ca ion-implanted Ti (Ca-Ti) *in vivo* and especially *in vitro*. Hanawa et al claimed that Ca ion-implantation enhanced the osseointegration and the formation of new osteoid tissue even at 2 days after surgery in a rat tibia model when compared to cpTi [Hanawa et al. 1997]. These authors implanted Ca ions into only one side of the Ti plates, which were then surgically inserted into the rat tibia for 2, 8, and 18 days. Rats were given injections of calcein (to label newly formed bone) and tetracycline (to label calcium phosphate deposits). After excision, the rat tibia tissues from around the plates were stained with Villanueva bone stain and the specimens were observed under a fluorescence microscope. Hanawa et al found that a

larger amount of new bone was formed on the Ca-treated side than on the untreated side, even at 2 days after surgery. Furthermore, at 8 days, tetracycline labeling was observed only on the Ca-implanted side of the Ti plates, which was indicative of an earlier formation of the mature bone. In contrast, on the untreated Ti control side, not only the bone formation was delayed, the bone also appeared to have made no contact with the surface. Absence of macrophage and/or inflammatory cell infiltration also indicated that Ca-implanted Ti was more biocompatible than the Ti alone [Hanawa et al. 1997]. In addition, these authors demonstrated an accelerated calcium phosphate formation on Ca-Ti surfaces in comparison with the non-implanted Ti upon exposure to SBF during culture of MC3T3-E1 cells. Based on these findings, it was concluded that a rapid precipitation of calcium phosphate and the formation of surface–modified layer of titanium dioxide may have been responsible for the enhanced biocompatibility of Ca-Ti surfaces *in vivo* [Hanawa et al. 1993; Hanawa et al. 1996a; Hanawa et al. 1996b; Hanawa et al. 1997; Hanawa et al. 1998]. However, these claims were challenged by Howlett et al due to the lack of both quantitative and surface topographic measurements [Howlett1999b]. The papers published by Hanawa group not only lack details of the exact ionic concentrations, but also contain questionable experimental parameters. An example of this is their use of Auger electron microscopy (AES) surface analysis to study the depth distribution of the implanted species without acknowledging the differing sputter rate of heavier particles as compared to the lighter ones [Howlett 1999b].

Ca ion-implantation has also been shown to reduce the Young's elastic modulus of Ti, which is known to be higher than bone [Hassan2004]. Young's elastic modulus is defined as coefficient of elasticity of a substance or a ratio between stress that acts to change the length of a body and the fractional change in length caused by this force. Since low elastic modulus enhances stress redistribution of the implant to the adjacent bone tissue and also minimizes the stress shielding, these authors concluded that Ca ion-implantation might eventually serve to prolong the survivability of these Ti implants [Hassan2004; Brown1997]. Jinno et al reported that a combination of corundumization (blasting 24-grit aluminium-oxide particles) and Ca ion-implantation offers a useful surface modification technique to achieve early fixation of Ti implants [Jinno et al. 2004]. Using a canine total hip arthroplasty model, Jinno et al showed that such surface-modified Ti femoral stems when inserted into dogs had greater bone apposition than the control (non-treated) Ti implants. Fifteen dogs underwent bilateral hip arthroplasties and were sacrificed at 1, 6, and 12 months post-operatively. Based on radiographic, SEM and histological evaluation, it was found that the Ca-implanted femoral stems were well integrated and had greater new bone apposition than non-Ca-implanted stems; the differences were significant as early as after 1 month [Jinno et al. 2004].

Reports of Ca ion-implantation into Ti with the aim of examining the biological response *in vitro* include the work of Krupa et al [Krupa et al. 2001a]. They demonstrated that, despite increased corrosion resistance in SBF under stationary conditions, there was no beneficial effect of Ca ion-implantation on the viability or the ALP activity of human bone-derived cells

(HBDC). Nevertheless, the same authors also reported an excellent spreading of osteoblastic cells cultured on Ti surfaces implanted with Ca ions at a dose of 1 x 10^{17} ions cm $^{-2}$. These authors did stress the need for further biocompatibility work, since no adverse reaction was elicited on the implanted surfaces [Krupa et al. 2001a].

However, in another study, Ca-Ti surfaces were shown to promote adhesion and colonisation of the oral bacteria *Porphyromonas gingivalis* and *Actinobacillus actinomycetemcomitans,* which can be detrimental as it increases the risk of dental plaque formation, peri-implantitis (infection around dental implants) and subsequent bone loss [Yoshinari et al. 2000]. Thus, while the *in vivo* findings, as those remarked upon by Howlett [Howlett1999b], are quite contradictory, very little *in vitro* work has been carried out to clarify the underlying mechanisms responsible for either beneficial or adverse cellular responses to Ca-Ti surfaces.

1.5 Aim of the study

The current research was carried out to investigate human bone cell responses to Ti surfaces implanted with Ca, K and Ar ions compared with non-implanted Ti *in vitro.* A number of biological parameters such as cell adhesion, cell spreading and morphology, cell proliferation, the cell cycle and bone cell function were examined.

This study has been carried out in parallel with the characterisation and physicochemical examination of the ion-implanted Ti surfaces, conducted by the Biomaterials and Tissue Engineering Division at the Eastman Dental Institute. A summary of their findings is presented in

Appendix A. Ti discs from each batch of ion-implantation were equally divided between the surface characterisation and the cell work.

1.6 Layout of the thesis

Brief descriptions of the basic principles of the different techniques employed in the current study, are presented in Chapter 2. The results of these investigations are then divided into four chapters (Chapters 3-6). Each chapter has its own introduction section which deals with the background information applicable to that specific chapter.

Chapter 3 deals with human alveolar bone and MG-63 cell attachment, growth and morphology on Ca, K and Ar-implanted Ti surfaces, while Chapter 4 presents a detailed assessment of osteoblastic adhesion in response to different levels of Ca ion-implantation. The effects of Ca-Ti surfaces on proliferation and progression of bone cells through different phases of the cell cycle were also investigated and are described in Chapter 5. Bone cell function in response to Ca ion-implantation was examined by measuring the expression of bone-associated antigens at the protein as well as gene levels and results are included in Chapter 6. Lastly, Chapter 7 offers final conclusion and some suggestions for targeting the future research.

Chapter 2

Techniques Used

2.0 Introduction

This chapter explains the basic principles of the ion-implantation process and the techniques which were employed to study the responses of human bone cells to the modified Ti surfaces *in vitro*. The selected approaches were directed to evaluate a range of cellular activities, such as cell adhesion, cell morphology and spreading, cell proliferation, cell cycle and cell function.

To circumvent the problem of visualising cells on the opaque Ti discs, scanning electron microscopy (SEM) and confocal laser scanning microscopy (CLSM) were utilised. SEM was used to assess the initial cell binding and the morphological characteristics of the attached cells, while CLSM was employed to analyse the effects of ion-implantation on the formation of cell adhesion plaques. In addition, the number of radioactively-labelled cells attached on Ti surfaces was determined by means of liquid scintillation spectroscopy.

Furthermore, the effects of ion-implantation on the chemical composition of Ti surfaces under tissue culture conditions were analysed by energy dispersive X-ray spectroscopy (EDS). A [^{3}H] thymidine incorporation assay was employed to measure the change in cell number in response to the ion-implantation of Ti surfaces; while flow cytometry (FCM) was used to investigate the effects of ion-implanted Ti on cell proliferation, cell cycle and also on cell function. Lastly, gene expression of bone-associated antigen by cells cultured on Ti surfaces was assessed using reverse transcriptase polymerase chain reaction (RT-PCR).

2.1 Preparation of titanium substrates

Cp Ti discs (grade 1, 99.6% pure, 14 and 8 x 1 mm diameter and 1mm thickness) (Goodfellow, Cambridge Ltd, UK) were polished on one face to a mirror finish using a RotoPol II polisher (Struers Ltd, Glasgow, Scotland).

Due to its inherently soft nature, Ti scratches easily and tends to facet during polishing which made it difficult to achieve a mirror finish. A number of different ways of mounting the Ti discs on the methyl methacrylate resin (MMA) jigs, to allow for their positioning on the polishing stage prior to grinding, were tried. Samples used in the present work were polished using the following protocol:

Ti discs embedded in MMA jigs using warm wax (Associated Dental Products Ltd., England) were incubated for 2-3 h at room temperature (RT). Once set, the grinding/polishing of Ti discs was carried out in three stages as described below in Table 2.1:

Table 2.1: Polishing protocol for Ti discs

Stage	Grit/cloth used	Speed (RPM)	Force (N)	Time (Sec)	Lubricant
1	1200 silicon carbide	300	25	45	H_2O
2	2400 silicon carbide	300	25	45	H_2O
3	chemical cloth (APCHE)	150	20	240	0.1 μm colloidal silica suspension + 5% H_2O_2 (4:1 v/v)

Suppliers of grits and chemical cloth: Struers Ltd, and H_2O_2: BDH laboratory supplies, Poole,UK.

Polished Ti discs were manually removed from MMA jigs and the remaining traces of wax were cleaned by sequential ultrasonication in toluene (Sigma-Aldrich Company Ltd., Gillingham, UK), HPLC grade acetone (BDH laboratory supplies, England) and ultra pure water (3 baths in fresh solvents, 5 min each). The samples were then air-dried and stored in a desiccator at RT prior to ion implantation.

2.2 Ion-implantation

Ion-implantation is a well-controllable and reproducible high vacuum technique that can induce intrinsic modifications within the surface, while preserving the bulk properties of the implanted material. The process of ion-implantation involves the bombardment of surfaces with ions that have been previously selected and accelerated in an electrostatic field to high velocities. The ions disrupt the surface of the materials due to their high kinetic energy, penetrating and becoming implanted within its atomic network. The penetration depth of the implanted ion is determined by the mass of the ion, the atomic mass of the substrate and the energy of implantation (Figure 2.1) [Ryssel and Ruge 1986; Sze1981].

For the current study, ion-implantation of Ti was carried out by Dr T. J. Tate at the Department of Electrical and Electronic Engineering, Imperial College of Science, London, UK using a Whickam 200 ion implanter, equipped with a Freeman ion source, a graphite arc chamber and tungsten filament. The ion-implanter was maintained at a background pressure of 2 x 10^{-7} mbar and the ion beam set at 40 keV was passing through a mass analysing magnet in order to achieve resolution equal to 1 atomic mass unit

(a.m.u). As shown in Figure 2.1, the entire ion source of the implanter was enclosed within a shielded high voltage enclosure. The ions generated in the primary ion beam were extracted at a preset energy and accelerated towards a mass analysing magnet which deflected the primary beam allowing only the passage of ions with the chosen mass/charge ratio. The substrate to be implanted was mounted onto a movable stage vertically positioned in the chamber and was scanned through the stationary ion beam (Figure 2.1).

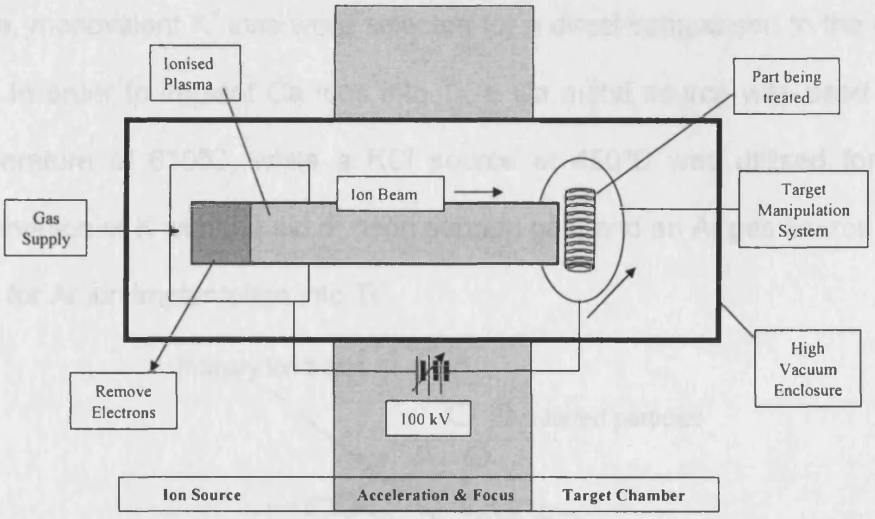

Figure 2.1: Schematic diagram of main components of an ion-implanter, adapted from the user's manual of Whickam 200 ion-implanter.

Figure 2.2 offers a schematic explanation of the ion-implantation process and the arising change in the substrate surface. Bombardment of the surface by primary ion beam can have direct physical effects on the Ti lattice causing a cascade of collisions within the surface atoms, resulting in sputtering of the oxide layer, creation of vacancies and defects at the surface (Figure 2.2) [Brown1989]. For this particular reason, it was imperative to

establish whether the ion-implantation process itself was not responsible for an enhanced biological response, previously reported for Ca-Ti surfaces (Chapter 1), but instead is solely due to the chemistry of the implanted ion and the resulting Ti surface. To test this, $^{39}K^{+}$ and $^{40}Ar^{+}$, in addition to $^{40}Ca^{+}$, were also implanted into the surface of Ti. Although these elements have similar masses and create similar damage on implantation, chemically they are quite different. Ar^{+}, being chemically inert, was selected as a control to assess any effects of the implantation process itself, while the chemically active, monovalent K^{+} ions were selected for a direct comparison to the Ca^{2+} ions. In order to implant Ca ions into Ti, a Ca metal source was used at a temperature of 610ºC, while a KCl source at 450ºC was utilised for the implantation of K with the aid of neon support gas, and an Ar gas source was used for Ar ion implantation into Ti.

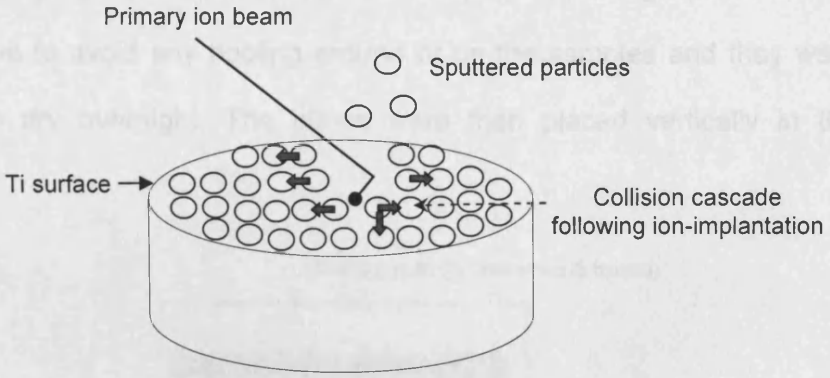

Figure 2.2: Schematic illustration of ion-implantation process

Based on the initial findings (Chapter 3), the later experiments primarily focused on the influence of ion-implantation of Ti with different levels of Ca by implanting three doses of this particular ion into the Ti lattice

and examining their effects on cellular responses *in vitro*. The type of ions and the doses at which they were implanted into Ti are shown in Table 2.2.

Table 2.2: Type and doses of ions implanted into Ti

Implanted ion	Implantation dose (ions cm^{-2})		
	Low	Medium	High
Ca^+	$1x10^{15}$	$1x10^{16}$	$1x10^{17}$
K^+			$1x10^{17}$
Ar^+			$1x10^{17}$

Prior to ion-implantation, Ti discs were mounted onto plates made of stainless steel, whose interference during the implantation process is negligible (Figure 2.3). One plate per ion was prepared using nail varnish as an adhesive to avoid any pooling around or on the samples and they were allowed to dry overnight. The plates were then placed vertically in the implanter.

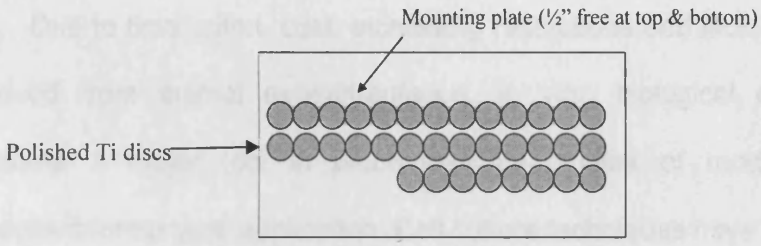

Figure 2.3: Schematic diagram of Ti discs mounted on stainless steel plate for ion-implantation

Following implantation, samples were gently removed from the mounting plates using acetone and were cleaned by sequential ultrasonication in HPLC grade acetone and deionised water (5 min each). Both the control (non-implanted) and the ion-implanted Ti discs were sterilized by exposing each side to the ultraviolet light (UV illuminator) for 1-2 h prior to cell culture. The sterile discs were stored in the 24 well tissue culture plates (Beckton-Dickinson Ltd, Oxford, UK) at room temperature (RT) in a desiccator.

2.3 Surface characterisation

Surfaces of both control and ion-implanted Ti discs were characterised by Dr F. H. Jones and other members of the Biomaterials group using X-ray photoelectron spectroscopy (XPS) and secondary ion mass spectroscopy (SIMS). A summary of their findings is presented in Appendix A.

2.4 *In vitro* model for testing bone cell response to the ion-implanted titanium

Due to time, effort, cost, increasing restrictions and lack of precise data derived from animal experimentation, *in vitro* biological evaluation has become a major tool in biocompatibilty studies of modified materials designed for surgical application. Cell culture techniques have the potential to provide fundamental information about the events which occur at bone/material interfaces, thereby enabling precise biological activities to be analysed in a controlled environment for the target cells cultured in direct contact with the implant material [Oreffo and Triffitt 1999].

It has been demonstrated previously that the biological responses to implant materials such as Ti are cell specific [Hunter et al. 1995]. Depending on the type of tissue being examined, *in vitro* studies have used cells such as fibroblasts and epithelial cells [Grill et al. 2000b; Grill et al. 2000a; Groessner-Schreiber et al. 2003; Prigent et al. 1998; Ruhling et al. 2001]. As bone formation is of great relevance in osseointegration, many research groups have studied the response of osteoblastic cells to dental and orthopaedic biomaterials [Ahmad et al. 1999; Anselme et al. 2000; Boyan et al. 1998; Cooper et al. 1999; Filippini et al. 2001; Howlett et al. 1994; Howlett et al. 1999a; Krause et al. 2000; Ku et al. 2002]. Osteoblasts, derived from undifferentiated mesenchymal stem cells, have the ability to synthesise and produce ECM. They control bone mineralization and thus play an important role in regulating the ingrowth of bone to the implant. Osteoblasts are therefore proposed to be key cells with regard to investigating implant performance, and assessing their behaviour may provide insight into the biocompatibility of a material [Aubin2001; Mackie2003; Schwartz et al. 1997]. As the material under investigation is being developed with the objective of bone implantation, osteoblast cell culture was chosen for the current study. The effects of ion-implantation of Ti were assessed by examining the responses of two types of human bone cells i.e. primary alveolar bone cells and MG-63 osteosarcoma cell line.

Fragments of normal human alveolar bone, which would otherwise be discarded (ethical approval was not required), were obtained from patients undergoing routine molar extraction at the UCL EDI, and processed as described in Chapter 3. The human alveolar bone cells, natural targets for

dental implants, were derived from these explant cultures. The primary cells derived from such explants express many of the characteristics of the osteoblastic phenotype including ALP activity, and an ability to synthesise osteoblast-specific collagenous and non-collagenous proteins [Oreffo and Triffitt 1999]. Primary osteoblasts also exhibit their osteogenic potential *in vitro* by forming mineralised bone-like nodules [Salih et al. 2001; Beresford et al. 1993]. However, the heterogeneity of cell populations obtained and the potential loss of osteoblast phenotype with sequential passaging or subculture, often limit their use [Oreffo and Triffitt 1999].

Permanent or immortal cell lines derived from osteosarcoma tumours have been extensively utilised to address factors that influence bone cell interactions with the implant material. They have several advantages over primary cell cultures; for example, they are homogeneous and represent clonal populations derived from early stages of the osteoblast lineage. In addition to that, a large number of such cells are available for analysis [Rodan and Noda 1991]. The MG-63 osteosarcoma cell line used for this project was derived from an osteogenic sarcoma of a 14 year old male [Clover and Gowen 1994]. It has been well-characterised and validated as a model to test the biocompatibility of various implant materials [Lajeunesse et al. 1990; Ferraz et al. 1999; Granchi et al. 1995a; Ku et al. 2002; Schwartz et al. 1999]. Despite being a tumour cell line, it exhibits many osteoblastic traits, including high levels of 1,25-$(OH)_2$ vitamin D_3-responsive ALP activity and inhibition of cell proliferation after 1,25-$(OH)_2$ vitamin D_3 treatment [Boyan et al. 1989]. Previous studies have also shown its ability to synthesise

osteocalcin and collagen type 1, which is characteristic of bone-forming cells [Lajeunesse et al. 1990; Lajeunesse et al. 1991].

2.5 Liquid scintillation counting

There are three main types of nuclear decay namely alpha (α), beta (β) and gamma (γ). Liquid scintillation counters are used mainly for detecting beta (β) decay, which are commonly used in biology. β Decay involves the loss or gain of an electron (negatron β^-) or its positive counterpart (positron β^+). Negatron β^--emitting isotopes of biological significance include tritium (^3H), ^{14}C, ^{32}P and ^{35}S. ^3H has a maximum energy of 18.61 keV and a half-life of 12.3 years. It is suitable for labelling organic molecules including DNA [Jones et al. 1994].

DNA is comprised of monomeric units called nucleotides, each of which consists of a five-carbon sugar, a phosphate group and a nitrogen containing base such as adenine, guanine, cytosine and thymine. If a phosphate is removed from a nucleotide, the remaining base-sugar unit is called a nucleoside. Thymidine is one such deoxynucleoside required for DNA synthesis [Lodish et al. 1996]. Since thymidine is a precursor of DNA, incorporation of ^3H thymidine by actively growing cells has also been used to determine DNA synthesis [Mujoomdar et al. 2004; Lincks et al. 1998; Schwartz et al. 1996; Martin et al. 1995; Hambleton et al. 1994]. In addition, ^3H thymidine has been used previously to tag cultured cells. Once radio-labelled, these cells have also been employed to measure cell adhesion *in vitro* [Okamura et al. 2000; Birkby et al. 1988; Hopper1986; Arisawa and Abiko 1984; Yoshinari et al. 2000].

In the current study, the influence of ion-implantation of Ti on the proliferation of bone cells was determined by employing [^{3}H] thymidine incorporation assay (Chapter 3), as previously described [Mustafa et al. 2001]. Moreover, to measure the effects of ion-implanted surfaces on cell attachment [^{3}H] thymidine was used as a radioactive tag to label cells (Chapter 3 and 4). In order to determine the radio-isotope counts, the sample was first dissolved in a suitable solvent called scintillant containing certain chemicals known as fluors. When radiation interacts with fluors, scintillations (fluorescence flashes) are produced which are measured by photomultiplier tubes of WALLAC 1409 liquid scintillation counter (Perkin Elmer Life Sciences, Cambridge, UK), which convert light pulses into electronic signals, the magnitude of which is directly proportional to the energy of the radioactive event [Jones et al. 1994]. Step-by-step details of both cell adhesion and cell growth assays are given in Chapter 3.

2.6 Scanning electron microscopy

SEM is a microscope that uses electrons rather than light to form an image. The combination of higher magnification, larger depth of focus, greater resolution (10 nm compared with 0.1μm for a conventional light microscope), and ease of sample observation makes SEM one of the instruments commonly used in research areas today. By scanning with an electron beam, an image is formed that is a three-dimensional representation of the sample surface [Goodhew et al. 2000].

As illustrated in Figure 2.4, a beam of electrons is produced in the electron gun at the top of the SEM by heating a metallic filament. This beam

is attracted through the anode, condensed by condenser lenses, and focused at a very fine point on the sample by the objective lens. The scanning coils are used to create a magnetic field which deflects the beam back and forth in a controlled pattern. Once the electron beam hits the sample, secondary electrons are ejected. Secondary electrons are produced by the interactions between energetic beam electrons and weakly bonded conduction-band electrons in metals. Detectors collect these secondary electrons and convert them to a signal that is sent to a viewing screen (Figure 2.4) [Goodhew et al. 2000].

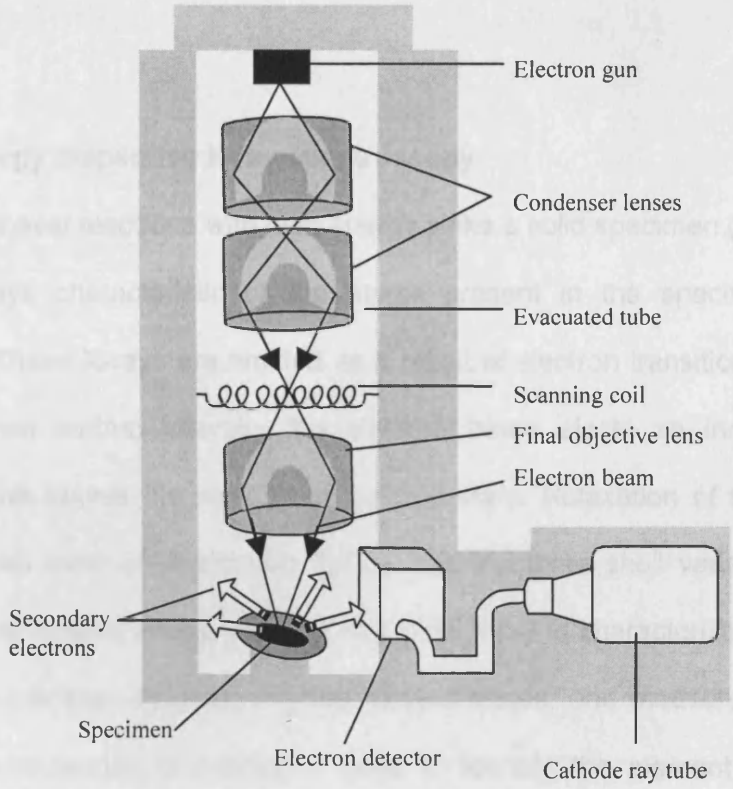

Figure 2.4: Simplified diagram of scanning electron microscopy, adapted from [Jones et al. 1994]

To study the influence of ion implantation on the morphology, anchorage and spreading of the cells in direct contact with the Ti, SEM analysis was carried out using Cambridge 90B SEM (LEO Electron Microscopy Ltd, Cambridge, UK) at an acceleration voltage of 15 kV. Images of representative random fields were digitally captured at lower and higher magnifications for a detailed assessment of the influence of ion implantation on the morphological features of the cells attached on these discs. In addition, the number of cells attached to the Ti discs and the extent of their spreading was determined by digital image analysis (Image-Pro Plus 4.01, Media Cybernetics, Crofton, USA) of these SEM micrographs (Chapter 3 and 4).

2.7 Energy dispersive X-ray spectroscopy

Whenever electrons with high energy strike a solid specimen (as in the SEM), X-rays characteristic of the atoms present in the specimen are produced. These X-rays are emitted as a result of electron transitions within the specimen atoms, whereby the electron beam ejects an inner shell electron. This leaves the atom in an excited state. Relaxation of the atom occurs by an outer shell electron 'falling' into the inner shell vacancy and releasing the excess energy as an X-ray. The X-ray is characterised by the difference in energy between the two excited states, and measurement of either its wavelength or energy is used to identify the element present [Garratt-Reed and Bell 2003; Goodhew et al. 2000].

In EDS, the energy of the X-rays is measured, typically using a silicon detector. The most intense X-rays emitted are generally associated with the

inner K shell of electrons (the K series) which can be excited for some elements with an electron beam of <10kV (typical accelerating voltages for SEM analysis being between 5 and 30kV). However, as the atomic number of the emitting element increases, the energy required to remove a K-shell electron also increases, until X-rays from this excitation can no longer be produced. X-rays corresponding to L and M shell electron excitation are then utilised [Garratt-Reed and Bell 2003].

For this study, in order to examine whether Ca implantation affects the surface chemical composition of Ti surfaces under tissue culture conditions, EDS analysis was carried out using INCA system (Oxford Instruments, High Wycombe, UK) attached to a SEM (1450 VP) (Leo, Cambridge, UK). Spectra were recorded from specific points on the SEM images of Ti surfaces and EDS spectral intensities were normalised to the Ti peak maximum, as explained in detail in Chapter 4.

2.8 Confocal laser scanning microscopy

CLSM offers good image resolution, excellent contrast and signal to noise ratio, and an ability to perform direct optical image sectioning and localisation of more than one fluorescently-labelled molecule within a sample [Sheppard and Shotton 1997].

In CLSM, a laser is used to illuminate one spot at a time in the specimen (dotted lines in Figure 2.5). The scanning mirrors move the spot in a given plane of focus through a precise pattern. The fluorescent light that is emitted from the specimen (solid lines in Figure 2.5) bounces off the same scanning mirrors and returns to the laser and is transmitted through the

dichroic mirror. A pinhole in the image plane blocks the extraneous rays that are out of focus. The light gets detected by a photomultiplier tube, and its signal is digitized and stored by a computer, as illustrated in Figure 2.5 [Becker et al. 1996].

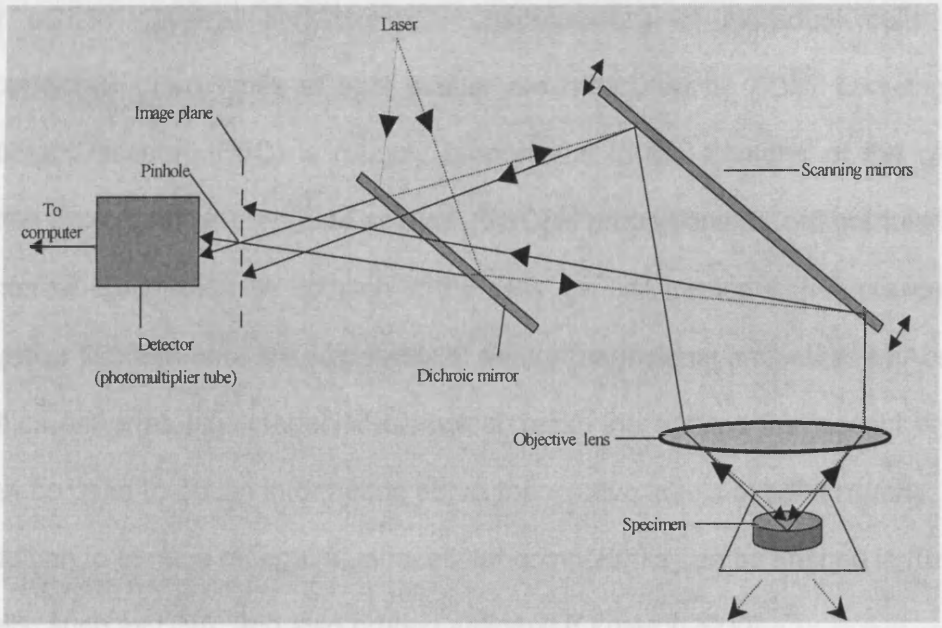

Figure 2.5: Schematic diagram of confocal laser scanning microscope, adapted from [Becker et al. 1996].

CLSM was employed in this study to investigate the effects of ion-implanted Ti surfaces on the adhesion of osteoblastic cells at a molecular level. Cells cultured on the Ti discs were immunostained for vinculin - a cell adhesion molecule, and the formation of vinculin-positive-focal adhesion plaques were examined using BioRad MRC-600 CLSM (BioRad Microscience Ltd, Hertfordshire, UK). Depth projection micrographs with a set of serial optical horizontal image sections using z-step and a 60x objective with oil were obtained throughout the samples. To measure the number of

vinculin-positive adhesion plaques formed per osteoblastic cell, digital image analysis of micrographs was carried out (Chapter 4).

2.9 Flow cytometry

Flow cytometry (FCM) is a technique that provides rapid measurement of certain physical and chemical characteristics of individual cells in suspension. Two types of light scatter are measured by FCM. Low-angle "forward scatter" (FSC) is roughly proportional to the diameter of the cell, while orthogonal, 90^{o} or "side scatter" (SSC) is proportional to cell granularity (internal complexity). In addition, if the cells are first treated with fluorescent dyes or fluorochrome-linked polyclonal and/or monoclonal antibodies (mAbs), which serve as highly specific biological 'tags', the emitted fluorescent light can be used to obtain information about the relative levels of cell antigens. In addition to surface receptors, intracellular components can be stained in fixed cells, such as DNA, and also protein antigens [Ormerod2000].

In a flow cytometer, small amount of a suspension of cells stained with a fluorescent antibody or a dye joins a larger amount of cell-free buffer called "sheath fluid". The fluids come together under laminar flow conditions so that they flow together evenly without mixing. The "sheath" fluid surrounds a thin core thread of sample. This spaces the cells out, so that only one passes the laser beam at a time, and keeps the cells centred in the flowing stream so that they pass the laser beam optimally centred. FCM instruments make measurements using this light as a source of excitation; fluorescent light emitted by each cell is recorded as it passes through the detection point rapidly. The momentary pulse of scattered and fluorescent lights emitted as

the cell crosses the beam is measured by photomultipliers at a 90 degree angle from the beam. Typically, 2-3 detectors are used with different wavelength bandpass filters, allowing the simultaneous detection of emissions at different wavelengths for different fluorochromes in each single cell. Finally, after conversion of the photon pulses into electronic signals and further computational processing, graphical display and statistical measurements are made, as illustrated in Figure 2.6 [Ormerod2000; Radbruch A.2000]

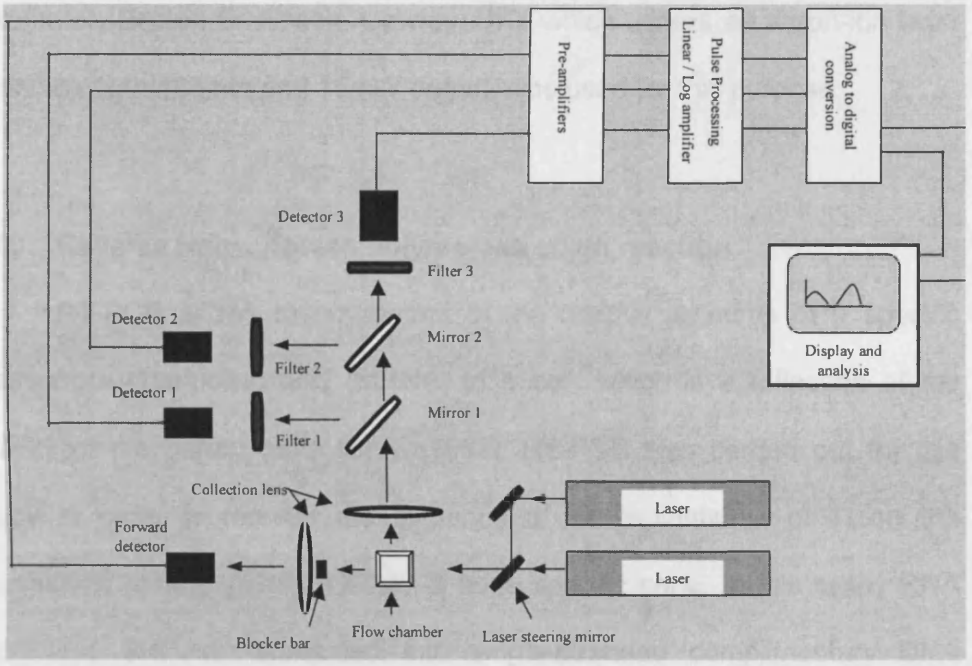

Figure 2.6: A schematic diagram of generalised flow cytometer system, adapted from [Ormerod 2000].

FCM is widely used for basic cellular and molecular research in the field of haematology and immunology. It allows specific measurement in heterogeneous cell populations without the need of physical separation of

individual cells [Radbruch2000; Scheffold and Kern 2000]. FCM has also been utilized to assess cellular responses to the novel orthopaedic and dental implant materials [Lopes et al. 1998; de Ruijter et al. 2001; Ferraz et al. 1999; Ferraz et al. 2000; Granchi et al. 1995a; Granchi et al. 1995b; Prigent et al. 1998]. For the current study, FCM analysis was carried out in order to examine the influence of ion-implantation of Ti on relative cell size, cell granularity and expression of cell adhesion molecules (Chapter 4), measurement of DNA content and DNA synthesis (Chapter 5), and expression of bone-associated antigens (Chapter 6). A FACScan flow cytometer (Becton Dickinson, Cowley, UK), which utilises an argon-ion laser of wavelength 488 nm and 15mW output, was used for this purpose.

2.10 Reverse transcriptase polymerase chain reaction

RT-PCR allows measurement of the relative amounts of a specific messenger ribonucleic acid (mRNA) in a cell, which is a reflection of the activity of the parent gene [Brown1997]. RT-PCR was carried out for this study in order to monitor the influence of ion-implantation of Ti on the expression of osteopontin (OPN) - a bone specific gene. In this assay RNA molecules are first converted into single-stranded complimentary DNA (cDNA) using reverse transcriptase. This enzyme is involved in the replication of several kinds of viruses and has a unique ability of synthesising the DNA strand complementary to the RNA template. Following reverse transcription, standard polymerase chain reaction (PCR) is carried out to amplify the specific sequence of cDNA (Figure 2.7) [Brown1997].

PCR is a method by which specific sequences of DNA can be copied many times. It is based on the ability of the DNA polymerase enzyme to carry out *in vitro* amplification of specific DNA sequences, using two specific oligonucleotide primers that hybridize to opposite strands and flank the region of interest in a specific DNA. The template in the case of RT-PCR is a specific single–stranded cDNA [Lodish et al. 1996]. A DNA chain synthesis begins as these specific oligonucleotides primers present at high concentration, hybridise with their complementary sequences in the DNA.

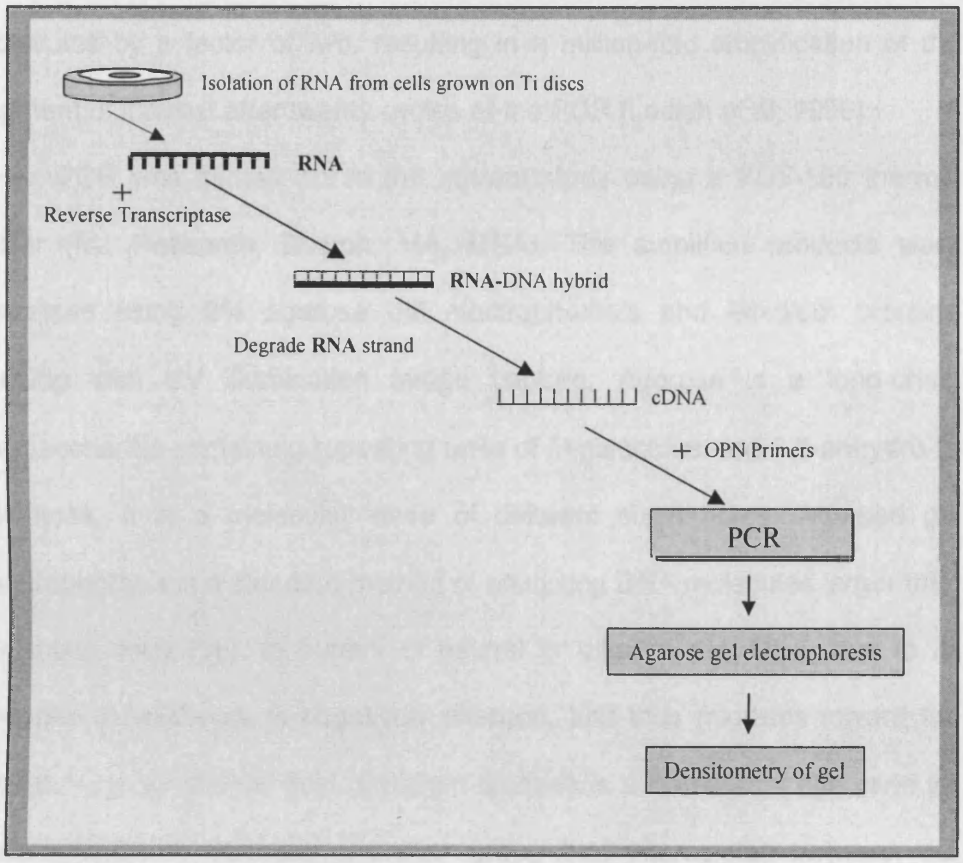

Figure 2.7: Flow chart showing scheme for evaluation of the effects of ion-implantation of Ti surfaces on OPN gene expression.

These hybridised oligonucleotides serve as primers for the extension, which is made possible due to the addition of a supply of deoxynucleotides and a temperature resistant DNA polymerase, such as *Taq polymerase*. Once the synthesis is complete, the whole mixture is heated to facilitate the melting (strand separation) of newly formed DNA duplexes. By lowering the temperature again, another cycle of synthesis begins, as excess primer is still available in the mixture. Repeated cycles of these cooling and melting steps quickly result in exponential amplification of the specific sequence of interest lying between the primer sites. In each cycle there is an increase in DNA molecules by a factor of two, resulting in a million-fold amplification of the segment of interest after twenty cycles of the PCR [Lodish et al. 1996].

PCR was carried out in the current study using a PCT-100 thermal cycler (MJ Research, Boston, MA, USA). The amplified products were visualised using 2% agarose gel electrophoresis and ethidium bromide staining with UV illumination image capture. Agarose is a long-chain polysaccharide containing repeating units of D-galactose and 3,6-anhydro-L-galactose. It is a molecular sieve of different sized holes. Agarose gel electrophoresis is a standard method of analysing DNA molecules larger than 200 base pairs (bp). In buffers of neutral or alkaline pH, DNA, due to its phosphate backbone, is negatively charged, and thus migrates toward the anode (+) in an electric field. Ethidium bromide is a fluorescent dye used for staining DNA. It contains a planar group that intercalates between the stacked bases of DNA. UV radiation absorbed by the DNA at 260 nm is transmitted to this dye and emitted in the red-orange region of the visible spectrum [Jones et al. 1994].

For the current study, expression of OPN gene by cells grown on Ti surfaces was assessed in parallel with that of a house keeping gene "glyceraldehyde-6-phosphate dehydrogenase (GAPDH)" (Chapter 6). GAPDH is a major metabolic gene which is constitutively transcribed in most primary cells and cell lines and is often used as an internal control for semi-quantification of target gene expression [Carre et al. 1991; Dukas et al. 1993; Ihl-Vahl et al. 1995]. Dukas et al confirmed that GAPDH represents a reliable standard for studies of gene expression as they found very small variations in its expression during the growth of AR4-2J pancreatic cells [Dukas et al. 1993]. Semi-quantitative determination of the effects of ion-implantation of Ti on the expression of OPN was achieved first by digitization of gels and then by densitometric evaluation using ScionImage software (Scion Corporation, Frederick, MD, USA). The values obtained for OPN were then normalised against band intensities measured for GAPDH.

Chapter 3

Bone Cell Interactions with Ion-Implanted Titanium

3.0 Introduction

In order to ensure a close apposition of bone to implants, the knowledge of cellular responses to the implants is essential. *In vitro* studies provide useful information about early events occurring at the cell-material interface which are known to affect subsequent cell and tissue reactions [Puleo and Nanci 1999]. Previous reports have shown that surface properties of implants play a vital role in dictating their biocompatibility. Besides reacting to surface physical properties such as topography and roughness [Lange et al. 2002; Zinger et al. 2004], bone-forming osteoblasts are known to be sensitive to differences in material surface chemistry [Krupa et al. 2001a; Howlett et al. 1999a; Zreiqat et al. 1999; Wieser et al. 1999], and even to implant surface cleanliness and sterilisation techniques [Stanford et al. 1994; Swart et al. 1992].

Since cells interact with the outermost atomic layer of the implant surfaces [Puleo and Nanci 1999], altering the surface chemistry via incorporation of ions through the ion-implantation process, is likely to alter the biocompatibility of Ti implants. Therefore, cell responses to the ion-implanted surfaces should be thoroughly addressed and investigated. The initial experiments, presented in this chapter, focused on assessing cell adhesion, morphology, spreading and growth of osteoblastic cells of human origin cultured on the non-implanted (control) and Ca, K and Ar-ion-implanted Ti surfaces. Ca ions were selected due to their previously-documented important biological functions [Dvorak and Riccardi 2004; Riccardi2000] (Chapter 1), while K and Ar ions were chosen as controls. Despite electrochemical differences, the atomic masses of K and Ar are similar to that

of Ca and were therefore expected to implant in a similar manner. This was important to test, since cellular responses were previously observed to alter solely due to the ion-implantation process [Suzuki et al. 1994]. These authors have demonstrated that the number of HeLa cells adhering to polystyrene surfaces were increased as a result of implantation of even chemically inert Ar and neon ions [Suzuki et al. 1994].

3.1 Background

3.1.1 Cell adhesion to titanium implants

The adhesion of cells to implants is an important indicator of their biocompatibility. Events occurring in this initial phase of the cell-material interactions influence the cell's capacity to grow on contact with the implant. It is widely known that cells do not interact with the bare implant materials either *in vivo* or *in vitro* [Anselme2000]. In the case of titanium, a strong and tightly bound 1-10 nm thick oxide layer is formed over the surface within a millisecond of exposure to air, which is capable of withstanding the physiological environment without disintegration [Brown1997]. Films on Ti implants retrieved from human tissue were found to be even two to three times thicker [Ask et al. 1989; Lausmaa et al. 1988; Sundgren et al. 1986]. This continued oxide growth reflects ongoing electrochemical events at the tissue-implant interface. Furthermore, surface analytical studies showed that the chemical composition of the oxide films present on Ti surfaces changes by incorporating Ca, P and S ions [Lausmaa et al. 1988; Ikeyama et al. 2000]. Ikeyama et al demonstrated that the surface oxide layer formed on

Ca-implanted Ti was much thicker than the oxide produced on non-implanted control surfaces [Ikeyama et al. 2000].

It has been reported that prior to cell adhesion, the implant surfaces are conditioned by the biological fluid components of plasma or serum [Chesmel et al. 1995; Derhami et al. 2001]. Chesmel et al demonstrated that proteins from serum used in the tissue culture medium were adsorbed on the material surfaces forming multiple molecular layers [Chesmel et al. 1995]. Similarly, Derhami et al showed adsorption of several serum-derived proteins such as albumin, alpha2-HS-glycoprotein, alpha-fetoprotein, plasminogen, thrombospondin 1, and serotransferrin onto the surfaces of cpTi [Derhami et al. 2001]. This adsorption layer was proposed to have a profound effect on the attachment and spreading of the cells to the surface of implant materials [Anselme2000]. The character of the adsorbed protein layer varies with the surface properties of Ti, with chemical, morphological and electrical features being important variables. These factors result in changes in the surface energy and therefore lead to variations in the amount and conformation of proteins adsorbed [Kasemo and Lausmaa 1988].

The numbers of cells attached to different substrates can be assessed by different methods. These may involve direct counting of the attached cells after detaching them from the substrates using trypsin; the cells may then be counted directly using a haemocytometer [Koulaouzidou et al. 1998] or a Coulter counter [Rao et al. 1996]. Another cell attachment assay employs radioactive techniques to label cells that are subsequently detached and counted in a liquid scintillation counter [Okamura et al. 2000; Birkby et al., 1988; Hopper1986; Arisawa and Abiko1984; Yoshinari et al. 2000] (Chapter

2). A previous study used [^{3}H] thymidine (a radioactive precursor of DNA) to label human alveolar bone and MG-63 cells in order to test the effects of ion-implantation / deposition on osteoblastic cell attachment [Howlett et al. 1999a]. The use of radioactively labelled cells was also appropriate for this study as it was previously shown that cells, once adhered firmly to Ti discs, could not be easily retrieved by a single trypsin treatment [Martin et al. 1995]. In addition, due to the opacity of Ti discs, which rendered light microscopy impossible, binding of cells to Ti surfaces was observed via SEM and image analysis was employed to measure the number of attached cells, as described earlier by Mustafa et al [Mustafa et al. 2000; Mustafa et al., 2001].

3.1.2 Morphology and spreading of cells attached to titanium

After initial attachment, the spreading of anchorage-dependent cells is generally believed to be required in order to maintain a stable cellular adhesion *in vitro*, and the cells that cannot adhere and spread often die *via* apoptosis (programmed cell death) [Puleo and Nanci 1999]. It was shown previously that the spreading of cells on the surfaces of substrates is of major importance for the subsequent cell growth [Chen et al. 1997]. In another study cell shape was found to be tightly correlated with the DNA synthesis and the growth of non-transformed cells [Folkman and Moscona 1978]. Chen et al demonstrated that the more cells spread on a substrate, the higher their rate of proliferation [Chen et al. 1997]. They cultured endothelial cells on micro-fabricated substrates containing fibronectin-coated islands of various defined shapes and sizes of a micrometer scale. Cells spread to the limits of the islands containing fibronectin substrate. When the spreading of cells was

restricted by smaller adhesive islands, proliferation was arrested, whereas larger islands permitted proliferation [Chen et al.1997].

A conventional method to assess the morphological characteristics of cells, adhered to opaque implant materials such as Ti, is to use SEM (Chapter 2) [Kirkpatrick et al. 1997; Foschi et al. 2004; Jayaraman et al. 2004; Satsangi et al. 2003; Weston et al. 1999]. In addition to this qualitative examination, the semi-quantitative assessment of cell spreading (measurements of area and shape factor of cells adhered to the substrate) on Ti discs is often carried out using digital image analysis [Ahmad et al. 1999a; Shah et al. 1999a]. Shah et al carried out a comparative analysis of primary human osteoblastic cell adhesion and spreading between two clinically relevant orthopaedic alloys, Ti-6Al-4V (Ti) and cobalt-chrome-molybdenum (CC). To examine cellular morphology on opaque Ti and CC surfaces, they stained osteoblasts with PKH-2 (a lipid soluble vital fluorescent dye that intercalates with the cell membrane) and visualized them using confocal laser scanning microscopy. Digital image analysis was used to determine total cell area and cell perimeter and then cell shape factor [(area/perimeter^2) x 4π] was calculated. Their findings revealed that cells on sandblasted roughened Ti surfaces were relatively less spread than those on rough CC [Shah et al.1999a]. Similarly, Ahmad et al measured spreading of human osteoblast-like cells cultured on cpTi discs by determining their shape factor. They found cpTi-induced differential morphologic changes in cells between grade 1 and 4 of the material [Ahmad et al. 1999a].

The effects of textured Ti-6Al-4V surfaces on the spreading and orientation of mouse calvarial MC3T3-E1cells were assessed by Soboyejo et

al [Soboyejo et al. 2002]. The test Ti-6Al-4V surfaces were produced by laser microgrooving, blasting with alumina particles and polishing. Cell-Ti interactions were studied using a combination of optical scanning transmission electron microscopy and atomic force microscopy. Their results showed that the MC3T3-E1 cells responded differently to Ti-6Al-4V surfaces of different surface topography and microchemistry. The 8-12 μm microgroove geometries were found to promote contact guidance along a narrow range of angles. In contrast, the smooth and alumina-blasted roughened surfaces promote random cell orientations that are likely to give rise to increased scar-tissue formation. In general, however, the alumina-blasted and the 8 and 12 μm microgrooved geometries caused restricted cell spreading compared to smooth Ti-6Al-4V surfaces [Soboyejo et al. 2002].

A previous *in vitro* study suggested that the modification of Ti surface chemistry by Ca ion- implantation influenced the morphological behaviour of human osteoblast-like cells [Krupa et al. 2001]. In this investigation human derived bone cells were cultured in direct contact with the Ca-implanted and non-implanted Ti discs and cell spreading was observed using SEM. Krupa et al demonstrated an excellent spreading of human bone-derived cells on Ti discs which were implanted with the Ca ions at a concentration of 1×10^{17} ions cm^{-2} in comparison with those on the non-implanted Ti [Krupa et al. 2001]. For the current study, all Ti surfaces were polished to a mirror finish prior to the ion-implantation process. Thus whilst keeping the surface topography constant, the aim was to investigate whether altering the surface chemistry of Ti discs would have an effect on the morphology and spreading of osteoblastic cells.

3.1.3 Bone cell growth in response to titanium implants

Growth of osteoblastic cells attached on the surface of implants is necessary for the successful "wound healing" or osseointegration *in vivo* [Puleo and Nanci 1999]. Since the long-term bone ingrowth is a consequence of initial cell attachment [Boyan et al. 2003], and one of the main regulators of proliferative rates of cells is shape [Chen et al. 1997; Folkman and Moscona 1978], the responses of osteoblastic cells to ion-implanted Ti discs were tested in the current study by quantifying cell adhesion and spreading and relating this to cellular proliferation.

For the evaluation of cell proliferation *in vitro*, the tests which are most frequently applied in the field of biomaterials research include [^{3}H] thymidine incorporation assay (previously explained in Chapter 2) [Hambleton et al. 1994; Lincks et al., 1998; Mujoomdar et al. 2004; Schwartz et al. 1996] and MTT [3-(4,5-dimethylthiazol-2-yl)-2,5-diphenyltetrazolium bromide] assay [Nishimura and Kawai1998; Yu et al. 2004; Cao et al. 2004; Mante et al. 2003; Groessner-Schreiber et al. 2003]. MTT assay is based on the ability of a mitochondrial dehydrogenase enzyme from viable cells to cleave the tetrazolium rings of the pale yellow MTT and to form dark blue formazan crystals. The number of surviving cells is directly proportional to the level of the formazan product created which is quantified colorimetrically [Mosmann1983]. More recently, the use of antibodies against certain proteins, such as proliferative cellular nuclear antigen (PCNA) and Ki-67 which are closely related to certain phases of the cell cycle and which are expressed in the dividing cells, has also been reported (Chapter 5) [Filippini

et al. 2001; Landberg et al. 1990; Scheidbach et al. 2004; Van Kooten et al. 2000; Katou et al. 1998; Calvo Mateo et al. 1998].

Several researchers have examined the effects of surface characteristics of Ti on the proliferation of cultured cells [Lincks et al. 1998; Anselme et al. 2000; Bordji et al. 1996; Boyan et al. 2003; Ku et al. 2002; Lauer et al. 2001; Lumbikanonda and Sammons2001; Mustafa et al. 2001; Degasne et al. 1999; Martin et al. 1995]. These studies suggest that the chemical, topographic and electrical surface features of implant materials markedly influence the growth of cells *in vitro*. Osteoblasts have been shown to respond differently when grown on Ti surfaces of varying microtopographies [Boyan et al. 2003]. Boyan et al demonstrated that on smooth Ti surfaces the osteoblasts attach and proliferate, but when grown on micro-rough Ti surfaces proliferation was relatively reduced [Boyan et al. 2003]. Similarly, Mustafa et al found that the proliferation of cells derived from human mandibular bone is affected by the surface roughness of Ti implants [Mustafa et al. 2001].

Previous studies have indicated that osteoblastic cells cultured on Ti do not grow as well as they do on the tissue culture plastic which is commonly used as a standard control [Degasne et al. 1999; Martin et al. 1996; Massas et al. 1993]. Martin et al measured the effects of altering Ti surface roughness on MG-63 cell proliferation using [^{3}H] thymidine incorporation assay. They showed that when compared to confluent cultures of cells on plastic, the number of cells was reduced on plasma-sprayed Ti but increased on the electro-polished Ti surfaces [Martin et al. 1995; Martin et al. 1996].

Modification of surface chemistry via the ion-implantation process has been previously employed for improving the biocompatibility of Ti implants using ions such as P, Mn, Mg, O, N and Ca [Leitao and Barbosa1998; Ikeyama et al. 2000; Johansson et al. 1993; Wieser et al. 1999]. *In vivo* studies of Ti modified by Ca-ion implantation have demonstrated increased formation of new osteoid tissue [Hanawa et al. 1997]. However, there are no reports examining the effects of Ca-implanted Ti on the growth of bone cells *in vitro*. Nevertheless, Krupa et al showed that Ca-implantation had no demonstrable effect on the viability and ALP (marker of cell differentiation) activity of human bone-derived cells *in vitro* [Krupa et al. 2001]. Therefore, experiments presented in the current chapter were aimed at examining the effects of Ca, K and Ar-implanted surfaces on the proliferation of both alveolar bone and MG-63 cells using [^{3}H] thymidine-incorporation assay.

3.2 Materials and methods

3.2.1 Preparation of ion-implanted titanium discs

A detailed protocol for the preparation of Ti substrate was previously presented in Chapter 2. Briefly, grade 1 cpTi discs were polished on one face to a mirror finish using 1200-2400 silicon carbide grit followed by chemical cloth with a colloidal silica suspension in 5% H_2O_2. They were then cleaned by ultrasonication in acetone followed by deionised water. Ion-implantation was carried out at Imperial College of Science using a Whickam 200 keV implanter, at an implantation energy of 40 keV. The Ti discs were implanted with $^{40}Ca^{+}$ (1×10^{17} cm^{-2}), $^{39}K^{+}$ (1×10^{17} cm^{-2}) and $^{40}Ar^{+}$ (1×10^{17} cm^{-2}) ions

and were subsequently used for cell culture work and for the surface chemical analysis (Appendix A).

3.2.2 Cell culture

Fragments of the normal human alveolar bone, obtained from the patients undergoing routine molar extractions at UCL EDI, which would otherwise be discarded, were placed in Dulbecco's modified Eagle's medium (DMEM) supplemented with 10% fetal calf serum (FCS), 100 IU/ml penicillin, 100 μg/ml streptomycin, 2 mM L-glutamine and 25 μg/ml fungizone (GIBCO Invitrogen Corporation, Paisley, UK). The fragments were cut into small pieces, washed with phosphate-buffered saline (PBS) and placed into 6 well plates in complete DMEM without fungizone. After 18 h of incubation at 37°C in a humidified atmosphere of 5% CO_2 in air, the bone chips were washed with PBS and treated with collagenase (10,000 IU) and 0.25% (w/v) trypsin (GIBCO Invitrogen) in PBS for 1 h at 37°C. The cells released into the digest were harvested by centrifugation, re-suspended in DMEM and incubated as above. The culture medium was changed twice weekly. The cells were sub-cultured by detaching the confluent layers with trypsin-EDTA (GIBCO Invitrogen), centrifuging, washing with fresh medium and seeding into tissue culture flasks (Beckton-Dickinson). They were serially passaged and used, in the following experiments, between the 1st and the 3rd passages.

The MG63 human osteosarcoma cell line derived from an osteogenic sarcoma of a 14-year-old male [Clover and Gowen 1994] was cultured in DMEM as for the alveolar bone cells. For all experiments, cells were cultured

on discs placed in 24 well plates (Beckton-Dickinson). Controls consisted of cells cultured directly on the non-implanted Ti (control) discs.

3.2.3 Characterisation of bone cell lineage

Primary osteoblastic cell populations are heterogeneous at any time due to differences in maturation and differentiation states between the individual cells, or to the existence of different subpopulations of cells in one culture [Aubin2001]. The Von Kossa staining method was; therefore, used in the current study to examine the formation of mineralising nodules, which are characteristic of bone cells *in vitro* [Beresford et al. 1993].

Human alveolar bone cells from passage 2 were seeded into 35 mm culture dishes (Beckton-Dickinson) at a density of $5x10^5$ cells per well and incubated for 5 weeks. They were divided into two groups, the control group receiving complete DMEM with no supplements, and the test group DMEM supplemented with 50 μg / ml ascorbic acid and 10 mM β-glycerophosphate (Sigma-Aldrich).

The media were replaced every 2-3 days during the 5 weeks, at which time monolayers were washed with PBS and fixed with acetone:methanol (1:1) for 10 min, washed with distilled water and examined for the formation of mineralised nodules by exposing them to 5% aqueous silver nitrate (Sigma-Aldrich) for 30 min in the dark, followed by 60 min in light. The presence of dark brown / black nodules was observed by phase contrast microscopy, and digital images of both the control and test cultures were captured using a Leica FW 4000 microscope (Leica Microsystems Ltd, Milton Keynes, UK).

3.2.4 Attachment of cells to titanium surfaces

For the quantitative measurement of cell adhesion, actively dividing bone cells in exponentially growing cultures were 'tagged' by radiolabeling for 18 h with [^{3}H] thymidine (1 μCi ml^{-1}; 44 Ci mmol^{-1}) (Amersham Biosciences UK Ltd, St Giles, UK), a radioactive precursor of DNA. The radiolabeled cells were harvested by trypsinisation, washed with PBS and resuspended in full DMEM. A sample was used to determine the number of cells. A second sample was used to measure the incorporation of isotope into DNA by liquid scintillation spectroscopy using WALLAC 1409 Liquid Scintillation Counter (Perkin Elmer). The specific activity was calculated as the dpm per 1 x 10^6 cells and was used to determine the number of adherent cells, as follows.

An aliquot of 0.05 ml of the radioactively labelled cells, containing 1 x 10^3 cells, was seeded onto 3 replicate Ti (control) and Ca-Ti, K-Ti and Ar-Ti discs which had been placed in 24 well plates (Beckton-Dickenson). These were incubated for 4 h at 37°C, the discs washed twice with PBS and the non-adherent cells discarded. 0.5 ml of 10% ice-cold trichloroacetic acid (TCA) was added for 10 min to precipitate the DNA and the discs washed twice again with cold 10% TCA. The DNA on the discs was dissolved in 0.25 ml of 1% sodium dodecyl sulphate (SDS), transferred to scintillation vials and the radioactivity which had remained associated with the discs determined by liquid scintillation spectroscopy. The level of isotope recorded was used to calculate the number of attached cells, based on the initial specific activity of the cells, as noted above.

3.2.5 Scanning electron microscopy

In order to examine the effects of ion-implantation of Ti on the morphology, anchorage, extent of spreading and binding of the alveolar bone cells and MG-63 cell line, SEM was carried out as follows: 1 x 10^3 cells were seeded on the surface of 3 replicate Ti (control), Ca-Ti, K-Ti and Ar-Ti discs and incubated for 4 h at 37°C in a humidified atmosphere of 5% CO_2 in air. The discs were then removed, transferred to fresh dishes, washed with PBS and fixed with 3% glutaraldehyde in 0.1 M cacodylic acid buffer overnight. After fixation, the discs were sequentially dehydrated in ethanol (20, 50, 70, 90 and 100%) for 10 min each, immersed for 1.5 min in hexamethyl disilazane solution (HMDS) (TAAB Laboratories Ltd., Aldermaston, UK), a critical point drying fluid, and air-dried for 1 h at room temperature. The discs were then mounted on metal stubs and a thin layer of gold / palladium was sputter coated using a Polaron E5000 (Emitech Ltd., Ashford, UK). The discs were then visualised using a Cambridge 90B SEM (LEO Electron Microscopy) at an acceleration voltage of 15 kV. The SEM micrographs were captured digitally at a magnification of x 100 for counting numbers and from x 499-2000 for the analysis of cell morphology.

3.2.6 Digital image analysis

In order to investigate the effects of ion-implantation of Ti on the extent of bone cell spreading, digital image analysis was carried out as follows: After manually tracing the cell outline, the average cell area (μm^2) and the shape factor [(area/perimeter^2) x 4π] of the cells cultured on control and ion-implanted Ti discs for 4 h were measured using Image-Pro Plus 4.01

software (Media Cybernetics) on five representative fields of the SEM micrographs. The shape factor of the cell indicated how circular an object was. A circle has a shape factor of 1.00, and a line has a shape factor approaching 0.0. For reference, the shape factor for an equilateral triangle is approximately 0.61, for a square 0.79, and for a pentagon 0.86 [Ahmad et al. 1999a; Shah et al. 1999a].

3.2.7 Measurement of bone cell growth

Changes in cell numbers were measured for 4 consecutive days by differences in DNA synthesis in sub-confluent cultures. A low number of bone cells ($1x10^3$) were seeded on the discs and, at the designated time points, medium containing 1 μCi ml^{-1} of [^{3}H] thymidine was added for 2 h. The discs were washed twice with cold PBS, then with TCA, and the level of incorporation of isotope into DNA measured, as described above. In these experiments, because of differences in cell attachment, the initial level of DNA synthesis at the first time point (24 h) was used as the 'time 0' baseline value for determining the initial number of cells present on each type of disc.

3.2.8 Statistical Analysis

Experiments were conducted three times each using three replicate samples and the standard error of the mean (SEM) was calculated for each set of experiments. Significant differences in bone cell responses were established using the Student's *t* test for paired samples using SPSS 11.0 software (SPSS, Chicago, IL, USA). A p value of ≤ 0.05 was considered to be statistically significant.

3.3 Results

3.3.1 Characterisation of alveolar bone cells

Von Kossa staining was carried out in order to characterise the osteoblastic potential of human alveolar bone cells which were employed in the current study, as described in section 3.2.3. The cultures of alveolar bone cells incubated with mineralising supplements for 5 weeks displayed readily detectable numbers of irregularly shaped brown/black bone-like nodules when exposed to silver nitrate, as shown in Figure 3.1A. However, Figure 3.1B showing control cultures of human alveolar bone cells incubated in media that did not contain the supplements, demonstrated an apparent absence of equivalent darkly-stained bone-like nodules (Figure 3.1B).

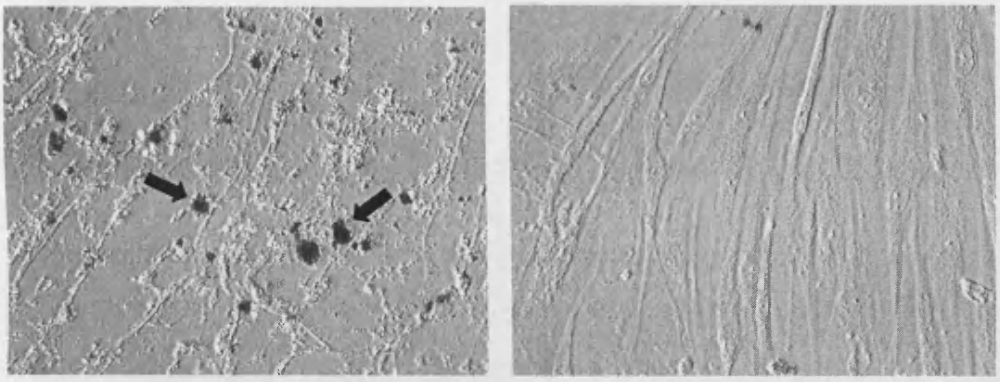

(A) (B)

Figure 3.1: Phase contrast micrographs of alveolar bone cells after 5 weeks of culture and staining using the Von Kossa method. (A) Cells cultured with mineralisation supplements and (B) control cells cultured in DMEM only, with no mineralisation supplements. The arrows show bone-like mineralising nodules in (A), while no nodules were seen in control cultures (B), magnification x 200.

3.3.2 Effects of ion-implantation on bone cell attachment

3.3.2.1 Radioactively-labelled cells

Measurements of human alveolar bone cell adhesion showed that approximately 44% (± 17) of the cells which had been seeded initially on the Ti (control) discs had attached after 4 h of incubation. However, the adhesion of the cells to the Ca-implanted Ti surface was found to be significantly reduced, to an average of only 63% of the control value, as shown in Figure 3.2 (*p = 0.03*). In contrast, cell attachment to both K-Ti and Ar-Ti was very similar to that on the Ti (control) discs (83% and 81%, respectively).

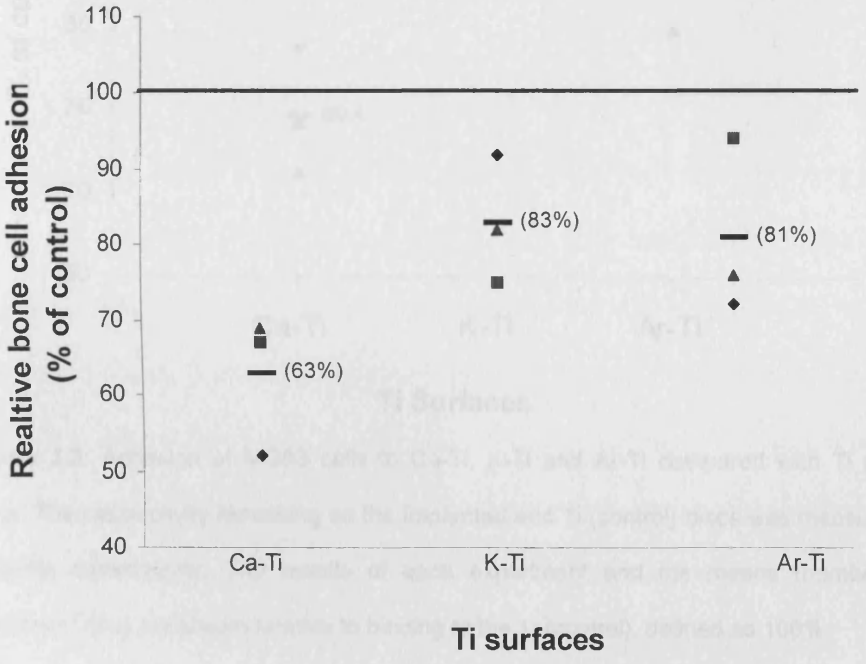

Figure 3.2: Adhesion of alveolar bone cells to the Ca-Ti, K-Ti and Ar-Ti discs relative to the Ti (control) discs, defined as 100%. The average number of cells which attached to the non-implanted Ti (control) discs was 440 cells ± 17. The 3 individual experiments are shown as ♦, ▲and ■ and the horizontal bar and numbers in brackets show the average of the 3 experiments.

The adhesion of radioactively-tagged MG-63 cells to the Ti discs was measured *in vitro,* as described in materials and methods. In 3 separate experiments it was found that 62, 57 and 43% (average 54%) of the cells which were added initially had attached to the Ti (control) discs during a period of 4 h.

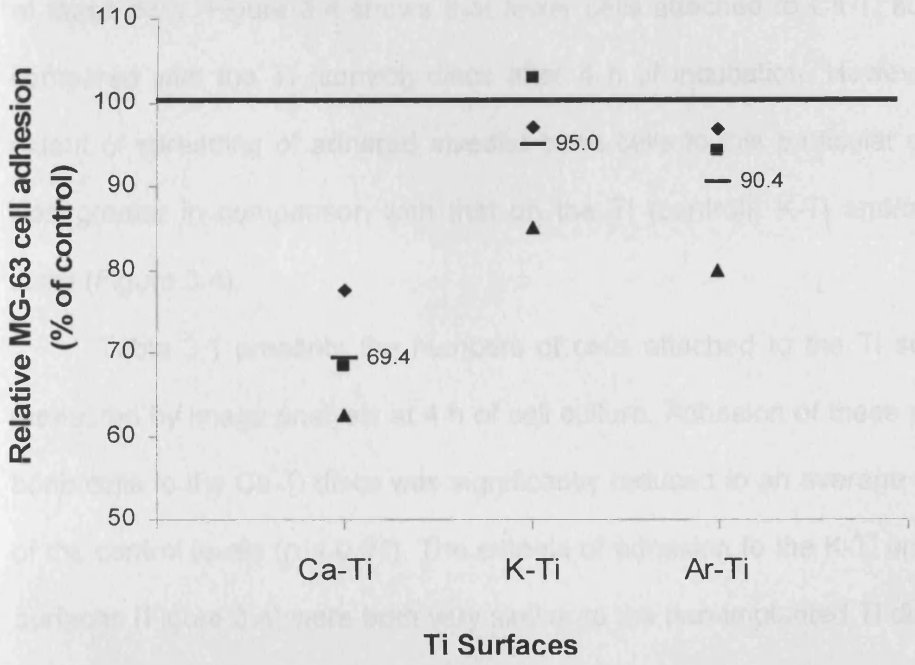

Figure 3.3: Adhesion of MG63 cells to Ca-Ti, K-Ti and Ar-Ti compared with Ti (control) discs. The radioactivity remaining on the implanted and Ti (control) discs was measured in 3 separate experiments. The results of each experiment and the means (numbers and horizontal lines) are shown relative to binding to the Ti (control), defined as 100%.

The results in Figure 3.3 show that, under the same conditions, the adhesion of MG63 cells to the K- and Ar-implanted Ti discs was similar to the non-implanted Ti (95.0 and 90.4% of that of the control, respectively). In contrast, the adhesion of osteoblast-like cells to the Ca-implanted Ti discs

was significantly reduced, to an average of 69.4% compared with the non-implanted Ti (control) levels ($p = 0.02$).

3.3.2.2 Scanning electron microscopy

Assessment of alveolar bone cell adhesion to the control and ion-implanted Ti surfaces based on the visual observation from SEM micrographs (Figure 3.4) suggests that ion-implantation affected the binding of these cells. Figure 3.4 shows that fewer cells attached to Ca-Ti surfaces compared with the Ti (control) discs after 4 h of incubation. However, the extent of spreading of adhered alveolar bone cells to this particular surface was greater in comparison with that on the Ti (control), K-Ti and/or Ar-Ti discs (Figure 3.4).

Table 3.1 presents the numbers of cells attached to the Ti surfaces measured by image analysis at 4 h of cell culture. Adhesion of these primary bone cells to the Ca-Ti discs was significantly reduced to an average of 59% of the control levels ($p = 0.01$). The extents of adhesion to the K-Ti and Ar-Ti surfaces (Figure 3.4) were both very similar to the non-implanted Ti discs (89 and 84% of control, respectively), as shown in Table 3.1. The presence of rounded cells which were attached but not yet flattened was noted on the SEM micrographs of Ar-Ti discs as shown in Figure 3.4. These measurements are consistent with the above mentioned results (section 3.3.2.1) of the adhesion of radioactively-labelled alveolar bone cells to the control and ion-implanted surfaces after 4 h of cell culture.

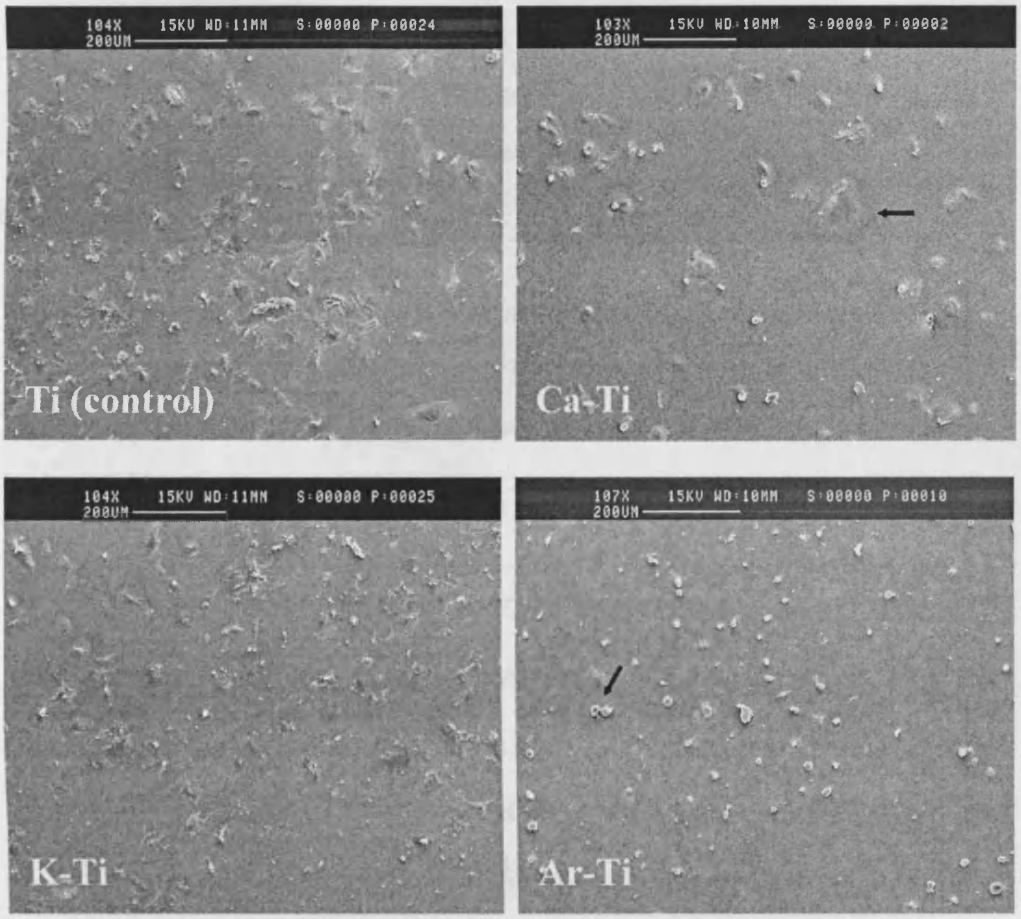

Figure 3.4: SEM micrographs of alveolar bone cells attached to Ti (control), Ca-Ti, K-Ti and Ar-Ti discs following 4 h of cell culture. Note the presence of fewer but well spread cells on Ca-Ti surfaces and in contrast attached but not yet spread cells on Ar-Ti discs, as indicated by the arrows (magnification x 100).

Table 3.1: Effects of ion-implantation on the binding of alveolar bone cells to Ti discs

Substrate	Number of attached cells	% of control
Ti (control)	580 ± 20	100
Ca-Ti	345 ± 15	**59***
K-Ti	515 ± 18	89
Ar-Ti	489 ± 25	84

Values shown are the averages (± SEM) of 3 replicate samples repeated 3 times. The numbers of the attached cells, after 4 h of incubation, were measured on 5 random fields of the SEM micrographs. The values relative to Ti (control) discs, defined as 100%, are also shown. * Indicates statistically significant differences compared with the control; shown in bold, $p = 0.01$.

Although, greater numbers of MG-63 cells appear to be adhering to Ti discs compared with the alveolar bone cells, Figure 3.5 shows that the pattern of binding of both types of bone cells was very similar (Figure 3.4 and Figure 3.5). It is apparent that fewer MG-63 cells adhered to the Ca-Ti discs in comparison with the Ti (control) following 4 h of incubation. However, MG-63 cell attachment does not seem to be substantially affected due to K or Ar ion implantation of Ti disc, as shown in Figure 3.5.

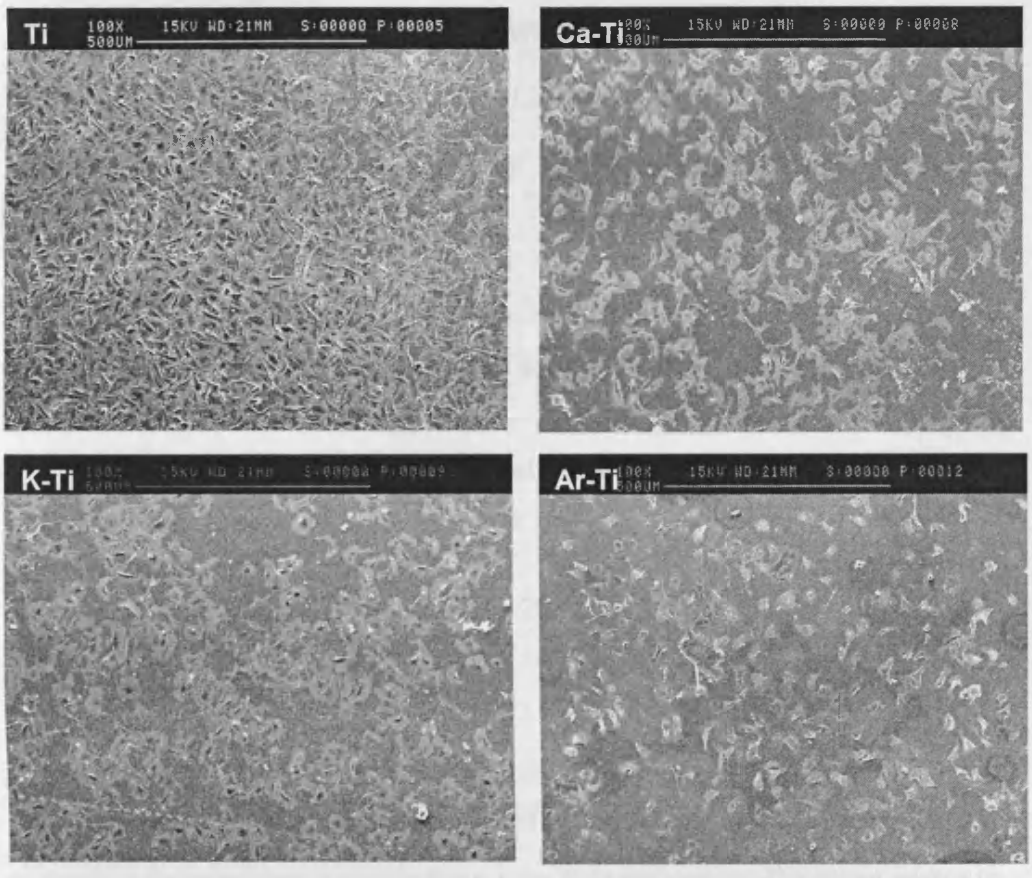

Figure 3.5: SEM micrographs showing binding of MG63 cells to Ti (control), Ca-Ti, K-Ti and Ar-Ti discs at 4 h of cell culture. Note reduced cell attachment on Ca-Ti surfaces compared with that on the Ti (control) discs (magnification x 100).

Table 3.2 shows that out of 1000 cells seeded initially on these substrates around, 880 ± 23 MG-63 cells were attached on the Ti (control) discs after 4 h of incubation. Visual assessment of cell binding by image analysis indicates that MG-63 adhesion was reduced on the ion-implanted discs in relation to that on the Ti (control), defined as 100%. A significant decrease in the cell numbers, to an average of 62% of the control level ($p = 0.04$) (Table 3.2) was measured on the Ca-Ti surface. In addition, cell binding on the K-Ti and Ar-Ti was apparently nearly as good as that on the Ti (control) following 4 h of cell culture.

Table 3.2: Effects of ion-implantation on the adhesion of MG-63 cells

Substrate	Number of attached cells	% of control
Ti (control)	880 ± 23	100
Ca-Ti	550 ± 19	**62***
K-Ti	702 ± 11	89
Ar-Ti	653 ± 22	84

The average numbers of attached cells (± SEM of 3 replicate samples repeated 3 times) shown were measured from 5 random fields of the SEM micrographs. The values relative to Ti (control) discs, defined as 100%, are also shown. Note the statistically significant difference, shown in bold, between Ti (control) and Ca-Ti surfaces as indicated by * ($p = 0.04$).

3.3.3 Ion-implantation and bone cell morphology

Human alveolar bone cells incubated on the Ti (control) discs exhibited a morphological appearance consistent with an osteobalstic

phenotype (i.e., polygonal shape with dorsal ruffles and numerous cell processes) [Leitao and Barbosa, 1998], as shown in Figure 3.6. At x 2000 magnification, cells attached on the control and ion-implanted surfaces showed fibrillar cell membranes, while the underlying surfaces appeared very smooth. The cells which had attached to the Ca-implanted Ti discs appeared to be more spread and highly flattened than those on the Ti (control) discs. A network of multiple cytoplasmic extensions was present between neighbouring cells on this particular surface (Figure 3.6).

In contrast, K implantation of Ti seemed to have no effect on the morphological appearance of the cells, as bone cells incubated on K-Ti displayed a cell morphology that was similar to those attached on the Ti (control) discs (Figure 3.6). Ar-implantation of Ti; however, resulted in a converse effect; a larger proportion of rounded cells with apparently reduced spreading were observed on this surface, as shown in Figures 3.4 and 3. 6. At high magnification, the SEM micrograph shows a picture of a representative cell attached on Ar-Ti surface with a granular cell body and relatively less cell to substrate contact ratio than those on the Ti (control) disc.

The effects of ion-implantation on the morphology of MG63 cells observed by SEM were largely in agreement with the response of alveolar bone cells, as described above. Figure 3.7 shows that although surface modification of the Ti discs by Ca-implantation enhanced the extent of MG-63 cell spreading at 4 h; nevertheless, it was not as pronounced as the alveolar bone cells (Figure 3.6). Cells seeded onto the Ca-Ti discs appeared to be

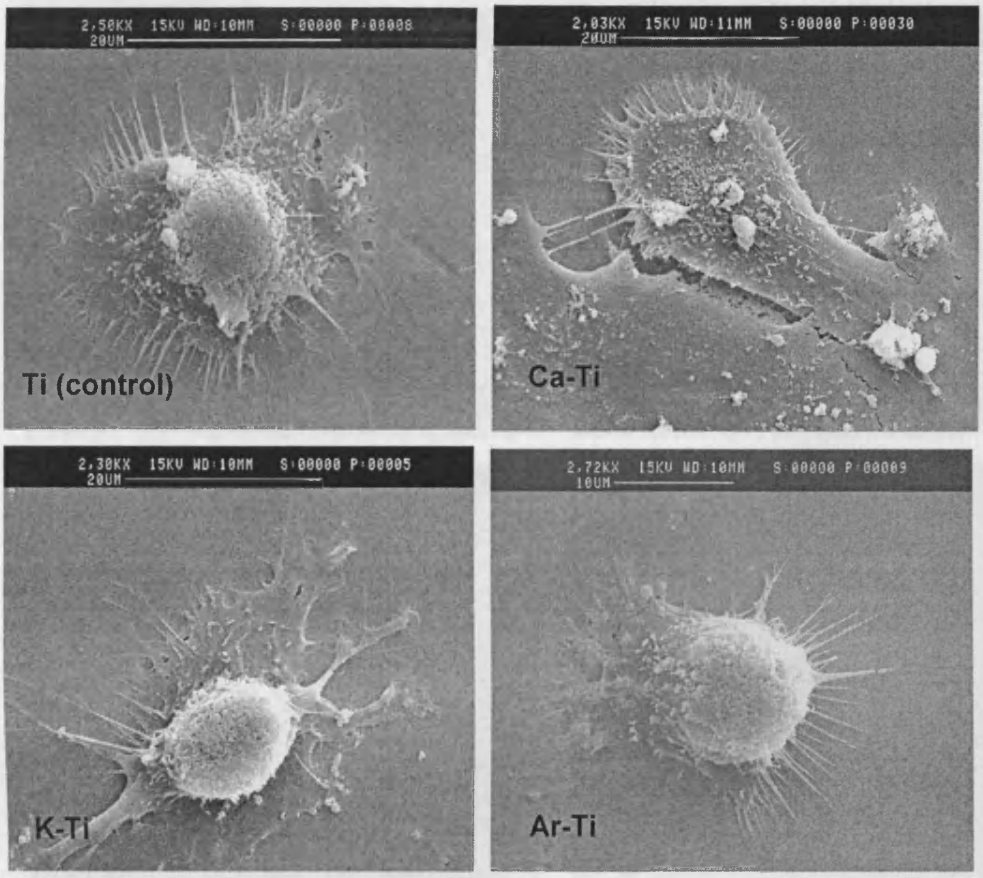

Figure 3.6: SEM micrographs show the morphology of a representative adherent alveolar bone cell following 4 h of incubation on Ti (control), Ca-Ti, K-Ti and Ar-Ti discs. Note the extent of cell spreading on the Ca-Ti compared with the Ti disc. The cell on K-Ti appears similar to the control, whereas distinctively rounded and attached but not yet spread cells were observed on the Ar-Ti surface (magnifications x 2000).

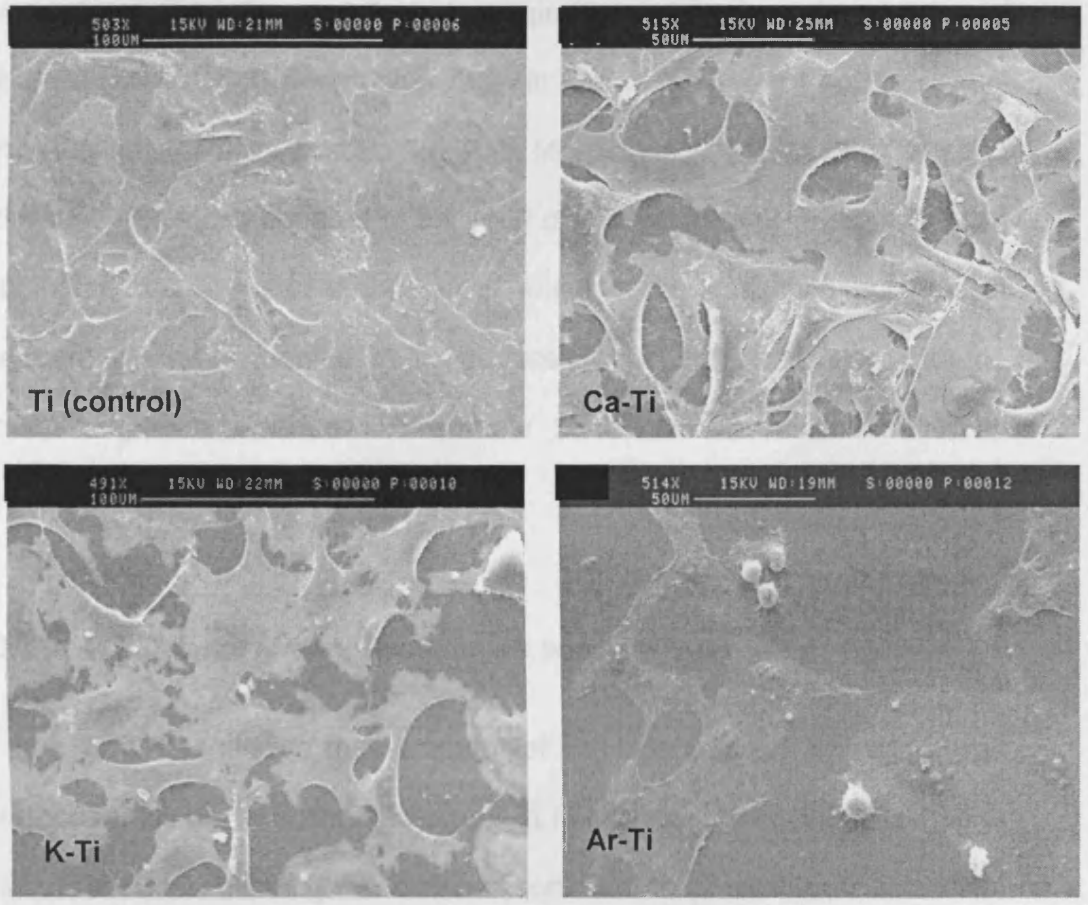

Figure 3.7: SEM micrographs of MG-63 cells attached on Ti (control), Ca-Ti, K-Ti and Ar-Ti discs after 4 h of incubation. Cells adhered on the Ca-Ti surfaces appear flattened with a high cell to substrate contact ratio compared with those on Ti (control). Extent of MG-63 cell spreading on K-Ti was as good as on Ti, while a higher proportion of rounded cells were detected on Ar-Ti (magnification x 491-500, as indicated).

slightly more spread, showing relatively increased cell to substrate contact ratio, than those seeded on the non-implanted Ti (control) discs (Figure 3.7). An apparent formation of a monolayer of MG-63 cells extending on this surface as early as after 4 h of incubation (Figure 3.7), indicates that the presence of Ca ions had an effect on the morphology of these osteoblast-like cells. In addition, Figure 3.7 shows a similar anchorage and spreading of MG-63 cells on K-Ti discs compared with the cells attached on the control non-implanted Ti after 4 h of cell culture. Most interestingly, although some of the cells which had adhered to the Ar-Ti discs appeared flattened as shown in Figure 3.7, a higher proportion of rounded cells, attached but not yet spread, was also observed on this surface. This effect is consistent with the morphological analysis of the alveolar bone cells to Ar-Ti surface, as described above.

3.3.4 Influence of ion-implantation on bone cell spreading

Semi-quantitative measurement of the extent of cell spreading was carried out by digital image analysis of SEM micrographs of cells attached to the Ti surfaces following 4 h of incubation. Results presented in Table 3.3, indicate that there was a significant increase in the average area of the alveolar bone cells incubated on the Ca-Ti surface (approximately 213% greater than those on the control discs; $p = 0.01$). The results in Table 3.3 also show that the spreading on the K-Ti discs was very similar to that on the control surfaces. In contrast, there was a notable reduction in the average area of cells incubated on Ar-Ti (by 24%), although this was not significantly less than the control value ($p = 0.06$).

Table 3.3: Effects of ion-implantation on the spreading of alveolar bone cells

Substrate	Average cell area (μm^2)	% of control
Ti (control)	719 ± 15	100
Ca-Ti	1532 ± 20	**213***
K-Ti	742 ± 30	103
Ar-Ti	548 ± 10	76

The averages values (± SEM) of 3 replicate samples repeated 3 times are shown. * Indicates statistically significant differences, shown in bold, measured between Ti (control) and Ca-Ti surfaces; *p = 0.01*.

Because spreading included changes in cell shape, the shape factor defined as (area/perimeter^2) x 4π was also calculated as a function of Ti surface chemistry. Shape factor is an inverse measure of cell spreading, such that a perfect circle has a value of 1 and a straight line has a value of 0; that is the lower the value of shape factor the more elongated the osteoblasts. Measurement of the shape factor of alveolar bone cells, further confirmed the significance of Ca ions implanted on the surface of Ti discs. Figure 3.8 shows that the cells attached on Ca-Ti had a shape factor of 0.27 ± 0.05, which is indicative of highly spread cells compared with control (*p = 0.02*). Similarly, cell spreading on K-Ti seems to be slightly increased compared with that on Ti (Figure 3.8) (0.53 ± 0.03 and 0.64 ± 0.02, respectively). In contrast, Ar implantation elicited a reduction in cell spreading after 4 h of cell culture (shape factor = 0.82 ± 0.03).

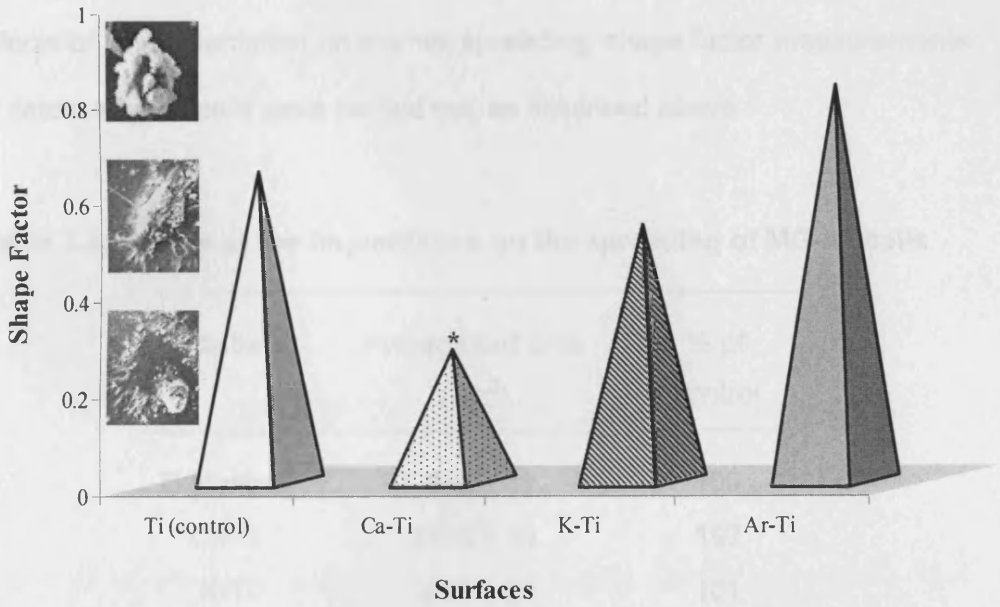

Figure 3.8: The effect of ion-implantation of Ti on the shape factor of alveolar bone cells following 4 h of cell culture. Asterisks denote significantly different shape factor values ($p = 0.02$) between Ti (control) and Ca-Ti discs. See insert as a guideline of decreasing shape factor value for rounded, spread and highly flattened cells from top to bottom.

Table 3.4 shows the effects of implanting Ti discs with Ca, K and Ar ions on the spreading of MG-63 cells which were incubated on these surfaces for 4 h, as described in section 3.2.5. A significant increase in the average area of the cells cultured on Ca-Ti discs was measured by image analysis (97% greater than those on control discs; $p < 0.05$). However, the response of these osteosarcoma cells on the K-Ti surface was very similar to those on the Ti (control), an average cell area of 672 ± 23 compared with 665 ± 12 was calculated for the K-Ti and Ti (control) discs, respectively (Table 3.4). As for alveolar bone cells MG-63 cell spreading was also reduced as a result of Ar ion implantation of Ti discs. A 21% drop in the average cell area

compared with the Ti (control) values defined as 100% was measured on this surface as presented below in Table 3.4. In order to further evaluate the effects of ion-implantation on the cell spreading, shape factor measurements of osteosarcoma cells were carried out, as described above.

Table 3.4: Effects of ion-implantation on the spreading of MG-63 cells

Substrate	Average cell area (μm^2)	% of control
Ti (control)	665 ± 12	100
Ca-Ti	1310 ± 19	**197***
K-Ti	672 ± 23	101
Ar-Ti	531 ± 18	79

Spreading of MG-63 cells was significantly enhanced on Ca-Ti surfaces compared to that on the Ti (control) discs, as indicated by an asterisk *; shown in bold, $p = 0.01$.

Figure 3.9 shows that the results are consistent with the findings for alveolar bone cells. A highly significant decrease in the average shape factor was calculated for the MG-63 cells incubated on Ca-Ti discs compared with those on the Ti (control) (0.20 ± 0.02 and 0.71 ± 0.04, respectively) ($p = 0.01$). Moreover, K ion implantation resulted in a 17% increased spreading of the cells compared with those in direct contact with the Ti (control) surfaces, as shown in Figure 3.9. In contrast, shape factor of the cells on Ar-Ti discs was measured as 0.79 ± 0.02, indicating the presence of rounded and not very well spread cells on this particular surface (Figure 3.9).

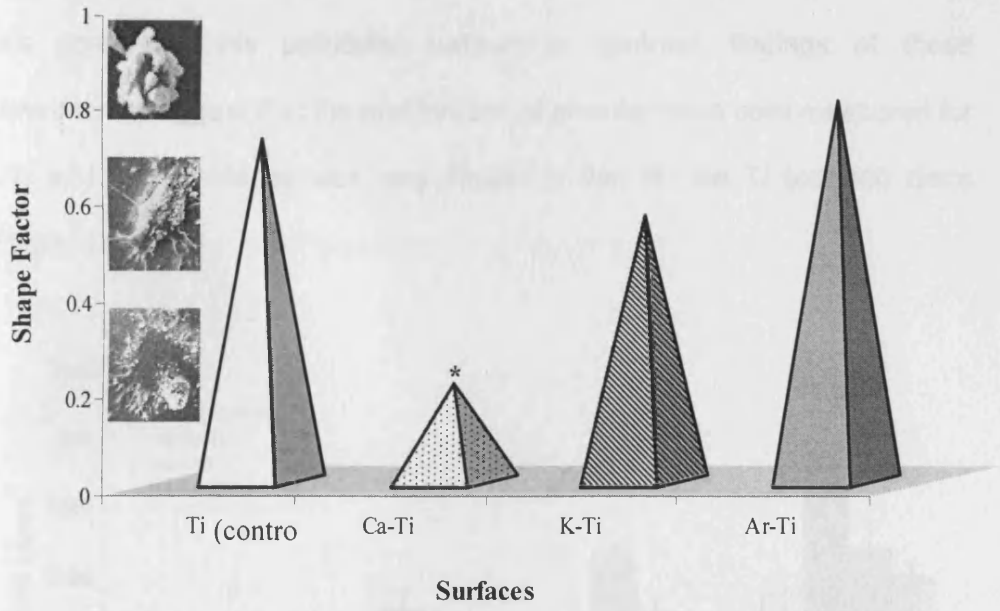

Figure 3.9: The effect of ion-implantation on the shape factor of MG-63 cells following 4 h of cell culture. Asterisks denote significantly different shape factor values ($p = 0.01$) between Ti (control) and Ca-Ti discs at 4 h.

3.3.5 Influence of ion-implantation on bone cell proliferation

The effects of ion-implanted surfaces on cell proliferation were determined by measuring the change in cell number for four consecutive days, as described in section 3.2.7. Figure 3.10 shows radioisotope counts, indicative of [^{3}H] thymidine incorporation into the DNA of proliferating alveolar bone cells cultured on the Ti (control), Ca-Ti, K-Ti and Ar-Ti discs, calculated after 24, 48, 72 and 96 h of incubation.

The results in Figure 3.10 point out that despite initial delay in cell growth seen at 24 h, the change in number of alveolar bone cells was greater on Ca-Ti surfaces in comparison with the non-implanted Ti (control) at all periods of incubation. Ca ion-implantation of Ti discs seemed to have caused a burst of DNA synthesis between 24 and 48 h, as shown in Figure 3.10. This

was followed by a steady increase in the number of cells measured at later time points on this particular surface. In contrast, findings of these experiments suggest that the proliferation of alveolar bone cells measured for K-Ti and Ar-Ti surfaces was very similar to that for the Ti (control) discs (Figure 3.10).

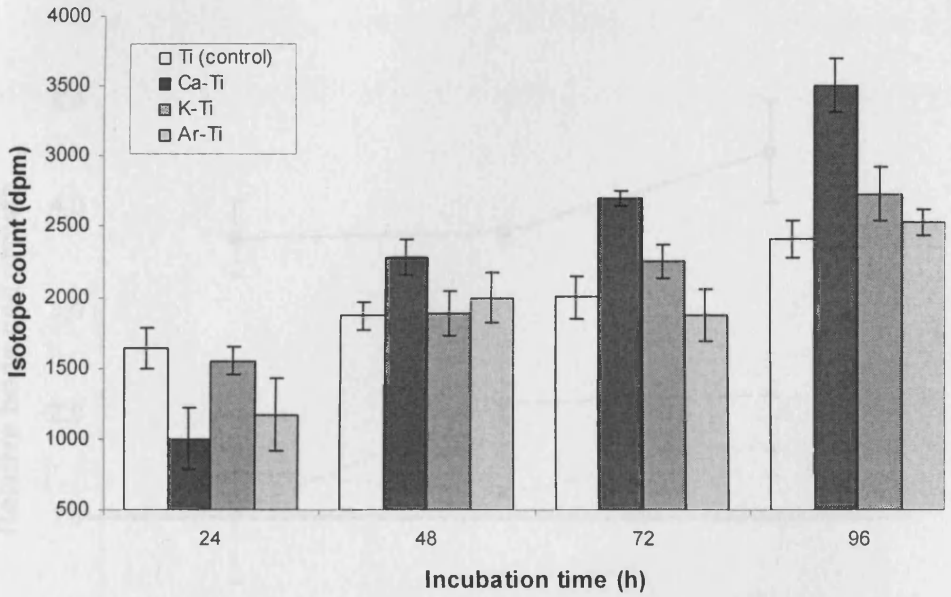

Figure 3.10: Measurement of the effects of ion-implantation on the proliferation of alveolar bone cells by [^{3}H] thymidine incorporation assay. Changes in the number of cells for Ti (control), Ca-Ti, K-Ti and Ar-Ti discs were determined at 24, 48, 72 and 96 h of cell culture. Values shown are average (± SEM) of 3 replicate experiments.

Figure 3.11 was plotted to show alveolar bone cell proliferation on Ca-Ti, K-Ti and Ar-Ti surfaces relative to that measured for the Ti (control) discs. Relative changes in cell number were adjusted for differences in the numbers of cells which had originally attached to the different surfaces, which was measured at 24 h (time 0) after seeding (Figure 3.10), as described in section 3.2.7. Figure 3.11 indicates that there was a significantly elevated level of

relative growth of the cells incubated on the Ca-Ti surfaces (p= *0.01*). At all times measured (48, 72 and 96 h the after initial seeding), this increased proliferation was approximately 400% greater than on the Ti (control) discs. In contrast, cells incubated on the surfaces of the K-Ti and Ar-Ti discs showed no significant difference in cell numbers compared to those on the control discs (Figure 3.11).

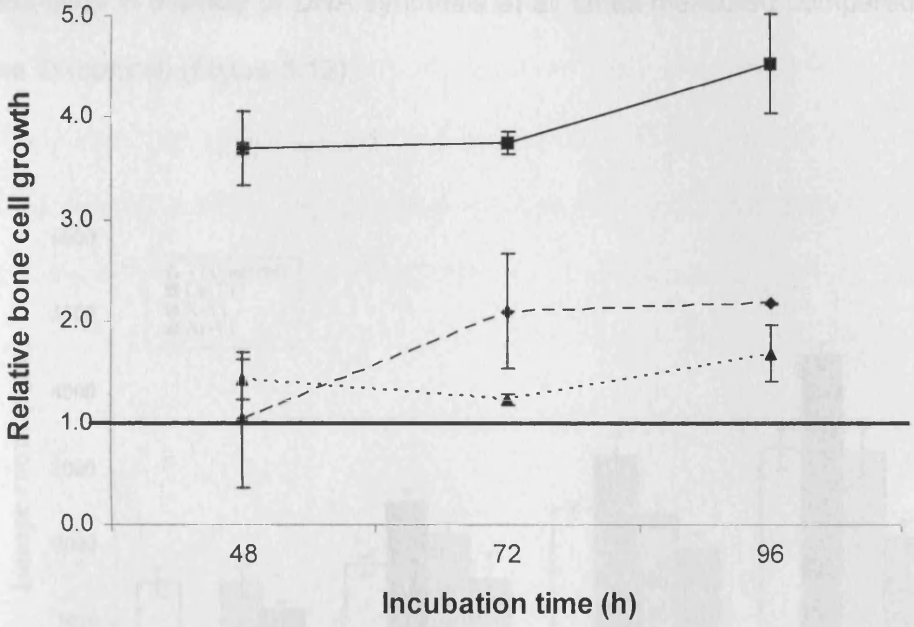

Figure 3.11: Growth of alveolar bone cells on the Ca-Ti (■—■), K-Ti (♦---♦) and Ar-Ti (▲...▲) discs measured at 48, 72 and 96 h after initial seeding. The values shown are relative to the growth on the Ti (control) discs, defined as 1.0. Note the significantly increased level of bone cell growth on Ca-Ti at all 3 incubation times (p = *0.01*).

Figure 3.12 shows the effects of ion-implantation of Ti discs on the 4 day growth of osteoblast-like cells. The results in Figure 3.12 suggest that the change in surface chemistry of Ti discs by Ca ion-implantation resulted in an enhanced rate of cell growth in comparison with the non-implanted Ti. Like

alveolar bone cells, the number of isotope counts obtained at 24 h for MG-63 cells cultured on Ca-Ti discs were less than those on the control surfaces. However, a 3-fold increase was measured from 24 to 48 h of incubation of these cells on this particular surface (Figure 3.12). Cell growth was shown to be greater for Ca-Ti after 48, 72 and 96 h of cell culture than that measured for any other surface. In contrast, K ion-implantation did not affect the proliferation MG-63 cells. However Ar-Ti surfaces seemed to have caused a reduction in the rate of DNA synthesis at all times measured compared with the Ti (control) (Figure 3.12).

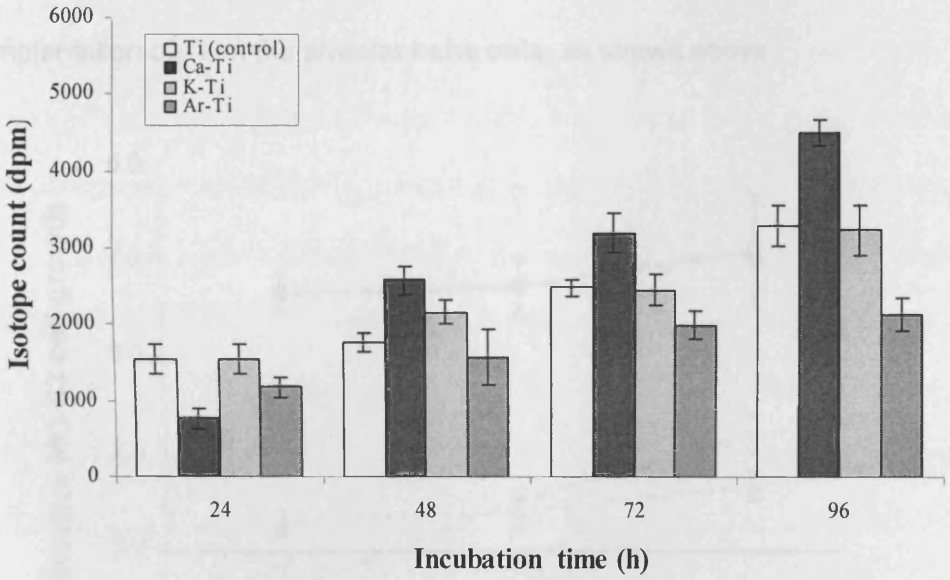

Figure 3.12: Change in the number of MG-63 cells measured by [^{3}H] thymidine incorporation assay after 24, 48, 72 and 96 h of cell culture on Ti (control), Ca-Ti, K-Ti and Ar-Ti discs. Values shown are average (± SEM) of 3 replicate experiments. Note the higher levels of cell proliferation on Ca-Ti surfaces in comparison to the Ti (control) at 48, 72 and 96 h of incubation.

To demonstrate the effects of ion-implantation of Ti surfaces on the proliferation of MG-63 cells, the values obtained from 3 replicate experiments were normalised for the non-implanted control levels. Figure 3.13 shows MG-63 cell growth on Ca, K and Ar ion-implanted surfaces relative to that on the Ti (control) discs after 48, 72 and 96 h of incubation of discs under physiological conditions. After adjustment of changes in cell number for the differences measured at 24 h (time 0) (Figure 3.12), a significant increase in relative proliferation was observed on Ca-Ti surfaces at all times compared with the control levels ($p = 0.01$). However, no marked increase in the relative cell growth was noticed on either K-Ti and/or Ar-Ti discs following 2, 3 or 4 days of cell culture. This finding is consistent with the effects of ion-implantation of Ti on the alveolar bone cells, as shown above.

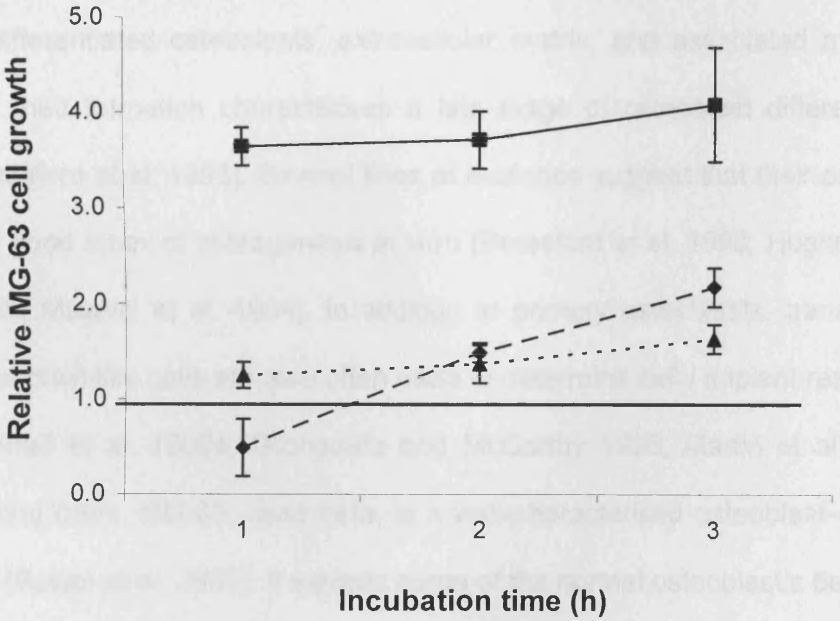

Figure 3.13: Proliferation of MG-63 cells on the Ca-Ti (■—■), K-Ti (♦---♦) and Ar-Ti (▲...▲) surfaces relative to the Ti (control) levels defined as 1.0, measured at 48, 72 and 96 h of cell culture. Note the significantly increased level of bone cell growth on Ca-Ti at all 3 incubation times ($p = 0.01$).

3.4 Discussion

Ti in its commercially pure form is one of the most commonly used implant materials in oral and cranio-facial surgery [Okabe and Hero 1995]. The quality and intensity of bone cell response to cpTi implants appear to depend on the surface characteristics of the material [Boyan et al. 1996; Ahmad et al. 1999a; Brett et al. 2004; Degasne et al. 1999; Howlett et al. 1994; Knabe et al. 2004; Rosa and Beloti 2003; Krupa et al. 2001; Krupa et al. 2005]. In the current investigation, the effects of modifying surface chemistry of cpTi discs via Ca, K and Ar ion-implantation were assessed on the response of human alveolar bone cells and MG-63 osteosarcoma cell line. The primary osteoblast cultures clearly comprised a proportion of osteoblast precursors, as evident by the finding that they were able to actively mineralize and form bone-like nodules *in vitro.* Bone nodules consist of differentiated osteoblasts, extracellular matrix, and associated minerals, and their formation characterises a late stage of osteoblast differentiation [Beresford et al. 1993]. Several lines of evidence suggest that their presence is a good index of osteogenesis *in vitro* [Beresford et al. 1993; Hughes et al. 1995; Malaval et al. 1994]. In addition to primary osteoblasts, transformed osteoblast-like cells are also often used to determine cell / implant responses [Ahmad et al. 1999a; Gronowicz and McCarthy 1996; Martin et al. 1995]. Among them, MG-63, used here, is a well-characterised osteoblast–like cell line [Boyan et al. 1989]. It exhibits some of the normal osteoblastic behaviour in culture, and therefore has been widely employed in previous investigations of cellular responses to the Ti surfaces [Martin et al. 1995; Massaro et al. 2001; Boyan et al. 1998; Martin et al. 1996]. Findings of the experiments

presented in this chapter suggest that the influences of ion-implanted Ti surfaces were largely consistent for both human alveolar bone cells and MG-63 osteosarcoma cell line.

3.4.1 Effects of ion-implantation on cell attachment and spreading

Results of the current study showed that both human alveolar bone and MG-63 cells readily attached to the Ti (control) and also to the K and Ar-implanted Ti surfaces. Ca implantation, however, markedly decreased their attachment following 4 h of incubation. It was initially speculated that the bombardment of high-energy Ca, K and Ar ions into Ti may give rise to altered surface topography by creating micro-or nano-scale pores or pits, as suggested by a previous study [Zinger et al. 2004]. The findings of the Biomaterials group of UCL EDI (Appendix A), however, suggested that the topographical roughness of the Ti surfaces were not significantly altered by the implantation conditions used in this work. Since Ti surfaces implanted with $^{40}Ar^{+}$ and $^{39}K^{+}$ ions have similar damage levels but different surface chemistry than $^{40}Ca^{+}$, therefore the reduced cell attachment observed on Ca-Ti surfaces at 4 h is unlikely to be due to the implantation process, and might have been induced by Ca ions specifically. Previous research has established that the surface characteristics of the implant materials, such as topography, chemistry or surface energy dictate the profile, conformation and the structural rearrangement of the molecules adsorbed on these biomaterials [Anselme2000; Boyan et al. 1996; Schwartz et al. 1997], which in turn may influence the initial cell adhesion to the implants [Juliano et al. 1993]. For example, a previous study showed that an alteration of Ti surface

chemistry/microcrystallinity directly influenced the adhesion of human bone derived cells possibly via changing the conformation and ability of the ECM proteins adsorbed on the material surface [Zreiqat and Howlett 1999]. Another study illustrated that the attachment of human bone-derived cells during the first 90 min of cell culture were a function of adsorption of the serum protein "vitronectin" onto the surface of Ti [Howlett et al. 1994]. In view of these results it appears that the implantation of Ti surfaces with Ca ions might have adversely affected the adsorption of ECM proteins on the Ti discs, which in turn possibly caused a reduction in the initial cell attachment.

In the current work, the morphological appearance and spreading of the attached alveolar bone and MG-63 cells was also found to be related to the type of ion implanted on the surface of Ti discs. Despite a significant reduction in the initial attachment of osteoblasts to the Ca ion-implanted surface, cells that attached to the Ca-Ti discs were found to be more flattened and had a network of fibrillar extensions, and thus might have retained a high degree of functional integrity than those on the Ti (control) [Leitao and Barbosa 1998]. While K-Ti surfaces caused no apparent change in the cell morphology, relative cell area and the shape factor, implantation of Ar ions resulted in a notably lower extent of cell spreading, with an enhanced proportion of the attached cells remaining rounded on the surface compared with the control, consistent with the previous reports of altered HeLa cell attachment to Ar-implanted polystyrene surfaces [Suzuki et al. 1994].

The apparently less than optimal spreading on the Ar-implanted surface is of particular interest in view of the inert nature of these implanted ions. Although the precise reason for these effects is not known, it is likely to

be related to the ion implantation process itself and the consequent modification of the Ti surface. It is possible that the presence of this inert element does not promo the adsorption of one or more species required for the cells to become well spread. A second possibility is that the cellular response is governed in this case by the disruption occurring to the surface during the ion implantation process itself. Since the radiation damage was expected to be similar for all the surfaces, similar effects might be expected for the three implanted surfaces. These were not observed. Their surface chemistries are differentially affected, i.e. the amount of Ar present at the immediate surface following implantation is very much less than the amount of Ca, possibly because the inert Ar is not trapped in the near surface region during implantation (Appendix A).

It is possible that the effect of surface damage may be outweighed by the presence of the "active" ions, such as in the K-Ti and Ca-Ti surfaces. Surface characterisation of the recently produced K-Ti samples by the Biomaterials group of UCL EDI reveal that despite high levels of K at the surface, K-concentrations further into the bulk of the Ti were not comparable to Ca concentrations in the Ca-Ti samples (Appendix A). Although these samples were prepared subsequently to those used in the current study, it is probable, that the earlier samples also contained much lower K levels in the bulk than expected, despite containing the expected levels of K at the surface. Following implantation and removal into the atmosphere, implanted K may be lost through reaction with oxygen at the same time as the Ti surface is oxidised, which might explain the reason for the similarities in bone cell response to K-Ti and the bare Ti (control) discs.

In agreement with the current study, Krupa et al demonstrated an excellent spreading of human osteoblasts in response to modification of Ti surfaces with calcium ions implanted at a dose of 1 x 10^{17} ions cm^{-2} [Krupa et al. 2001]. These authors also demonstrated that Ca-implanted Ti surfaces augment the formation of hydroxyapatite-like calcium phosphate on exposure to simulated body fluids [Krupa et al. 2001]. The Ca-Ti surfaces used in the current study have also shown some evidence of more rapid formation of calcium phosphates in simulated biofluids than the other types of the surfaces (Appendix A). Since the appearance of calcium phosphate precipitates on surfaces is indicative of an improved 'biocompatibility' [Maitz et al. 2002; Zinger et al. 2004], the formation of a calcium phosphate layer may explain the enhanced bone cell spreading shown here and previously on the Ca-implanted Ti [Krupa et al. 2001].

3.4.2 Influence of ion-implanted Ti surfaces on cell growth

One of the main regulators of proliferative rate in anchorage dependent cells is shape. Cells in a rounded configuration divide at a lower rate than those flattened and well spread on a substratum [Archer et al. 1982; Folkman and Moscona 1978]. Consequently, cells which attach to materials but spread little will show lower proliferative rates than those materials which allow greater spreading. The present finding of an extensive network of cellular processes mediating the spreading of bone cells to the Ca-implanted Ti, suggests that this substrate provided a highly favourable surface for biological responses, as indicated by the subsequent growth of the cells. This was evident from the current experiments as a highly significant increase in

cell numbers following prolonged incubation on the Ca-Ti discs, relative to the Ti (control) surfaces was measured. In contrast, no increase in relative cell growth was observed on the K-Ti or Ar-Ti discs determined at 48, 72 and 96 h after seeding. Since proliferation and cell cycle of bone cells are known to be tightly correlated, this Ca-induced increase in cell growth could be due to stimulation of the cell cycle progression, possibly by accelerating the emergence of the post-trypsinised cells from the G0/G1 phase and their re-entry into the cycle, in contrast to Ti alone [Ryhänen et al. 2003].

The precise mechanisms governing this behaviour remain unknown. During implantation, the transfer of energy to the atoms and ions in the Ti/oxide lattice causes their displacement and / or sputtering out of the surface (Chapter 2). One possibility is that the nature of the implanted ion significantly affects the re-growth of the oxide layer. It is notable that only the Ca-Ti discs were observed to undergo a reflective colour change following immersion in the culture medium. Such a colour change may be due to a light interference phenomenon, which occurs when a surface layer of appropriate thickness is formed on the reflective Ti. Findings of the Biomaterials group also confirmed thickening of the oxide layer only on the Ca-Ti surfaces upon immersion in solution (Appendix A). In agreement, Ikeyama et al demonstrated that the surface oxide layer formed on Ca implanted Ti was thicker than the oxide on non-implanted control surfaces [Ikeyama et al. 2000]. Since only Ca-Ti discs and not those implanted with K and Ar, which are of the same atomic mass but differ electrochemically, affected bone cell response, it is possible that, the surface electric charge [Ikeyama et al. 2000],

the surface adsorbed protein layer [Zreiqat and Howlett 1999], as well as the thickened oxide layer (Appendix A) may all have contributed to these effects.

3.5 Conclusions

- Both qualitative and quantitative analyses indicate that the ion implantation of Ti surfaces has a profound effect on the response of bone cells *in vitro.*
- This influence, although consistent for both the primary and the osteosarcoma cells, was dependent on the nature of the implanted ion.
- Bone cell response to the K-Ti surfaces was very similar to the Ti (control). In contrast, the chemically inert Ar ions implanted on the surface of Ti caused an apparent reduction in cell spreading and cell growth.
- Despite reduced cell adhesion at 4 h, Ca-Ti surfaces elicited a significant increase in the spreading and subsequent growth of bone cells compared with the control.

Chapter 4

Effects of Different Levels of Calcium Ions on Bone Cell Adhesion

4.0 Introduction

Previous findings of the current study indicated that despite significantly enhanced morphology and growth, the initial attachment of human bone cells to Ca-Ti discs implanted with 1 x 10^{17} ions cm^{-2} was not as good as on the non-implanted Ti (control) (Chapter 3). Since cell adhesion mechanisms are likely to influence signal transduction and regulation of gene expression, this Ca-induced decrease in bone cell binding could adversely affect host responses to the Ti implants [Anselme2000]. Previous studies have emphasised the importance of dose dependency of biomaterials on the cellular response [Franks et al. 2002; Jones et al. 2001; Xynos et al. 2000; Maroothynaden and Hench 2001]. For example, it was shown that the calcification of mouse embryonic long bones was dependent on the concentrations of ions which were leaching out from the soluble bioactive glasses [Maroothynaden and Hench 2001]. The second part of the current investigation was; therefore, undertaken to determine the effects of Ti surfaces implanted with different concentrations of the biologically important Ca ions [Lodish et al. 1996; Anghileri2000] on a number of aspects of bone cell adhesion at the cellular as well as at the molecular level.

Results presented in Chapter 3 established that the responses to the ion-implanted Ti surface were largely consistent for both types of osteoblastic cells. In order to avoid the inevitable variations of primary bone cells obtained from different cell sources and of different passages, and also due to the limited availability of ion-implanted Ti discs, only MG-63 cells, which consistently and reproducibly exhibit the osteoblastic phenotype [Clover and Gowen 1994] (Chapter 2), were used for the remainder of this project.

A previous study reported that osteosarcoma-derived human osteoblasts responded to even minor variations in the chemical composition and topography of cpTi surfaces. They demonstrated that the adhesion of such cells was time-dependent, as the rate of cell attachment to grade 1 and grade 4 cpTi significantly differed between 4 and 24 h of cell culture [Ahmad et al. 1999a]. Therefore, for the current study the initial attachment of MG-63 cells to control and Ca-Ti discs was examined following 4 and 24 h of incubation under physiological conditions. Moreover, the effects of Ti surfaces implanted with different doses of Ca ions on the spreading and morphological characteristics of MG-63 cells were also assessed.

Further, to understand cell-material interactions at a molecular level, the expression of integrins, which are involved in mediating cell-substrate adhesion [Sinha and Tuan 1996; Hynes2002], and the formation of vinculin-positive adhesion plaques, which is one method of characterising the physical association of cells with Ti surfaces [Okumara et al. 2001], were also examined. In addition, since tissue culture conditions have previously been shown to influence cell responses to biomaterials [Ferraz et al. 2000], the effects of pre-immersion of the Ca-implanted Ti in cell culture medium on cell attachment were also measured and correlated with specific chemical changes at the Ti surfaces. The following section gives a brief overview of these biological parameters and also discusses their importance in screening biocompatibility of the implant materials.

4.1 Background

4.1.1 Cell adhesion

Cell adhesion is a fundamental process involved in embryogenesis, maintenance of tissue integrity, wound healing, immune response, cancer metastasis and also tissue integration of the implants. A complete understanding of osteoblastic cell adhesion is essential in order to optimise events occurring at the bone/biomaterial interface. Cell adhesion comprises a sequence of events which includes initial cell attachment, cell spreading, organization of an actin cytoskeleton and formation of focal adhesions [Anselme2000; LeBaron and Athanasiou 2000]. It is a critical first step involving the interaction of numerous proteins such as ECM proteins (fibronectin, vitronectin, collagen, laminin) [Gronowicz and McCarthy 1996; Howlett et al. 1994], cytoskeletal proteins (actin, talin, vinculin) [Puleo and Bizios 1992b; Puleo and Nanci 1999] and membrane receptors (integrins) [Hynes1987; Aplin et al. 1999; Hynes2002]. Binding of these proteins to their specific receptors induces signal transduction, gene expression and protein synthesis which directly influences cell growth, cell migration and cell differentiation [Hynes1987; Kornberg and Juliano 1992; Kornberg et al. 1991; Krause et al. 2000; LeBaron and Athanasiou 2000; Hynes2002].

The control and consequences of cell adhesion are of major importance in the context of orthopaedic and/or dental implants as these factors dictate their clinical performance and longevity [Puleo and Nanci 1999]. Previous *in vitro* evaluations established that the physicochemical characteristics of Ti surfaces have a substantial influence on the adhesion of MG-63 cell, which are also used in the experiments described in this chapter

[Kim et al. 2004; Lange et al. 2002a; Lincks et al. 1998; Zinger et al. 2004]. For example, Lincks et al examined the effect of chemical composition and surface roughness of Ti on the attachment of MG-63 cells. Smooth and rough cpTi (grade 2) and Ti-6Al-4V alloy discs were prepared by either machining/fine-polishing or grinding, respectively, and the number of cells adhering to these discs was measured. Compared to control (standard tissue culture plastic), MG-63 cell adhesion was reduced on the smooth cpTi surfaces, while it was equivalent on the Ti-6Al-4V surfaces. However, roughened cpTi surfaces increased the initial cell attachment compared with the smooth cpTi discs [Lincks et al. 1998]. Zinger et al investigated the effects of specific micro-architectural features of Ti surfaces in modulating the osteoblast behavior. On electrochemically micro-structured surfaces with hemispherical cavities of 30 or 100 μm in diameter, the MG63 cells were able to go inside, adhere and spread, whereas they did not recognize the 10 μm diameter cavities, covering them up as if they did not exist [Zinger et al. 2004].

In another recent study, it was demonstrated that the anodized Ti surfaces significantly enhanced the adhesion of human osteoblast-like MG-63 cells [Kim et al. 2004]. These authors carried out anodic oxidation of the Ti which resulted in the formation of rough, thick and porous crystalline oxide layer with an average pore size of 0.79 ± 0.27 μm. MG-63 cells on these surfaces were shown to have attached and spread better, typically containing filopodia and lamillopodia-like extensions, compared to the control machined surface [Kim et al. 2004]. Furthermore, Lang et al analysed the effects of machined, glass particle-blasted, corundum-blasted and vacuum plasma-

sprayed Ti surfaces on the adhesion of MG-63 cells. Although the components of cell adhesion were influenced by the surface roughness of Ti discs, no straight correlation was established with the degree of roughness. An increased spreading of MG-63 cells was seen on surfaces with low roughness. In contrast, integrin expression was enhanced on roughened Ti surfaces compared with the polished material. Furthermore, the organization of the actin cytoskeleton and fibronectin (FN) was impaired on extremely rough i.e. corundum-blasted and vaccum plasma-sprayed Ti surfaces [Lange et al. 2002].

4.1.2 Integrins

Adhesion of osteoblasts on implant materials has also been considered in relation to the expression of cell adhesion proteins [Castoldi et al. 1997; Schneider and Burridge 1994; Sinha et al. 1991; Gronowicz and McCarthy 1996]. Upon adhesion cells require signals from the ECM, and these signals are transduced by transmembrane receptor proteins called "integrins" [Puleo and Nanci 1999]. Integrins are a large family of heterodimeric glycoproteins connected to the cytoskeleton of the cells. Each integrin is composed of α and β subunits, non-covalently bonded, forming the large globular extracellular head region which binds to the ligands. Most integrins have more than one adhesive ligand, and more than one integrin can bind to the same ligand at the same time. At present, eighteen α and eight β subunits have been identified which are known to assemble into 24 different receptors. Changes in either α or β subunit of integrins alter their

specificity for ligands and thus affect their function [Juliano and Haskill 1993; Hynes1987; Akiyama1996].

Integrins mediate interactions between the cells and also amid cytoskeleton and the ECM *via* a complex spectrum of ligands which are present on the surface of cells and on the ECM proteins [Hynes1987]. ECM proteins contain the amino acid sequence, Arg-Gly-Asp (RGD), which is recognised by integrins as their cell binding sites. In addition to connecting cells with ECM molecules, integrins play a major role in transmembrane signalling involving molecules such as mitogen-activated protein kinase, focal adhesion kinase (FAK) and integrin-linked kinase. Integrin-mediated adhesion of cells to the substrates triggers the intracellular signalling pathways by enhanced tyrosine phosphorylation of these proteins [LeBaron and Athanasiou 2000]

Several integrin subunits (e.g., β1, α5, α6, αv) have been identified in bone cells and in osteosarcoma cell lines [Chiang et al. 1995; de Ruijter et al. 2001]. Osteoblastic cells mainly use integrins for initial attachment to various substrates *in vitro* [Gronowicz and McCarthy 1996]. Integrin expression in osteoblastic cells from various sources has been characterised on different orthopaedically relevant surfaces, with adhesion to the surfaces concluded to be either primarily dependent on or not mediated through integrins, depending on the study and the cell source [Gronowicz and McCarthy 1996; Castoldi et al. 1997; Schneider and Burridge 1994; Sinha et al. 1991]. Gronowicz and McCarthy showed that when osteoblast-like Saos-2 cells attach to the Ti surface, various integrin subunits (predominantly β1) appear on the cell surface [Gronowicz and McCarthy 1996]. Another study

emphasised the importance of the β1 integrin subunit in cell adhesion to Ti surfaces. They demonstrated a decreased adhesion and spreading of Saos-2 cells cultured on the Ti discs as a result of the addition of anti β1 monoclonal antibody in the culture medium [Degasne et al. 1999]. Therefore, for the current study the effects of different levels of Ca ion-implantation of Ti were tested on the expression of β1 integrin subunit by MG-63 cells.

4.1.3 α5β1 integrin

Cells that are attachment dependent interact with the substrate through a number of mechanisms including specific binding of integrins to components of ECM, as well as to proteins adsorbed on the material surface [Puleo and Nanci 1999]. One of the integrins that mediate bone function and binding of osteoblasts to proteins containing the RGD motif is α5β1 [Schaffner and Dard 2003]. This integrin was identified as a receptor for FN, an ECM protein which functions as a link between the substratum and the cytoskeleton of many types of cells [Hynes1987].

It is known that ECM molecules, as deposited on a substrate surface, have striking effects on the behaviour of the cell. The binding of α5β1 integrin with FN adsorbed onto the surface of Ti indirectly modulates cell adhesion by initiating a signalling cascade across the membrane resulting in gene expression and protein synthesis [Puleo and Nanci 1999]. Degasne et al showed that the presence of FN was critical for adhesion, spreading and proliferation of cells on Ti surfaces [Degasne et al. 1999]. Another study showed reduced fibroblast attachment with a concomitant decrease in the adsorption of FN on cpTi surfaces compared with that on the tissue culture

plastic [Derhami et al. 2000]. The surface characteristics of Ti were also shown to affect the expression of integrin receptors specific for FN [Hormia and Kononen 1994]. Furthermore, Zreiquat et al proposed that cell adhesion to biomaterial surfaces is probably mediated by $\alpha5\beta1$ and $\beta1$ integrins [Zreiqat et al. 2002]. Therefore, for the current study, in addition to $\beta1$ integrin subunit, the effects of Ca ion-implantation of Ti were also assessed on the expression of $\alpha5\beta1$, a receptor for FN.

4.1.4 Focal adhesions

Focal adhesions are highly specialised distinct entities of the cell that link molecules of the ECM to components of the cell's actin cytoskeleton. These most frequently observed cell–substrate interactions of the adherent cells are approximately 0.1-2 μm wide and 2-10 μm in length, characterised by a spacing of 10-15 nm between the cell membrane and the substrate [Puleo and Nanci 1999]. Focal adhesions have been shown to appear at the cell periphery within 20 minutes of the cell interacting with the surface [Sinha et al. 1994].

Membrane proteins such as vinculin, talin, paxillin, α-actinin and FAK constitute focal adhesions. These focal adhesion proteins mediate transmembrane signalling via interaction with integrins [LeBaron and Athanasiou 2000]. They also play a role in the organization of the actin cytoskeleton by directing the positioning of the actin filaments, which are responsible for contractile mechanisms of the cells, and thus control the cytoskeleton, cell shape and behaviour of the cell [Baxter et al. 2002].

4.1.5 Vinculin

Vinculin, a ubiquitous protein with a molecular weight of 130 kDa [Anselme2000], has been frequently used as a immunofluorescent marker for assessing the formation of focal adhesions by osteobalstic cells on opaque Ti surfaces [Okumara et al. 2001; Sinha et al. 1994; Ahmad et al. 1999a]. Furthermore, due to its presence on the focal adhesion sites as early as 3 h of cell attachment [Baxter et al 2002], it is a suitable focal adhesion protein to assess the effects of ion-implantation on the initial stages of cell adhesion. Vinculin is one of the connecting molecules in the hierarchy of integrin-mediated cytoskeletal molecules. It is known to play an important role in transmitting signals from integrins on the cell surface to cytoskeletal actin filaments [Anselme2000; Juliano and Haskill 1993; Miyamoto et al. 1995].

Vinculin has been shown to be expressed by the cells which were cultured on Ti surfaces [Ahmad et al. 1999a; Kooten et al. 1997; Linez-Bataillon et al. 2002; Shah et al. 1999a; Zinger et al. 2004]. Kooten et al seeded human umbilical vein endothelial cells (HUVEC) directly on the Ti surfaces and determined the expression of vinculin by these cells. They showed that HUVEC cells which had adhered to Ti were able to form focal adhesions [Kooten et al. 1997]. In another study, a comparative analysis of primary human osteoblastic cell adhesion and spreading on Ti-6Al-4V and cobalt-chrome-molybdenum (CC) was carried out [Shah et al. 1999a]. Using confocal laser scanning microscopy, Shah et al observed that, during the first 12 h of contact with the substratum, focal adhesion contacts, as indicated by vinculin immunostaining, were distributed throughout the cells adhering to Ti, but were relatively sparse and localized to cellular processes on CC.

Vinculin-positive adhesion plaques were identified at all membrane-to-surface contact points on both Ti and CC, however on Ti, these contact points closely followed the surface contour, while on CC, they were restricted to relative topographic peaks only [Shah et al. 1999a].

Linez-Bataillon et al investigated the role of the surface roughness of Ti6Al4V on the expression of cell adhesion proteins such as actin, FN, collagen I and vinculin: Five different surface preparations were used i.e. sandblasted, 80, 1200, and 4000 grade polished and mirror polished. Their results indicated that after 3 days of MC3T3-E1 mouse osteoblast culture on Ti surfaces, the expression of adhesion proteins varied with respect to the surface roughness [Linez-Bataillon et al. 2002]. Zinger et al also used MG63 cells to assess the role of micrometer and submicrometer roughness of the Ti surfaces on the early phase of cell-Ti interactions. Using double immunofluorescent labeling of vinculin and actin, they found that the MG-63 cells responded to nanoscale roughness by a higher cell thickness and a delayed appearance of the focal contacts [Zinger et al. 2004].

4.1.6 Influence of pre-immersion of titanium discs on surface chemistry and cell adhesion

Ti, a leading implant material does not encourage calcium phosphate precipitation on its surface. To improve its biocompatibility, HA, a crystalline form of calcium phosphate is frequently coated on the surface using plasma spray techniques. However, there are certain disadvantages of this method such as formation of thick unstable layer with internal fractures causing poor

adherence of coating to the substrate and problems with the integrity of HA structure and composition [Ratner et al. 2004] (Chapter 1).

An alternative technique of encouraging calcium phosphate deposition is the pre-immersion of ion-implanted Ti surfaces in physiological fluids [Pham et al. 2000a]. Modification of Ti surfaces by ion-implantation, where ions are implanted below the surface, has been previously reported to augment the formation of HA-like calcium phosphate on exposure to SBF [Maitz et al. 2002a; Pham et al. 2000a]. Previous studies of calcium phosphate formation on ion-implanted Ti have generally utilised primarily SBF of the Kokubo type (i.e. containing mainly inorganic components) [Kokubo et al. 1990]. It has been reported by Maitz et al that Ti surfaces modified in a controlled way by Na ion–implantation induced calcium phosphate precipitation following pre-immersion in SBF prior to cell culture. Such surfaces were shown to enhance bone cell growth, compared with the non-treated Na-implanted Ti surfaces, *in vitro* [Maitz et al. 2002a]. Similarly, Na ion-implantation with subsequent thermal treatment of the Ti surfaces has also been observed to promote HA nucleation and growth in SBF [Pham et al. 2000a].

Hanawa et al implanted Ca ions on the surface of cpTi and found that this modification of surface chemistry resulted in an accelerated precipitation of calcium phosphate [Hanawa et al. 1998]. Krupa et al and Pham et al also reported similar effects for Ca-implanted Ti surfaces [Pham et al. 2000b; Krupa et al. 2001a]. Pham et al demonstrated that upon exposure of cpTi discs to SBF the precipitation of HA was enhanced with increasing concentration of Ca ions implanted on the surface [Pham et al. 2000b]. Other

studies carried out double implantation of Ca and P ions into Ti and found enhanced nucleation and growth of HA in SBF on ion-implanted surfaces relative to that on the control cpTi [Wieser et al. 1999; Krupa et al. 2005] (Chapter 1).

A previous *in vitro* study demonstrated that the pre-immersion of biomaterials in the tissue culture medium apparently improved the response of human osteosarcoma cells [Ferraz et al. 2000]. These authors examined the influence of pre-immersed HA and P2O5-based bioactive glasses on the growth and function of MG-63 cells using the MTT assay and FCM analysis, respectively. Their results showed that the increase in numbers of viable cells was the same or elevated following incubation on the pre-immersed HA and glass-reinforced HA coatings compared with the non-immersed materials. In addition, the expression of bone sialoprotein (BSP) and FN, two key connective tissue antigens, was up-regulated in cultures grown on the pre-immersed surfaces compared with the non-treated materials [Ferraz et al. 2000]. For these reasons, the current study measured the effects of pre-immersion of the Ca-implanted Ti discs in tissue culture medium on MG-63 cell attachment and correlated them with the specific chemical changes occurring at the Ti surfaces.

4.2 Materials and methods

4.2.1. Preparation of titanium discs

CpTi discs (grade 1, 8 x 1 mm) (Goodfellow Cambridge, UK) were polished, as described in Chapter 2. Ion-implantation was carried out using high, medium and low doses of $^{40}Ca^{+}$ ions i.e. 1×10^{17}, 1×10^{16} and 1×10^{15}

ions cm^{-2}, respectively. Following implantation, the samples were removed from the mounting plates using acetone and washed in deionised water. Both the Ti (control) and Ca-implanted Ti discs were sterilized by UV light prior to cell culture and stored at RT in a desiccator.

4.2.2 Cell culture

MG-63 cells were cultured in DMEM supplemented with 10% FCS, 100 IU ml^{-1} penicillin, 100 μg ml^{-1} streptomycin and 2 mM L-glutamine (GIBCO Invitrogen). In order to measure bone cell responses, a suspension of the cells was seeded onto the surfaces of the Ca-implanted and non-implanted Ti (control) discs which had previously been placed in 24 well tissue culture plates (Becton-Dickinson). Three replicate discs per sample were used and each experiment was repeated 3 times.

4.2.3 Adhesion of radioactively-labelled cells

In order to quantitatively measure cell adhesion, actively dividing MG-63 cells were first tagged by radiolabeling for 18 h with 1 μCi ml^{-1} of [^{3}H] thymidine (44 Ci $mmol^{-1}$) (Amersham Biosciences). One sample was used to count the number of cells and a replicate sample was used to measure the amount of isotope incorporated into the DNA. The radiolabeled cells were harvested, washed and seeded in triplicate onto the discs at a density of 1x 10^3 cells in 0.05 ml of DMEM. These were incubated for 4 and 24 h at 37°C, the later time point selected to examine whether Ca levels also affected cell attachment following prolonged incubation. The discs were then processed, as described in detail in Chapter 3 (section 3.2.4), and the radioactivity which

had remained associated with them was measured by using WALLAC 1409 Liquid Scintillation Counter (Perkin Elmer).

To determine the effect of pre-immersion on cell adhesion, the control and Ca-Ti discs were first incubated without cells in DMEM at 37°C for 4 and 24 h prior to cell culture. The cell binding assay was then carried out for 4 h, as described above.

4.2.4 Scanning electron microscopy

SEM was carried out in order to determine whether differences in the concentration of Ca ions implanted on the surface of Ti would affect the morphology and spreading of MG-63 cells. Cells were seeded (1×10^3 cells/disc) on the Ti (control), Ca (med)-Ti and Ca (high)-Ti surfaces and incubated at 37°C in a humidified atmosphere of 5% CO_2 in air for 4 h. The discs were then removed, transferred to fresh dishes, washed and then processed for SEM visualisation, as described in detail in Chapter 3. SEM micrographs were captured digitally for the detailed morphological analysis of the adhered bone cells.

4.2.5 **Digital image analysis**

For semi-quantitative analysis of cell binding and cell spreading on the different Ti surfaces digital image analysis was carried out as described previously (Chapter 3). Briefly, the number of attached cells, average cell area, and cell perimeter were measured on five representative fields of the SEM micrographs of the cells incubated for 4 h on Ti (control), Ca (high)-Ti, Ca (med)-Ti and Ca (low)-Ti discs, using Image-Pro Plus 4.01 analysis software (Media Cybernetics).

4.2.6 Flow cytometry

In the present experiments, FCM was used to determine whether the presence of different levels of Ca ions at the surface of Ti discs influences the light scattering properties of the cells and the expression of integrins (Chapter 2). In each experiment, FSC and SSC data dot plots were obtained using a FACScan Flow Cytometer (Becton-Dickinson) equipped with an argon ion laser (488 nm). The threshold was set on FSC parameter during data acquisition. Cell aggregates and doublets were excluded during data analysis. The green fluorescence signals generated by each cell, as a result of positive immunostaining, were also collected and analyzed, as described below.

4.2.7 Analysis of integrin expression

To determine whether the modification of Ti discs by implanting different doses of Ca ions affected the expression of integrins, the cells were cultured on the control and Ca-implanted discs (high and low) for 4 and 24 h and immunostained for the integrins β1 sub-unit, which identifies all β1-containing integrins, and for the specific α5β1 integrin, a high affinity fibronectin receptor involved in initiating bone cell attachment to the substrate [Hynes1987].

The MG-63 cells were cultured at a uniform density (1 x 10^4 cells / disc) for 4 and 24 h, after which the discs were washed with PBS and the cells detached using 20 mM EDTA (GIBCO Invitrogen) instead of trypsin to avoid proteolytic destruction of the cell surface integrins. After washing with PBS, the cells were fixed with 1% paraformaldehyde (PFA) in PBS for 30 min

at RT. They were then washed, centrifuged and resuspended in wash buffer (PBS supplemented with 2% FCS and 0.05% sodium azide) and incubated for 60 min at RT with fluorescein isothiocyanate (FITC)-conjugated mouse anti-human integrin β1 monoclonal antibody (mAb) (1:200 dilution) (Caltag Laboratories, Burlingame, CA, USA). A replicate aliquot of cells was reacted with anti-human α5β1 mAb (1:100 dilution) (Dako, High Wycombe, UK) and then, after washing, with FITC-labeled rabbit anti-mouse IgG (Dako) diluted 1:50 in wash buffer for 30 min at RT. Non-specific mouse serum (5% in wash buffer) (Dako) was used as a negative control for α5β1.

After immunostaining, the cells were centrifuged, washed and suspended in 500 µl of wash buffer and the fluorescence intensities of 5,000 individual cells were measured by FCM using the FACScan, as described above. Net expression levels were adjusted for each antigen by subtracting data from the negative control (i.e., cells treated with non specific immunoglobulin (Ig) instead of the primary antibody). The data were analyzed using WinMDI software (version 2.8) (http://facs.scripps.edu/software.html) and the level of antigen expression is shown as the average fluorescence intensity (AFI) of 5000 individual cells.

4.2.8 Confocal laser scanning microscopy of vinculin adhesion plaques

Immunofluorescence microscopy of the cell adhesion protein vinculin was carried out to determine the influence of Ca (high)-Ti on the formation of focal adhesion plaques. MG-63 cells (1 x 10^3 cells/disc) were incubated on the discs for 4 and 24 h. The cells which had remained attached to the discs were fixed with absolute methanol for 10 min at 4°C and the non-adherent

cells were removed by washing twice with PBS. Non-specific Ig binding sites were blocked with 5% normal mouse serum in PBS for 1 h at RT and the cells then incubated with a 1:40 dilution of mouse anti-human vinculin mAb (Sigma-Aldrich) for 1 h at RT. After washing with PBS the cells were incubated for 1 h at RT with goat anti-mouse IgG conjugated to the fluorochrome Cy3 (Serotec Ltd., Kidlington, Oxford, UK), which emits a red fluorescent signal. Control cultures were treated with normal mouse serum instead of the primary mAb. The Ti discs were mounted on glass slides using clear nail varnish as an adhesive and covered with coverslips using Citifluor medium (Agar Scientific, Stansted, UK).

The samples were examined with a BioRad MRC-600 CLSM (BioRad Microscience), equipped with an argon ion laser source. Depth projection micrographs were obtained from 15-30 serial horizontal image sections using a z-step of 0.01 μm and a x 60 oil objective. Image analysis was carried out using Image-Pro Plus 4.01 analysis software (Media Cybernetics) to measure the number of triangle-shaped vinculin-positive focal adhesion plaques on 30 randomly selected cells per sample.

4.2.9 Effects of pre-immersion on the titanium/cell interface

EDS was carried out to examine whether Ca implantation affects the surface chemical composition of Ti surfaces under tissue culture conditions. The Ti (control) and Ca (high)-Ti discs were first pre-immersed in DMEM at 37°C for 4 and 24 h, then washed with PBS and the MG-63 cells (1 x 10^3 cells/disc) seeded for 4 h, as described above (one set of both types of pre-immersed Ti discs was prepared without the cells as a control). After washing with PBS, the cells were fixed with 3% glutaraldehyde in 0.1 M cacodylic acid

buffer, as described above. They were then mounted on metal stubs, air-dried for 1 h at RT and stored in a desiccator prior to analysis. EDS microanalysis was carried out using the INCA system (Oxford Instruments, High Wycombe, UK) attached to a SEM (1450 VP) (Leo) set at a beam current of 500 pA and an acceleration voltage of 10 kV. Spectra were recorded from specific points on the SEM images of Ti surfaces. EDS spectral intensities were normalised to the Ti peak maximum.

4.2.10 Statistical Analysis

Experiments were conducted three times using three replicate samples each and SEM was calculated for each set of experiments. Significant differences in MG-63 bone cell responses were established using the Student's *t* test for paired samples, with significance levels of $p \leq 0.05$.

4.3 Results

4.3.1 Effects of different levels of calcium on bone cell adhesion

Figure 4.1 shows quantitative measurement of the adhesion of pre-labelled MG-63 cells to the Ti surfaces implanted with different doses of Ca ions. The results of 3 replicate experiments indicate that cell adhesion to the Ca (high)-Ti discs was significantly reduced (by 43%; $p = 0.02$) at 4 h compared with the control Ti (Figure 4.1). While no significant differences were found for MG-63 cell attachment to the Ca (med)-Ti and Ca (low)-Ti discs, which were 85 and 105% of the control levels, respectively.

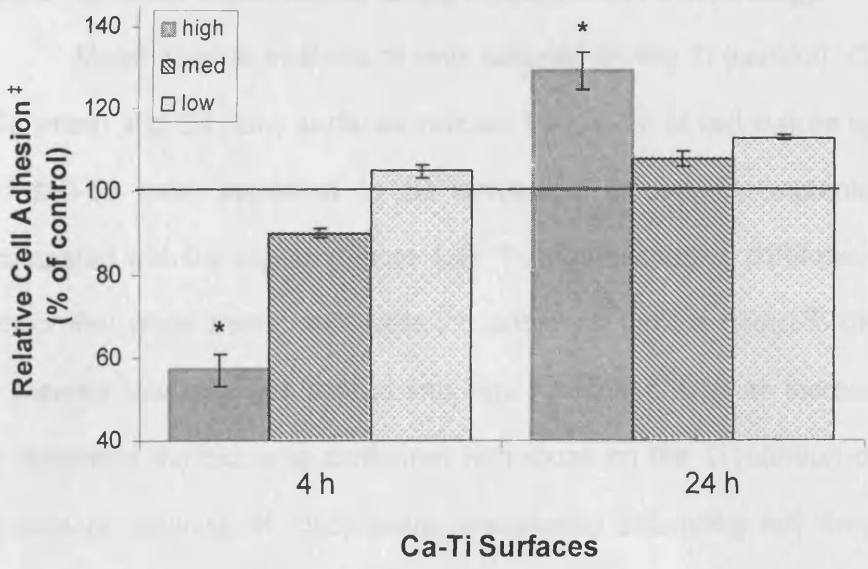

Figure 4.1: MG-63 cell adhesion to Ti discs implanted with high, medium and low levels of Ca. The bars show the average adhesion of the cells on the Ca-implanted surface ‡ relative to the numbers on the Ti (control) surface after 4 and 24 h of cell culture, which is defined as 100%. The error bars show the ± SEM of 3 replicate experiments. The average cell adhesion to the control (non-implanted) Ti surfaces was 571 cells at 4 h and 668 cells at 24 h (approximately 58 and 69% of the cells added initially, respectively). * Denotes statistically significant differences in cell adhesion between the Ca (high)-Ti and Ti (control) surfaces at 4 and 24 h ($p = 0.02$ and 0.01, respectively).

However, when the incubation time was extended to 24 h, the number of cells which had adhered to the Ca (high)-Ti discs increased to a level which was significantly higher than on the non-implanted Ti (129%; $p = 0.01$), whereas cell attachment to the Ca (low)-Ti and Ca (med)-Ti surfaces were similar to the control Ti discs. Thus, despite a relatively low level of cell adhesion at 4 h of cell culture, prolonged incubation (for 24 h) markedly enhanced the binding of the MG-63 cells to the Ca (high)-Ti discs (Figure 4.1).

4.3.2 Calcium-implantation levels and bone cell morphology

Morphological analysis of cells adhered on the Ti (control), Ca (high), Ca (med) and Ca (low) surfaces indicate that at 4 h of cell culture spreading of MG-63 cells appeared to be enhanced on the Ca-implanted discs compared with the control (Figure 4.2). The representative SEM micrographs show that when these cells were incubated on the Ca (high)-Ti discs they appeared relatively well spread and highly flattened, with an increased cell-to-substrate contact ratio compared with those on the Ti (control) discs. An extensive network of cytoplasmic processes, extending not only to the underlying substrate but also established between neighbouring cells, was observed on Ca (high)-Ti discs. In contrast, cells on the Ti (control) discs, which remained mainly rounded at 4 h of cell culture, had far fewer and much shorter fibrillar extensions (Figure 4.2).

The difference could be explained by the fact that MG-63 cells were more spread out and covered the totality of the Ca (high)-Ti surface in contrast with Ti (control) where the area occupied by cells appeared to be smaller, leaving the Ti disc exposed. It must be noted that like Ca (high)-Ti, MG-63 cells incubated on Ca (med)-Ti and Ca (low)-Ti discs also exhibited a flattened morphology, with prominent dorsal ruffles and numerous cytoplasmic processes which were clearly associated with the cell body, compared with the control discs. Figure 4.2 also reveals that despite seemingly enhanced spreading, increasing concentrations of implanted Ca ions caused an apparent reduction in the numbers of attached MG-63 cells after 4 h of incubation.

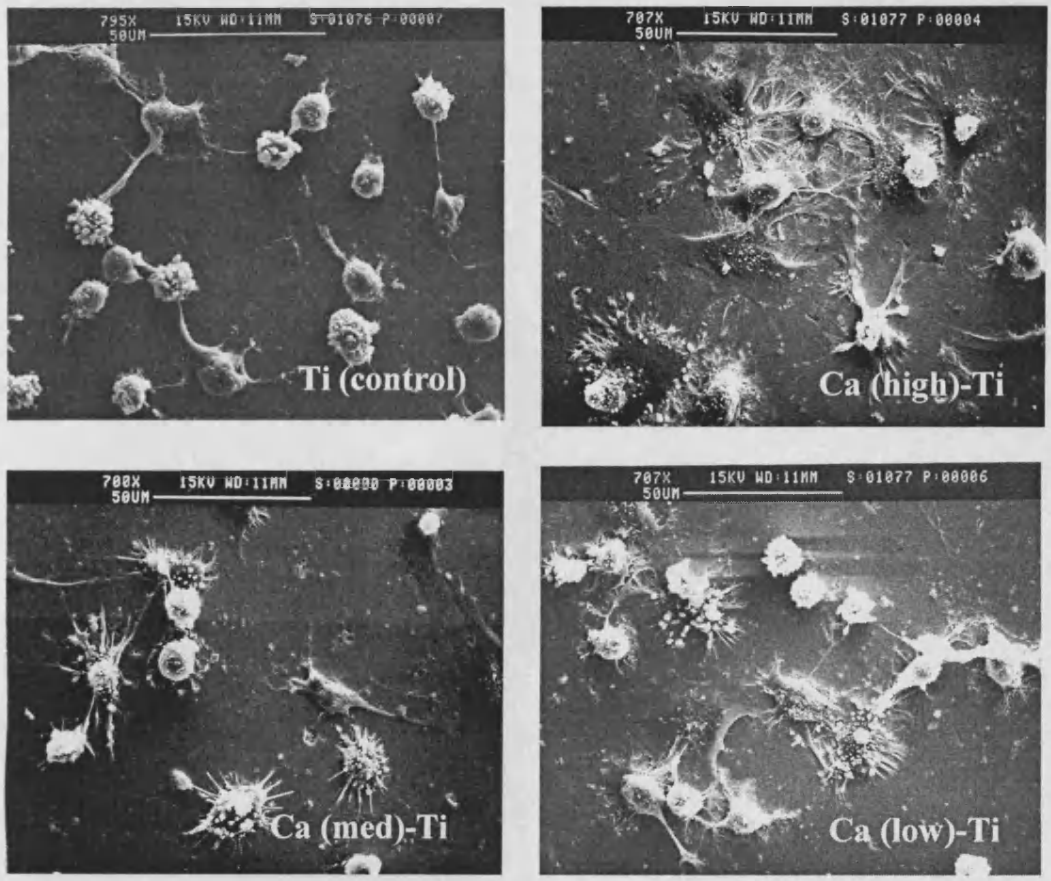

Figure 4.2: SEM micrographs of adherent MG-63 cells following 4 h of incubation on Ti (control), Ca (high)-Ti, Ca (med)-Ti and Ca (low)-Ti discs. Note the presence of fewer but much more highly spread cells particularly on the Ca (high)-Ti compared with the Ti (control) discs. Magnification x 700-795, as indicated.

4.3.3 Calcium-implantation levels and bone cell spreading

Digital image analysis of the SEM micrographs showed that the number of MG-63 cells which attached to the Ca (high)-Ti discs was only 61% of the control (non-implanted Ti disc) level (401 compared with 653 cells, respectively; *p=0.02*) (Table 4.1). In contrast, no significant differences were measured in the binding of cells to either Ca (med)-Ti or Ca (low)-Ti discs compared with that on the Ti (control) surfaces.

Table 4.1: Effects of Ca levels on binding and spreading of MG-63 cells

Surfaces	Number of attached cells	% of control	Average cell area (μm^2)	% of control
Ti (control)	653 ± 22	100	682 ± 15	100
Ca (high)-Ti	401 ± 24	**61***	1405 ± 10	**206***
Ca (med)-Ti	559 ± 19	86	1013 ± 30	148
Ca (low)-Ti	672 ± 15	103	1106 ± 20	162

Values shown are the average (± SEM) of 3 replicate samples repeated 3 times. The numbers and spreading of attached cells, after 4 h of incubation, were measured on 5 random fields of the SEM micrographs. The values relative to control Ti discs, defined as 100% are also shown. * Indicates statistically significant differences, shown in bold, compared with control; $p \leq 0.05$.

This finding is in agreement with the above-mentioned results which described the adhesion of radioactively-labeled MG-63 cells to the Ti (control) and Ca-Ti surfaces (Figure 4.1). Values presented in Table 4.2 also show that despite reduced cell binding to the Ca (high)-Ti, the spreading (i.e., average cell area) of the cells which had attached to this particular surface was significantly greater than that on the Ti (control) (206%; *p=0.01*) (Table

4.1). Although average cell area of MG-63 cells was also enhanced on Ca (med)-Ti and Ca (low)-Ti discs compared with the control, it was nevertheless not as markedly increased as on Ca (high)-Ti surfaces (Table 4.2).

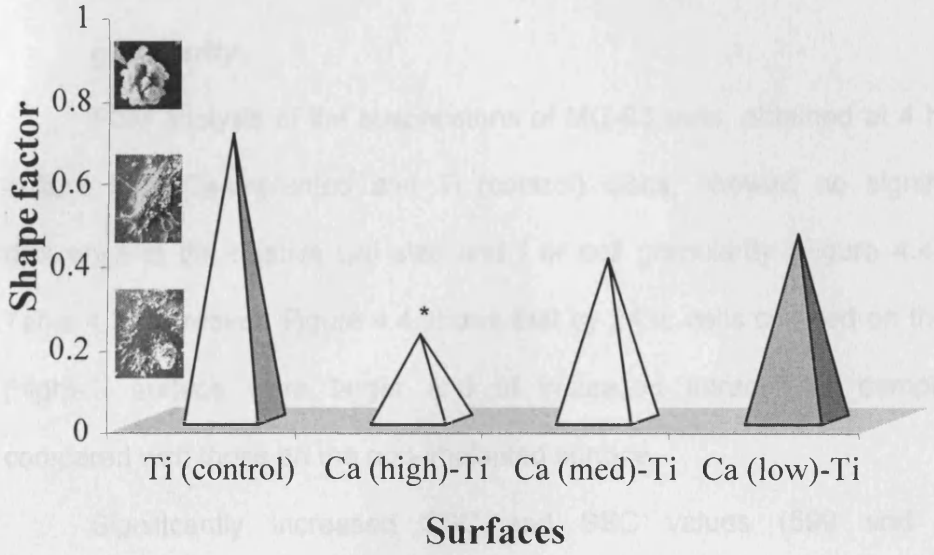

Figure 4.3: The effect of Ca implantation levels on the shape factor of MG-63 cells following 4 h of cell culture. The shape factor of a perfect circle is defined as 1 and that of a straight line as 0.00. The SEM micrographs on the left show a representative cell which is highly circular (top) to one which is highly flattened and spread, with many cytoplasmic processes (bottom). * Denotes significant differences between the Ca (high)-Ti and control Ti discs; $p = 0.01$.

In addition, the results in Figure 4.3 show that the shape factor [(area x perimeter^2) 4π] value of these cells, which is inversely related to the roundness of the cell, was also significantly lower than on the control Ti discs (0.21 compared with 0.69; $p=0.01$). As with cell attachment and cell spreading, the shape factors of cells on the Ca (med)-Ti and particularly on the Ca (low)-Ti discs were not significantly different from the control values

after 4 h of incubation. Due to cell-cell interactions at 24 h, which affect cell shape and spreading, measurements were not performed at this later time point.

4.3.4 Influence of different levels of calcium on cell size and cell granularity

FCM analysis of the suspensions of MG-63 cells, obtained at 4 h cell culture from Ca-implanted and Ti (control) discs, showed no significant difference in the relative cell size and / or cell granularity (Figure 4.4 and Table 4.2). However, Figure 4.4 shows that by 24 h, cells cultured on the Ca (high)-Ti surface were larger and of increased intracellular complexity compared with those on the non-implanted surface.

Significantly increased FSC and SSC values (599 and 553, respectively) were found on this particular surfaces compared with the non-implanted discs (520 and 472, respectively) ($p=0.02$ and $p= 0.01$) (Figure 4.4 and Table 4.2). On the contrary, implantation of Ti discs with low concentrations of Ca ions seemed to have no significant effect on the size and/or granularity of MG-63 cells after 4 and 24 h of cell culture (Figure 4.4 and Table 4.2). Table 4.2 shows that both FSC and SSC values of MG-63 cells cultured on Ca (low)-Ti discs were very similar to those on the Ti (control) surfaces at both periods of incubation.

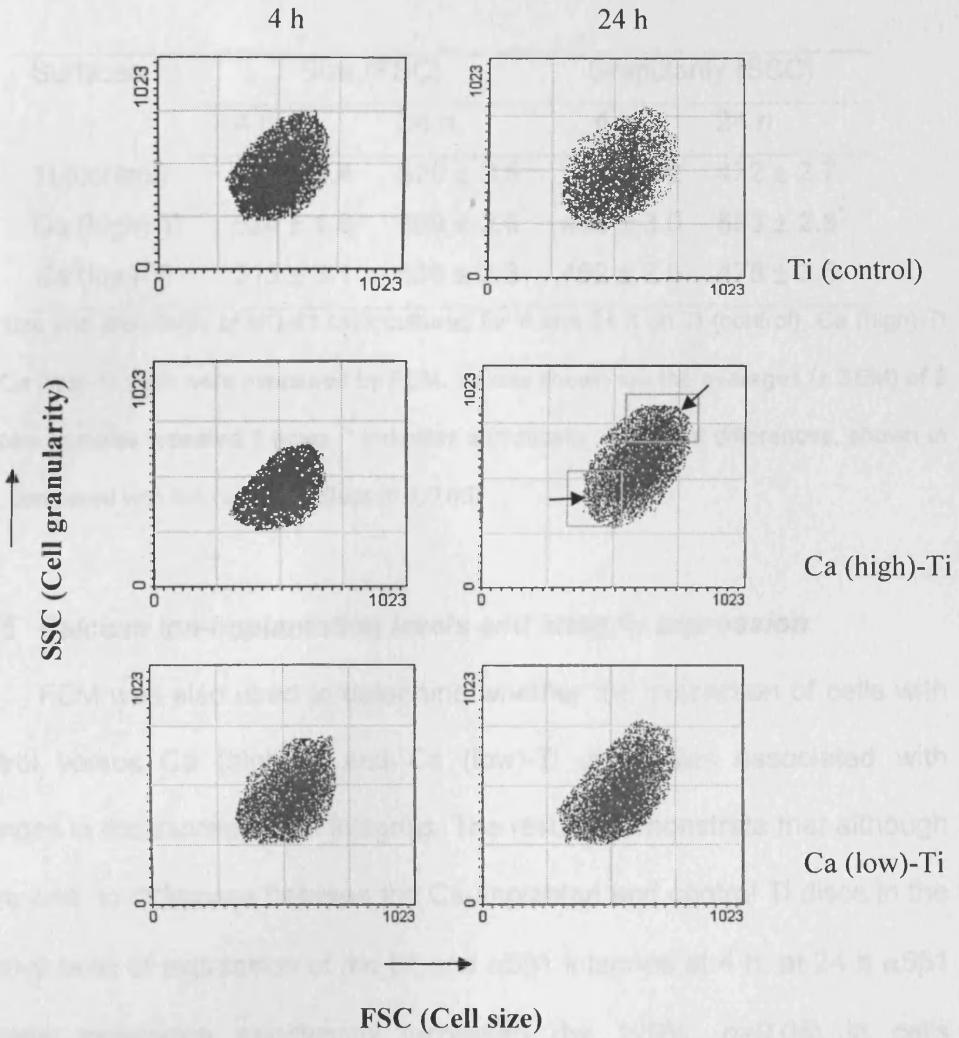

Figure 4.4: FCM profiles showing light scatting characteristics, indicative of relative size and granularity, of the MG-63 cells which were incubated on the surface of the Ti (control), Ca (high)-Ti and Ca (low)-Ti discs for 4 and 24 h under standard tissue culture conditions. Note significantly increased FSC and SSC values (marked by boxes and arrows) of cells collected from Ca (high)-Ti discs following 24 h of cell culture.

Table 4.2: Effects of Ca ion-implantation levels on size and granularity of MG-63 cells

Surfaces	Size (FSC)		Granularity (SSC)	
	4 h	24 h	4 h	24 h
Ti (control)	512 ± 2.4	520 ± 3.5	469 ± 3.2	472 ± 2.7
Ca (high)-Ti	524 ± 1.9	**599 ± 2.6***	455 ± 3.0	**553 ± 2.8***
Ca (low)-Ti	515 ± 3.1	539 ± 2.3	462 ± 2.6	478 ± 3.5

The size and granularity of MG-63 cells cultured for 4 and 24 h on Ti (control), Ca (high)-Ti and Ca (low)-Ti discs were measured by FCM. Values shown are the averages (± SEM) of 3 replicate samples repeated 3 times. * Indicates statistically significant differences, shown in bold, compared with the control Ti discs ($p \leq 0.05$).

4.3.5 Calcium ion-implantation levels and integrin expression

FCM was also used to determine whether the interaction of cells with control versus Ca (high)-Ti and Ca (low)-Ti discs was associated with changes in the expression of integrins. The results demonstrate that although there was no difference between the Ca-implanted and control Ti discs in the relative level of expression of the β1 and α5β1 integrins at 4 h, at 24 h α5β1 integrin expression significantly increased (by 120%; $p=0.05$) in cells incubated on the Ca (high)-Ti surface (Table 4.3 and Figure 4.6).

Figure 4.5 shows that the levels of the β1 antigen, common to all integrins of the 'β1 family', were not affected by the modification of Ti surface chemistry by Ca ion-implantation (Figure 4.5 and Table 4.3). However, compared with the control, the expression of α5β1 by MG-63 cells was significantly up-regulated on Ca (high)-Ti surfaces following 24 h of incubation ($p = 0.05$) (Figure 4.6 and Table 4.3).

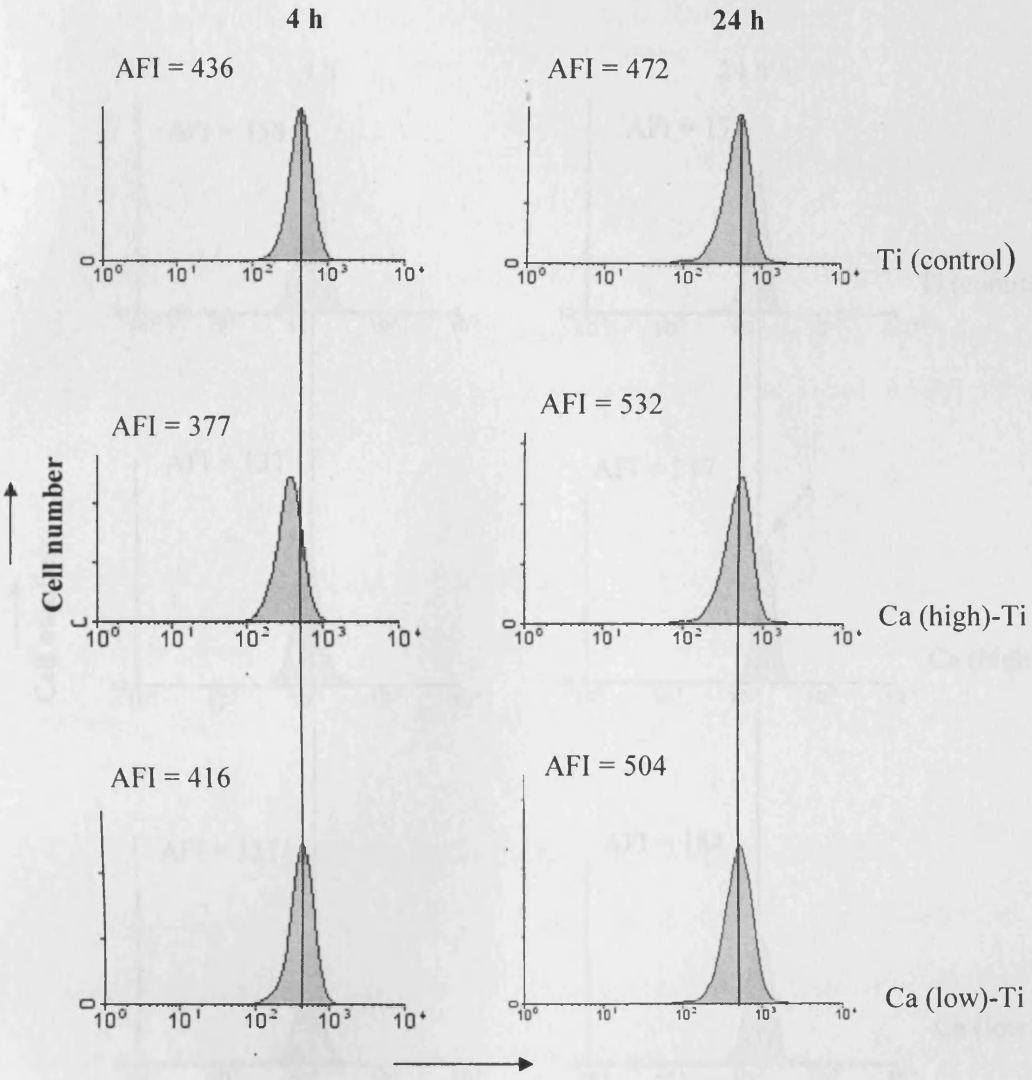

Figure 4.5: The representative data of β1 integrin expression by flow cytometric analyses. The effects of Ca-implantation on the expression of β1 integrin by MG-63 cells were measured after 4 and 24 h of incubation on Ti discs. For background staining, the primary antibody β1-FITC was appropriately replaced with mouse IgG1-FITC. The net AFI is shown for each histogram.

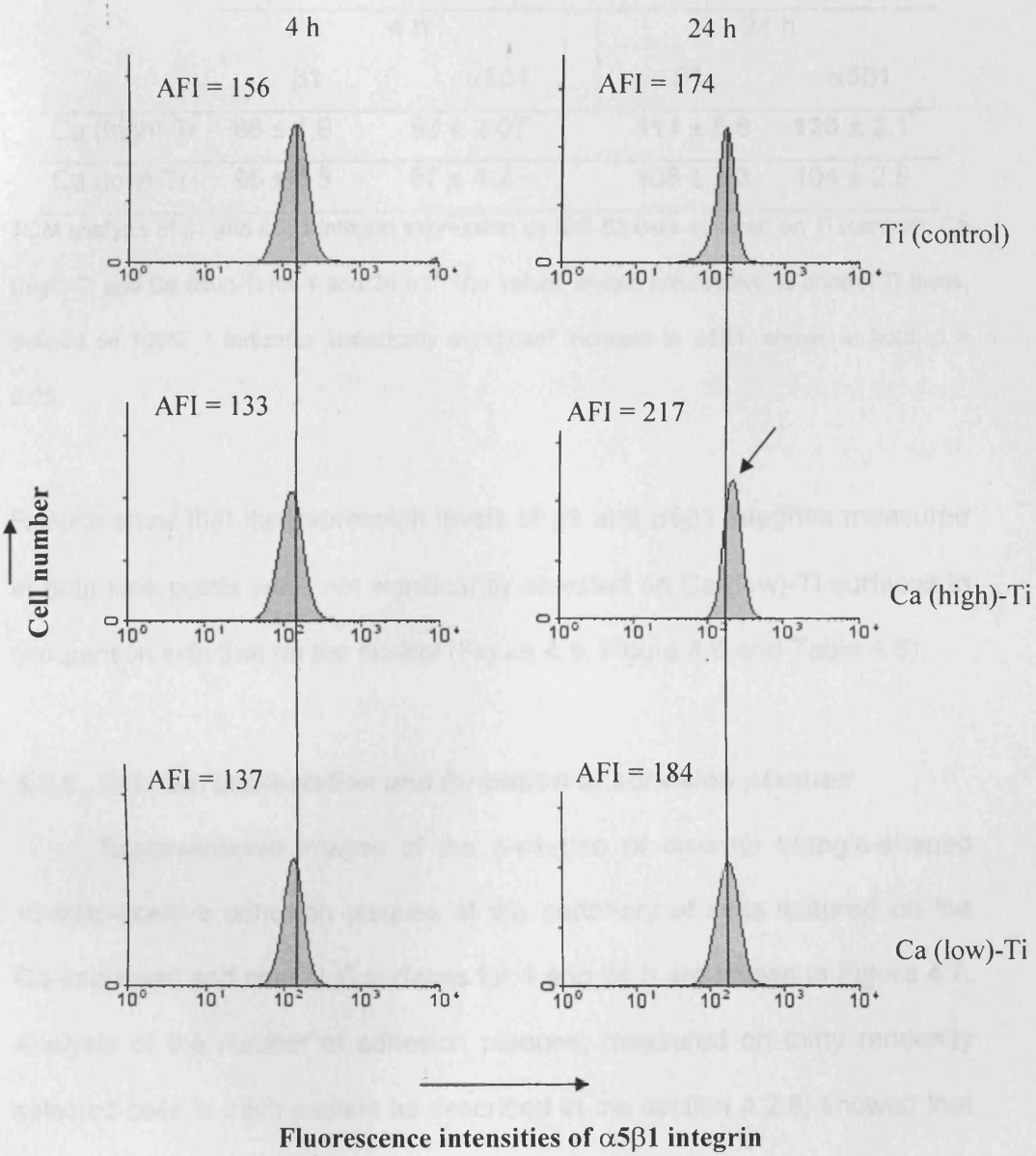

Figure 4.6: Representative FCM histograms showing cell surface expression of α5β1 integrins by MG-63 cells following 4 and 24 h of incubation on control and Ca-implanted Ti discs. Compared with control, cells cultured on Ca (high)-Ti for 24 h significantly enhanced the fluorescence intensity of α5β1 integrins, as indicated by the arrow ($p = 0.05$).

Table 4.3: Effect of Ca-implanted Ti on integrin expression by MG-63 cells

Ti surfaces	Relative antigen levels (% of control) [a]			
	4 h		24 h	
	β1	α5β1	β1	α5β1
Ca (high)-Ti	86 ± 1.9	83 ± 2.07	114 ± 5.8	**120 ± 2.1***
Ca (low)-Ti	95 ± 5.3	87 ± 4.2	108 ± 3.3	104 ± 2.5

FCM analysis of β1 and α5β1 integrin expression by MG-63 cells cultured on Ti (control), Ca (high)-Ti and Ca (low)-Ti for 4 and 24 h. [a] The values shown are relative to control Ti discs, defined as 100%. * Indicates statistically significant increase in α5β1, shown in bold, $p = 0.05$.

Results show that the expression levels of β1 and α5β1 integrins measured at both time points were not significantly elevated on Ca (low)-Ti surfaces in comparison with that on the control (Figure 4.5, Figure 4.6 and Table 4.3).

4.3.6 Calcium implantation and formation of adhesion plaques

Representative images of the presence of discrete triangle-shaped vinculin-positive adhesion plaques at the periphery of cells cultured on the Ca-implanted and control Ti surfaces for 4 and 24 h are shown in Figure 4.7. Analysis of the number of adhesion plaques, measured on thirty randomly selected cells in each sample as described in the section 4.2.8, showed that there was a significantly greater number on the Ca (high)-Ti surface compared with the Ti (control) (Table 4.4).

Table 4.4: Effects of different Ca levels on the formation of adhesion plaques by MG-63 cells

Ti surfaces	Number of adhesion plaques / cell	
	4 h	24 h
Ti (control)	12 ± 2.5	19 ± 1.86
Ca (high)-Ti	**34 ± 1.3***	**48 ± 1.9***

The numbers of adhesion plaques/cell were measured following 4 and 24 h of culture on the Ti (control) and Ca-Ti (high) discs. * Significant differences compared with Ti (control), shown in bold, were observed in the number of vinculin-positive adhesion plaques on Ca (high)-Ti at 4 and 24 h ($p = 0.01$ and 0.03 respectively).

Results show that the number of adhesion plaques increased in cells on both surfaces during the experimental culture period, with the greatest number in cells on Ca (high)-Ti at both time points (34; $p=0.01$ and 48; $p = 0.03$ sites per cell at 4 and 24 h, respectively) (Figure 4.7 and Table 4.4). Figure 4.7 demonstrates that after 24 h in culture, there were still significantly more immuno-reactive (vinculin-positive) sites on the cells incubated on the Ca-implanted surface compared with those on the Ti (control) discs (Figure 4.7).

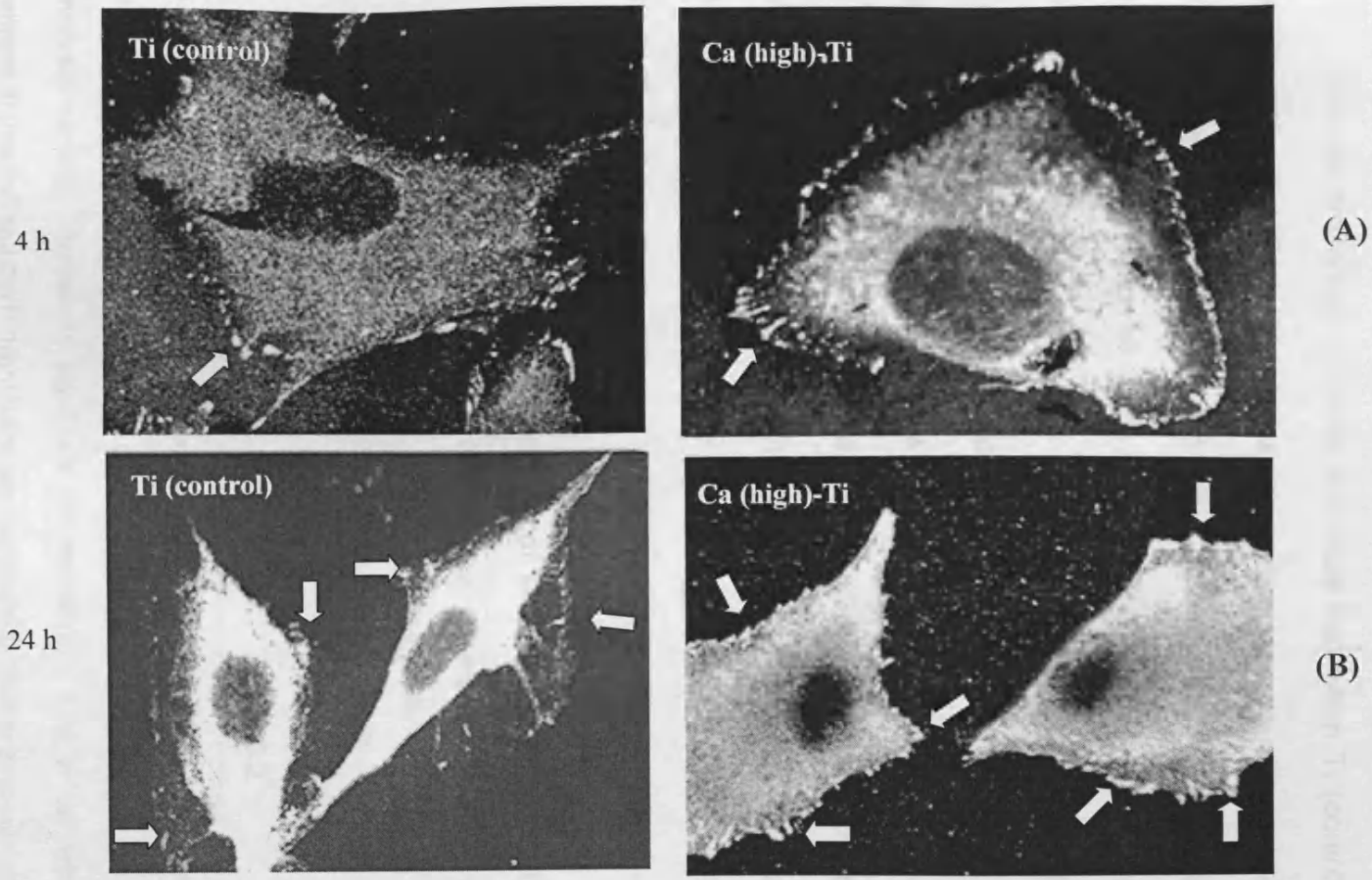

Figure 4.7: Immunostaining of vinculin in MG-63 bone cells cultured for 4 h (A) and 24 h (B) on the Ti and Ca (high)-Ti discs. The arrows indicate the triangle-shaped vinculin–positive adhesion plaques on the cell periphery. Note that the cells on the Ca (high)-Ti discs formed more adhesion plaques than those on the control Ti at both time points, magnification x 800-1200.

4.3.7 *Influence of pre-immersion of titanium discs on cell adhesion and surface elemental composition*

Results presented in Table 4.5 show that when Ti (control) discs were pre-immersed for 4 h in tissue culture medium and then incubated with MG-63 cells for a further 4 h, the number of radioactively-labelled attached cells increased by an average of 150% compared with the level on non-immersed Ti discs (Table 4.5). In contrast, 4 h pre-immersion of the Ca (high)-Ti discs substantially reduced cell adhesion to 68% compared with that on the non-immersed Ca (high)-Ti discs. Likewise, when the Ti discs were pre-immersed for 24 h in DMEM, the level of cell attachment to Ti (control) surfaces remained at a similarly elevated level (162% of the non-immersed Ti), however, cell binding to the Ca (high)-Ti discs significantly increased to 247% of the non-immersed Ca (high)-Ti ($p=0.01$) (Table 4.5).

Table 4.5: Effects of pre-immersion of Ti discs on MG63 cell adhesion

Ti surfaces	Relative cell adhesion [a] / %	
	Pre-immersion period	
	4 h	24 h
Ti (control)	150 ± 1.5	162 ± 0.72
Ca-Ti (high)	68 ± 2.5	**247 ± 5.2***

Values (± SEM of 3 replicate experiments) presented are [a] relative to cell adhesion on both non-immersed Ti (control) and Ca-Ti (high) discs, each defined as 100% for the respective pre-immersed surface. * Statistically significant differences ($p = 0.01$) in cell adhesion is shown between Ti (control) and Ca-Ti (high) discs pre-immersed for 24 h prior to cell culture.

Thus, while the duration of pre-immersion did not affect the elevated level of cell attachment to the control Ti surface, prolonged pre-immersion of the Ca (high)-Ti discs markedly reversed the initial reduction of MG-63 cell binding to this surface. These findings suggest that the chemical changes occurring at the Ti surfaces had an effect on cell adhesion, and may partly elucidate the underlying mechanisms responsible for the differences in the attachment of MG-63 cells on Ca (high)-Ti observed at 4 and 24 h of cell culture (Figure 4.1). To further investigate whether Ca implantation affects the chemical composition of Ti surfaces under tissue culture conditions, X-ray microanalysis was carried out, as described in section 4.2.9.

The EDS spectra recorded from the SEM images are shown in Figure 4.8 (pre-immersed Ti discs with cells) and Figure 4.9 (pre-immersed Ti discs without cells). A representative SEM image of the control Ti surface after 4 h of pre-immersion and 4 h of cell culture (Figure 4.8A) showed large flat areas of surface between the cells. In addition to the two peaks corresponding to Ti, spectra recorded from these flat surface regions also showed presence of O and C on the surface, which was expected following immersion of Ti discs in an organic medium like DMEM (Figure 4.8 A and Figure 4.9 A). Figure 4.8 B shows that a large number of small precipitates appeared both underneath as well as between the cells adhered on the Ca (high)-Ti surfaces. Although Ti (control) discs were incubated under the same conditions as Ca (high)-Ti, no such deposits were detected in the SEM images of cells attached on these surfaces (Figure 4.8 B). It must be noted that these precipitates were also observed on

Figure 4.8: Changes in the surface chemistry after pre-immersion of the Ti (control) and Ca (high)-Ti discs in DMEM at 37°C for 4 and 24 h prior to cell culture for 4 h. The arrows on the SEM micrographs of Ti surfaces indicate representative areas from which spectra were recorded. The black regions in each image correspond to the nucleus of the adherent cell and the grey region to the cytoplasm of the cell body. The pale areas correspond to the Ti surface between the cells. All spectra were recorded from the following areas away from the cells: (A), a flat surface region of the Ti (control) discs after 4 h of pre-immersion; (B), a flat surface region between the precipitated material found to be deposited on the Ca (high)-Ti discs after 4 h of pre-immersion; (C), the precipitated material deposited directly on the Ca (high)-Ti discs after 4 h of pre-immersion; (D), a flat surface region of the Ti (control) discs after 24 h of pre-immersion; and (E), a flat surface region of the Ca (high)-Ti discs after 24 h of pre-immersion. Note the absence of the P peak at 24 h in (E) compared with 4 h in spectrum (C), as above.

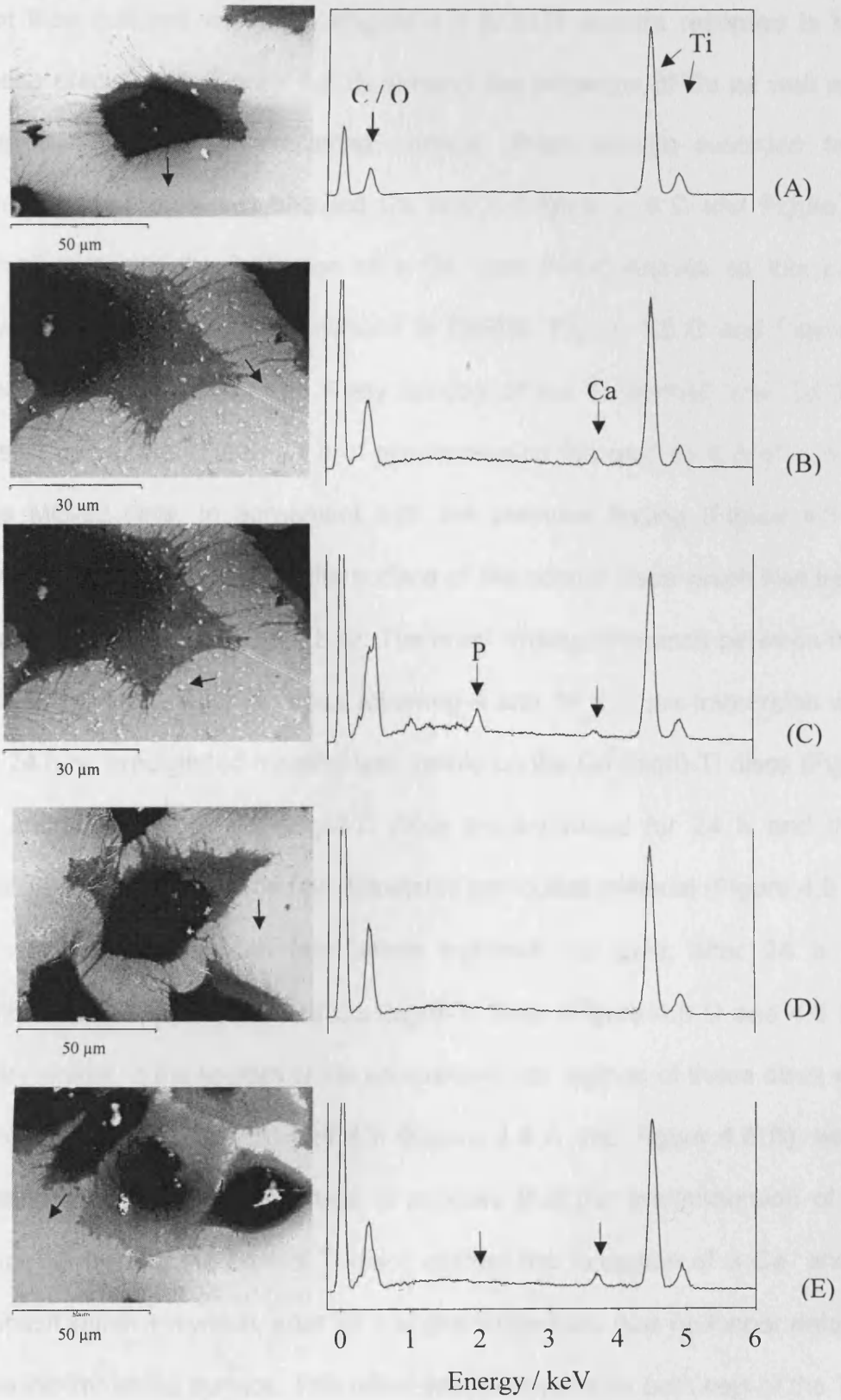
C / O
Ti
(A)
50 µm
Ca
(B)
30 µm
P
(C)
30 µm
(D)
50 µm
(E)
50 µm
0 1 2 3 4 5 6
Energy / keV

the Ca (high)-Ti surfaces which were pre-immersed for 4 h in DMEM but were not then cultured with cells (Figure 4.9 B).EDS spectra recorded in between these precipitates (Figure 4.8 B) showed the presence of Ca as well as Ti, as expected for the ion-implanted surface. X-ray spectra recorded from the precipitates themselves showed Ca and P (Figure 4. 8 C and Figure 4.8 C), which suggests the formation of a Ca- and P-rich deposit on this particular surface after 4 h of pre-immersion in DMEM. Figure 4.8 D and Figure 4.8 E show the SEM images and X-ray spectra of the Ti (control) and Ca (high)-Ti discs, respectively, after 24 h of pre-immersion followed by 4 h of culture with the MG-63 cells. In agreement with the previous finding (Figure 4.8 A), no deposits were observed on the surface of the control discs which had been pre-immersed for 24 h (Figure 4.8 D). The most striking difference between the SEM image of the Ca (high)-Ti discs following 4 and 24 h of pre-immersion was that at 24 h no precipitated material was visible on the Ca (high)-Ti discs (Figure 4.8 B and 4.8 E). The Ca (high)-Ti discs pre-immersed for 24 h and then not cultured with cells also had no detectable particulate material (Figure 4.9 E).

Spectra recorded from areas between the cells after 24 h of pre-immersion of the control and Ca (high)-Ti discs (Figure 4.8 D and 4.8 E) were very similar to the spectra of the comparable flat regions of these discs after the shorter pre-immersion time of 4 h (Figure 4.8 A and Figure 4.8 B), with no P detected in any of these areas. It appears that the pre-immersion of the Ca (high)-Ti but not the control Ti discs elicited the formation of a Ca- and P-rich deposit within 4 h which, after 24 h of pre-immersion, was no longer detected on this ion-implanted surface. This effect was persistent for both sets of the Ti discs

Figure 4.9: EDS spectra showing changes in the surface chemistry after pre-immersion of the Ti (control) and Ca (high)-Ti discs in DMEM at 37°C for 4 and 24 h in the absence of MG-63 cells. The boxes and arrow on the SEM micrographs of Ti surfaces indicate representative areas from which spectra were recorded. All spectra were recorded from the following areas: (A), a representative region of the Ti (control) discs after 4 h of pre-immersion; (B), a representative flat surface region between the precipitated material found to be deposited on the Ca (high)-Ti discs after 4 h of pre-immersion; (C), the precipitated material deposited directly on the Ca (high)-Ti discs after 4 h of pre-immersion; (D), a flat surface region of the Ti (control) discs after 24 h of pre-immersion; and (E), a flat surface region of the Ca (high)-Ti discs after 24 h of pre-immersion. Note the absence of the P peak at 24 h in (E) compared with 4 h in spectrum (C), as above.

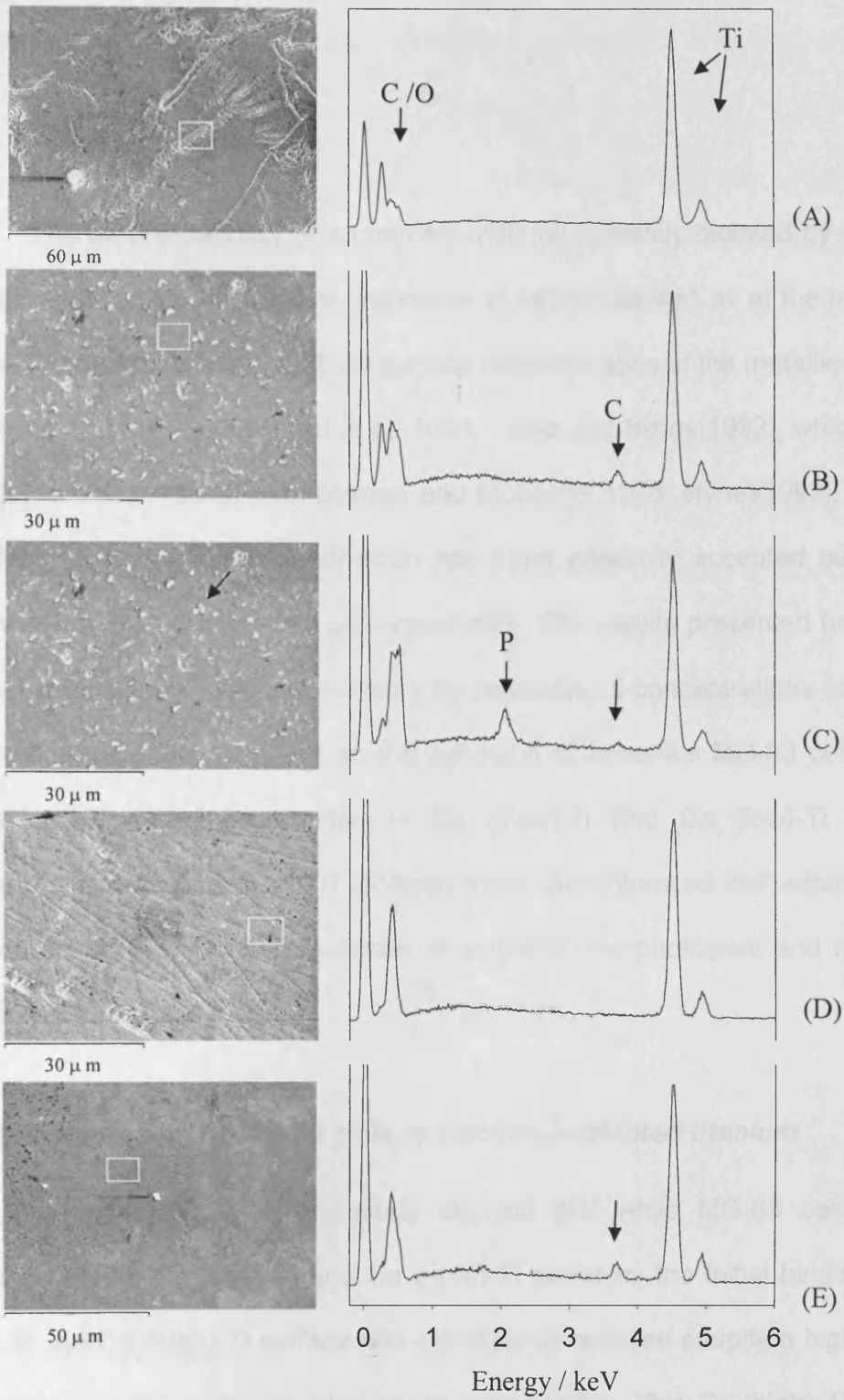
C /O
Ti
(A)
60 μ m
C
(B)
30 μ m
P
(C)
30 μ m
(D)
30 μ m
(E)
50 μ m
0 1 2 3 4 5 6
Energy / keV

regardless of the presence or absence of cells, as shown in Figure 4.8 and Figure 4.9, respectively.

4.4 Discussion

The biocompatibility of an implant material is mainly dictated by its ability to elicit appropriate host tissue responses at cellular as well as at the molecular levels [Puleo and Nanci 1999]. As surface characteristics of the metallic implants influence cell adhesion [Kornu et al. 1996; Puleo and Bizios 1992], which in turn regulates cell proliferation [Folkman and Moscona 1978; Hynes1992], analysis of different aspects of cell adhesion has been generally accepted as a good indicator of implant materials biocompatibility. The results presented here show that alteration of Ti surface chemistry by implanting 3 concentrations of Ca ions had a dose-dependent effect on the adhesion of bone-like MG-63 cells. While adhesion of osteoblastic cells on Ca (med)-Ti and Ca (low)-Ti surfaces appeared similar to that on Ti (control) discs, an enhanced cell adhesion was measured on Ca (high)-Ti surfaces, at physical, morphological and molecular levels, as discussed below.

4.4.1. Attachment of MG-63 cells to calcium-implanted titanium

Results of the current study showed that while MG-63 cells readily adhered to the Ca (low)-Ti and Ca (med)-Ti surfaces, the initial binding of the cells to the Ca (high)-Ti surface was significantly reduced despite a high level of spreading on this particular surface, as noted below. This Ca (high)-Ti-induced reduction in cell attachment, observed at 4 h (Chapter 3), appeared to be

completely reversed following prolonged culture for 24 h. At this later period of incubation, cell adhesion was significantly enhanced which is indicative of higher proliferation capacity of this surface compared with the control.

A number of factors may have contributed to this time-related effect. Firstly, during the ion-implantation process an amorphous oxide surface layer is formed [Hanawa et al. 1993], which has a different chemical composition to the native oxide on the non-implanted Ti and is likely to carry a different charge on immersion in solution. Such amorphous layers could differentially interact with inorganic ions in solution via the electrical double layer which forms in the interfacial region of the electrolytic fluid, possibly resulting in a supersaturated solution and the precipitation of ionic compounds as well as influencing interactions with biomolecules in solution. In addition, the surface oxide layer, which thickens on ion implantation [Hanawa et al. 1996b; Wieser et al. 1999], may thicken even further on prolonged incubation. It is notable that only the Ca (high)-Ti discs were observed to undergo a reflective colour change in culture medium. This effect was most probably due to the light interference effect that occurs when a surface layer of certain thickness and refractive index is formed on a reflective surface such as the Ti substrate. In experiments conducted by the Biomaterials group (Appendix A), an increase in the surface oxide thickness on Ca (high)-Ti discs and considerable further thickening on immersion in solution was found, compared with that on the Ti (control). Thus, the enhanced MG-63 cell attachment following prolonged incubation of Ca (high)-Ti discs in DMEM could be related to the formation of a thicker oxide layer, as has been

reported to also cause stronger bone integration and enhanced tissue responses in rabbit tibia *in vivo* [Sul et al. 2001].

In addition to thickening of the oxide layer, previous studies have reported the time-dependent dissolution and leaching of ions from the Ca-implanted surface on immersion in nitric acid, phosphate buffer, saline [Hanawa et al. 1996a] and deionised water (Appendix A). Continuing loss of Ca ions from the substrate would affect the surface charge and would also alter the local pH and ion concentration in the solution, potentially having marked effects on cellular activity. Thus, many features of the Ti surface, particularly following implantation with high levels of Ca ions, are likely to be considerably different after 24 h in culture medium compared with the initial 4 h period of cell attachment.

4.4.2 Spreading and morphological characteristics of bone cells

The results of the experiments described in this chapter revealed that implantation of Ti with Ca ions strongly influenced the spreading of MG-63 cells both qualitatively and quantitatively and moreover, this effect depended on the level of Ca ions which had been implanted into the Ti surface. Changes in the extent of spreading were also found to be associated with marked differences in the morphological appearance of the cells. Thus, increasing doses of Ca ions caused a significant increase in spreading and cell area compared with the control Ti. Cells on Ca (high)-Ti surface appeared to flatten, spread well and formed cellular bridges with the adjacent cells and also extended fibrillar

processes towards the surface of the Ti substrate, as observed and quantified from the SEM micrographs.

This is an important finding as it has been suggested by other researchers that such initial cell response will eventually cause an enhancement in the rate of proliferation of cells cultured on the surface of implant materials [Dalby et al. 2002]. Dalby et al assessed fibroblast reaction to the islands produced by polymer demixing of polystyrene and polybromostyrene. They found that the spreading of fibroblasts cultured on 13-nm-high islands was enhanced compared with those on the planar surfaces. They showed that the well-spread cells adhered on the islands also caused broad gene up-regulation, notably in the areas of cell signalling, proliferation, cytoskeleton, and production of ECM proteins [Dalby et al. 2002].

The importance of cell spreading on their proliferation has also been emphasised by experiments that used endothelial cells cultured on microfabricated substrates containing fibronectin-coated islands of various defined shapes and sizes of a micrometer scale. Cells spread to the limits of the islands containing fibronectin substrate. When the spreading of cells was restricted by smaller adhesive islands, proliferation was arrested, whereas larger islands permitted proliferation [Chen et al. 1997]. It has been previously established that physical cues such as the cell shape may play an important role in regulating the cell function [Mrksich et al. 1996]. Self–assembled monolayers (SAMs) of alkanethiolates on gold, adhesive micrometer-scale islands of ECM proteins or RGD peptides separated by nonoadhesive regions were manufactured using soft lithography (the formation of surfaces with well-defined

molecular characteristics and complex topographies), and the size and geometry of the islands were shown to determine cell shape [Mrksich et al. 1996] and ultimately gene expression [Chen et al. 1997; Whitesides et al. 2001]. Thus an enhanced spreading (increased cell area and reduced cell shape factor) of MG-63 cells cultured on Ca (high)-Ti discs compared with the control may be indicative of an improved biocompatibility of these modified surfaces.

4.4.3 Flow cytometry and confocal microscopy analyses

The level of Ca ion implantation and duration of cell culture was also found to affect the relative size and granularity of individual cells, with Ca (high)-Ti showing a statistically significant increase compared with the Ti (control) surface, but again only after 24 h of incubation. This increase in volume and complexity of intracellular organelles suggests that cells incubated on the Ca (high)-Ti surface for 24 h are likely to have elevated metabolic and mitotic activity [Ormerod2000; Radbruch A.2000]. However, FCM analysis showed that cells incubated on Ti implanted with the lower doses of Ca did not become similarly activated.

In the current study, the effects of Ca implantation levels on the expression of integrins by MG-63 cells were analysed. Integrins, which are closely associated with adhesion to substrata as well as cell activation, have been previously reported to be expressed by osteoblasts [de Ruijter et al. 2001; Sinha and Tuan 1996]. de Ruijter et al showed that osteosarcoma cell lines provide a reliable *in vitro* model to analyse integrin expression in response to differences in the chemical composition of the implant materials [de Ruijter et al.

2001]. The expression of integrin subunits β1, α3, α4, α5, α6, and αv by U2OS cells cultured on various well-defined calcium phosphate (Ca-P)-coated implant substrates was quantitatively analysed. These osteosarcoma cells expressed high levels of β1, low levels of α4, α5 and α6, and moderate levels of α3 and αv integrin subunits on the various biomaterial substrates. de Ruijter et al concluded that Ca-P-coated implant substrates modulate expression patterns of integrin receptors, which are the sensors of the cell [de Ruijter et al. 2001]. Results presented in this chapter showed that at 24 h, but not at 4 h, the α5β1 integrin by MG-63 cells was specifically and significantly up-regulated on the Ca (high)-Ti surface compared with the control Ti. Moreover, lower doses of Ca did not result in similar significant up-regulation.

Poor cell adhesion to orthopaedic and dental implants may result in implant failure. Cellular adhesion to biomaterial surfaces is primarily mediated by integrins, which act as signal transduction and adhesion proteins. Several studies have investigated the factors which affect integrin expression by cells cultured on different substrates. Different levels of integrin were expressed depending on the type of cells used, composition and topography of the substrate on which the cells were cultured [Gronowicz and McCarthy 1996; Sinha et al. 1994; Sinha and Tuan 1996]. Cell spreading, which is an active process and also involves expression of integrins, was reduced on more rough surfaces, which is in agreement with an earlier study that demonstrated an improved attachment and spreading of osteoblastic cells on smooth Ti surfaces [Anselme et al. 2000; Shah et al. 1999]. In contrast, Lange et al showed that the

expression of two β- and three α- integrin receptor subunits by MG-63 cells was increased on rough compared to polished Ti surfaces [Lange et al. 2002a].

Although the precise reason for the delayed response of α5β1, by cells cultured on the Ca (high)-Ti surfaces, is not yet understood, this integrin mediates cell adhesion to substrates *via* binding to FN, a process which also generates intracellular signals that lead to the progression of cells through the cell cycle and increased cell proliferation [Juliano and Haskill 1993; Roovers et al. 1999]. Furthermore, a previous study demonstrated that the addition of anti α5 or β1 antibody significantly reduced the mineralization of osteoblasts *in vitro*. This effect was reversible following the removal of the anti-integrin antibody. Therefore, it was proposed that the integrin-mediated adhesion and signalling events may contribute to the progressive differentiation of the osteoblast and to the initiation of a mineralized matrix. [Schneider et al. 2001].

Integrin's functions depend on divalent cations such as Mg and Ca which are present in mm concentrations *in vivo* and regulate the interaction of integrins with their cognate ligands [Hynes2002]. Zreiqat et al investigated the effects of modification of bioceramic substrate via Mg ion supplementation on HBDC adhesion, integrin expression, and activation of intracellular signalling molecules [Zreiqat et al. 2002]. They showed that the adhesion of HBDC to Al(2)O(3)-Mg(2+) was increased compared to on the Mg(2+)-free Al(2)O(3). In addition, when α5β1 and β1 integrins were blocked by functional blocking antibodies, HBDC adhesion significantly decreased. They concluded that cation-promoted cell adhesion to biomaterial surfaces is probably mediated by α5β1 and β1

integrins. Furthermore, their results suggest that this integrin-mediated cell adhesion may have triggered a signal transduction pathway involving the key signalling protein Shc, which subsequently resulted in enhanced gene expression of the ECM proteins [Zreiqat et al. 2002].

Another study demonstrated that integrin function is critically dependent on the concentration of divalent cations [Ajroud et al. 2004]. It is therefore possible that the presence of a sufficiently high level of Ca ions, released from or contained within the Ca (high)-Ti surfaces (Appendix A), might trigger enhanced ligand binding of the integrin receptors, thereby stimulating integrin-mediated activation signalling pathways. Ajroud et al proposed an integrin-metal-ligand ternary complex where the affinity of metal ions to integrins is itself regulated by the activation state of these receptors and by certain ligands. They reported that the Ca ions regulate the interaction of integrins with their cognate ligands [Ajroud et al. 2004].

Results of the current study also showed that incubation of MG-63 cells on the Ca (high)-Ti surface caused a significant increase in vinculin-positive focal adhesion plaques. In agreement with the current study, vinculin was previously shown to be expressed at high levels by well-spread cells on Ti-6Al-4V and CC surfaces [Shah et al. 1999]. Diener et al recently demonstrated that the surface topographical differences of Ti regulate the number and size of vinculin-positive focal adhesion plaques formed by MG-63 cells [Diener et al. 2005]. Zinger et al showed that cells can respond not only to micrometric but also to nanometric surface topographical variations. They demonstrated that the formation of vinculin-positive adhesion plaques by MG-63 cells varied on Ti

surfaces with nanoscale differences in roughness [Zinger et al. 2004]. In another study, a differential expression of vinculin was reported by Saos-2 cells when cultured on grade 1 and grade 4 cpTi discs [Ahmad et al. 1999a].

Vinculin is one of the connecting molecules in the cascade of integrin–mediated cell adhesion and signal transduction. Integrins first aggregate on the cells attached on the Ti surface and then bind to the ECM molecules secreted by these cells, this induces accumulation of vinculin, talin and α-actinin (a homodimer that binds to integrin on the cytoplasmic face). Finally integrins trigger tyrosine phosphorylation of signalling molecules, such as FAK, which results in cytoskelatal reorganisation *via* cross-linking of the actin filaments. Thus, the mechanisms of cell adhesion to the ECM which are of fundamental importance for function, survival, and growth of cells involve the formation of focal adhesions to facilitate integrin signalling [Hynes1987; Kornberg and Juliano 1992; Kornberg et al. 1991]. The concomitant up-regulation of α5β1 integrin and vinculin by bone-like cells adhered on Ca (high)-Ti surfaces, may therefore highlight some of the molecular events occurring at the cell-Ti interface.

4.4.4 Surface analysis and cell attachment following pre-immersion of titanium surfaces

Ti has been shown to naturally form a calcium phosphate film in electrolyte solution whose composition resembles that of extracellular fluid. However, the calcium phosphate layer formed on Ti was found to be only a few

nm thick after 30 day immersion in the SBF. Such a thin calcium phosphate layer does not effectively exhibit bioactive properties of HA, because the surface is electronically affected by titanium oxide and Ti as substrates [Hanawa and Ota 1991]. Modification of Ti surfaces by ion-implantation has previously been reported to augment the formation of HA-like calcium phosphate on exposure to SBF. This has been demonstrated for Ti implanted with Ca, both as a single ionic species [Krupa et al. 2001a] and co-implanted with P [Krupa et al. 2001b], and for Ti implanted with Na [Maitz et al. 2002b; Pham et al. 2000a], although some of these studies utilised samples which were heat-treated and therefore likely to have altered surface chemistry [Krupa et al. 2001b; Pham et al. 2000a; Pham et al. 2000b]. While the appearance of calcium phosphate precipitates on surfaces has generally been taken as a sign of an improved 'bioactivity' or 'biocompatibility', the precise mechanisms governing their formation, structure and stability are not fully understood. Precipitation may depend on the availability of Ti-OH groups acting as nucleation sites [Maitz et al. 2002b], while local ion concentrations and changes in pH, as noted above, may also be important in determining the supersaturation point at the surface.

In the present study, pre-immersion experiments were also carried out in order to study the effects of tissue culture conditions on the attachment and surface chemistry of the Ti discs. The EDS analysis carried out here conclusively demonstrated that a Ca- and P-rich particulate deposit had formed only on the Ca (high)-Ti surfaces after a relatively brief period (4 h) of pre-immersion in culture medium. However, the presence of this precipitate was found to be accompanied by a significantly reduced attachment of the MG-63

cells which, nevertheless, retained the morphological appearance indicative of a metabolically active cell population. This suggests the possibility that the initial formation of Ca- and P-containing particles on the Ti surface implanted with the high levels of Ca ions was, at least partially, responsible for the reduction in cell adhesion. Although it is not yet known whether this was primarily a physical effect of surface topography (for example by blocking attachment sites available to the cells) or an effect of the altered surface chemistry, these particles nevertheless did not appear to exert any deleterious effect on the cells. Most notably, the precipitated material was no longer present after more prolonged (24 h) pre-immersion, at which time cell attachment to the Ca (high)-Ti surface was very substantially enhanced. Thus, while the chemical changes which may have occurred at this surface by 24 h remain unclear, they do not appear to have involved the presence of an apatite layer at that time, as evidenced by the absence of P ions across the surface.

Previous studies have generally shown formation of calcium phosphate on ion-implanted Ti following relatively long-term immersion in SBF [Maitz et al. 2002b], but nucleation of calcium phosphates after 24 h in SBF has also been reported [Pham et al. 2000a]. In contrast, when cell attachment was measured at 14 days, in a full protein-containing medium as used here, no inorganic calcium phosphate precipitate was detected at this time [Maitz et al. 2002a], in agreement with the type of changes found at 24 h in the present study. Results presented here suggest that differences in the observed levels of cell attachment may at least partly be due to modification of nucleation and precipitation processes on Ca (high)-Ti surfaces following exposure to high

levels of amino acids and proteins. These surface changes are likely to depend on molecular and ionic interactions between the material and the aqueous environment, including release of certain ionic species, local modification of pH and also adsorption of biologically active molecules from the medium onto the surface.

4.5 Conclusions

- Ca implantation can affect the adhesion of MG-63 cells both qualitatively and quantitatively. However, this effect appears to depend on the level at which Ca ions are implanted.
- Initial reduction in cell adhesion on Ca (high)-Ti was not only restored but substantially increased with progressing culture times.
- A significantly enhanced cell spreading, formation of focal adhesion plaques and expression of integrins were measured on Ca (high)-Ti surface. In contrast, no marked differences were observed in cell behaviour on Ca-Ti (low and medium).
- Pre-immersion studies indicated that the decrease in cell attachment to Ca (high)-Ti at early time periods may be linked to the presence of Ca- and P-rich particles on the surface. The absence of these particles at 24 h was consistent with a significant increase in cell attachment.

Chapter 5

Effects of Calcium-Implanted Titanium on the Proliferation and Cell Cycle of MG-63 Cells

5.0 Introduction

Once the cells are adhered to the substrate, they are confronted with the next challenge: they need a different set of cues to start proliferating. Upon cell adhesion, a spatial redistribution and clustering of transmembrane receptors occurs, which in turn triggers a restructuring of the cytoskeleton. Depending on the characteristics of the cell adhesions formed and the associated cytoplasmic protein complexes, alternate cell signalling pathways can be triggered that regulate gene expression and ultimately cell migration, differentiation, apoptosis, quiescence, or entry into the cell cycle resulting in cell proliferation [Anselme2000; Aplin et al. 1999; Puleo and Nanci 1999]. The cell cycle is controlled by evolutionarily conserved mechanisms that ensure the strict regulation of the division process and the accurate segregation of the genome in two daughter cells. An inhibition or elevation in cell proliferation has been strongly linked to the mechanisms which regulate movement of cells through different phases of the cell cycle [Johnson and Walker 1999; Murray2004; Norbury and Nurse 1992]. These mechanisms are able to integrate intra- and extracellular signals and, therefore, play a central role in the control of cell proliferation [Ryhänen et al. 2003].

Current testing of implant materials for potential clinical application frequently involves the measurement of overall change in cell number *in vitro*, which is usually equated with the level of 'biocompatibility'[Vogel and Baneyx 2003]. While the effect of implant materials on cell growth is undeniably an important feature of the cellular response, such data provide only limited understanding of cell-implant interactions and the molecular basis whereby

implant materials exert their biological effects. However, a number of cellular 'markers' such as the nuclear antigen Ki-67 are known to delineate actively proliferating cells specifically [Danova et al. 1988; Landberg et al. 1990] , while progression through the various coordinated stages of the cell cycle is also now considered to be a major determinant of cell growth [Johnson and Walker 1999; Murray2004; Norbury and Nurse 1992].

In order to clarify the effects of Ca ion-implantation of Ti on bone cells, the present study has used FCM to determine, for the first time, whether these novel Ca-Ti surfaces modulate Ki-67 expression and the progression of synchronised cultures of MG-63 cells through the G0/G1, S and G2/M phases of the cell cycle. Experiments presented in this chapter evaluated the effects of different levels of Ca ion-implantation of Ti on MG-63 cell proliferation via [^{3}H] thymidine incorporation assay and Ki-67 immunostaining method, as described below.

5.1 Background

5.1.1 Cell proliferation

Controlling surface chemistry by ion-implantation has been previously shown to invoke a favourable cellular response (Chapter 1). For example, Ca-ion implantation of Ti has reported to increase the formation of new osteoid tissue *in vivo* as early as after 2 days of implant insertion [Hanawa et al. 1997]. However, these claims [Hanawa et al. 1997] were previously challenged by Howlett et al due to the lack of both quantitative and surface topographic measurements [Howlett, 1999b], as discussed earlier in Chapter 1.

Krupa et al investigated the effects of Ca ion-implantation of Ti surfaces on bone cell response *in vitro* [Krupa et al. 2001a]. Human osteoblasts were seeded on the surfaces of both the Ca ion-implanted (at a dose of 1×10^{17} ions cm^{-2}) and non-implanted Ti samples (6.2 mm in diameter and 2 mm high Ti cylinders placed at the bottom of 96-well culture dishes). After one week, viability of the cells was determined by means of the XTT assay. This test is based on the capacity of mitochondrial dehydrogenase enzymes in living cells for converting the XTT substrate (2,3-bis(2-methoxy-4-nitro-5-sulfophenyl)-5-[(phenyloamino) carboxyl]-2H-tetrazolium hydroxide) into a water-soluble formazan product, which in this study was measured by the ELISA (enzyme linked immunosorbent assay) reader. Their results demonstrated that the Ca-Ti surfaces had no effect on the viability of cultured cells [Krupa et al. 2001a]. In contrast to the findings of Krupa et al, initial results of the current study showed that the growth of alveolar bone and MG-63 cells was enhanced on the Ca (high)-Ti discs compared to that on the non-implanted control (Chapter 3). To test whether this increased proliferation of MG-63 cells was dependent on the concentration at which Ca ions were implanted, two cell proliferation assays were employed i.e. [^{3}H] thymidine incorporation (described earlier in Chapter 2), and a Ki-67 staining method, which is explained in the following section.

5.1.1.1 Cell proliferation associated Ki-67 antigen

A quantitative method to assess cell proliferation is one essential prerequisite for testing biomaterial cytocompatibility *in vitro*. Several nuclear and surface proteins are expressed in varying amounts during different phases of the

cell cycle. Studying these proteins permit a better understanding of the mechanisms regulating proliferation and provide kinetic parameters for describing the cell cycle. Proliferating cell nuclear antigen (PCNA) and Ki-67 are two such nuclear proteins which are expressed in cycling, but not in G0 cells. Statin, on the contrary, is expressed only in resting G0 cells. However, the expression of the c-ras product is not strictly related to the cell cycle phases [Danova et al. 1990].

Ki-67, selected in the current study to examine the effects of Ca ion-implantation levels on cell growth, was previously demonstrated to be associated with only actively proliferating cells [Danova et al. 1988; Landberg et al. 1990]. For example, Danova et al measured the expression of Ki-67 in the breast carcinoma MCF-7 cell lines, human leukemic cells and the glioblastoma cells using FCM. These authors found that the Ki-67-reactive antigen is expressed only by the actively proliferating cells which are in G1, S, and G2-M phases of the cell cycle [Danova et al. 1988]. Similarly, Landberg et al measured the expression of Ki-67 in seven human hematopoietic cell lines using a monoclonal antibody and a phycoerythrin-conjugated anti-mouse antibody. These authors showed that cycling cells expressed the Ki-67 antigen with increasing levels during the S phase, while a maximum level was detected in M phase. Landberg et al concluded that the determination of Ki-67 expression levels by FCM is a good method of measuring cell proliferation *in vitro* [Landberg et al. 1990].

5.1.2 An overview of the cell cycle

The cell cycle is defined as a highly co-ordinated sequence of events which stretches from a cell's "birth" by cell division to the completion of its own division [Murray and Hunt 1993]. When a cell divides into two daughter cells, the genetic information present in the nucleus of the parent cell is duplicated for each daughter cell. The cell cycle is divided into five distinct phases, as illustrated in Figure 5.1 [Murray and Hunt 1993; Pagano1995].

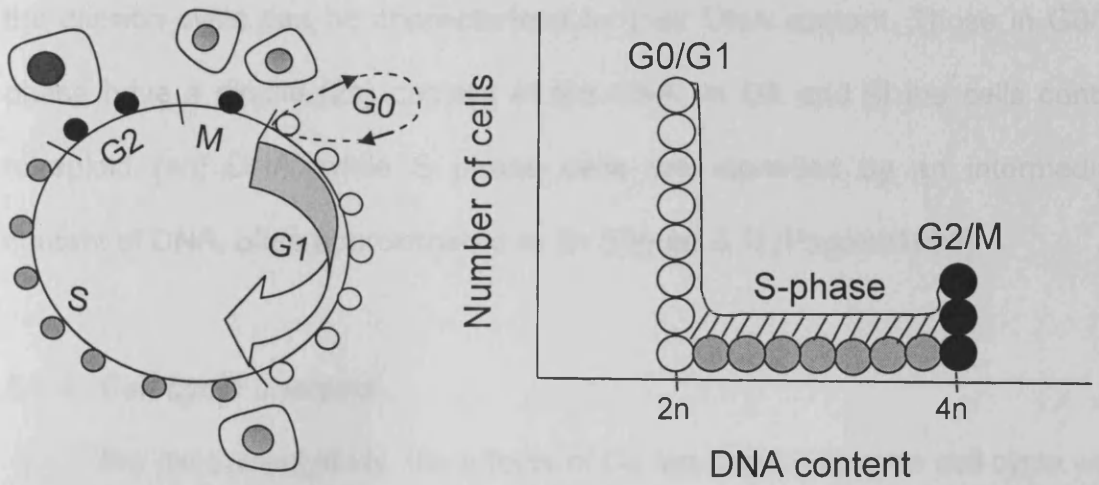

Figure 5.1: Schematic illustration of different phases of a typical mammalian cell cycle and corresponding DNA content of actively cycling cell population, adapted from [Givan2005].

A quiescent cell, which is resting and not involved in cell division is often referred to as being in the "G0" state. Once division is triggered, cells enter into the pre-synthetic phase called gap 1 or "G1", during which the amount of RNA increases and certain proteins required for DNA replication are synthesised. The next stage of the cell cycle is the "S" or DNA synthesis phase where cells double their DNA content, often measured by [^{3}H] thymidine incorporation and/or

bromodeoxyuridine (BrdU) uptake. At the end of DNA synthesis cells enter in the post-synthetic or "G2" phase of the cell cycle. During G2, cells have to ensure that DNA replication is adequately completed.

Finally, cells enter mitosis or "M" phase. During this phase, after a cascade of events involving chromatin condensation, cytoskeletal re-organisation occurs, which culminates in the division of a cell into two daughter cells (Figure 5.1) [Murray and Hunt 1993; Pagano1995]. At the end of M phase, cells will either rest in G0, or go through a new cell cycle. Cells in each stage of the division cycle can be characterised by their DNA content. Those in G0/G1 phase have a diploid (2n) content of the DNA, in G2 and M the cells contain tetraploid (4n) DNA, while S phase cells are identified by an intermediate content of DNA, often approximated to 3n (Figure 5.1) [Pagano1995].

5.1.3 Cell cycle analysis

For the current study, the effects of Ca ion-implantation on cell cycle were firstly assessed by monitoring progression of MG-63 cells through the G0/G1, S and G2/M phases using FCM, and secondly, by microscopically quantifying the numbers of mitotic cells. The influences of control and Ca-Ti discs on cell cycle progression were determined by measuring total DNA content in conjunction with DNA synthesis, as explained below.

The DNA content of cells is measured to determine the percentages of cells in G1, S, and G2/M phases of the cell cycle [Ormerod2000; Pagano1995]. Several types of fluorescent dyes can be used to bind the DNA, for example diamino-2-phenylindole (DAPI), acridine orange, Hoechst 33342 and 33258,

chromomycin A3, LDS 751, TO-PRO-3 and propidium iodide (PI) [Ormerod2000]. PI, used in the current study to determine the proportion of cells cultured on Ti (control) and Ca-Ti surfaces in different phases of the cell cycle at any designated time point, reacts with DNA by intercalating between the stacked bases of the double helix [Givan2005].

Like [^{3}H] thymidine (Chapter 2), bromo-deoxyuridine (BrdU) is also used to measure DNA synthesis [Pagano1995]. BrdU is incorporated by cells which are actively synthesising DNA. The proportion of cells with positively tagged nuclei can be detected by using anti-BrdU mAb conjugated with a fluorescent dye, and quantified either by direct counting in the microscope or by FCM analysis. While, [^{3}H] thymidine incorporation assay measures total DNA synthesis, BrdU uptake not only determines DNA synthesis per cell but also the percentage of S phase cells. The radioactive method measures the total amount of DNA being synthesised and is dependent upon the number of cells counted, whereas the FCM data reflects proportion of cells that are in the S phase and it does not change by changing the total number of cells counted [Givan2005]. A previous study investigated the effects of orthopaedic implant materials on the progression of MG-63 cells through different phases of the cell cycle by measuring BrdU incorporation in conjunction with PI staining and found it to be extremely valuable assay [Granchi et al. 1995a]. They showed that using this method, the cells in the S phase, marked by the anti-BrdU antibody, can be distinguished from the cells in G0/G1 and G2/M phase which were marked with PI only. Cells in the G2 /M phase having 4n DNA content, in comparison with

G0/G1 cells with 2n DNA, showed double fluorescence intensity when analysed by FCM [Granchi et al. 1995a; Pagano1995].

M, the last phase of cell cycle is classically divided into four stages: prophase, metaphase, anaphase and telophase, as illustrated in Figure 5.2. During prophase chromosomes condense, the nuclear membrane disaggregates into small vesicles and the mitotic spindle forms by the

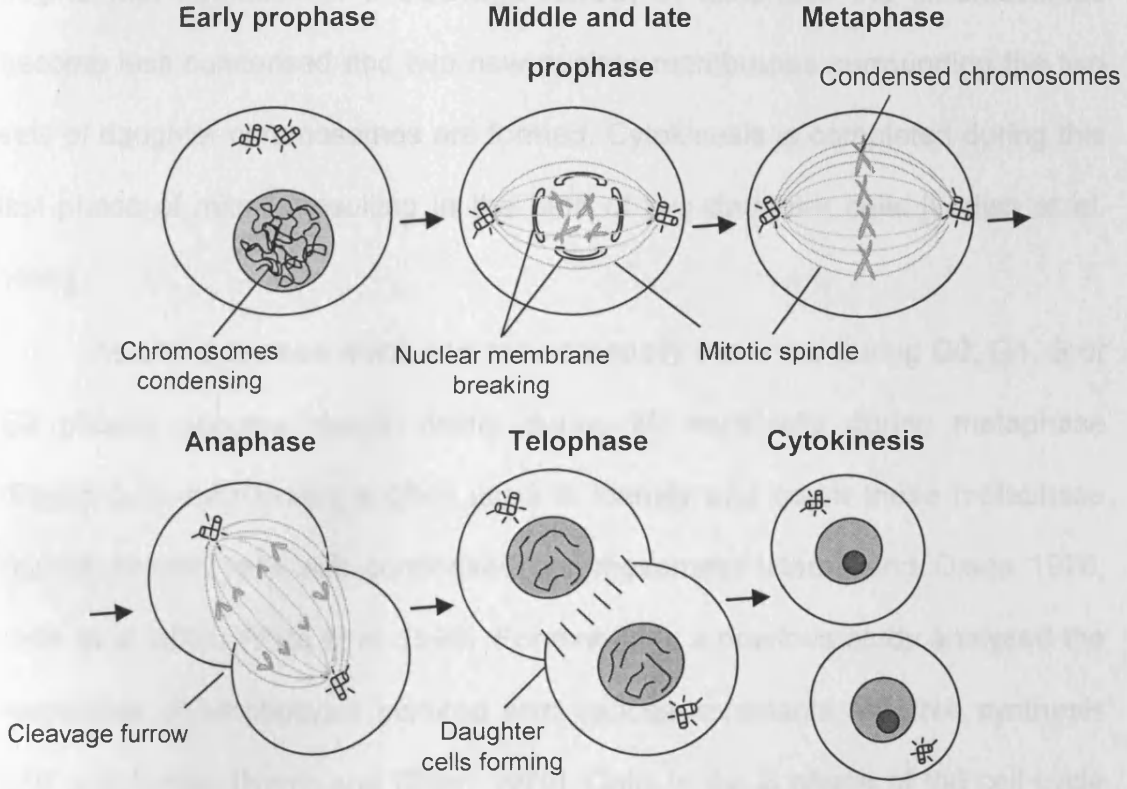

Figure 5.2: A schematic diagram illustrating different stages of mitosis, during which the mitotic spindle segregates the duplicated, condensed chromosomes into two daughter nuclei and the cytoplasm divides to produce two genetically identical daughter cells, adapted from [Lodish et al. 1996].

polymerisation of microtubules. The microtubules form the scaffold of the mitotic cell; they provide the tracks along which chromosomes move and ensure that the chromosomes are equally distributed between the two daughter cells. In metaphase, the chromosomes align in a central plane perpendicular to the long axis of the spindle. During anaphase the paired chromosomes separate into individual chromosomes which are pulled to the opposite poles of the spindle. Simultaneously, the cell elongates and cytokinesis (division of cell cytoplasm) begins with formation of a cleavage furrow. In telophase the chromosomes become less condensed and two new nuclear membranes surrounding the two sets of daughter chromosomes are formed. Cytokinesis is completed during this last phase of mitosis resulting in the birth of two daughter cells [Lodish et al. 1996] .

As chromosomes which can not be visually observed during G0, G1, S or G2 phases become clearly visible during M, especially during metaphase (Figure 5.2), microscopy is often used to identify and count these metaphase figures (mitotic cells with condensed chromosomes) [Harris and Olsen 1976; Ojok et al. 2001; White et al. 1998]. For example, a previous study analysed the responses of lymphocytes cultured with various stimulants on DNA synthesis and cell division [Harris and Olsen 1976]. Cells in the S phase of the cell cycle were counted using [^{3}H] thymidine incorporation assay and autoradiography. To determine the number of dividing cells, mitotic counts were performed. Cells were embedded in araldite and autoradiographs of the sections were prepared. The cells were then fixed in formal saline before staining with toluidine blue. Metaphase cells were readily identified and mitotic counts were estimated

[Harris and Olsen 1976]. In another study, both light and electron microscopy were used to examine the femoral bone marrow of rats which were experimentally infected with different doses of *Trypanosoma congolense* (a major livestock pathogen in Africa). Femoral bone marrow samples were taken from all animals and after fixation were stained with haematoxylin and eosin. These authors counted the metaphase figures in the bone marrow samples, and found that in the acute stage of trypanosomosis infection, a vast majority of haemopoietic cells were in mitosis [Ojok et al., 2001]. Similarly, White et al studied the effects of gapstatin, a surface-associated component of *Actinobacillus actinomycetemcomitans* (a bacterium which is a major pathogen in human periodontal disease), on the number of MG-63 cells in M phase of the cell cycle. Cells grown on glass coverslips were exposed to gapstatin for 24 h. The cells were fixed and then stained with haematoxylin to microscopically visualise relative cell and nuclear dimensions, and to determine the presence and proportions of metaphase figures [White et al. 1998]. For the current study, the effects of Ca-implantation of Ti on the number of MG-63 cells in mitosis were determined by microscopically identifying the metaphase figures, as previously described [White et al. 1998], and counting these M phase cells using digital image analysis.

5.1.4 Rationale for the use of hydroxyurea and colcemid

Cells growing in cultures are not all at the same stage of the cell cycle. Understanding the molecular and biochemical basis of cellular growth and

division involves the investigation of regulatory events that most often occur in a cell-cycle phase-dependent fashion. To study cell cycle progression *in vitro*, it is essential to have cells that are growing in the same phase of the cell cycle [Davis et al. 2001].

The procedure by which cells are arrested in specific phases of the cell cycle is termed synchronisation. Cell synchronisation can be achieved by either exposure of cells to special conditions or their treatment with drugs, as illustrated in Figure 5.3. These procedures which cause growth arrest at a specific stage of the cell cycle are often completely reversible. Once cells are released from the block, they recover and proceed through the cell cycle in a relatively uniform manner [Pagano1995; Davis et al. 2001].

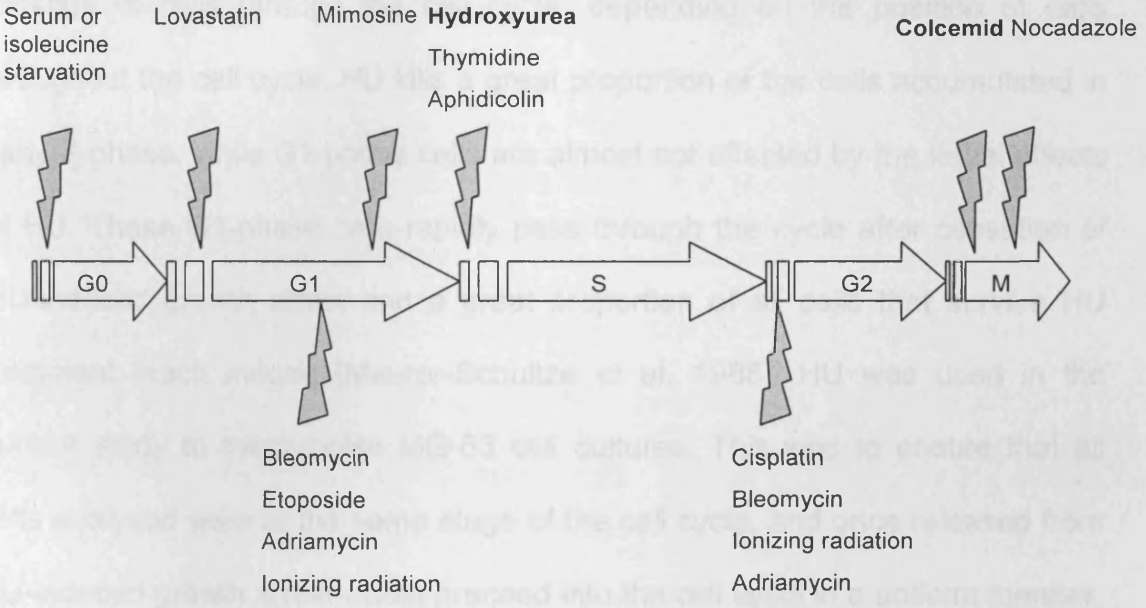

Figure 5.3: An illustration of different conditions and chemicals that can be employed to induce synchronisation, causing growth arrest at a specific point in the cell cycle, adapted from [Pagano1995].

In order to investigate the effects of Ca ion-implantation of Ti on bone cell cycle progression in a cell-cycle phase independent fashion, hydroxyurea (HU) and colcemid were used in the current study for the synchronisation of MG-63 cell cultures. The following section explains the mode of action of these two drugs and the reason for their selection in this study.

HU is classified as a cytostatic drug. After exposure to this drug, cells are entrapped at the G1/S interface (Figure 5.3) [Ormerod2000]. HU exerts a direct effect on the synthesis of DNA by inhibiting ribonucleotide reductase, an enzyme which is responsible for the production of the deoxyribonucleotides (precursors required for DNA synthesis) [Lori and Lisziewicz 2000]. It was previously described by Maurer-Schultze et al that HU synchronises cells by influencing the passage of cells through the cell cycle, depending on the position of cells throughout the cell cycle. HU kills a great proportion of the cells accumulated in early S-phase, while G1-phase cells are almost not affected by the lethal effects of HU. These G1-phase cells rapidly pass through the cycle after cessation of HU-induced growth arrest and a great proportion of all cells that survive HU treatment reach mitosis [Maurer-Schultze et al. 1988]. HU was used in the current study to synchronise MG-63 cell cultures. This was to ensure that all cells analysed were at the same stage of the cell cycle, and once released from HU-induced growth arrest would proceed into the cell cycle in a uniform manner, thus, allowing measurement of the effects of Ca ion-implantation of Ti in a cell cycle phase-independent fashion.

Colcemid is a mitotic inhibitor which causes arrest of cells at metaphase (Figure 5.3). It exerts its effect by preventing assembly of the mitotic spindle and by interfering with microtubule stability, both of which are pre-requisites for cell division (Figure 5.2) [Rieder and Palazzo 1992]. It has been reported by Kranenburg et al that the treatment of Adenovirus-transformed cell cultures with cell cycle inhibitory drug colcemid resulted in an inability of these cells to divide, as they were trapped at metaphase [Kranenburg et al. 1996]. These authors labeled cells with BrdU and the percentage of BrdU-positive nuclei was determined by immunofluorescence. To analyse whether transformed cells would divide in the presence of colcemid, cell proliferation was measured by direct cell counting and by BrdU incorporation assay. Staining of the nuclei was carried out using Hoechst 33258 dye. Their results showed that the cells treated with colcemid continued to synthesize DNA but did not divide [Kranenburg et al. 1996].

White et al investigated the effects of bacterial surface protein "gapstatin" on the control of human cell cycle. HU and colcemid were used in this study to achieve the synchronisation of cell cycle progression. They compared the DNA content of PI-stained cells exposed to HU, colcemid and gapstatin for 24 h. Results showed that like colcemid-treated cells, a majority of gingival fibroblasts and MG-63 cells exposed to gapstatin had 4n DNA content. However, microscopic examination of cells exposed to this bacterial fraction failed to reveal any metaphase figures, as mentioned above (section 5.1.3). Taken together, their observations suggested that gapstatin might have blocked the

mammalian cells prior to M, probably in the G2 phase of the cell cycle [White et al. 1998]. For the current study, colcemid was used in conjunction with HU to achieve synchronization of MG-63 cell cycle progression. In order to trap cells which entered mitosis and to block their escape into the next cycle, HU-synchronised cells, once released, were simultaneously treated with colcemid. In addition, as colcemid blocks cells at metaphase, it was also used to identify and to microscopically quantify M cells based on their characteristic condensed metaphase nuclei (Figure 5.2), as previously described [White et al. 1998],

5.2 Materials and methods

5.2.1 Preparation of titanium discs

CpTi discs were polished on one face to a mirror finish, as detailed in Chapter 2, and Ca ions were implanted onto the surface of Ti discs at 3 different doses (Chapter 4).

5.2.2 Cell culture

For all experiments, MG-63 cells were cultured on Ca-implanted Ti discs placed in 24 well plates (Beckton-Dickinson). Controls consisted of cells cultured on the non-implanted Ti discs, as described in previous chapters. With the aim of measuring possible changes in cell proliferation and cell-cycle progression, all cultures were initiated at a low cell density in order to ensure that they would subsequently be able to grow exponentially.

5.2.3 *Measurement of cell growth by [^{3}H] thymidine incorporation*

The influence of 3 different levels of Ca ion-implantation of Ti on the proliferation of MG-63 cells was assessed by measuring DNA synthesis in the sub-confluent cultures using [^{3}H] thymidine incorporation assay on 4 consecutive days. To take into account differences in initial cell attachment which were observed between Ca-implanted and control Ti surfaces (Chapter 3), the level of DNA synthesis at 24 h was used as the initial 'time 0' baseline value for calculating the number of cells present on each type of disc. Briefly, MG-63 cells were seeded on the surfaces of Ti (control), Ca (high)-Ti, Ca (med)-Ti and Ca (low)-Ti at a density of 1 x 10^3 cells/disc. At 24, 48, 72 and 96 h, cells were pulse-labelled with 1 μCi ml^{-1} of [^{3}H] thymidine for 2 h and radioisotope counts were measured using liquid scintillation spectroscopy, as described earlier in Chapter 3.

5.2.4 *Immunostaining of the cell proliferation-associated Ki-67 antigen*

To measure the effects of Ca implantation levels on the proportion of proliferating cells over a period of three days, Ki-67 staining was carried out as follows. MG63 cells were cultured on the surface of the Ti (control), Ca (high)-Ti, Ca (med)-Ti and Ca (low)-Ti discs, at an initial density of 1 x 10^3 cells/disc. After 24, 48 and 72 h of incubation, the discs were washed with PBS and cells were detached from the surface using trypsin-EDTA (GIBCO Invitrogen). After washing with PBS, the cells were fixed with 1% PFA in PBS containing 0.1% v/v saponin for 30 min at RT. Saponin was used to permeabilise cell membranes in

order to allow access of antibody to the nuclear Ki-67 antigen. Cells were then washed, centrifuged at 1100 rpm for 5 min and resuspended in wash buffer (PBS supplemented with 2% FCS, 0.05% sodium azide and 0.1% v/v saponin).

The cells were incubated for 60 min at RT with FITC-conjugated mouse anti-Ki-67 monoclonal antibody (mAb) (MCA289T) (Serotec), diluted 1:100 in wash buffer. IgG1-FITC mouse mAb (Dako) was used as the negative control. The cells were centrifuged, washed and resuspended in 500 µl of wash buffer. The fluorescence intensity of 1 x 10^4 individual cells/sample was measured using FCM, as described below, and the data analysed using WinMDI software (version 2.8) (http://facs.scripps.edu/software.html). The percentage of the total cell population positive for Ki-67 was equivalent to the proportion of proliferating cells.

5.2.5 DNA content and synchronisation of MG-63 cell cultures

Cells in exponentially growing cultures are distributed through all of the phases of the cell cycle [Davis et al. 2001]. In order to determine the effects of Ca-Ti surfaces on the progression of the cells through each of the specific stages of the cell cycle, it was first necessary to obtain cultures in which all the cells were at the same stage. This was achieved by 'synchronising' MG-63 cell cultures with the cell cycle inhibitor HU [Lori and Lisziewicz 2000].

MG-63 cells were seeded into 3 replicate tissue culture flasks at a relatively low density (1 x 10^4 cells per 25 cm^3 flask). Cells from the control culture (flask 1) were harvested after 18 h of cell incubation. After washing with PBS, cells were detached from the flask by trypsin-EDTA (G1BCO Invitrogen),

centrifuged and washed again with PBS. They were then fixed using 1 ml of 70% ethanol and stored at -20°C for 18 h. The harvested MG-63 cell pellets were washed in PBS and resuspended in 400 µl of wash buffer containing 0.1% saponin. To ensure that only DNA, but no RNA, was stained with the fluorescent intercalating dye PI, cell suspensions were first incubated with 1 µl of ribonuclease (RNase) (Sigma-Aldrich) (5 µg ml^{-1}) at 37°C for 10 min and then were stained with 20 µl of PI (Sigma-Aldrich) (50 µgml^{-1}) for 2 h at RT.

To obtain synchronised cultures, cells in the second flask were blocked at the G1/S boundary by adding HU (1 µM) for 18 h. HU was then removed by washing with warm PBS, the cells harvested and PI staining of this 'arrested' culture carried out as described above. In order to allow the blocked cells to progress through the cycle, the third flask was arrested with HU, then released by removing HU and re-incubated for 12 h in the presence of colcemid (0.1 µM). This drug was included because it is an inhibitor of M phase of the cell cycle, causing metaphase arrest by preventing assembly of the mitotic spindle and interfering with microtubule stability, both of which are pre-requisites for cell division [Davis et al. 2001]. Cells in this culture thus accumulate in M, do not divide and do not enter the next cell cycle. Their DNA content was also determined by PI staining and by FCM, as described below.

5.2.6 Measurement of S phase

To determine whether Ca-implantation of Ti modifies the time of re-entry and duration of HU-synchronised cells in the S phase of the cell cycle, BrdU

(bromo-deoxyuridine; used as a marker of DNA synthesis) uptake was measured in conjunction with total DNA content at 2, 4, 6, 8, 10 and 12 h following release from growth arrest.

MG63 cells were seeded on the Ti (control) and Ca (high)-Ti surfaces at a density of 3 x 10^3 cells per disc. Replicate sets of 15 discs per sample were placed in 24-well tissue culture plates. 24 h after the initial seeding, the sub-confluent cultures were incubated with 1 μM HU for 18 h, then washed with warm PBS to remove the HU. Fresh DMEM containing 0.1 μM colcemid was added to prevent possible 'escape' of dividing cells into the next cell cycle once they had progressed to M phase. After 15 min, cells on replicate sets of the discs were exposed to 1 μM BrdU for 2 h, then washed in PBS, detached from the control and Ca-Ti surfaces using trypsin-EDTA and fixed in 70% ethanol at -20°C for 18 h. This 2 h BrdU labelling procedure was repeated for replicate cells at 4, 6, 8, 10 and 12 h following HU removal from the culture medium.

S phase (BrdU-containing) cells were detected using FITC-conjugated anti-BrdU antibody, which recognises the epitope only in single–stranded DNA [Pagano1995]. Cell pellets were therefore harvested, washed with PBS and the DNA denatured by re-suspending the cells in 2 M HCl for 30 min at RT, with regular mixing. After washing twice with PBS, the cells were washed in PBS-T (PBS with 0.1% BSA and 0.2% of Tween 20, pH 7.4) and the cell pellets incubated with 2 μl of FITC-conjugated anti-BrdU antibody (1:100 dilution) for 1 h at RT. After washing with PBS the cells were re-suspended in 400 μl of wash buffer, 1 μl of RNase (5μg ml^{-1}) was added and the cells incubated at 37°C for

10 min. The DNA was stained by adding 20 µl of PI (50 µg ml^{-1}) to the cells and incubating for 2 h at RT prior to FCM analysis, as described below.

5.2.7 Flow cytometry analysis

For each measurement of cell proliferation (Ki-67) and the cell cycle (BrdU + PI), data (1 x 10^4 single cell events) were collected using a FACS Scan flow cytometer (Becton-Dickinson). In cell proliferation experiments, FITC (FL1 channel, green fluorescence) signals resulting from Ki-67-positive immunostaining were collected in the logarithmic mode. Similarly, for cell cycle analysis, positive immunostaining of the cells with FITC-conjugated BrdU antibody produced green fluorescence which was also collected in the logarithmic mode, while PI (FL3 channel, red fluorescence) was collected in the linear mode. Cell aggregates and doublets were excluded during data analysis, and net fluorescence levels for each antigen were calculated by subtracting the negative control values (i.e., cells treated with non specific IgG) from those obtained using the specific primary antibody. Since the fluorescent dyes used here have substantial spectral overlap [Ormerod2000], the compensation was adjusted so that the FITC-labelled cells (peak emission 520 nm) were detected only in the FLI channel and the PI-labelled cells (peak emission 639 nm) only in the FL3 channel. The data were analyzed using WinMDI software (version 2.8).

5.2.8 Measurement of mitotic figures

To determine whether Ca implantation of Ti affected the M phase of the cell cycle, the numbers of metaphase figures, i.e. mitotic cells showing

characteristic condensed nuclei (Figure 6.2), were quantified using phase contrast microscopy, as follows. MG-63 cells cultured on the Ti (control) and Ca (high)-Ti discs were synchronised using HU, released from G1/S arrest and re-cultured in the presence of colcemid, as described above. The cells were harvested from the discs at 2, 4, 6, 8, 10 and 12 h after HU removal and fixed in 70% ethanol at -20°C for 18 h. The fixed cells were washed with PBS and 5 µl were placed on poly l-lysine coated slides, air dried and stained with haematoxylin to visualise metaphase figures, as previously described [White et al. 1998]. A total of 250 cells were counted in 10 separate fields under a phase contrast microscope at a magnification of x 200. Based on the cell/nuclear dimensions, the mitotic cells were identified and their numbers were scored for both the Ti (control) and Ca-Ti surfaces using digital image analysis.

5.2.9 *Statistical analysis*

The SEM was determined for the results of all the experiments, which were conducted 3 times. Data were analysed by the Student's *t*-test for paired samples using SPSS 11.0 software (SPSS). A p value of ≤ 0.05 was considered to be statistically significant.

5.3 Results

5.3.1 Effects of calcium-implantation levels on MG-63 cell proliferation

The incorporation of [^{3}H] thymidine by MG-63 cells cultured on Ti (control), Ca (high)-Ti, Ca (med)-Ti and Ca (low)-Ti discs was measured over a period of 4 consecutive days, as described in section 5.2.3.

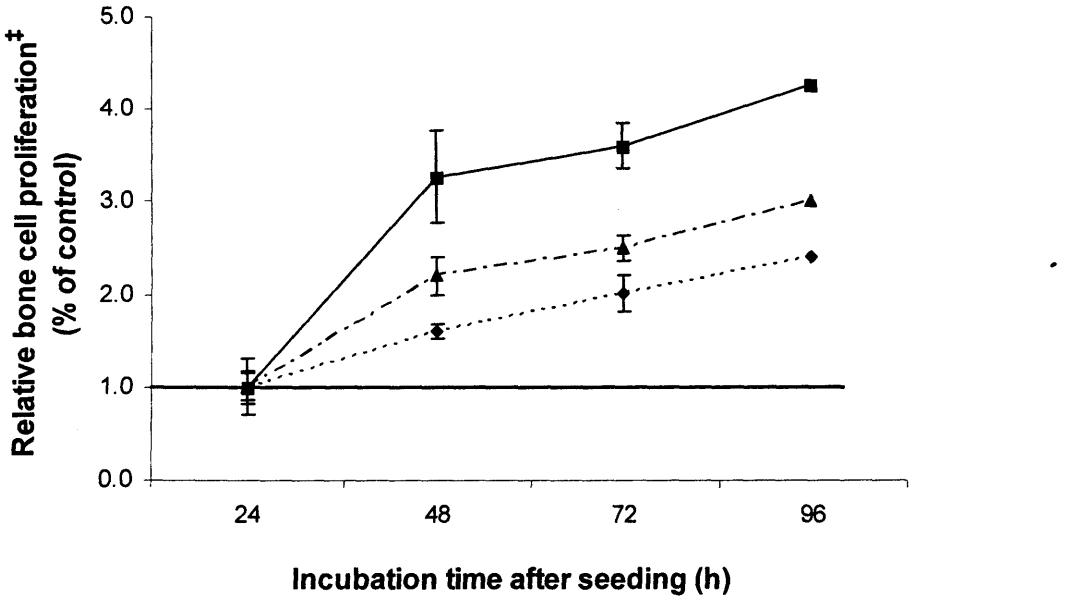

Figure 5.4: Growth of MG-63 cells on Ca (high)-Ti (■—■), Ca (med)-Ti (▲– · – ▲) and Ca (low)-Ti (♦- -♦) discs measured at 48, 72 and 96 h after initial seeding. Relative changes in cell number were adjusted for differences in the numbers of cells which had originally attached to the different surfaces, which was measured 24 h after seeding, as described in the Materials and Methods. ‡The values shown are relative to the number of cells present on the Ti (control) discs, defined as 1.0 on each day indicated by the horizontal bar. Note the significantly increased number of bone cells on Ca (high)-Ti at 48, 72 and 96 h of incubation ($p \leq 0.05$).

Figure 5.4 shows the proliferation of MG-63 cells on these Ca-Ti discs relative to the numbers of cells on Ti (control) surfaces after 48, 72 and 96 h of cell culture. Ca (high)-Ti surfaces seemed to have elicited a significant enhancement in the growth of cells compared with that on the Ti (control) discs (Figure 5.4). An initial burst (approximately 3-fold increase) in DNA synthesis was measured on Ca (high)-Ti discs from 24 ($5x10^3$cells) to 48 h ($1.3x10^4$) after cell culture ($p = 0.02$). This was followed by a gradual increase in [^{3}H] thymidine uptake by cells on this particular surface, such that by 96 h of incubation a 4-fold

increase in the number of cells cultured on Ca (high)-Ti discs was seen compared with the Ti (control) surfaces ($p = 0.01$). Although the numbers of cells measured each day on Ca (med)-Ti and Ca (low)-Ti were also greater than the control values (Figure 5.4), the differences were found not to be of statistical significance ($p > 0.05$).

5.3.2 Influence of calcium ion-implantation on the proportion of Ki-67 positive cells

The expression of the proliferation-associated Ki-67 antigen by MG-63 cells cultured on the Ti (control), Ca (high)-Ti, Ca (med)-Ti and Ca (low)-Ti discs was determined on 3 consecutive days, as described in section 5.2.4. The results presented in Figure 5.5 show that there was a significantly higher percentage of Ki-67 positive cells on the Ca (high)-Ti discs at all times tested (52% ±1.8, 61% ±1.2 and 70% ±2.4 on days 1, 2 and 3 respectively) compared with those cultured on the Ti (control) discs (34% ±2, 44% ±3.5 and 50% ±1.2, respectively). Thus, compared with the control, implantation of high doses of Ca ions on Ti surfaces caused a statistically significant increase in the proliferation of osteoblast-like MG-63 cells ($p = 0.02$, 0.05 and 0.01 on days 1, 2 and 3, respectively). In contrast, both Ca (med)-Ti and Ca (low)-Ti surfaces failed to elicit any significant increase in the proportions of Ki-67 positive cells, which were determined each day, in comparison with the control (Figure 5.5) ($p > 0.05$). For these reasons, Ca (med)-Ti and Ca (low)-Ti surfaces were not

included in the experiments conducted to examine the effects of Ca ion-implantation of Ti on the specific phases of the cell cycle.

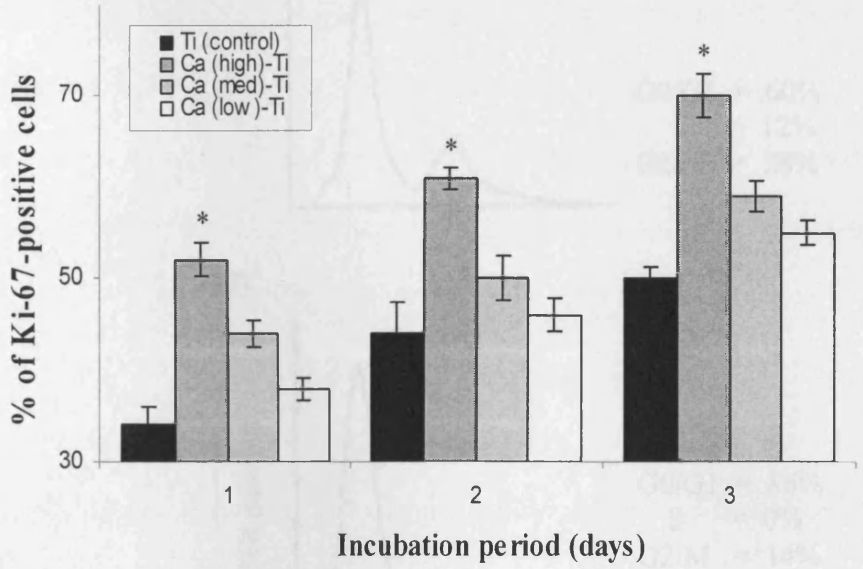

Figure 5.5: The proportion of cells positive for Ki-67 antigen after growth on Ti (control), Ca (high)-Ti, Ca (med)-Ti and Ca (low)-Ti surfaces measured on 3 consecutive days. Error bars show SEM from 3 replicate experiments. Note the significantly higher percentage of cycling cells each day on Ca (high)-Ti compared with the substantially lower proportions on Ti (control), as denoted by the asterisk ($p \leq 0.05$).

5.3.3 Synchronisation of MG-63 cells by hydroxyurea and colcemid

The ability of HU and colcemid to synchronize MG63 cell cultures was examined by measuring the DNA content of replicate untreated control and drug-treated cultures. The results in Figure 5.6 (A) shows that in exponentially growing control cultures there are two main peaks, the left peak representing 60% of the total cells which have a 2n DNA content (124 AFI units), while the

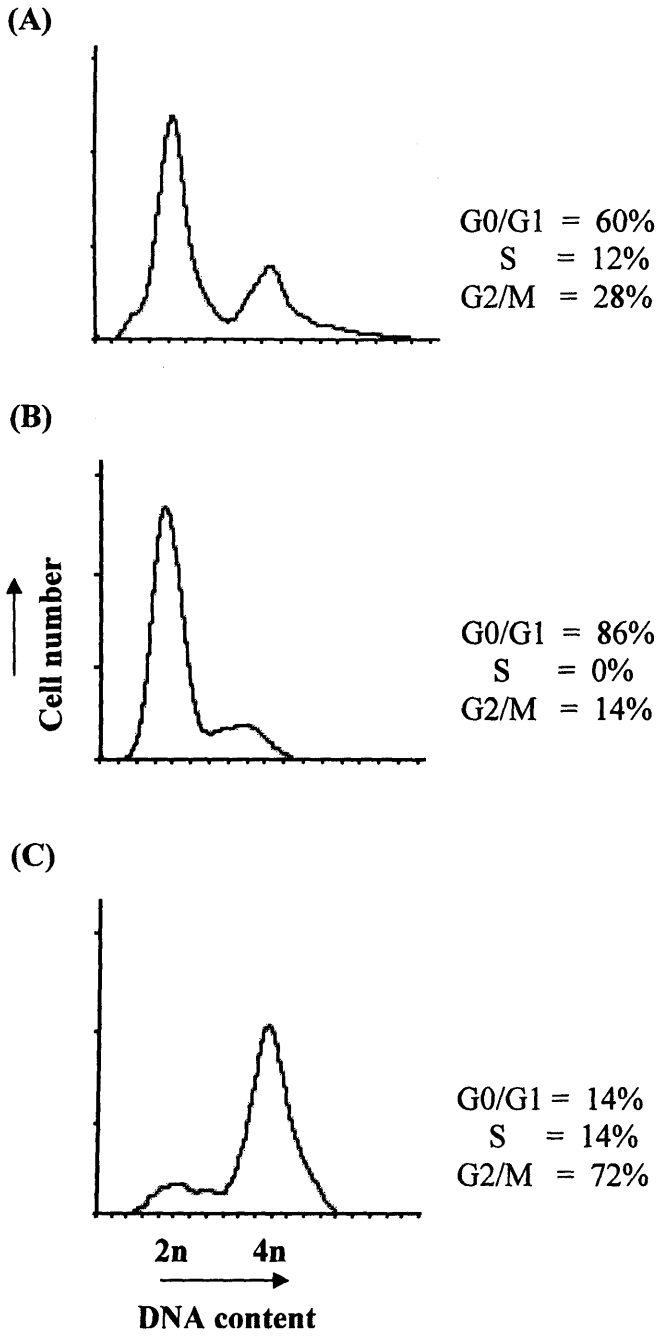

Figure 5.6: FCM analysis of PI-stained MG-63 cells showing the DNA content of control (untreated) (A), HU treated (B) and colcemid treated (C) cultures. Note two prominent peaks of cells with 2n and 4n levels of DNA in control cultures, while most of the cells in (B) and (C) primarily had either 2n or 4n DNA content, respectively.

right peak comprises 28% of the total cells which are in the G2/M phase of the -63 cell cell cycle (having a DNA content of 4n). S phase cells were therefore calculated to comprise approximately 12% of the population. However, treatment of the MG-63 cells with HU was found to have effectively synchronised them, as 86% were found to have 2n DNA and 14% were in G2/M, with no cells calculated to be in S phase (Figure. 5.6 (B)). The removal of HU and re-culture for 12 h in the presence of colcemid resulted in the progression of the majority of the cells (72%) into G2/M, with only 14% remaining in G0/G1 and 14% still in S phase (Figure 5.6 (C)). These findings confirm that HU can be used to achieve synchronisation of MGcultures and further, that treatment with colcemid arrests them at 4n and largely prevents their 'escape' into the next cell cycle.

5.3.4 Influence of calcium-implantation on cell cycle progression

To measure the effects of Ca (high)-Ti surfaces on the movement of cells through the different phases of the cell cycle, changes in DNA synthesis were assessed in conjunction with changes in DNA content at different time points after cessation of HU-induced growth arrest. MG63 cells cultured on the Ti (control) and Ca (high)-Ti discs were released from HU arrest and harvested after 2, 4, 6, 8, 10 and 12 h, then double-stained with PI and BrdU-FITC. Figure 5.7 (A) shows that at 2 h following cessation of HU-induced growth arrest, 72% of the Ti (control) cells were still in the G0/G1 phase but only 36% of the Ca-Ti cells had a 2n DNA level. Moreover, this relatively low proportion of G0/G1 cells on the Ca (high)-Ti discs was accompanied by a significantly elevated proportion

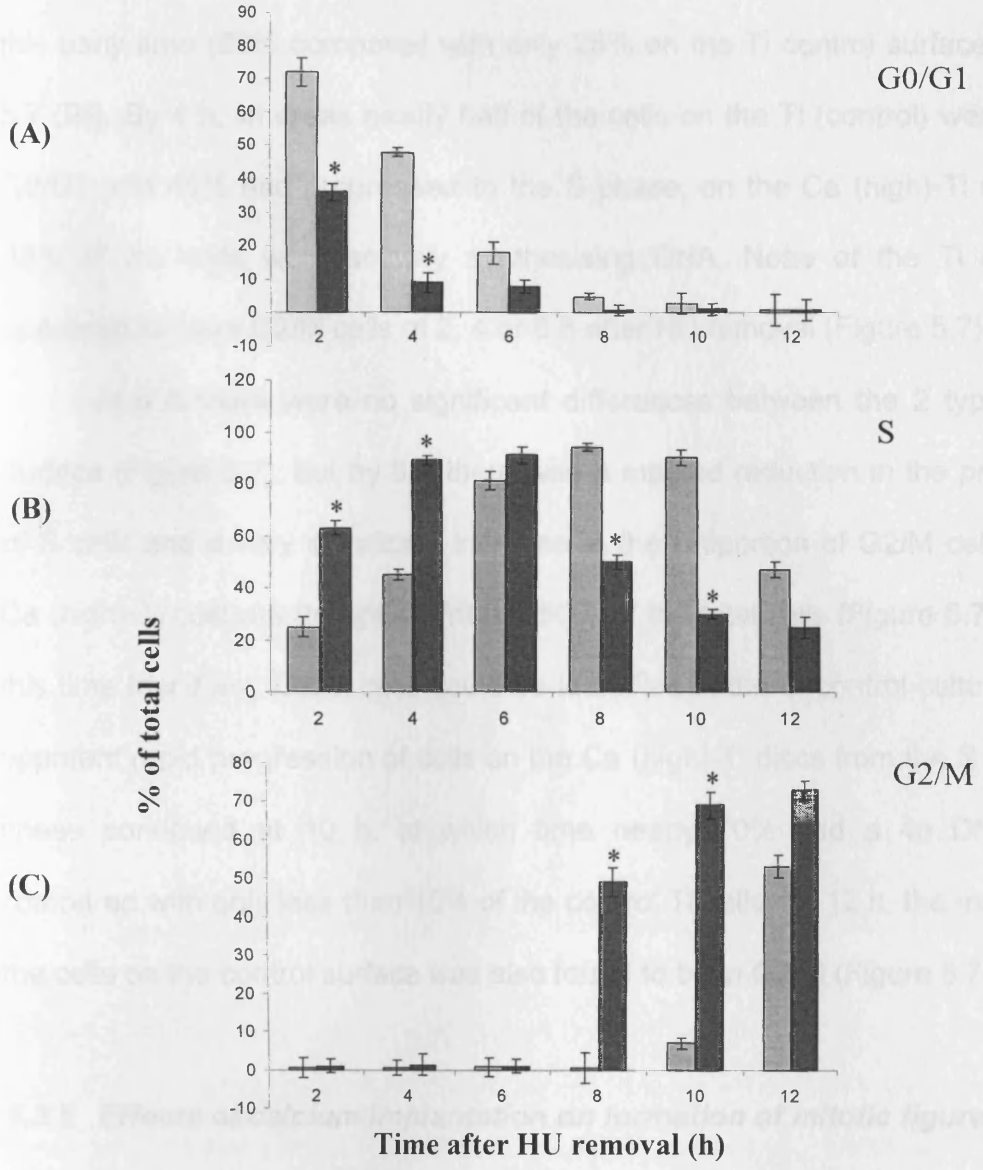

Figure 5.7: Progression of cells through different phases of the cell cycle in response to Ca ion-implantation of Ti. MG-63 cells were incubated on Ti (control) discs (grey bars) and Ca (high)-Ti surfaces (black bars). Data are presented as the percentage of total cells measured by FCM at each time point after the removal of HU and show a summary of three replicate experiments (error bars indicate average values ± SEM). Significant differences, between Ti (control) and Ca-Ti surfaces, in the proportion of cells accumulating in G0/G1 (A), S (B) and G2/M (C) phases of cell cycle are indicated by asterisks ($p \leq 0.05$).

of cells which had progressed into S phase (BrdU-positive) on this surface at this early time (63% compared with only 25% on the Ti control surface (Figure 5.7 (B)). By 4 h, whereas nearly half of the cells on the Ti (control) were still in G0/G1 and 45% had progressed to the S phase, on the Ca (high)-Ti surfaces 89% of the cells were actively synthesising DNA. None of the Ti surfaces appeared to have G2/M cells at 2, 4 or 6 h after HU removal (Figure 5.7).

At 6 h there were no significant differences between the 2 types of Ti surface (Figure 5.7), but by 8 h there was a marked reduction in the proportion of S cells and a very significant increase in the proportion of G2/M cells in the Ca (high)-Ti cultures (to approximately 50% of the total cells (Figure 5.7 (C)). At this time few if any G2/M cells could be identified in the Ti control cultures. The apparent rapid progression of cells on the Ca (high)-Ti discs from the S to G2/M phase continued at 10 h, at which time nearly 70% had a 4n DNA level compared with only less than 10% of the control Ti cells. By 12 h, the majority of the cells on the control surface was also found to be in G2/M (Figure 5.7 (C)).

5.3.5 Effects of calcium implantation on formation of mitotic figures

In order to identify M cells specifically, since both these and G2 cells have a 4n DNA content, the numbers of mitotic cells were microscopically quantified. The representative phase contrast micrographs in Figure 5.8 show that 8 h after HU removal, the Ca (high)-Ti surfaces contain a relatively high proportion of large rounded cells with condensed chromosomes compared with the Ti (control) cultures, in which few if any of these mitotic cells were observed. Analysis of the changes in numbers of M cells following release from HU-

induced growth arrest in the presence of colcemid is summarised in Table 5.1, and shows that there was a statistically significant increase in the proportion of mitotic cells on the Ca (high)-Ti surfaces compared with the Ti (control) discs at 8, 10 and 12 h (p = 0.01, 0.03 and 0.01, respectively) following HU removal. At 8 h after cessation of HU-induced growth arrest only 1% of cells on the control surfaces were identified as mitotic in comparison with a noticeable 36% on the Ca (high)-Ti discs (Table 5.1).

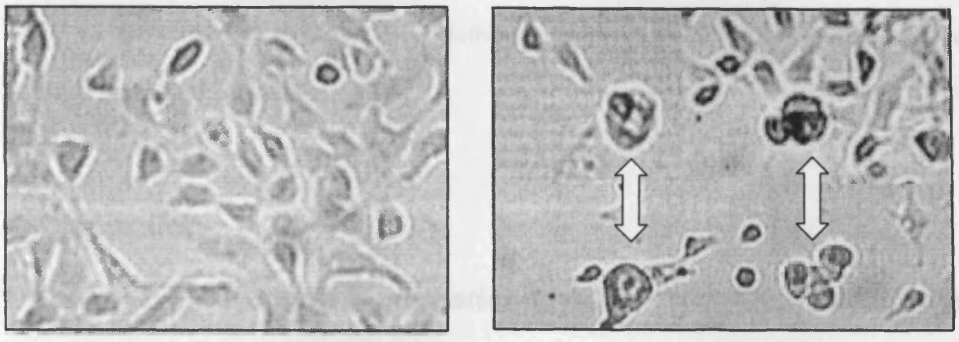

Ti (control) **Ca (high)-Ti**

Figure 5.8: Effects of Ca (high) implantation of Ti on mitotic counts of colcemid treated MG-63 cells 8 h after HU removal. Cells trapped in metaphase were stained with haematoxylin and visualised by phase contrast microscope at a magnification of x 400. Mitotic figures were not detected among the cells from Ti (control) surfaces at this time point. In contrast, a greater proportion of cells in metaphase arrest (indicated by arrows) were seen for Ca (high)-Ti. Note that the nuclei in these cells appear to be larger than those in cultures from control discs.

Table 5.1: Effects of Ca (high)-implantation of Ti on mitotic counts

Time after HU removal (h)	Number of mitotic figures		% of total cells counted	
	Ti (control)	Ca (high)-Ti	Ti (control)	Ca (high)-Ti
2	0	2	0%	0%
4	1	4	0%	1%
6	2	20	0%	8%
8	4	89	1%	**36%***
10	13	144	5%	**58%***
12	66	159	27%	**64%***

A total of 250 cells from 10 random fields of phase contrast micrographs were counted at each time point, as described in Materials and Methods. Statistically significant differences at 8, 10 and 12 h are denoted by asterisks ($p \leq 0.05$).

5.4 Discussion

5.4.1 Influence of calcium implantation levels on MG-63 cell proliferation

Experiments presented in this chapter measured the effects of different levels of Ca ion-implantation on cell proliferation. The results demonstrated that both the change in the number of [^{3}H] thymidine labelled cells and the proportion of Ki-67 positive (non-G0/G1 cycling) cells were enhanced on Ca ion-implanted surfaces compared with the Ti (control) discs. However, this response was dependent on the dose at which Ca ions were implanted on the surfaces of Ti discs. While the proliferation of bone-like cells on Ca (high)-Ti surfaces was significantly elevated over a period of 3-4 days, the same increase was not observed on the Ca (med)–Ti and/or Ca (low)–Ti surfaces, which remained very similar to the control levels.

Although expression levels of cell proliferation-associated Ki-67 antigen have previously been shown to be affected by the nature of the substrate [Van Kooten et al. 2000], the current study is the first to establish that the Ca ion-implantation of Ti enhanced the proportion of Ki-67 positive cells *in vitro*. Van Kooten et al cultured human umbilical vein endothelial cells in direct contact of Ti, NiCr alloy, and CoCr alloy discs and assessed expression of Ki-67 antigen by these cells using immunofluorescence and FCM after 48 and 72 h of incubation. Differences in the expression patterns of Ki-67 antigen by endothelial cells were observed between substrates and at different periods of incubations [Van Kooten et al. 2000].

Cells derive Ca ions from both internal and external sources. Ca ions can act within milliseconds in highly localized regions [Berridge et al. 1995; Berridge1998; Berridge2001]. Previous studies measured the release of Ca ions from Ti discs implanted with 1 x 10^{17} Ca ions cm^{-2}, into nitric acid solutions and phosphate citric acid buffers [Hanawa et al. 1996a; Hanawa et al. 1996b]. The findings of the experiments conducted by the Biomatrials group also confirmed the release of Ca ions from Ca (high)-Ti surfaces in water using ion-chromatography (Appendix A). After 2 min immersion at 37°C in 1 ml water; Ca ion concentrations of 0.13 (± 0.09) ppm were detected, compared to control values of 0.07 (± 0.07). After 4 h immersion, the Ca concentration had increased to 1.27 (± 0.18) ppm. The reactivity of Ca-implanted surfaces was also examined by XPS. The results showed that after 24 h immersion in water at 37°C, the Ca/Ti ratio was reduced to around a third of its original value

(Appendix A). It is noteworthy that the levels of Ca detected were very much lower than the levels present in simulated biofluids such as HBSS (66 ppm) and DMEM (95 ppm) (Appendix A). Nevertheless, concurrent with the previous findings of Ca ion dose-dependence of cell adhesion (Chapter 4), the present results of the effects of different levels of Ca ion-implantation on cell proliferation *in vitro* indicate that the quantities of Ca ions released only from the Ca (high)-Ti surfaces but not from Ca (med)-Ti or Ca (low)-Ti, might have been biologically beneficial. This hypothesis was further strengthened by the findings of a previous *in vivo* study which reported that the early bone formation around Ti implanted with 1×10^{17} Ca ions cm^{-2} was favoured by the local microdissolution of Ca ions [Hanawa et al. 1997].

Cells are guided by physical and chemical signals received from their environments. Integrins act as signalling receptors and transmit growth regulatory signals from the ECM to the cell [Hynes2002; Hynes1992; Juliano and Haskill 1993]. Integrin-mediated cell anchorage to the ECM activates downstream cell-signalling pathways, in particular, $\alpha 5\beta 1$ is central to regulating the downstream events such as cell-cycle progression and cell growth. [Vogel and Baneyx 2003; Varner et al. 1995; Roovers et al. 1999]. Since Ca (high)-Ti surface caused an up-regulation of $\alpha 5\beta 1$ integrin expression by osteoblast-like cells (Chapter 4), it can be speculated that the enhanced proportion of cycling Ki-67-positive cells and the increased DNA synthesis found on Ca (high)-Ti discs in the current study, may have been triggered specifically via $\alpha 5\beta 1$-mediated cell-signalling pathway. Varner et al previously reported that the

binding of α5β1 integrin receptor in HT29 colon carcinoma cells to a fibronectin substratum activated a signalling pathway which lead to proliferation of these transformed cells [Varner et al. 1995]. A previous study suggested that integrin α5β1 mediates fibronectin-induced epithelial cell proliferation through activation of the epidermal growth factor receptor (EGFR). Human integrin α5 was transfected into the integrin α5β1–negative intestinal epithelial cell line Caco-2 to study EGFR and integrin α5β1 signalling interactions involved in epithelial cell proliferation. Their results showed that EGFR kinase activity was necessary for integrin α5β1–mediated cell proliferation. EGFR activation occurred when either the integrin α5–transfected or control cells were cultured on fibronectin. They concluded that a coordinated input from both growth factor receptors and integrins is necessary for cell proliferation [Kuwada and Li 2000]. Thus the enhanced cell proliferation seen here on the Ca (high)-Ti surfaces may have been triggered, at least partly, due to the α5β1-mediated intracellular signalling pathways.

5.4.2 Effects of calcium-implantation on cell cycle progression

To elucidate the possible mechanisms that could mediate enhanced cell proliferation on Ca (high)-Ti discs, analysis of the cell cycle was carried out. Results of the current study show that the synchronised MG-63 cells cultured on the Ca (high)-Ti surfaces and released from HU-induced cell cycle arrest at the G1/S boundary were found to progress significantly more rapidly from G0/G1 into S phase, and from S phase in G2/M compared with cells which had been

cultured on the non-implanted Ti discs. In addition, Ca ion-implantation of Ti also induced a significantly more rapid increase in the proportion of mitotic cells.

The results presented in this chapter also show that a greater proportion of synchronised MG-63 cells present on the Ca-Ti surfaces progressed out of G0/G1 and entered the S phase as early as 2 h after the removal of HU. In contrast to this apparent Ca implantation-induced acceleration, MG-63 cells on the non-implanted Ti re-entered the cell cycle much more slowly, possibly because they may have been blocked at some point prior to or at the G1/S transition. Notably, a previous study of the effects of orthopaedic cements on MG63 cells showed that their effect was also mediated via initiation of the replication cycle [Granchi et al. 1995a, Granchi et al. 1995b]. Granchi et al investigated the effects of orthopaedic implant materials on the progression of MG-63 cells through different phases of the cell cycle by measuring BrdU incorporation in conjunction with PI staining [Granchi et al. 1995a]. Five different cements were mixed and extracted at different time intervals. Cell cycle phases of MG63 cells were evaluated at 24, 48 and 72 h by FCM; the DNA content was assessed using PI uptake and the percentage of cells in the S phase was determined using BrdU uptake. The cements examined in this study were shown to have inhibited cell proliferation and the MG-63 cells exposed to the most toxic cements had more difficulties in starting their replication cycle [Granchi et al., 1995a]. Similarly, when Lopes et al studied the effects of HA and P_2O_5 glass-reinforced HA composite on the progression of MG-63 cell cycle, a statistically significant reduction in the proportion of S phase cells on the glass-reinforced HA composite discs was observed. FCM profiles were obtained for the DNA

content of PI-stained cells 36 h after plating on these substrates. Compared with both the control (cells grown on polystyrene culture dishes) and HA, a greater proportion of MG-63 cells on glass-reinforced HA composite discs accumulated in the G0/G1 of the cell cycle. It was suggested that the glass-reinforced HA composite might have caused some inhibition of cell cycle progression, possibly by delaying the entry of G0/G1 cells into the S phase [Lopes et al. 1998].

In order to pursue an ordered series of molecular events, the initiation of an event during cell cycle progression is dependent on the successful completion of an earlier event. Transition of cells from G1 to S phase is considered to be the most critical step in the control of cell proliferation. It is during the G1 phase that the cell integrates mitogenic and growth inhibitory signals and makes the decision to proceed, pause, or exit the cell cycle [Norbury and Nurse, 1992]. Although the precise mechanisms are not known, delayed movement of MG-63 cells cultured on Ti (control) surfaces could be due to down-regulation of some of the important proteins required for transition from G1 to S phase. The overall process of the control of progression through decision points of the cell cycle is very complicated and involves coordinated regulation of the multiple biochemical pathways. Cyclins were identified as key components providing the primary means of cell cycle regulation [Murray, 2004]. These proteins whose accumulation and degradation oscillated during the cell cycle, were first identified in marine invertebrates [Rosenthal et al. 1980].

Mammalian cells contain multiple cyclins which bind with cyclin-dependent kinases (cdks) to regulate the cell cycle progression. Cdk activities are regulated by cyclin binding and phosphorylation of a tumour suppressor

retinoblastoma protein (pRb). As cells progress through G1, cyclin D/cdk4 complexes once activated, phosphorylate pRb. Next, cyclin E/cdk2 complexes are formed and phosphorylate pRb in a sequential manner. The hyperphosphorylation of pRb enables the activity of E2F transcription factors, which, in turn, regulate the expression of numerous proteins required for S phase progression. As cells enter S phase, cyclin A/cdk2 becomes activated, and remains activated into G2 phase. In late G2, cyclin B/cdk1 (cdk1 in higher eukaryotes and cdc2 in yeasts) is activated, allowing entry into mitosis. Specific cdk inhibitors (CKI) proteins have been identified which associate with cdk or cyclin/cdk complex to prevent activation. The two classes of CKI are the p21/p27 family, whose members associate with both cdk2 and cdk4, and the p15/p16 family, whose members associate with only cdk4/cdk6 [Norbury and Nurse 1992; Johnson and Walker 1999; Murray2004; Zhu et al. 1996; Jackman et al. 2003].

The sequential synthesis, activation, and subsequent inactivation of cyclin/cdk complexes govern transitions during the cell cycle phases. Cyclin E is a positive regulator of the G1 to S phase transition of the cell cycle. In complex with cdk2 it is responsible for committing the cell to another round of cell division [Wingate et al. 2003]. A previous study demonstrated the significance of cyclin E-cdk2 complex in the regulation of G1 phase in the MG-63 cells [Merli et al. 1999]. These authors investigated the role of cyclin E, cyclin D1, cdk2, cdk4, phosphorylation of pRb, and cell cycle inhibitors p21 in the cell cycle progression of MG-63 cells. To detect expression levels of these proteins MG-63 cells were treated with tumor necrosis factor-alpha (TNF-alpha) and interleukin-6 (IL-6).

Cell proliferation analysis demonstrated an increased proliferation of MG-63 cells with IL-6, while TNF-alpha acted as an anti-proliferative agent. Using immunoblotting technique, they showed an increased expression of p21 with TNF-alpha and its complex with cdk2. Although TNF-alpha reduced the expression of the cyclin E/cdk2 complex, it did not affect the amount of cyclin D1, cyclin E, cdk4, cdk2, and of cyclin D1-cdk4 complex. Treatment with IL-6 decreased p21 expression and its complex with cdk2, while it increased the expression of cyclin E/cdk2 complex, cyclin D1 and cdk4 expression and their complex did not change on exposure of MG-63 cell cultures to IL-6. Moreover, hyperphosphorylated/dephosphorylated pRb protein ratio was reduced with TNF-alpha, whereas it increased with IL-6. Based on these findings Merli et al suggested that cyclin E-cdk2 complex and p21 play an important role in the G1 phase regulation of MG-63 cells through pRb phosphorylation [Merli et al. 1999]. Therefore, it can be speculated that, in the current study, the Ca (high)-Ti surfaces might have increased the cell cycle progression by affecting the transition of HU-synchronised MG-63 cells from G1 to S phase possibly via increasing the activity of cyclin E/cdk2 complex as a result of pRb phosphorylation or by down-regulating the expression of cell cycle inhibitor p21.

5.4.3 Influence of calcium-implantation of titanium on mitosis

By using colcemid and counting mitotic figures it was possible to separate the M phase specifically from the G2+M, the results showing that although the Ca-Ti surfaces had no effect on the proportion of 4n DNA cells, there was nevertheless a significantly greater proportion of mitotic cells present on this

surface compared with the Ti (control) discs. Thus, at 12 h after release from HU-induced growth arrest, the majority of cells on the Ca-Ti surface had already progressed from the G2 to M phase, whereas the majority of 4n cells seen on the Ti (control) discs were still in G2. Ca implantation of Ti therefore not only enhanced the transition of the MG-63 cells from G1 to S, but also appears to have prompted a more rapid progression from the G2 to M phase of the cell cycle.

Although not yet completely understood, the sequence of events that constitutes the cell cycle is carefully regulated. A part of this regulation depends upon the ubiquitous Ca signalling system. Ca, an intracellular second messenger, is known to be a growth-regulating divalent cation [Berridge et al. 1995; Berridge1998; Berridge2001]. Regulation of the cell cycle by Ca ions has been extensively reviewed in the past [Kahl and Means 2003; Means1994; Lu and Means 1993; Takuwa et al. 1995]. While the precise role of the Ca implanted into Ti remains unclear, this ion, and its ubiquitous intracellular receptor calmodulin, is well known to be a major growth-regulating molecule [Berridge et al. 1998; Berridge1995; Berridge2001] to have a fundamental role in cell cycle control [Kahl and Means 2003; Means1994; Lu and Means 1993; Takuwa et al. 1995], with the Ca-calmodulin complex generating a cascade of events which activates the immediate early genes responsible for inducing resting G0 cells to re-enter the cell cycle [Kahl and Means 2003] and also promoting the initiation of DNA synthesis at the G1/S transition [Means1994]. Additionally, the G2/M and metaphase/anaphase transitions in M phase are known to be sensitive to the concentration of both calmodulin and Ca ions [Kahl

and Means 2003; Means1994; Lu and Means 1993; Takuwa et al. 1995]. To address the underlying molecular mechanisms by which Ca/calmodulin regulated cell cycle progression, Lu and Means used single-celled eukaryotic organism such as *Asperigillus nidulans* [Lu and Means, 1993]. Using this system, these authors demonstrated that Ca and calmodulin are selectively required for the activation of two mitotic protein kinases cdk1(cdc2) and NIMA, during the G2 to M transition in *A. nidulans* [Lu and Means, 1993]. It is thus possible that the presence of Ca ions at the Ti surface may be an important factor in activation of the cyclin B/cdk1 complex, and hence the apparently brisk progression of the MG-63 cells from G2 to M phase of the cell cycle.

5.5 Conclusions

- Ca ion-implantation of Ti surfaces affected the proliferative activity of the cultured osteoblast-like cells in a dose-dependent manner.
- The proportion of cycling cells which were actively synthesising DNA was markedly enhanced on the Ca (high)-Ti surfaces compared with the Ti (control) discs.
- Synchronised MG-63 cells cultured on the Ca (high)-Ti surfaces progressed through G0/G1, S and G2/M phases of the cell cycle more rapidly than those on the control discs.
- Ca (high) implantation of Ti induced a significant increase in the proportion of actively dividing mitotic cells.

Chapter 6

Effects of Calcium Ion-Implantation of Titanium on MG-63 Cell Function

6.0 Introduction

Bone is a complex tissue consisting of mineral and cellular phases. Osteoblasts are the cuboidal, basophilic cells found on the bone surfaces with eccentric nuclei, large Golgi complex, abundant mitochondria and extensive endoplasmic reticulum studded with ribosomes [Aubin2001]. These features are the hallmarks of a cell with considerable capability for synthesising protein and this is reflected in the wide range of products formed by the osteoblasts [Mackie2003].

Previous studies have shown that, following proliferation, osteoblasts differentiate and secrete a complex array of extracellular matrix (ECM) components which subsequently mineralizes to form mature calcified bone [Friedenstein et al. 1987; Mackie2003]. Osteoblasts contribute to the process of mineralization (deposition of HA crystals) through the provision of certain ECM proteins. The ECM itself also exerts a profound effect on cell function [Locci et al., 1997], including on the production of essential bone-associated constituents such as alkaline phosphatase (ALP), bone sialoprotein (BSP), osteonectin (ON), osteopontin (OPN) and growth factors (for example, bone morphogenetic protein, BMP) [Boskey1989; Denhardt and Guo 1993; Mundy1995; Suzawa et al. 1999]. Evaluation of such osteogenic 'markers' can thus be used to gain valuable information about the potential biocompatibility of new or modified implant materials *in vivo* [Kirkpatrick et al. 1997], and the experiments presented in this chapter have therefore evaluated the effects of Ca ion-implantation of Ti on the expression of these key bone components by osteoblast-like MG-63 cells *in vitro*.

6.1 Background

6.1.1. Alkaline phosphatase

ALP is an enzyme which regulates phosphate metabolism. It is expressed during the post-proliferative period. Osteoblasts have high levels of this membrane-bound enzyme, which is also a receptor for tissue-specific hormones, such as parathyroid hormone, as well as cytokines, other hormones and growth factors, which regulate bone growth, differentiation and metabolism [Rodan and Noda 1991]. ALP plays a role in matrix mineralization There is good evidence from experimental manipulation *in vitro* and from ALP mutations leading to hypophosphatasia (a rare inheritable disorder characterised by defective bone mineralization due to deficiency of ALP activity) in man, that ALP is involved in the bone mineralization process [Aubin2001]. ALP affects progressive differentiation of pre-osteoblasts into mature osteoblasts [Aronow et al., 1990;Mackie, 2003] and is therefore extensively used as a marker of bone differentiation *in vitro* [Boyan et al. 1998; Lincks et al. 1998; Martin et al. 1995; Montanero et al. 2002]. By forcing expression of ALP by transfection of a variety of cell lines, it has been suggested that this molecule regulates cell proliferation, migration and differentiation, and thus can also be used as an osteogenic marker of these transformed cells [Hui et al. 1996].

It has been shown previously that the micro-topographical differences of Ti surfaces markedly influence ALP specific activity in osteoblast-like MG-63 cells [Boyan et al. 1998; Lincks et al. 1998; Martin et al. 1995; Montanero et al. 2002]. Boyan et al cultured MG63 cells on Ti surfaces roughened via acid

etching, sand-blasting or plasma-spraying with Ti particles, and the cellular responses measured were compared with the control standard tissue culture polystyrene [Boyan et al. 1998]. These authors reported that the ALP activity was affected by Ti surface roughness; as the surface became rougher, the MG-63 cells showed a significant increase in ALP activity [Boyan et al. 1998].

Another study determined the effect of chemical composition and surface roughness of cpTi and Ti-6Al-4V (Ti-A) on MG63 cells. Ti discs were machined and either fine-polished or wet-ground, resulting in smooth (S) and rough (R) finishes, respectively [Lincks et al. 1998]. Standard tissue culture plastic was used as a control. The effects on ALP specific activity were evaluated 24 h post-confluence. When compared to plastic, the stimulatory effect of surface roughness on ALP specific activity was more pronounced on the rougher surfaces, with enzyme activity on Ti-R being greater than on Ti-A-R. Lincks et al. 1998 further reported that the surface composition of Ti discs also played a role in cell differentiation, since cells cultured on Ti-R surfaces had more ALP specific activity than those cultured on Ti-A-R [Lincks et al. 1998]. In another study, MG63 osteoblast-like cells were seeded onto two fluorohydroxyapatite (FHA)-coated Ti6Al4V materials differing in roughness [LR-FHA (Ra = 5.6 microm) and HR-FHA (Ra = 21.2 microm) [Montanero et al. 2002]. Their results established that both types of coatings caused a significant increase in ALP activity with respect to the control, and that the roughest surfaces exhibited a more prolonged effect [Montanero et al. 2002].

It was reported that when cells, derived from the same patient, were grown on Ti discs, they responded even to small differences in the material

surface chemistry and/or microcrystallinity [Zreiqat and Howlett 1999]. These authors investigated the influence of cpTi and Ti-6Al-4V on the expression of osteoblastic proteins such as ALP, thrombospondin, OPN, OC, ON, Col I and BSP by HBDCs grown for 5, 7, 10, and 14 days. At the four predetermined time points, cells grown on either cpTi or Ti-6Al-4V generally expressed similar mRNA levels, while levels of their respective proteins, measured using a quantitative immunohistochemistry assay, differed. Cells on cpTi had peak levels for most proteins at day 7, and those on Ti-6Al-4V peaked at either day 5 and/or day 7. At day 5, cells grown on Ti-6Al-4V had higher levels of ALP, Col I, ON, OC, and BSP than those in cpTi [Zreiqat and Howlett 1999].

Changing the surface chemistry of cpTi discs by the ion-implantation process has been reported to have no effect on the specific activity of ALP [Krupa et al. 2001a; Krupa et al. 2002]. Krupa et al measured the ALP activity after 8 days of exposure of human osteoblasts to the Ti samples. The differences in the enzymatic activity of ALP by HBDC cultured on Ca- and/or P ion-implanted Ti discs compared to the non-implanted Ti were found to be of no statistical significance [Krupa et al. 2001a; Krupa et al. 2002]. In contrast to the approach of Krupa et al, the effects of Ca-Ti surfaces on the expression levels of ALP were measured in the current study. Thus instead of measuring ALP specific activity, as a marker of bone differentiation, its expression by osteoblast-like MG-63 cells was determined in order to investigate the influence of Ca-Ti surfaces on bone cell function *in vitro*, as previously described [Zreiqat and Howlett 1999].

6.1.2 Bone morphogenetic protein receptor

Growth factors are naturally occurring biological mediators that may act locally or systemically to affect the growth and function of the cells. Osteoblasts are known to produce a variety of the growth factors such as insulin-like growth factors I and II (IGF-I, IGF-II) transforming growth factor (TGF-β1, TGF-β2), platelet-derived growth factor and basic and acidic fibroblast growth factor. These growth factors secreted by bone cells have acute effects on their neighbouring osteoblastic cells (paracrine action) or on themselves (autocrine action) [Baylink et al. 1993; Mohan and Baylink 1991; Mundy1995].

Bone morphogenetic protein (BMP), named for their ability to induce the formation of bone [Urist1965; Wozney et al. 1988], belong to a large family of structurally related growth factors called TGF-β superfamily. Over 20 BMP family members have been identified to date. BMPs stimulate osteoblast proliferation differentiation and also the production of ECM [Ten et al. 2003]. Like other members of TGF-β family, BMPs exert their effects through serine/threonine kinase receptors which are expressed on the target cells. Binding of BMPs with their receptors results in the activation of intracellular signalling pathways which control the cell function. Three kinds of type I and type II BMP receptors (BMPR) have been identified. Activin receptor-like kinase-2 (ALK-2), BMP type IA receptor (BMPR-IA) and BMPR-IB/ALK-6 are the three BMP type I receptors, while, type II receptors include BMPR-II, activin type II receptor (ActR-II) and ActR-IIB. [Ten et al. 2003; Chen et al. 2004]

Shah et al previously reported that BMP-2 treatment of osteoblastic cells, for 12 h prior to plating on Ti-6Al-4V, affected bone cell growth and function *in vitro*. Using confocal microscopy, these authors demonstrated that cytoskeletal and ECM organization, expression of FN and of $\alpha 5$ and $\beta 1$ integrin, and the levels and phosphorylation of focal adhesion kinase (p125FAK), were significantly enhanced in the BMP-2 treated osteoblasts compared with the untreated control cells cultured on the Ti surfaces [Shah et al. 1999b]. In view of these results, the current study assessed the effects of Ca ion-implantation of Ti on the expression levels of BMPR-IB, a known receptor of BMP-2 [Yoshikawa et al. 2004; Nohe et al. 2004], previously detected in three osteosarcoma cell lines [Guo et al. 1999], by MG-63 cells *in vitro*.

6.1.3 Bone sialoprotein

BSP, initially isolated from bovine bone tissue by Herring et al in 1972, was eventually characterised in 1983 [Fisher et al. 1983; Herring1972]. It is a phosphorylated protein which is rich in acidic amino acids and contains the RGD cell-attachment sequence. BSP belongs to the small integrin-binding ligand *N*-linked glycoprotein (SIBLING) family of proteins which also includes OPN. However, unlike OPN, the tissue distribution of BSP is restricted exclusively to mineralized tissue including bone, dentin, mineralizing cartilage and cementum [Qin et al. 2004]. BSP was found at the sites of bone formation and has been shown to play a central role in the mineralization process of bone and dentine [Hunter et al. 1996; Mackie2003].

MacNeil et al conducted experiments to determine the role of BSP in tooth root formation. Developing murine molar tooth germs at sequential stages of development (developmental days 21-42) were analyzed using immunohistochemical and *in situ* hybridization techniques. These authors showed that BSP was localized to alveolar bone and odontoblasts early in development, and to the cemental root surface at latter periods. *In situ* hybridization confirmed that cells lining the root surface express BSP. It was suggested that this protein is involved in cementoblast differentiation and/or early mineralization of the cementum matrix [MacNeil et al. 1995]. Similarly, another study localized BSP during de novo mineralization by single and double immuno-histochemistry. Since BSP was found to be expressed prior to the mineralization, it was suggested that this specific ECM protein is necessary for the initiation of bone mineralization process [Roach1994].

Previously the effects of chemically modifying Ti-6Al-4V surfaces with a common RGD sequence, a 15-residue peptide containing GRGDSP (glycine-arginine-glycine-aspartate-serine-proline), on the expression of BSP protein were examined [Zreiqat et al. 2003]. Human bone derived cells were grown for 7 and 14 days on the chemically-modified Ti surfaces. BSP levels were reported to be significantly higher in HBDC cultured for 7 days on RGD-modified Ti surfaces compared with the production by HBDC grown on the native Ti-6Al-4V [Zreiqat et al. 2003]. In view of these findings, the experiments presented in the current chapter selected BSP, an important bone specific antigen, to examine whether changing surface chemistry of Ti discs by Ca ion-implantation would have any effect on bone cell function *in vitro*.

6.1.4 Osteonectin

ON is also known as SPARC (secreted protein acidic rich in cyteine). In bone, ON is one of the most abundant non-collagenous matrix protein [Lackie and Dow, 2000;Hunter et al., 1996]. It is an important glycoprotein that is expressed in the remodelling tissue such as bone, gut mucosa, and healing wounds, and is necessary for normal development [Brekken and Sage 2001]. In adult, the expression of ON is limited largely to tissues undergoing repair or remodelling due to wound healing, disease, or natural processes. It is involved in the regulation of important physiological processes (e.g. angiogenesis, cell proliferation, and cell migration) that entail the modulation of cell-ECM and cell-growth factor interaction [Brekken and Sage 2001]. ON has been shown to affect bone mineralization process both *in vivo* and *in vitro* [Muriel et al. 1991; Delany and Canalis 1998]. Osteoblasts from patients with osteogenesis imperfecta (brittle-bone disease) and osteoblasts derived from the *fro/fro* mouse, an animal with fragile bones, produce decreased amounts of ON [Muriel et al. 1991]. Conversely, murine osteoblastic cell line MC3T3-E1 induced to form nodules *in vitro* produce more ON as the matrix matures and mineralizes [Delany and Canalis 1998]. In a cell free *in vitro* system, ON inhibited *de novo* formation of apatite [Boskey1989] and slowed down HA crystal growth by blocking growth sites [Doi et al. 1992]. Taken together, it was concluded that since slowing down crystal growth may regulate the growth and size of HA crystals, ON might be playing a role in preventing excessive mineralization [Roach1994].

Ku et al reported that the treatment of Ti-6Al-4V surfaces using ageing (thermal treatment in deionised distilled boiling water) and passivation techniques (using 30% nitric acid for 1 h) did not affect the expression of ON gene by osteoblast-like human SaOS-2 cells after 1 week of incubation [Ku et al. 2002]. These authors examined the effect of different Ti-6Al-4V surface treatments on ON, OPN, OCN gene expression, total protein amount, ALP activity and FN production by SaOS-2 cell line between 1-4 weeks of cell culture. At week 1, no difference in the ON, OPN, and OCN gene expression was found between samples. There was no difference in the expression of FN for the different surface treatments. The peak of ALP activity appeared earlier at week 2 for the control surface compared with the passivated and aged surfaces. They proposed that the different surface treatments induced different metal ion release kinetics and surface properties, which influenced only the ALP activity of osteoblast-like cells [Ku et al. 2002]. In contrast, Zreiqat and Howlett demonstrated that cells cultured on the Ti-6Al-4V discs had higher levels of ON protein expression than those on cpTi [Zreiqat and Howlett 1999]. These authors investigated the influence of cpTi and Ti-6Al-4V on the expression of ON by human bone-derived cells grown for 5, 7, 10, and 14 days [Zreiqat and Howlett 1999]. The above results indicate that the expression levels of ON by cells cultured on Ti discs may have been altered in response to minor differences in the Ti surface chemistry, and for these reasons, the effects of Ca ion-implantation of Ti on the expression of this very important bone-associated protein were also examined here.

6.1.5 Osteopontin

OPN was first described as a secreted 60-kDa transformation-specific phosphoprotein [Senger et al. 1979]. Like BSP, OPN is a phosphorylated, acidic non-collagenous glycoprotein belonging to the SIBLING family of proteins. It can function both as a cell attachment protein and as a cytokine, delivering signals to cells via a number of receptors including the integrins $\alpha_v(\beta_1, \beta_3, \text{or } \beta_5)$ and $(\alpha_4, \alpha_5, \alpha_8, \text{or } \alpha_9)\beta_1$, and certain variant forms of CD44 (a cell surface glycoprotein that serves as an adhesion molecule in cell-substrate or cell-cell interactions) [Katagiri et al. 1999]. Interaction of OPN with these receptors, via the RGD amino acid sequence, mediates cell adhesion which directly or indirectly activates intracellular signalling pathways [Denhardt and Guo 1993; Denhardt et al. 2001a].

The ability of OPN to stimulate cell activity through multiple receptors linked to several interactive signalling pathways may account for much of its functional diversity. This secreted protein is found in all body fluids and also in the proteinaceous matrix of mineralized tissue. OPN is a prominent component of the mineralized ECMs of bones and teeth. In addition to mineralization of osseous tissues, OPN is also associated with calcification [Sodek et al. 2000]. It was previously co-localized with calcified deposits in atherosclerotic lesions [Hirota et al. 1993]. OPN is characterized by the presence of a polyaspartic acid sequence and sites of Ser/Thr phosphorylation that causes it to bind strongly to the calcium phosphate crystals in mineralized tissues and to inhibit crystal growth [Sodek et al. 2000; Jono et al. 2000]. Although, it is not required for normal bone formation and development, the presence of OPN on the bone

surface is critical for the remodelling of mature bone. OPN also plays important roles in inflammation, tissue injury and wound healing processes [Johnson et al. 2004; Butler1989; Goldberg and Hunter 1995].

It was previously shown that Ti surface characteristics affect the expression of OPN by osteoblast-like cells. SaOS-2 cells were cultured on cpTi discs with three different surface roughness i.e. smooth (S), sandblasted (SB) and Ti plasma sprayed (TPS). OPN was shown to be detected largely on the SB and TPS surfaces, while only minimal production was observed on the S surfaces, indicating that surface properties may be able to modulate the osteoblast phenotype [Postiglione et al. 2004]. Puleo et al studied the expression of OPN gene by osteoblasts cultured in direct contact with Ti by using Northern blotting and RT-PCR techniques. They demonstrated that mRNAs encoding OPN were expressed during a 5 week period of interaction of osteoblasts with Ti [Puleo et al. 1993]. Therefore, experiments presented in the current study were carried out to determine whether changes in surface chemistry of Ti discs via Ca ion-implantation would have any effect on the expression of multifunctional OPN by MG-63 cells both at the protein as well as at the gene levels.

6.1.6 Rationale for the use of monensin

ECM components are normally secreted from the cells in which they are produced and only a proportion of these antigens is retained either intracellularly or expressed on the surface of the cell [Mundy1995], which makes it difficult to measure the correct expression levels of matrix proteins using FCM analysis. The effects of Ca ion-implantation on the expression levels of normally secreted

bone ECM antigens i.e. BSP, ON and OPN were therefore assessed using a procedure whereby a replicate set of MG-63 cells cultured on Ti (control) and Ca-Ti discs were treated with monensin, an inhibitor of protein secretion, as previously described [Kuru et al. 1998].

Monensin induces an intracellular accumulation of secreted proteins primarily by blocking Golgi/ER transport of newly synthesised proteins [Rieman et al. 2001]. Kuru et al treated cultured gingival fibroblasts and periodontal ligament (PDL) cells with monensin in order to measure the expression levels of FN, collagen 1 and tenascin *in vitro* using FCM. They reported that when the PDL cells were exposed to monensin, secretion of FN was blocked, as cell-associated FN levels increased to 70%, whereas FN expression increased by less than 5% in gingival fibroblast cultures. However, while incubation in the presence of monensin increased the cell-associated collagen 1 levels in the PDL cells by 15%, antigen levels in the gingival fibroblasts increased by 120%. In contrast, the expression of another ECM protein tenascin in both types of cells showed the same increase, approximately 20% each [Kuru et al. 1998]. In another study, the presence of monensin caused viral proteins to remain trapped intracellularly [Suikkanen et al. 2003]. In addition, Nylander and Kalies reported that monensin was able to completely block secretion of cytokine CD69 by mice splenocytes [Nylander and Kalies 1999]. Similarly, upon exposure of human osteoclast-like cells to monensin, cells were seen loaded with FN containing vesicles, and hence blocking FN secretion [Grano et al. 1994]. These findings confirm the efficiency of monensin in blocking protein secretion in a variety of cell types, and thus support its use in the current study to determine

the effects of Ca-Ti surfaces on the expression of certain bone ECM proteins i.e. BSP, ON and OPN.

6.2 Materials and Methods

6.2.1 Preparation of Ca-implanted Ti discs

Mirror polished Cp Ti discs (grade 1, 8 x 1 mm in diameter) (Goodfellow) were implanted with high doses of Ca ions (1 x 10^{17} Ca ions cm^{-2}). Both the non-implanted Ti (control) and Ca-Ti discs were sterilised by UV light prior to cell culture and stored at RT in a desiccator, as described earlier (Chapter 2)

6.2.2 Cell culture

Suspensions containing 1 x 10^4 MG63 cells, cultured in complete DMEM (GIBCO Invitrogen), were seeded onto the surfaces of the Ti (control) and Ca-Ti discs. Fifteen replicate discs per sample were used and each experiment was repeated 3 times. In all experiments, the discs were placed into 24 well plates (Beckton-Dickinson) and incubated at 37°C in a humidified atmosphere of 5% CO_2 in air, as described in detail in Chapter 3.

6.2.3 Treatment with monensin

In some experiments, in order to determine the effects of Ca-implantation on bone proteins which are normally secreted (BSP, ON, OPN), the drug monensin (1 μM; Sigma-Aldrich) was added for 4 h to block protein secretion. After washing, fixation and permeabilization, the antigens which had accumulated within the cell were immunostained. Since ALP and BMP-RIB are

membrane-bound proteins i.e. they are not secreted by the cells, the monensin treatment was not carried out for measuring the effects of Ca-Ti surfaces on their expression levels.

6.2.4 Immunofluorescent staining of bone-associated antigens

After 6 days of incubation of Mg-63 cells on Ti (control) and Ca-Ti surfaces the tissue culture medium was removed and the discs were washed twice with PBS. The cells were detached from the discs using 20 mM EDTA (i.e. with no trypsin) (GIBCO Invitrogen) for 5 min at 37°C. Trypsin was not applied because its protease activity would be likely to remove cell-membrane associated proteins. The cells were then centrifuged and fixed for 30 min at RT with 1% w/v PFA (BDH) in PBS containing 0.1% of the non-ionic detergent saponin (Sigma-Aldrich) in order to permeabilise cell membrane and allow the entry of detecting antibodies [Sumner et al. 1991]. After centrifugation, the cells were washed, resuspended in wash buffer (2% FCS, 0.05% sodium azide and 0.1% saponin in PBS) and immunostained for ALP, BMPR-IB, BSP, ON and OPN expression, as described below.

Replicate aliquots of the cells were incubated for 60 min at RT with the following primary antibodies: rabbit polyclonal antibodies (pAb) against human ALP, and BSP; mouse monoclonal antibodies (mAb) against BMPR-IB (Dako), ON and OPN (kindly provided by Dr. L. Fisher; NIH, Bethesda, MD USA). All primary antibodies were used at a 1:100 dilution in the washing buffer. Normal non-immune rabbit serum (Dako) and mouse IgG1 (Dako) served as the

negative controls for the pAb and mAb, respectively. After washing the cells, FITC-labelled swine anti-rabbit IgG (Dako), diluted 1:20 in PBS, was added for 30 min at RT to the pAb-treated cells. FITC-labelled rabbit anti-mouse IgG (Dako), diluted in 1:50 in PBS was added for the same time to the mAb-treated cells. The cells were then washed and resuspended in 500 µl of wash buffer and the forward light scatter (FSC) (proportional to cell size), side light scatter (SSC) (proportional to intracellular granularity) and fluorescent intensities of 10,000 individual cells measured by FCM, as described below.

6.2.5 Flow cytometry analysis

The light scattering properties and the fluorescence of each cell stained with FITC were measured on a FACScan flow cytometer (Becton-Dickinson). The FSC, SSC and fluorescence values obtained were dependent on the electronic input and detection settings of the FACScan, which were kept constant in the experiments described, and on the specific antibody used.

For the analysis of antigen levels, the signals corresponding to debris and cell aggregates were first gated out by using the FSC and SSC display. The AFI of the cell population was calculated for each antigen after subtraction of the AFI of the negative control samples (non-specific serum and IgG) from the AFI of the test samples (cells treated with the specific antibody). For ALP and BMPR-IB, the net AFI values of the Ca-Ti and Ti (control) cells were compared directly. For BSP, ON and OPN, the effects of Ca-Ti were determined by comparing the change in AFI values in the presence of monensin with the change in the AFI of

cells incubated on the Ti (control) discs in the presence of the drug, as previously described [Kuru et al., 1998].

All data were analysed using WinMDI software (version 2.8) (www.facs.sripps.edu/software.html). Since each antibody has a unique reactivity for its corresponding antigen, the AFI values obtained using different antibodies cannot be compared with each other.

6.2.6 RNA extraction

The effects of Ca-Ti surfaces on the expression of OPN at the gene level were evaluated by RT-PCR. MG-63 Cells were cultured on the Ti (control) and Ca-Ti discs for 24 h and 6 days and the total RNA was isolated and purified using RNeasy mini columns (Quiagen, Crawley, West Sussex, UK), as follows. Buffers A, B and C, mentioned below, were provided in the Quiagen kit as buffer RLT, RW1 and RPE, respectively, and their chemical compositions were not specified. Cell pellets obtained by trypsinisation were first lysed by adding 350 µl of "buffer A". This is a highly denaturing buffer which immediately inactivates RNases and thus allows isolation of intact RNA [Quiagen manual]. Secondly, to shear genomic DNA, samples were homogenised by mixing with pipette and vortex for 1 min. Then, 350 µl of 70% ethanol were added to each sample and mixed well using a pipette. This step was recommended to adjust the binding conditions for the adsorption of isolated RNA to RNeasy columns [Quiagen manual]. Approximately 700 µl of the total liquid from each tube was then applied to an RNeasy mini column which was placed in a 2 ml collection tube (supplied with the Quaigen kit). The tubes were then centrifuged for 15 s at

10,000 rpm. The 'flow through' (liquid collected at the bottom of the tube) was discarded and the RNeasy mini columns were placed in new collection tubes.

To ensure removal of any contaminants from the RNeasy mini columns [Quiagen manual], two subsequent wash spins in "buffer B" and "buffer C" were carried out. First, 700 µl of buffer B were added to each column and they were centrifuged for 15 s at 10,000 rpm. This was followed by discarding the flow through, replacing the collection tube and adding 500 µl of buffer C to the RNeasy mini column, which was then centrifuged as before. This was further repeated by adding another 500 µl of buffer C to each RNeasy mini column. Following centrifugation for 2 min at 10,000 rpm, the columns were placed in the new collection tubes and spun at full speed for 1 min in a micro-centrifuge.

Finally to elute RNA, columns were placed in new collection tubes and 50 µl of RNase free H_2O were added directly onto the RNeasy silica gel membranes. After mixing well with a pipette, tubes were centrifuged for 1 min at 10,000 rpm. The eluate obtained for each sample was the purified RNA which was stored in a RNase free tube at -70°C prior to reverse transcription.

6.2.7 Reverse transcription

The collected RNA from the cells (5 µg of total RNA from each sample; quantified by measuring absorbance at 260nm) was reversibly transcribed to cDNA using a cells-to-cDNA™ kit (Ambion, Inc. Huntingdon, Cambridgeshire, UK). Reagents added to an aliquot of 10 µl of RNA were: 4 µl of dNTP mix, 2 µl of oligo (dT) primers and 4 µl of nuclease free H_2O. After mixing thoroughly by vortex and brief centrifugation, samples were placed in PCT-100 thermal cycler

(MJ Research) for 3 min at 70°C. After cooling for 5 min at -20°C and a brief centrifugation, the remaining reagents required for reverse transcription were 2 µl of 10x RT buffer, 1 µl of M-MLV reverse transcriptase and 1 µl of RNase inhibitor were added to each tube. Following mixing via vortex and brief centrifugation, tubes were incubated in a PCT-100 thermal cycler (MJ Research) for 60 min at 42°C to allow preparation of cDNA. The reaction was terminated by subsequent incubation at 90°C for 10 min. The cDNA samples obtained were stored at -20°C before continuing with amplification via PCR.

6.2.8 Polymerase chain reaction

Five microlitres of cDNA was used for PCR with 0.5 µl of REDtaq DNA polymerase (2.5 U), 5 µl of 1x REDtaq PCR buffer, 2 µl of dNTP mix (2.5 mM each), 3 µl of $MgCl_2$ (1.5mM), 32.5 µl of nuclease free H_2O and 1 µl each of the sense and anti-sense primers for OPN. Replicate reactions contained the primers for the housekeeping gene GAPDH (Chapter 2) (all from Sigma-Genosys, Pempisford, UK). PCR was carried out using a PCT-100 thermal cycler (MJ Research) with an initial 3 min 94°C denaturation step, followed by cycles of 30 s at 94°C, 2 min at 61°C, 2 min at 72°C, respectively and a 10 min 72°C termination step. 35 Cycles were used for OPN and 32 for GAPDH. The primer sequences and expected PCR product sizes (base pairs; bp) for the OPN and GAPDH genes are shown below.

	Primer sequence (5'–3')	Product size (bp)
OPN	5': CCAAGTAAGTOCAACGAAAG 3': GGTGATGTCCTCGTCTGTA	347
GAPDH	5': CCACCCATGGCAAATTCCCATGGCA 3': CTGGACGGCAGGTCAGGTCCACC	600

Figure 6.1: Sequence of PCR amplification primer sets for OPN and GAPDH genes, adapted from Sigma-Genosys information sheet.

The molecular sizes of the amplified PCR products were determined by their electrophoretic mobility in 2% agarose gels which were stained with ethidium bromide, using the UV illumination image capture. Images of the OPN bands, compared with a 1 Kbp DNA ladder used as a size marker, were scanned by densitometry using ScionImage software (Scion Corporation). The expression of OPN mRNA by cells cultured on the Ca-Ti and Ti (control) discs was calculated relative to GAPDH, which is defined as 1.0 [Dukas et al. 1993].

6.2.9 Statistical analysis

The results of triplicate experiments are shown as ± SEM. Differences in the levels of antigen and gene expression by cells cultured on Ca-Ti discs relative to those on Ti (control) surfaces were determined using SPSS 11.0 software (SPSS) and the Student's *t* test for paired samples, with $p \leq 0.05$ considered as statistically significant.

6.3 Results

6.3.1 Effects of Ca ion-implantation on bone protein expression

Figure 1 shows representative FCM profiles of ALP, BMPR-IB, BSP, ON and OPN expression by MG-63 cells on the Ca-Ti and Ti (control) discs after 6 days of cell culture. These histograms indicate that growth of the cells on the Ca-implanted Ti up-regulated the expression of BMPR-IB, BSP and OPN, but appeared to have little if any effect on the levels of ALP and ON.

The average net AFI values of these bone-associated markers, obtained from three replicate experiments, confirm that while these latter 2 antigens were unaffected by the Ca-implanted surface, the level of BMPR-IB expressed by MG-63 cells cultured on the Ca-Ti discs was significantly higher compared with cells incubated on the Ti (control) discs ((255 ± 8.0 compared with110 ± 4.6) (p = *0.05*) (Table 1)). BSP levels similarly increased after culture on the Ca-Ti discs, to a level which was 2.9 times greater than that on the Ti (control) (p = *0.04*; Table 1). Most strikingly, Table 1 also shows that OPN expression by cells on the ion-implanted discs increased 470% (from a net AFI of 120 on the control to 315 on the Ca-Ti discs in the presence of monensin). In view of this highly significant up-regulation (p =*0.01*) of this antigen by culture on the Ca-Ti surface compared with the Ti (control), OPN expression was further evaluated at the gene level by RT-PCR, as described in the Materials and Methods. In summary, the findings of these experiments indicate that out of the five bone-associated antigens analysed, BMPR-IB, BSP and OPN were all up-regulated in response to Ca ion-implantation of Ti

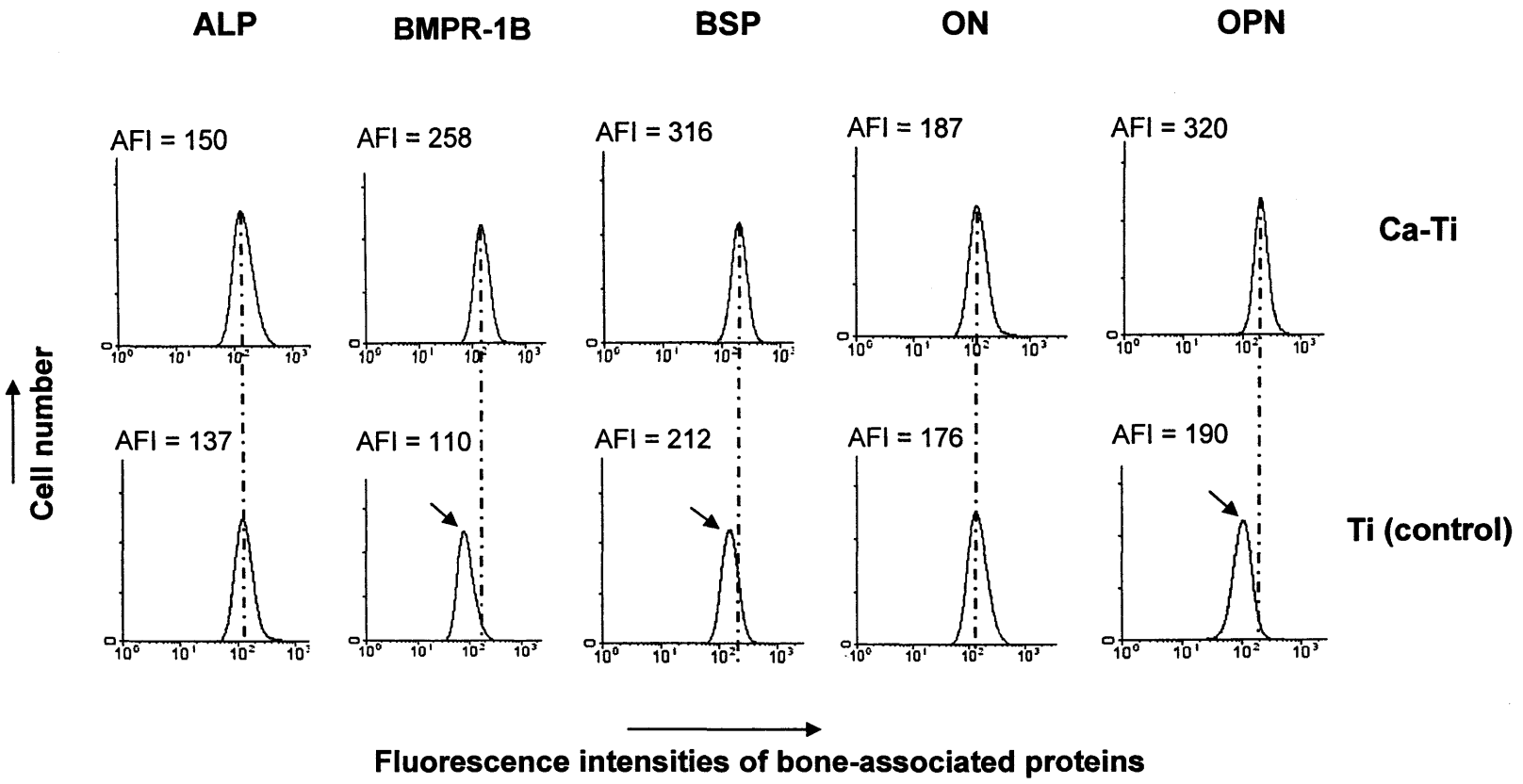

Figure 6.2: Representative FCM profiles of the effects of Ca implanted Ti on ALP, BMPR-IB, BSP, ON and OPN antigen expression by MG-63 cells after 6 days of culture. The BSP, ON and OPN proteins were measured after 4 h of incubation with monensin, as described in the Materials and Methods. Note the higher expression levels of BMPR-IB, BSP and OPN on the implanted surface (upper histograms) compared with the Ti (control) surface (lower histograms), as indicated by the arrows.

Table 6.1: Effects of Ca-Ti surfaces on the expression of bone-associated antigens

Antigen	Net AFI		Change in AFI		Relative [a] AFI
	Ca-Ti	Ti (control)	Ca-Ti	Ti (control)	
ALP	152 ± 4.8	140 ± 3.9			1.08
BMPR-IB	255 ± 8.0	110 ± 4.6			**2.31***
BSP	320 ± 7.0	200 ± 12.2	58	20	**2.90***
ON	185 ± 5.3	172 ± 3.4	23	19	1.21
OPN	315 ± 6.0	120 ± 7.6	112	24	**4.70***

Net AFI values shown are the averages (± SEM) of 15 replicate samples repeated 3 times. Changes in the AFI values of BSP, ON and OPN were measured for MG-63 cells cultured on the Ca-Ti and Ti (control) and surfaces treated with and without monensin, as described in the Materials and Methods. [a] The fluorescence intensity of each antigen on the Ca-Ti surface relative to the Ti (control) discs, defined as 1.0. * Indicates statistically significant increase in BMPR-IB, BSP and OPN expression, shown in bold (*p = 0.05, 0.04 and 0.01,* respectively).

6.3.2 Influence of calcium-implantation on osteopontin gene expression

Figure 6.3 (A) shows a representative RT-PCR experiment of the OPN mRNA gene product in cells cultured for 24 h and 6 days on the Ca-Ti and Ti (control) discs. This indicates that the implanted surface may have mediated an increase in gene activity (relative to the change in GAPDH levels; lanes 2 and 4 compared with 1 and 3 for the control surface, at 24 h and 6 days, respectively). The intensities of the bands corresponding to the OPN and GAPDH genes were therefore measured in 3 separate experiments, and the

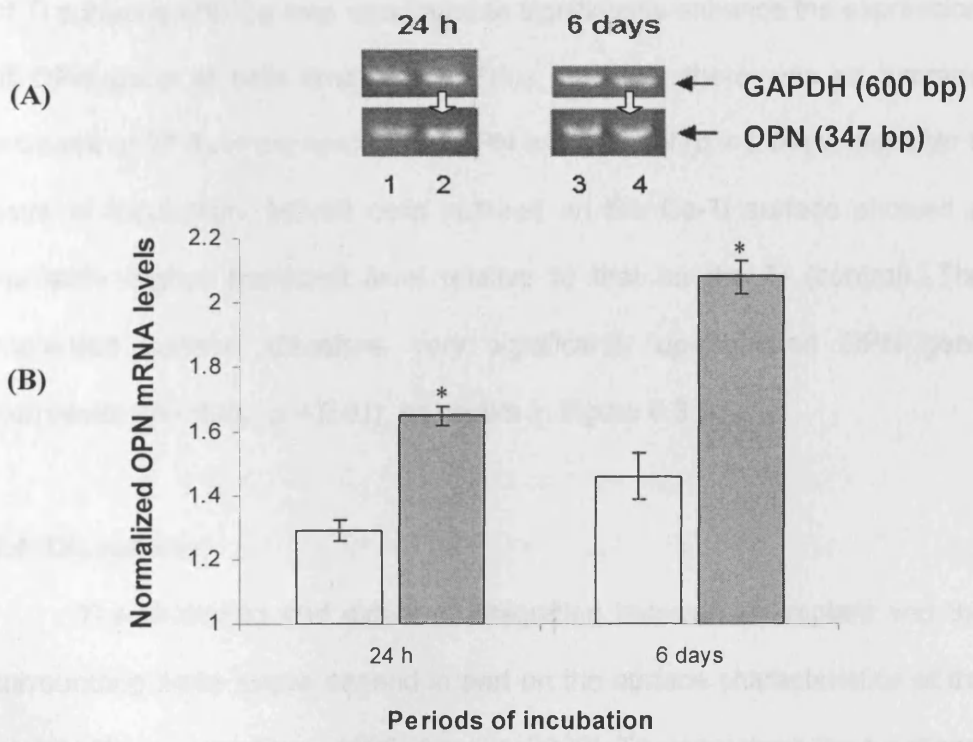

Figure 6.3: RT-PCR analysis of the effects of Ca-implanted Ti on the activity of the OPN gene in MG-63 cells after 24 h and 6 days of culture. 1 Kbp DNA ladder was used to identify the 600 and 347 bp bands corresponding to the GAPDH and OPN gene products. In (A), lanes 1 and 3 show the mRNA derived from cells on the Ti (control) discs, while lanes 2 and 4 are derived from the Ca-implanted surface. The white arrows indicate the possibly increased band intensities of OPN on the Ca-Ti surfaces compared with those on the control, relative to the GAPDH band intensity in each sample. The histogram in (B) shows the average level of OPN gene expression normalised to that of the GAPDH gene, defined as 1.0, by cells incubated on the Ti (control) (white bars) and Ca-Ti discs (grey bars). *Note the significant increase in the relative levels of the OPN transcript at both time periods in cells incubated on the ion-implanted Ti surface ($p = 0.04$ and 0.01, respectively).

results in Figure 6.3 (B) show the average values ± SEM of the OPN mRNA levels normalised against the GAPDH transcript, defined as 1.0. Implantation of Ti surfaces with Ca ions was found to significantly enhance the expression of OPN gene at both time points. Thus, at 24 h, there was an average increase of 27 % in the normalised OPN mRNA level ($p = 0.04$) while, after 6 days of incubation, MG-63 cells cultured on the Ca-Ti surface showed a markedly higher transcript level relative to that on the Ti (control). The implanted surface; therefore, very significantly up-regulated OPN gene expression (by 40%; $p = 0.01$), as shown in Figure 6.3 B.

6.4 Discussion

The likelihood and extent of integration between an implant and the surrounding bone tissue depend in part on the surface characteristics of the implant [Puleo and Nanci 1999; Anselme2000]. To understand the functional consequences of the modification of Ti surface chemistry by Ca ion-implantation, the present *in vitro* study measured the effects of this novel surface on the expression of ALP, BMPR-IB, BSP, ON and OPN, previously shown to be key osteogenic markers [Bowers et al. 1992; Chehroudi et al. 1992; Mustafa et al. 2000; Piattelli et al. 1994; Wennerberg et al. 1997; Cooper et al. 1999].

6.4.1 Expression of ALP and BMPR-IB on calcium-implanted titanium

Ca ion-implantation seemingly failed to influence the expression of the ALP antigen by MG-63 cells, even after 6 days of culture. Krupa et al previously reported that there was also no significant difference in the

enzymatic activity of ALP in human bone-derived cells which had been similarly cultured on Ca-implanted Ti surfaces [Krupa et al. 2001a]. However, the present experiments showed that BMPR-IB, another membrane-associated antigen which also plays an important part in bone growth and differentiation [Yoshikawa et al. 2004; Nohe et al. 2004], was significantly up-regulated by the implanted Ti. Although the reasons for this effect are not yet understood, the functional consequences of increased BMPR-IB expression are likely to involve the role of Ca ions as a major and ubiquitous cell activation molecule.

Cell signalling via this transmembrane receptor is mediated following its binding to the BMP [Scherer and Graff 2000]. BMPR-IB was previously demonstrated to interact with BMP-2 which in turn activates the Smad (a combination of the gene names from *C.elegans*, Sma, and *Drosophila*, Mad) signalling pathway [Yoshikawa et al. 2004; Nohe et al. 2004]. BMP receptors and nuclear effector Smad proteins control cell growth and differentiation by regulating the transcription of specific genes [Korchynskyi and Ten 2002; Miyazono1999]. Several pivotal BMP target genes that dictate cell fate, including the inhibitors of differentiation (Id) proteins, have been identified. Although BMP activates the Smad pathway to modulate gene transcription, there is growing evidence that other pathways distinct from the Smad pathway, are initiated downstream of the BMP-2/BMPR-1B receptor complex. For example, other members of TGF-β family have been shown to activate small GTP-binding proteins and MAP kinases in certain cells [Korchynskyi and Ten 2002; Miyazono1999]. Scherer and Graff previously reported the presence of a cross-talk between three major signalling cascades i.e.

Ca/calmodulin signalling cascade, receptor tyrosine kinase, and TGF-β pathways [Scherer and Graff 2000]. In addition, Xu et a proposed that calmodulin can bind Smad in a Ca dependent manner, however the effects on TGF-β signalling remained unclear [Xu et al. 1999].

To summarize the findings of above studies it can be stated that the cell signalling via BMPR-1B is mediated in part by the intracellular Smad pathway that regulates the transcription of a number of essential growth and differentiation genes and which is, in turn, regulated by Ca ion-dependent binding to calmodulin [Yoshikawa et al. 2004; Nohe et al. 2004; Korchynskyi and Ten 2002; Miyazono1999; Scherer and Graff 2000]. Thus, the activation of Ca-based signal transduction which may occur on Ca-implanted Ti could be partially responsible for the apparently enhanced biocompatibility of this surface *in vivo* [Hanawa et al. 1997].

6.4.2 Effects of Ca-Ti on the expression of bone matrix proteins

ECM proteins adsorbed onto the surface of Ti are either exogenously derived from serum or endogenously synthesised by cells [Puleo and Nanci, 1999; Anselme, 2000]. Surface properties of implant materials influence the adsorption of serum-derived ECM proteins *in vitro.* Additionally, the expression of ECM proteins by cells is also affected by physicochemical differences of Ti surfaces [Puleo and Nanci 1999; Anselme2000; Kasemo and Gold 1999]. Compared with the control non-implanted discs, Ca ion-implantation of Ti caused an up-regulation of BSP and most significantly OPN proteins by osteoblast-like cells. In contrast, no significant increase was found in ON expression by MG-63 cells on Ca-Ti discs in comparison with

the control. Although it is not known whether monensin treatment completely prevented the secretion of all the matrix proteins that were examined, the measurement of altered antigen levels is in agreement with the previous studies which showed increased intracellular accumulation of ECM proteins following exposure to monensin [Grano et al. 1994; Kuru et al. 1998].

OPN and BSP are believed to play a role in the adhesion of cells to implant materials [Puleo and Nanci, 1999;Anselme, 2000]. Both of these non-collagenous proteins contain the RGD sequence and therefore can bind with integrin receptors including $\alpha 5\beta 1$ [Denhardt et al. 2001b]. Results in Chapter 4 have shown that Ti surfaces implanted with the high doses of Ca ions can induce a significantly enhanced expression of $\alpha 5\beta 1$ integrin. Together with the elevated levels of BSP and OPN induced by the Ca-Ti surface as shown here, this may further trigger integrin-mediated pathways leading to bone cell activation, growth and particularly Ca-dependent bone mineralization [Schneider et al. 2001].

Both OPN and BSP proteins are known to regulate the bone mineralization process via binding to Ca and HA [Boskey1989]. A previous study demonstrated that integrin-mediated adhesion and subsequent intracellular signalling of osteosarcoma cells play a role in the mineralization of bone ECM by BSP [Schneider et al. 2001]. The proteins necessary for the initiation of mineralization are likely to be present at the "mineralization front" i.e. just ahead of the mineralised matrix. Notably, a previous study demonstrated that both BSP and OPN were present at sites of mineralising new bone matrix whereas the expression of ON, which is shown in the current study to be unaffected by the Ca-Ti surface, was not detected

[Roach1994]. Therefore, an up-regulation of BSP and OPN seen here may suggest that the Ca ion-implantation of Ti possibly enhanced the osteoblast-like cell function by initiating the bone mineralization process.

6.4.3 Influence of Ca-Ti surfaces on OPN gene expression

OPN is encoded by a single gene, much of which is highly conserved in vertebrates [Denhardt et al. 2001b]. OPN affects the function of osteoblasts in several ways, e.g. via stimulating cell-cell adhesion, increasing cell-ECM communication, augmenting tissue mineralization and promoting calcium phosphate deposition [Johnson et al. 2004; Butler1989; Goldberg and Hunter 1995]. It is also required for stress-induced bone remodelling. A previous study has shown that during the process of osseointegration, the bonding between bone/teeth and the implants was promoted by OPN [McKee and Nanci 1996]. A highly significant up-regulation of such a multifunctional antigen, found in the current study on Ca-Ti surfaces, was further evaluated at the gene level. Results presented in the current chapter show that the effects of the Ca-implanted surface appear to be mediated at the level of gene transcription. Although RT-PCR of the other genes studied here were not carried out, semi-quantitative analysis of relative OPN mRNA levels demonstrated unequivocally that OPN transcripts were clearly elevated in response to growth on Ca ion-implanted Ti, as was the corresponding antigen.

Ti surface characteristics, such as microtopographical differences, have previously been shown to influence osteoblast gene expression [Schneider et al. 2003], including that of OPN [Takeuchi et al. 2005]. For

example, OPN gene activity in rat bone marrow-derived osteoblasts cultured on acid-etched Ti was found to be elevated compared with cells on the smooth surface [Takeuchi et al. 2005]. However, in human bone-derived cells an acid-etched and sandblasted Ti surface was found to elicit greater OPN protein but not mRNA expression compared with smooth Ti [Knabe et al. 2004], while in the SaOS bone cell line this gene was unresponsive to ageing and passivation of the Ti surface [Ku et al. 2002], and the presence of RGD peptides chemically bound to Ti [Zreiqat et al. 2003]. Nevertheless, the present finding of up-regulation of this highly conserved bone-associated gene by Ca ion-implanted Ti suggests that this material may be of substantial benefit in OPN-stimulated bone cell adhesion, ECM communication, calcium phosphate deposition and augmentation of tissue mineralization [Johnson et al. 2004; Butler1989; Goldberg and Hunter 1995] leading to improved bone remodelling [McKee and Nanci 1996].

6.5 Conclusions

- Ca ion-implantation enhanced the expression of bone specific antigens such as: BMPR-IB, BSP and most significantly OPN.
- This marked up-regulation of OPN protein on Ca-Ti discs increased in parallel with OPN mRNA levels.
- Compared with the non-implanted Ti, Ca-Ti surfaces may possess a higher potency to enhance bone cell function.

Chapter 7

Conclusions

7.1 Conclusions

The ultimate goal in studying the response of osteoblastic cells to the modified implant surfaces is to use the information obtained for promoting bone formation and osseointegration of the implants. To achieve osseointegration, the adhesion between the implant material and hard and soft tissues needs to be optimal; new bone should be able to form and regenerate as in a normal wound healing process; the union between bone and the implant material must enable the transferring of functional loads from the implant to bone; and the properties of normal bone should be largely restored. Moreover, these changes should occur as rapidly as possible with maximum bone formation along the entire length of the implant [Skalak and Brånemark 1994; Zarb and Albrektsson 1998]. In order for all these expectations to be fulfilled, there is a need to expand our limited understanding of the events occurring at the cell-material interface [Aubin2001; Mackie2003; Schwartz et al. 1997]. Rigorous efforts have recently been made to reduce the occurrence of implant failures [Esposito et al. 1999]. For example, various surface modification techniques have been carried out in order to improve the biocompatibility of Ti implants [Brunette et al. 2001; Donley and Gillete 1991; Esposito et al. 1999]. To achieve Ti implant surfaces that would optimise osseointegration, a continued acquisition of the fundamental knowledge of bone cell responses to specific material characteristics is necessary.

Findings of the Biomaterial group established that the ion-implantation technique altered the surface chemistry of Ti discs in a controlled and reproducible manner (Appendix A); and the results of this current study

showed that the osteoblasts responded to these differences in the Ti surface chemistry. However, this influence appears to be dependent on the nature and concentration of the implanted ion. Thus, although K-Ti and Ar-Ti surfaces failed to have any effect on human alveolar bone cells and MG-63 cell line, implantation of Ti surfaces only with high doses of Ca ions elicited an enhanced bone cell response *in vitro.* The relatively enhanced osteoblastic response to the Ti discs implanted with 1 x 10^{17} Ca ions cm^{-2}, suggest that cells on these surfaces were biologically more activated than their counterparts on the non-implanted Ti.

Both qualitative and quantitative biological parameters examined here may provide means to conduct in-depth analysis of the bone cell-material interactions *in vitro*. This study is the first to demonstrate that modifying Ti surface chemistry via Ca ion-implantation modulated expression of key signalling proteins such as $\alpha 5\beta 1$, vinculin, BMPR-1B, BSP and OPN. In addition, present findings establish for the first time that altering Ti surface chemistry can have an effect on the bone cell cycle. The concomitant up-regulation of $\alpha 5\beta 1$ integrin and vinculin by bone-like cells adhered on Ca-Ti surfaces, may highlight some of the molecular events occurring at the cell-Ti interface. The mechanisms of cell adhesion to the ECM, which are of fundamental importance for function, survival, and growth, are known to involve the formation of focal adhesions which may facilitate integrin signalling [Hynes1987; Kornberg and Juliano 1992; Kornberg et al. 1991]. Thus, an increase in the expression of $\alpha 5\beta 1$ integrin and focal adhesion protein vinculin in response to Ca ion-implantation may give clues about stimulation of a signal transduction pathway possibly involving ECM proteins.

This hypothesis was strengthened by the present findings of a significant increase in the expression levels of major ECM proteins such as BSP and OPN in response to Ca ion-implantation. OPN, in particular was shown to be up-regulated at both protein as well as gene levels. Both OPN and BSP contain the RGD sequence and therefore can bind with the integrin receptors including $\alpha 5\beta 1$ [Denhardt et al. 2001]. Based on these current findings, it can be speculated that interaction of these ECM proteins with $\alpha 5\beta 1$ might have triggered integrin-mediated intracellular signalling pathways [Denhardt et al. 2001].

In order to clarify the effects of Ca-implanted Ti on bone cells, the present study has used FCM to measure, for the first time, whether this novel surface modulates Ki-67 expression and the progression of synchronised cultures of MG-63 cells through the G0/G1, S and G2/M phases of the cell cycle. An enhanced proportion of Ki-67 positive cells and a rapid progression of cell through different phases of the cell cycle may possibly explain the underlying cause of an enhanced cell proliferation on Ca-Ti surfaces. The enhanced progression of cells cultured on Ca-Ti surfaces through G1, S and G2/M phases of the cell cycle could be due to up-regulation of cyclins and the subsequent activation of the cyclin/cdk complexes (key components providing the primary means of cell cycle regulation), in particular cyclin E/cdk2 (required for transition from the G1 to the S phase) [Merli et al. 1999] and cyclin B/cdk1 (required for the initiation of mitosis) [Jackman et al. 2003]. Moreover, since BMP-2 binding to BMPR-1B activates the Smad signalling pathway [Yoshikawa et al. 2004; Nohe et al. 2004], the present findings of

the enhanced expression of BMPR-1B might imply that Ca ion-implantation of Ti possibly stimulated this specific pathway.

It remains unclear as to the precise mechanisms governing this behaviour. The ion implantation process influences the surface characteristics in a number of ways. During implantation, the transfer of energy to the atoms and ions in the Ti/oxide lattice causes their displacement and/or sputtering out of the surface. The implanted surfaces also tend to contain a higher amount of hydroxide/water and carbon than the non-implanted surfaces, with some of the carbon present as carbide, all of which could affect biological reactivity [Ryssel and Ruge 1986; Sze1981; Ziegler1988]. In solution, several reactions may occur. The surface oxide layer may thicken or dissolve and inorganic species may precipitate onto the surface. Previous research has established that the surface characteristics of the implant materials such as topography, chemistry or surface energy dictate the profile, conformation and the structural rearrangement of the molecules adsorbed on these biomaterials [Anselme2000; Boyan et al. 1996; Schwartz et al. 1997].

An enhanced *in vivo* response to Ca ion-implantation has previously been attributed to the thickening of the oxide layer, formation of the Ca-P rich apatite layer, and/or release of the implanted ion from the modified Ca-Ti surfaces [Hanawa et al. 1997; Hanawa et al. 1996a; Hanawa et al. 1996b]. The altered bone cell response to Ca-Ti surfaces observed here *in vitro,* may have also been elicited by one or more of these physicochemical factors. Firstly, the results of Biomaterials group demonstrated an increase in surface oxide thickness on Ca-implanted Ti discs and considerable further thickening

on immersion in solution (Appendix A). Thus, the increased cell response to the Ca-Ti surfaces observed in the present study could be related to the formation of a thicker oxide layer, as has been reported to also cause stronger bone integration and enhanced tissue responses in rabbit tibia *in vivo* [Sul et al. 2001].

Secondly, since the appearance of calcium phosphate precipitates on surfaces has generally been taken as a sign of improved 'biocompatibility', an enhanced bone cell response to Ca-Ti surfaces could possibly be due to deposition of a Ca and P rich layer, as suggested by the enhanced response of rabbit osteoblasts to apatite-coated Ti *in vitro*, apparently as a result of the presence of Ca and P on the surface [Feng et al. 2004]. Modification of Ti surfaces by ion-implantation has previously been reported to augment the formation of a HA-like calcium phosphate on exposure to SBF [Krupa et al. 2001a; Krupa et al 2001b; Krupa et al. 2002; Maitz et al. 2002; Pham et al. 2000]. In addition, the findings of the current study established that a Ca- and P-rich particulate deposit is also formed upon immersion of Ca-Ti discs in culture medium after short immersion times for which such features were not observed on Ti (control) discs. Results of Biomaterials group also confirmed the presence of significantly greater amounts of P on the Ca-Ti surface, with a P/Ti ratio of ~0.6 compared to ~0.1 for control cp Ti. It was shown that the deposition of calcium phosphate species was faster on Ca-Ti than on other surfaces (Appendix A). In agreement, a previous study reported that similarly produced Ca-Ti surfaces induced accelerated calcium phosphate precipitation following immersion in HBSS [Hanawa1999].

Lastly, a gradual release of Ca ions from the Ca-Ti surfaces into the solution was detected by the Biomaterials group (Appendix A) and also by Hanawa et al [Hanawa et al. 1996b]. However, the amounts of Ca ions released are likely to be very much less (at least 2 orders of magnitude) than the amount of Ca present in the cell culture medium (Appendix A). Nonetheless, the possibility of changes in ionic concentrations and/or pH in the vicinity of the cells could subsequently generate a local microenvironment in which the ionic and molecular concentrations differ significantly from those of the overall surrounding environment, having profound effects on cellular responses. The leached out Ca ions can enter into the cytoplasm via channels in the cell membrane [Lodish et al. 1996; Anghileri2000] and/or exert their effects in a hormone-like fashion without crossing the plasma membrane. Bone cells express Ca^{+2}–sensing receptors (CaR) which respond to changing Ca ion concentrations in the ECM [Dvorak and Riccardi 2004; Riccardi2000]. Recent studies indicate that the osteoblast-derived cell lines MC3T3-E1, UMR-106, and SaOS-2 also express CaR mRNA and protein [Yamaguchi et al. 1998a; Yamaguchi et al. 1998b]. Activation of CaR by Ca ions triggers an intracellular cascade of second messengers producing a variety of biological effects depending on the cell type [Dvorak and Riccardi 2004; Riccardi2000; Riccardi and Gamba 1999; Yamaguchi et al. 1998a]. It was previously reported that raising extracellular levels of Ca ions induced a proliferative response in the osteoblasts [Brown1991]. A previous study has shown that calcium phosphate coatings on Ti implants released higher local concentrations of Ca and P ions, which provided favourable conditions for the proliferation and differentiation of osteoblast-like cells [Becker et al. 2001]. In

another study, rapid Ca ion release was linked to enhanced osteoblastic activity around calcium carbonate coated Ti alloy plates [Berrere et al. 2001].

Thus, thickening of the Ti oxide layer, the formation of calcium phosphate layer and the release of Ca ions may all have contributed to the enhanced response of bone cells to the Ca-implanted Ti surfaces *in vitro*, as reported here. Results presented here indicate that Ca ion-implantation may contribute to successful osteoblast adhesion, growth and function at the skeletal tissue-device interface. Although the intracellular signalling cascades triggered by Ca-Ti surfaces remains largely unknown, the present findings may explain, at least partly, the underlying mechanisms responsible for the improved osseointegration on the Ca-implanted Ti implants compared with the non-implanted Ti, reported *in vivo* [Hanawa et al 1997]. It is difficult, however, to extrapolate the present *in vitro* findings to the clinical situation as the bone cell culture model used here does not represent the *in vivo* situation. Nevertheless, these *in vitro* studies enable the response of cells to be evaluated in order to develop and carry out *in vivo* investigations [Oreffo and Triffitt 1999].

7.2 **Suggestions for future work**

- Future experiments may be aimed at determining bone cell responses to the Ti surfaces implanted with other biologically beneficial ions. Similarly, ion-implantation of other metallic implant materials may be carried out and responses of cultured osteoblastic cells to such modified surfaces could also be investigated in detail.

- Further exploration of the material-dependent effects reported here may involve the study of intracellular signal transduction pathways. Since integrins are known to be a major part of the signal transduction process [Kuwada and Li 2000; Roovers et al. 1999; Varner et al. 1995], an up-regulation of $\alpha 5\beta 1$ integrin seen here suggest that the enhanced bone cell responses to the Ca-Ti surfaces may have been specifically manifested by integrin-mediated pathways. A recent study showed that modification of Ti surface chemistry enhanced activation of Mapkinase pathway and up-regulated Shc, a common point of integration between integrins and the Ras/Mapkinase pathway. The signalling pathway involving c-fos (member of the activated protein-1) was also shown to be upregulated in osteoblasts cultured on the Mg ion-implanted Ti-6Al-4V [Zreiqat et al. 2005]. Future experiments might, therefore investigate the effects of Ca ion-implantation on the expression of Shc, Erk (member of Mapkinase superfamily) and c-fos proteins, as described before [Zreiqat et al. 2005].

- Future experiments may also involve the analysis of protein adsorption, as previously tested using FN [Kilpadi et al. 2001], on the ion-implanted Ti surfaces and the effects of such modified surfaces on human bone cells *in vitro*.

- Since Ca implantation enhanced the progression of cells through different phases of the cell cycle, the effects of this change in Ti surface chemistry on the expression of cyclins and the subsequent

activation of the cyclin/cdk complexes [Murray2004; Zhu et al. 1996] may also be addressed. Moreover, In order to accept the proposed hypothesis that locally released Ca ions might have triggered formation of Ca/calmodulin complex resulting in a rapid cell cycle progression [Takuwa et al. 1995], future investigation could measure the effects of Ca-Ti surfaces on intracellular Ca levels [Berger et al. 2001], and also the binding of Ca ions with calmodulin *in vitro* [Quadroni et al. 1998].

- Previous studies have generally shown deposition of calcium phosphate on ion-implanted Ti following relatively long-term immersion in SBF [Maitz et al. 2002]. For example, Hanawa et al reported that Ca ion-implantation induced accelerated calcium phosphate precipitation following 30 days immersion in HBSS [Hanawa1999]. Future experiments may, therefore analyse the effects of Ca implantation on calcium phosphate deposition by pre-immersing the Ti discs in DMEM for longer periods of incubation (1-6 weeks). The response of osteoblastic cells to these modified surfaces could then be studied by measuring cell adhesion, cell proliferation and cell function.

- Both OPN and BSP protein, up-regulated in the current study, are known to regulate the bone mineralization process. Mineralization of newly-formed bone is essential for the proper functioning as it confers upon bone the property of mechanical rigidity [Hunter et al. 1996]. The influence of the change in surface chemistry of Ti discs by Ca ion-

implantation may, therefore be assessed on the bone mineralization processes *in vitro*, for example, by using Alizarin red assay, as described before [Chaudhary et al. 2004].

- DNA arrays are used to measure gene expression for many genes simultaneously and in a quantitative fashion [Lockhart and Winzeler 2000]. To have a comprehensive description of the cell-implant interaction with ion-implanted Ti at a gene level, cDNA microarray technology may also be carried out. This may reveal involvement of some novel genes which may possibly be responsive to changes in the Ti surface chemistry.

- A previous study reported an increased bacterial adhesion and colonisation on Ca ion-implanted Ti *in vitro* [Yoshinari et al. 2000]. This can be detrimental, as it not only increases the risk of infection at the supra and sub-gingival sites around dental implants but also causes a subsequent bone loss [Yoshinari et al., 2000]. In order to thoroughly evaluate possible adverse effects of Ca ion-implanted Ti surfaces, a series of future experiment may examine immune reactions *in vitro,* as described before [Hallab et al. 2000; Petty1979]. Another likely route would be to assess the effects of ion-implanted surfaces on cell death by apoptosis [Kylarova et al. 2002] and/or necrosis [Catelas et al. 2005].

- After thorough investigations *in vitro,* the effects of Ca-Ti implants may be examined *in vivo* possibly using the animal models.

References

Ahmad M, Gawronski D, Blum J, Goldberg J, Gronowicz G (1999a) Differential response of human osteoblast-like cells to commercially pure (cp) titanium grades 1 and 4. *J Biomed Mater Res* **46**: 121-131

Ahmad M, McCarthy MB, Gronowicz G (1999b) An in vitro model for mineralization of human osteoblast-like cells on implant materials. *Biomaterials* **20**: 211-220

Ajroud K, Sugimori T, Goldmann WH, Fathallah DM, Xiong JP, Arnaout MA (2004) Binding Affinity of Metal Ions to the CD11b A-domain Is Regulated by Integrin Activation and Ligands. *J Biol Chem* **279**: 25483-25488

Akiyama SK (1996) Integrin in cell adhesion and signalling. *Hum Cell* **9**: 181-186

Albrektsson B, Johansson C (1991) Quantified bone tissue reactions to various metallic materials with reference to the so-called osseointegration concept. In *The bone-biomaterial interface*, Davies JE (ed) pp 357-363. University of Toronto Press

Alonso F, Arizaga A, Quaintons S, Ugarte JJ (1995) Mechanical properties and structure of Ti6Al4V alloy implanted with different light ions. *Surf Coat Technol* **74-75**: 986-992

Anghileri LJ (2000) *Role of calcium in biological systems*. CRC Press

Anselme K (2000) Osteoblast adhesion on biomaterials. *Biomaterials* **21**: 667-681

Anselme K, Linez P, Bigerelle M, Le Maguer D, Le Maguer A, Hardouin P, Hildebrand HF, Iost A, Leroy JM (2000) The relative influence of the topography and chemistry of Ti-6Al-4V surfaces on osteoblastic cell behaviour. *Biomaterials* **21**: 1567-1577

Aplin AE, Howe AK, Juliano RL (1999) Cell adhesion molecules, signal transduction and cell growth. *Curr Opin Cell Biol* **11**: 737-744

Archer CW, Rooney P, Wolpert L (1982) Cell shape and cartilage differentiation of early chick limb bud cells in culture. *Cell differen* **11**: 245-251

Arisawa Y, Abiko Y (1984) Fibronectin mediated human gingival fibroblasts attachment to bone. *Gen Pharmacol* **15**: 293-299

Aronow MA. Gerstenfeld LC. Owen TA. Tassinari MS, Stein GS, and Lian JB. (1990) Factors that promote progressive development of the osteoblast phenotype in cultured fetal rat calvarial cells. *J.Cell Physiol* **143**: 213-221

Arys A, Philippart C, Dourov N, He Y, Le QT, Pireaux JJ (1998) Analysis of titanium dental implants after failure of osseointegration: combined histological, electron microscopy, and X-ray photoelectron spectroscopy approach. *J Biomed Mater Res* **43**: 300-312

Ask M, Lausmaa J, Kasemo B (1989) Preparation and surface spectroscopic characterization of oxide films on Ti-6Al-4V. *App Surf Sci* **35**: 283-301

Aubin JE (2001) Regulation of osteoblast formation and function. *Rev Endocr Metab Disord* **2**: 81-94

Baxter LC, Frauchiger V, Textor M, ap G, I, Richards RG (2002) Fibroblast and osteoblast adhesion and morphology on calcium phosphate surfaces. *Eur Cell Mater* **4**: 1-17

Baylink DJ, Finkelman RD, Mohan S (1993) Growth factors to stimulate bone formation. *J Bone Miner Res* **8 Suppl 2**: S565-S572

Becker P, Neuman HG, and Zeggel P (2001) Resorbable calcium phosphate coatings on orthopaedic and dental implants. European Society of Biomaterials (ESB 16), 78

Becker WM, Reece JB, Poenie MF (1996) *The world of the cell.* The Benjamin/Cummings publishing company

Beresford JN, Graves SE, Smoothy CA (1993) Formation of bone nodules by bone-derived cells in vitro: a model of bone formation? *Am J Med Genet* **45**: 163-178

Berger CE, Rathod H, Gillespie JI, Horrocks BR, Datta HK (2001) Scanning electrochemical microscopy at the surface of bone-resorbing osteoclasts: evidence for steady-state disposal and intracellular functional compartmentalization of calcium. *J Bone Miner Res* **16**: 2092-2102

Berrere F, Habibovic P, van Blitterswijk CA, deGroot K and Layrolle P (2001). Preparation of biomimetic calcium carbonate caotings on Ti-6Al-4V. European Society of Biomaterials (ESB 16), 77

Berridge MJ (1995) Calcium signalling and cell proliferation. *Bioessays* **17**: 491-500

Berridge MJ, Bootman MD, Lipp P (1998) Calcium--a life and death signal. *Nature* **395**: 645-648

Berridge MJ (2001) The versatility and complexity of calcium signalling. *Novartis Found Symp* **239**: 52-64

Birkby CA, Curtis AS, McGrath M, Ripley BD (1988) MHC control of cell position *in vitro*. *J Cell Sci* **89 (Pt 2)**: 167-174

Bordji K, Jouzeau JY, Mainard D, Payan E, Netter P, Rie KT, Stucky T, Hage-Ali M (1996) Cytocompatibility of Ti-6Al-4V and Ti-5Al-2.5Fe alloys according to three surface treatments, using human fibroblasts and osteoblasts. *Biomaterials* **17**: 929-940

Boskey AL (1989) Noncollagenous matrix proteins and their role in mineralization. *Bone Miner* **6**: 111-123

Bowers KT, Keller JC, Randolph BA, Wick DG, Michaels CM (1992) Optimisation of surface micromorphology for enhanced osteoblast responses in vitro. *Int J Oral Maxillofac Implants* **7**: 302-310

Boyan BD, Schwartz Z, Bonewald LF, Swain LD (1989) Localization of 1,25-$(OH)_2$ D_3-responsive alkaline phosphatase in osteoblast-like cells ROS 17 / 2.8, MG-63, and cartilage cells in culture. *J Biol Chem* **264**: 11879-11886

Boyan BD, Hummert TW, Kieswetter K, Schraub DM, Dean DD, Schwartz Z (1995) Effect of titanium surface characteristics on chondrocytes and osteoblasts *in vitro*. *Cells Mater* **5**: 335

Boyan BD, Hummert TW, Dean DD, Schwartz Z (1996) Role of material surfaces in regulating bone and cartilage cell response. *Biomaterials* **17**: 137-146

Boyan BD, Batzer R, Kieswetter K, Liu Y, Cochran DL, Szmuckler-Moncler S, Dean DD, Schwartz Z (1998) Titanium surface roughness alters responsiveness of MG63 osteoblast-like cells to 1 alpha,25-(OH)2D3. *J Biomed Mater Res* **39**: 77-85

Boyan BD, Lossdorfer S, Wang L, Zhao G, Lohmann CH, Cochran DL, Schwartz Z (2003) Osteoblasts generate an osteogenic microenvironment when grown on surfaces with rough microtopographies. *Eur Cell Mater* **6**: 22-27

Brånmark PI (1983) Osseointegration and its experimental background. *J Prosthet Dent* **50**: 399-410

Brånmark PI (1985) Introduction to osseointegration. In *Tissue-Integrated Prosthesis*, Brånmark PI, Zarb GA, Albrektsson B (eds) pp 11-76. Quintessence Publishing Co. Inc

Brekken RA, Sage EH (2001) SPARC, a matricellular protein: at the crossroads of cell-matrix communication. *Matrix Biol* **19**: 816-827

Brett PM, Harle J, Salih V, Mihoc R, Olsen I, Jones FH, Tonetti M (2004) Roughness response genes in osteoblasts. *Bone* **35**: 124-133

Brown WL (1989) Ion beam induced chemical changes in molecular solids. *Nuc Instr Meth B* **37-38**: 270-274

Brown EM (1991) Extracellular Ca2+ sensing, regulation of parathyroid cell function, and role of Ca2+ and other ions as extracellular (first) messengers. *Physiol Rev* **71**: 371-411

Brown D (1997) All you wanted to know about titanium, but were afraid to ask. *Br Dent J* **182**: 393-394

Brown TA (1997) *Gene cloning an introduction.* Chapman and Hall

Brunette DM, Tengvall P, Textor M, Thomsen P (2001) *Titanium in Medicine.* Springer

Buchanan RA, Ridney ED, Williams JM (1987a) Ion-implantation of surgical Ti-6Al-4V for improved resistance to wear-accelerated corrosion. *J Biomed Mater Res* **21**: 355-366

Buchanan RA, Rigney ED, Jr., Williams JM (1987b) Wear-accelerated corrosion of Ti-6Al-4V and nitrogen-ion-implanted Ti-6Al-4V: mechanisms and influence of fixed-stress magnitude. *J Biomed Mater Res* **21**: 367-377

Buchanan RA, Lee IS, Williams JM (1990) Surface modification of biomaterials through noble metal ion implantation. *J Biomed Mater Res* **24**: 309-318

Butler WT (1989) The nature and significance of osteopontin. *Connect Tissue Res* **23**: 123-136

Calvo Mateo MA, Ruiz Marcellan MC, Banares Agustin MV, Padros FA, Sada ME (1998) Morphological and immunohistochemical aspects of the biological seal in Klockner's dental implants: study of 15 cases. *Implant Dent* **7**: 103-112

Cao H, Chen HQ, Wu J, Li L (2004) Effect of titanium particles loading on the viability of mesenchymal stem cells after osteoblastic induction. *Sichuan Da Xue Xue Bao Yi Xue Ban* **35**: 323-326

Carre PC, Mortenson RL, King TE, Jr., Noble PW, Sable CL, Riches DW (1991) Increased expression of the interleukin-8 gene by alveolar macrophages in idiopathic pulmonary fibrosis. A potential mechanism for the recruitment and activation of neutrophils in lung fibrosis. *J Clin Invest* **88**: 1802-1810

Castoldi M, Pistone M, Caruso C, Puddo A, Filanti C, Piccini D, Tacchetti C, Manduca P (1997) Osteoblastic cells from rat long bone, 11: Adhesion to substrata and integrin expression in primary and propagated cultures. *Cell Biol Int* **21**: 7-16

Catelas I, Petit A, Vali H, Fragiskatos C, Meilleur R, Zukor DJ, Antoniou J, Huk OL (2005) Quantitative analysis of macrophage apoptosis vs. necrosis induced by cobalt and chromium ions in vitro. *Biomaterials* **26**: 2441-2453

Chaudhary LR, Hofmeister AM, Hruska KA (2004) Differential growth factor control of bone formation through osteoprogenitor differentiation. *Bone* **34**: 402-411

Chehroudi B, Ratkay J, Brunette DM (1992) The role of implant surface geometry on mineralisation *in vivo* and *in vitro*: a transmission and scanning electron microscopic study. *Cells Mater* **2**: 89-104

Chen CS, Mrksich M, Huang S, Whitesides G, Ingber DE (1997) Geometric control of cell life and death. *Science* **276**: 1425-1428

Chen CC, Huang TH, Kao CT, Ding SJ (2005) Characterization of functionally graded hydroxyapatite/titanium composite coatings plasma-sprayed on Ti alloys. *J Biomed Mater Res B Appl Biomater* [Epub ahead of print]

Chen D, Zhao M, Mundy GR (2004) Bone morphogenetic proteins. *Growth Factors* **22**: 233-241

Chesmel KD, Clark CC, Brighton CT, Black J (1995) Cellular responses to chemical and morphologic aspects of biomaterial surfaces. 11. The biosynthetic and migratory response of bone cell populations. *J Biomed Mater Res* **29**: 1101-1110

Chiang HS, Yang RS, Huang TF (1995) The Arg-Gly-Asp containing peptide, rhoostomin, inhibits in vitro cell adhesion to extracellular matrices and platelet aggregation caused by Saos-2 human osteosarcoma cells. *Brit J Cancer* **71**: 265-266

Clover J, Gowen M (1994) Are MG-63 and HOS TE85 human osteosarcoma cell lines representative models of the osteoblastic phenotype? *Bone* **15**: 585-591

Cooper LF, Masuda T, Whitson SW, Yliheikkila P, Felton DA (1999) Formation of mineralizing osteoblast cultures on machined, titanium oxide grit-blasted, and plasma-sprayed titanium surfaces. *Int J Oral Maxillofac Implants* **14**: 37-47

Dalby MJ, Yarwood SJ, Riehle MO, Johnstone HJH, Affrossman S, Curtis ASG (2002) Increasing fibroblast response to materials using nanotopography: morphological and genetic measurements of cell response to 13 nm-high polymer demixed islands. *Exp Cell Res* **276**: 1-9

Danova M, Riccardi A, Giordano M, Girino M, Mazzini G, Dezza L, Ascari E (1988) Cell cycle-related proteins: a flow cytofluorometric study in human tumors. *Biol Cell* **64**: 23-28

Davies JE (1998) Mechanisms of endosseous integration. *Int J Prosthodont* **11**: 391-401

Davis PK, Ho A, Dowdy SF (2001) Biological methods for cell-cycle synchronization of mammalian cells. *Biotechniques* **30**: 1322-1

de Ruijter JE, ter Brugge PJ, Dieudonne SC, van Vliet SJ, Torensma R, Jansen JA (2001) Analysis of integrin expression in U2OS cells cultured on various calcium phosphate ceramic substrates. *Tissue Eng* **7**: 279-289

Degasne I, Basle MF, Demais V, Hure G, Lesourd M, Grollleau B, Mercier L, Chappard D (1999) Effects of roughness, fibronectin and vitronectin on attachment, spreading and proliferation of human osteoblast-like cells (Saos-2) on titanium surfaces. *Calcif Tissue Int* **64**: 499-507

Delany AM, Canalis E (1998) Basic fibroblast growth factor destabilizes osteonectin mRNA in osteoblasts. *Am J Physiol* **274**: C734-C740

Denhardt DT, Guo X (1993) Osteopontin: a protein with diverse functions. *FASEB J* **7**: 1475-1482

Denhardt DT, Giachelli CM, Rittling SR (2001a) Role of osteopontin in cellular signaling and toxicant injury. *Annu Rev Pharmacol Toxicol* **41**: 723-749

Denhardt DT, Noda M, O'Regan AW, Pavlin D, Berman JS (2001b) Osteopontin as a means to cope with environmental insults: regulation of inflammation, tissue remodeling, and cell survival. *J Clin Invest* **107**: 1055-1061

Derhami K, Zheng J, Li L, Wolfaardt JF, Scott PG (2001) Proteomic analysis of human skin fibroblasts grown on titanium: novel approach to study molecular biocompatibility. *J Biomed Mater Res* **56**: 234-244

Diener A, Nebe B, Lüthen F, Becker P, Beck U, Neumann HG, Rychly J (2005) Control of focal adhesion dynamics by material surface characteristics. *Biomaterials* **26**: 383-392

Doi Y, Horiguchi T, Kim SH, Moriwaki Y, Wakamatsu N, Adachi M, Ibaraki K, Moriyama K, Sasaki S, Shimokawa H (1992) Effects of non-collagenous proteins on the formation of apatite in calcium beta-glycerophosphate solutions. *Arch Oral Biol* **37**: 15-21

Donley, Gillete WB (1991) Titanium endosseus implant-soft tissue interface: literature review. *J Periodontol* **62**: 153-160

Doundoulakis JH (1987) Surface analysis of titanium after sterilization: role in implant-tissue interface and bioadhesion. *J Prosthet Dent* **58**: 471-478

Dukas K, Sarfati P, Vaysse N, Pradayrol L (1993) Quantitation of changes in the expression of multiple genes by simultaneous polymerase chain reaction. *Anal Biochem* **215**: 66-72

Dvorak MM, Riccardi D (2004) Ca2+ as an extracellular signal in bone. *Cell Calcium* **35**: 249-255

Ellingsen JE (1998) Surface configuration of dental implants. *Periodontology 2000* **17**: 36-46

Esposito M, Hirsch JM, Lekholm U, Thomsen P (1998) Biological factors contributing to failure of osseointegrated oral implants (II) etiopathogenesis. *Eur J Oral Sci* **106**: 721-764

Esposito M, Lausmaa J, Hirsch JM, Thomsen P (1999) Surface analysis of failed oral titanium implants. *J Biomed Mater Res* **48**: 559-568

Estessabi, A. M., Otsuka, T., and Tsuboi, Y. Quantitative measurement of metal ion release from orthopaedic and dental implants. Fifth World Biomater. Congress. 1996. 31-5-1996

Feller HG, Kllinger R, Benecke W (1985) Tribo-enhance diffusion of nitrogen implanted into steel. *Mater Sci Eng* **69**: 173-180

Feng B, Weng J, Yang BC, Qu SX, Zhang XD (2004) Characterization of titanium surfaces with calcium and phosphate and osteoblast adhesion. *Biomaterials* **25**: 3421-3428

Ferraz MP, Knowles JC, Olsen I, Monteiro FJ, Santos JD (1999) Flow cytometry analysis of effects of glass on response of osteosarcoma cells to plasma-sprayed hydroxyapatite/CaO-P(2)O(5) coatings. *J Biomed Mater Res* **47**: 603-611

Ferraz MP, Knowles JC, Olsen I, Monteiro FJ, Santos JD (2000) Flow cytometry analysis of the effects of pre-immersion on the biocompatibility of glass reinforced hydroxyapaptite plasma-sprayed coatings. *Biomaterials* **21**: 813-820

Filippini P, Rainaldi G, Ferrante A, Mecheri B, Gabrielli G, Bombace M, Indovina PL, Santini MT (2001) Modulation of osteosarcoma cell growth and differentiation by silane-modified surfaces. *J Biomed Mater Res* **55**: 338-349

Fisher LW, Whitson SW, Avioli LV, Termine JD (1983) Matrix sialoprotein of developing bone. *J Biol Chem* **258**: 12723-12727

Folkman J, Moscona A (1978) Role of cell shape in growth control. *Nature* **273**: 345-349

Foschi F, Nucci C, Montebugnoli L, Marchionni S, Breschi L, Malagnino VA, Prati C (2004) SEM evaluation of canal wall dentine following use of Mtwo and ProTaper NiTi rotary instruments. *Int Endod J* **37**: 832-839

Franks K, Salih V, Knowles JC, Olsen I (2002) The effect of MgO on the solubility behavior and cell proliferation in a quaternary soluble phosphate based glass system. *J Mater Sci Mater Med* **13**: 549-556

Friedenstein AJ, Chailakhyan RK, Gerasimov UV (1987) Bone marrow osteogenic stem cells: *in vitro* cultivation and transplantation in diffusion chambers. *Cell Tissue Kinet* **20**: 263-272

Garratt-Reed AJ, Bell DC (2003) *Energy dispersive X-ray analysis in the electron microscope*. BIOS Scientific Publishers

Givan AL (2005) *Flow Cytometry: First Principles*. John Wiley & Sons, Inc.

Goldberg HA, Hunter GK (1995) The inhibitory activity of osteopontin on hydroxyapatite formation in vitro. *Ann N Y Acad Sci* **760**: 305-308

Goodhew PJ, Cartwright LE, Humphreys FJ, Beanland R (2000) *Electron microscopy and analysis*. Taylor and Francis

Granchi D, Stea S, Ciapetti G, Cavedagna D, Stea S, Pizzoferrato A (1995a) Endodontic cements induce alterations in the cell cycle of in vitro cultured osteoblasts. *Oral Surg Oral Med Oral Pathol Oral Radiol Endod* **79**: 359-366

Granchi D, Stea S, Ciapetti G, Savarino L, Cavedagna D, Pizzoferrato A (1995b) In vitro effects of bone cements on the cell cycle of osteoblast-like cells. *Biomaterials* **16**: 1187-1192

Grano M, Zigrino P, Colucci S, Zambonin G, Trusolino L (1994) Adhesion properties and integrin expression of cultured human osteoclast-like cells. *Exp Cell R* **212**: 209-218

Grill V, Sandrucci MA, Di LR, Basa M, Narducci P, Martelli AM, Bareggi R (2000a) In vitro evaluation of the biocompatibility of dental alloys: fibronectin expression patterns and relationships to cellular proliferation rates. *Quintessence Int* **31**: 741-747

Grill V, Sandrucci MA, Di LR, Dorigo E, Narducci P, Martelli AM, Bareggi R (2000b) Cell proliferation rates and fibronectin arrangement as parameters for biocompatibility evaluation of dental metal alloys in vitro. *J Oral Sci* **42**: 1-7

Grinnell F, Feld M (1981) Adsorption properties of fibronectin in relationship to biological activity. *J Biomed Mater Res* **15**: 363-381

Groessner-Schreiber B, Neubert A, Muller WD, Hopp M, Griepentrog M, Lange KP (2003) Fibroblast growth on surface-modified dental implants: an in vitro study. *J Biomed Mater Res A* **64**: 591-599

Gronowicz G, McCarthy MB (1996) Response of human osteoblasts to implant materials: integrin-mediated adhesion. *J Orthop Res* **14**: 878-887

Guo W, Gorlick R, Ladanyi M, Meyers PA, Huvos AG, Bertino JR, Healey JH (1999) Expression of bone morphogenetic proteins and receptors in sarcomas. *Clin Orthop Relat Res* 175-183

Hallab NJ, Mikecz K, Jacobs JJ (2000) A triple assay technique for the evaluation of metal-induced, delayed-type hypersensitivity responses in patients with or receiving total joint arthroplasty. *J Biomed Mater Res* **53**: 480-489

Hambleton J, Schwartz Z, Khare A, Windeler SW, Luna M, Brooks BP, Dean DD, Boyan BD (1994) Culture surfaces coated with various implant materials affect chondrocyte growth and metabolism. *J Orthop Res* **12**: 542-552

Hanawa T (1991) Titanium and its oxide film: a substrate for formation of apatite. In *The bone-biomaterial interface*, Davies JE (ed) pp 49-61. University of Toronto Press

Hanawa T, Ukai H, Murakami K (1993) X-ray photoelectron spectroscopy of calcium-ion-implanted titanium. *J Electron Spectrosc Relat Phenom* **63**: 347-354

Hanawa T, Asami K and Asaoka K (1996a) AES studies on the dissolution of surface oxide from calcium-ion-implanted titanium in nitric acid and buffer solutions. *Corrosion Sci* **38[11]**: 2061-2067

Hanawa T, Asami K, Asaoka K (1996b) Microdissolution of calcium ions from calcium-ion-implanted titanium. *Corrosion Sci* **38**: 1579-1594

Hanawa T, Kamiura Y, Yamamoto S, Kohgo T, Amemiya A, Ukai H, Murakami K, Asaoka K (1997) Early bone formation around calcium-ion-implanted titanium inserted into rat tibia. *J Biomed Mater Res* **36**: 131-136

Hanawa T, Asami K, Asaoka K (1998) Repassivation of titanium and surface oxide film regenerated in simulated bioliquid. *J Biomed Mater Res* **40**: 530-538

Hanawa T (1999) *In vivo* metallic biomaterials and surface modifications. *Mater Sci Eng* **A267**: 260-266

Harris G, Olsen I (1976) Cell division and deoxyribonucleic acid (DNA) synthesis in cultures of stimulated lymphocytes. *Immunology* **31**: 195-204

Herring GM (1972) The organic matrix of bone. In *The biochemistry and physiology of bone*, Bourne GH (ed) pp 127-189. Academic Press

Hirota S, Imakita M, Kohri K, Ito A, Morii E, Adachi S, Kim HM, Kitamura Y, Yutani C, Nomura S (1993) Expression of osteopontin messenger RNA by macrophages in atherosclerotic plaques. A possible association with calcification. *Am J Pathol* **143**: 1003-1008

Hopper KE (1986) Kinetics of macrophage recruitment and turnover in peritoneal inflammatory exudates induced by Salmonella or thioglycollate broth. *J Leukoc Biol* **39**: 435-446

Hormia M, Kononen M (1994) Immunolocalization of fibronectin and vitronectin receptors in human gingival fibroblasts spreading on titanium surfaces. *J Periodontal Res* **29**: 146-152

Howlett CR, Evans MD, Wildish KL, Kelly JC, Fisher LR, Francis GW, Best DJ (1993) The effect of ion implantation on cellular adhesion. *Clin Mater* **14**: 57-64

Howlett CR, Evans MD, Walsh WR, Johnson G, Steele JG (1994) Mechanism of initial attachment of cells derived from human bone to commonly used prosthetic materials during cell culture. *Biomaterials* **15**: 213-222

Howlett CR, Zreiqat H, Wu Y, McFall DW, McKenzie DR (1999a) Effect of ion modification of commonly used orthopedic materials on the attachment of human bone-derived cells. *J Biomed Mater Res* **45**: 345-354

Howlett CR (1999b) Early bone formation around calcium-ion-implanted titanium inserted into rat tibia. *J Biomed Mater Res* **44**: 352-353

Hughes FJ, Collyer J, Stanfield M, Goodman SA (1995) The effects of bone morphogenetic proteins-2, -4, -6 on differentiation of rat osteoblast cells in vitro. *Endocrinology* **136**: 2671-2677

Hui MZ, Sukhu B, Tenenbaum HC (1996) Expression of tissue non-specific alkaline phosphatase stimulates differentiated behaviour in specific transformed cell populations. *Anat Rec* **244**: 423-436

Hunter GK, Hauschka PV, Poole AR, Rosenberg LC, Goldberg HA (1996) Nucleation and inhibition of hydroxyapatite formation by mineralized tissue proteins. *Biochem J* **317 (Pt 1)**: 59-64

Hynes RO (1987) Integrins: a family of cell surface receptors. *Cell* **48**: 549-554

Hynes RO (1992) Integrins: versatility, modulation, and signaling in cell adhesion. *Cell* **69**: 11-25

Hynes RO (2002) Integrins: bidirectional, allosteric signaling machines. *Cell* **110**: 673-687

Ihl-Vahl R, Marquetant R, Bremerich J, Strasser RH (1995) Regulation of beta-adrenergic receptors in acute myocardial ischemia: subtype-selective increase of mRNA specific for beta 1-adrenergic receptors. *J Mol Cell Cardiol* **27**: 437-452

Ikeyama M, Nakao S, Morikawa H, Yokogawa Y, Wielunski LS, Clissold RA, Bell T (2000) Surface hardness changes induced by O-, Ca- or P-ion implantation into titanium. *Colloids Surf B Biointerfaces* **19**: 263-268

Jackman M, Lindon C, Nigg EA, Pines J (2003) Active cyclin B1-Cdk1 first appears on centrosomes in prophase. *Nat Cell Biol* **5**: 143-148

Jayaraman M, Meyer U, Buhner M, Joos U, Wiesmann HP (2004) Influence of titanium surfaces on attachment of osteoblast-like cells in vitro. *Biomaterials* **25**: 625-631

Jennissen HP (2002) Accelerated and improved osteointegration of implants biocoated with bone morphogenetic protein 2 (BMP-2). *Ann N Y Acad Sci* **961**: 139-142

Jinno T, Kirk SK, Morita S, Goldberg VM (2004) Effects of Calcium ion implantation on osseointegration of surface-blasted titanium alloy femoral implants in a canine total hip arthroplasty model. *J Arthroplas* **19**: 102-109

Johansson CB, Lausmaa J, Rostlund T, Thomsen P (1993) Commercially pure titanium and Ti-6Al-4V implants with and without nitrogen implantation: surface characterization and quantitative studies in rabbit cortical bone. *J Mater Sci: Mater Med* **4**: 132-141

Johnson DG, Walker CL (1999) Cyclins and cell cycle checkpoints. *Annu Rev Pharmacol Toxicol* **39**: 295-312

Johnson GA, Burghardt RC, Bazer FW, Spencer TE (2004) Osteopontin: roles in implantation and placentation. *Biol reproduc* **69**: 1458-1471

Jones A, Reed R, Weyers J (1994) *Practical skills in biology.* Addison Wesley Longman Limited

Jones JR, Sepulveda P, Hench LL (2001) Dose-dependent behavior of bioactive glass dissolution. *J Biomed Mater Res* **58**: 720-726

Jono S, Peinado C, Giachelli CM (2000) Phosphorylation of osteopontin is required for inhibition of vascular smooth muscle cell calcification. *J Biol Chem* **275**: 20197-20203

Juliano DJ, Saavedra SS, Truskey GA (1993) Effect of the confrontation and orientation of adsorbed fibronectin on endothelial cell spreading and the strength of adhesion. *J Biomed Mater Res* **27**: 1103-1113

Juliano RL, Haskill S (1993) Signal transduction from the extracellular matrix. *J Cell Biol* **120**: 577-585

Kahl CR, Means AR (2003) Regulation of cell cycle progression by calcium/calmodulin-dependent pathways. *Endocr Rev* **24**: 719-736

Kasemo B, Lausmaa J (1986) Surface science aspects on inorganic biomaterials. *CRC Crit Rev Biocomp* **2**: 335-380

Kasemo B, Lausmaa J (1988) Biomatrial and implant surfaces: A surface science approach. *Int J Oral Maxillofac Implants* **3**: 247-259

Kasemo B, Gold J (1999) Implant surfaces and interface processes. *Adv Dent Res* **13**: 8-20

Katou F, Ohtani H, Nagura H, Motegi K (1998) Procollagen-positive fibroblasts predominantly express fibrogenic growth factors and their receptors in human encapsulation process against foreign body. *J Pathol* **186**: 201-208

Kilpadi KL, Chang PL, Bellis SL (2001) Hydroxylapatite binds more serum proteins, purified integrins, and osteoblast precursor cells than titanium or steel. *J Biomed Mater Res* **57**: 258-267

Kim HM, Miyaji F, Kokubo T, Nakamura T (1996) Preparation of bioactive Ti and its alloys via simple chemical surface treatment. *J Biomed Mater Res* **32**: 409-417

Kim HM, Miyaji F, Kokubo T, Nishiguchi S, Nakamura H (1999) Graded surface structure of bioactive titanium prepared by chemical treatment. *J Biomed Mater Res* **45**: 100-107

Kim Y, Jang JH, Ku Y, Koak JY, Chang IT, Kim HE, Lee JB, Heo SJ (2004) Microarray-based expression analysis of human osteoblast-like cell response to anodized titanium surface. *Biotechnol Lett* **26**: 399-402

Kirkpatrick CJ, Wagner M, Kohler H, Bittinger F, Otto M, Klein CL (1997) The cell and molecular biological approach to biomaterial research: a perspective. *J Mater Sci Mater Med* **8**: 131-141

Knabe C, Howlett CR, Klar F, Zreiqat H (2004) The effect of different titanium and hydroxyapatite-coated dental implant surfaces on phenotypic expression of human bone-derived cells. *J Biomed Mater Res* **71A**: 98-107

Kokubo T, Kushitani H, Sakka S, Kitsugi T, Yamamuro TJ (1990) Solutions able to reproduce *in-vivo* surface-structure changes in bioactive glass-ceramic A-W3. *J Biomed Mater Res* **24**: 721-734

Kooten TG, Klein CL, Kohler H, Kirkpatrick CJ, Williams DF, Eloy R (1997) From cytotoxicity to biocompatibility testing in vitro: cell adhesion molecule expression defines a new set of parameters. *J Mater Sci Mater Med* **8**: 835-841

Korchynskyi O, Ten DP (2002) Identification and functional characterization of distinct critically important bone morphogenetic protein-specific response elements in the Id1 promoter. *J Biol Chem* **277**: 4883-4891

Kornberg L, Juliano RL (1992) Signal transduction from the extracellular matrix: the integrin-tyrosine kinase connection. *Trends Pharmacol Sci* **13**: 93-95

Kornberg LJ, Earp HS, Turner CE, Prockop C, Juliano RL (1991) Signal transduction by integrins: increased protein tyrosine phosphorylation caused by clustering of beta 1 integrins. *Proc Natl Acad Sci U S A* **88**: 8392-8396

Kornu R, Maloney WJ, Kelly MA, Smith RL (1996) Osteoblast adhesion to orthopaedic implant alloys: effects of cell adhesion molecules and diamond-like carbon coating. *J Orthop Res* **14**: 871-877

Koulaouzidou EA, Papazisis KT, Beltes P, Geromichalos GD, Kortsaris AH (1998) Cytotoxicity of three resin-based root canal sealers: an in vitro evaluation. *Endod Dent Traumatol* **14**: 182-185

Kranenburg, O., Van der Eb, A. J., and Zantema, A (1996) Induction of polyploidy in Adenovirus E1-transformed cells by the mitotic inhibitor colcemid. *Virus Res* **40**: 185-190.

Krause A, Cowles EA, Gronowicz G (2000) Integrin-mediated signaling in osteoblasts on titanium implant materials. *J Biomed Mater Res* **52**: 738-747

Krupa D, Baszkiewicz J, Kozubowski JA, Barcz A, Sobczak JW, Biliniski A, Lewandowska-Szumiel MD, Rajchel B (2001a) Effect of calcium-ion implantation on the corrosion resistance and biocompatibility of titanium. *Biomaterials* **22**: 2139-2151

Krupa D, Baszkiewicz J, Kozubowski JA, Barcz A, Sobczak JW, Biliniski A, Rajchel B (2001b) The influence of calcium and/or phosphorous ion-implantation on the structure and corrosion resistance of titanium. *Vacuum* **63**: 715-719

Krupa D, Baszkiewicz J, Kozubowski JA, Barcz A, Sobczak JW, Biliniski A, Lewandowska-Szumiel MD, Rajchel B (2002) Effect of phosphorous-ion implantation on the corrosion resistance and biocompatibility of titanium. *Biomaterials* **23**: 3329-3340

Krupa D, Baszkiewicz J, Kozubowski JA, Barcz A, Sobczak JW, Bilinski A, Lewandowska-Szumiel M, Rajchel B (2005) Effect of dual ion implantation of calcium and phosphorus on the properties of titanium. *Biomaterials* **26**: 2847-2856

Ku CH, Pioletti DP, Browne M, Gregson PJ (2002) Effect of different Ti-6Al-4V surface treatments on osteoblasts behaviour. *Biomaterials* **23**: 1447-1454

Kuru L, Parkar MH, Griffiths GS, Newman HN, Olsen I (1998) Flow cytometry analysis of gingival and periodontal ligament cells. *J Dent Res* **77**: 555-564

Kuwada SK, Li X (2000) Integrin alpha5/beta1 mediates fibronectin-dependent epithelial cell proliferation through epidermal growth factor receptor activation. *Mol Biol Cell* **11**: 2485-2496

Kylarova D, Prochazkova J, Mad'arova J, Bartos J, Lichnovsky V (2002) Comparison of the TUNEL, lamin B and annexin V methods for the detection of apoptosis by flow cytometry. *Acta Histochem* **104**: 367-370

Lackie JM, Dow JAT (2000) *The dictionary of cell and molecular biology.* Academic press

Lajeunesse D, Frondoza CG, Schoffield B, Sactor B (1990) Osteocalcin secretion by the human osteosarcoma cell line MG-63. *J Bone Miner Res* **5**: 915-922

Lajeunesse D, Kiebzak GM, Frondoza CG, Sacktor B (1991) Regulation of osteocalcin secretion by humna primary bone cells and by the human osteosarcoma cell line MG-63. *J Bone Miner Res* **14**: 237-250

Landberg, G, Tan EM, and Roos G (1990) Flow cytometric multiparameter analysis of proliferating cell nuclear antigen / cyclin and Ki-67 antigen: a new view of the cell cycle. *Exp Cell Res* **187**:111-118.

Lange R, Luthen F, Beck U, Rychly J, Baumann A, Nebe B (2002) Cell-extracellular matrix interaction and physico-chemical characteristics of titanium surfaces depend on the roughness of the material. *Biomol Eng* **19**: 255-261

Lauer G, Wiedmann-Al-Ahmad M, Otten JE, Hubner U, Schmelzeisen R, Schilli W (2001) The titanium surface texture effects adherence and growth of human gingival keratinocytes and human maxillar osteoblast-like cells in vitro. *Biomaterials* **22**: 2799-2809

Lausmaa J, Kasemo B, Rolander U, Bjursten LM, Ericson LE, Rosander L (1988) Preparation, surface spectroscopic and electron microscopic characterization of titanium implant materials. In *Surface characterization of biomaterials*, Ratner BD (ed) pp 161-174. Elsevier Academic Press

LeBaron RG, Athanasiou KA (2000) Extracellular matrix cell adhesion peptides: functional applications in orthopedic materials. *Tissue Eng* **6**: 85-103

LeGeros RZ, Orly I, Gregoire M, Daculsi G (1991) Substrate surface dissolution and interfacial biological mineralization. In *The bone-biomaterial interface*, Davies JE (ed) pp 76-88. University of Toronto Press

Leitao and Barbosa MA (1998) In vitro testing of surface-modified biomaterials. *J Mater Sci: Mater Med* **9**: 543-548

Li P, Ducheyne P (1997). Quasi-biological apatite film induced by titanium in a simulated body fluid. *J.Biomed.Mater Res* **41**, 341-348. 1997.

Lincks J, Boyan BD, Blanchard CR, Lohmann CH, Liu Y, Cochran DL, Dean DD, Schwartz Z (1998a) Response of MG63 osteoblast-like cells to titanium and titanium alloy is dependent on surface roughness and composition. *Biomaterials* **19**: 2219-2232

Lincks, J., Boyan, B. D., Cochran, D. L., Liu, Y., Blanchard, C., Dean, D. D., and Schwartz, Z (1998b). Cell type and maturation state determine cell response to surface roughness and composition. *J.Dent.Res* **77**(966), 2678.

Linez-Bataillon P, Monchau F, Bigerelle M, Hildebrand HF (2002) In vitro MC3T3 osteoblast adhesion with respect to surface roughness of Ti-6Al-4V substrates. *Biomol Eng* **19**: 133-141

Locci P, Becchetti E, Pugliese M, Rossi L, Belcastro S, Calvitti M, Pietrarelli G, Staffolani N (1997) Phenotype expression of human bone cells cultured on implant substrates. *Cell Biochem and Funct* **15**: 163-167

Lockhart DJ, Winzeler EA (2000) Genomics, gene expression and DNA arrays. *Nature* **405**: 827-836

Lodish H, Baltimore D, Berk A, Zipursky SL, Matsudaira P, Darnell J (1996) *Molecular cell biology*. Scientific American Books

Long M, Rack HJ (1998) Titanium alloys in total joint replacement-a materials science perspective. *Biomaterials* **19**: 1621-1639

Lopes MA, Knowles JC, Kuru L, Santos JD, Monteiro FJ, Olsen I (1998) Flow cytometry for assessing biocompatibility. *J Biomed Mater Res* **41**: 649-656

Lori F, Lisziewicz J (2000) Rationale for the use of hydroxyurea as an anti-human immunodeficiency virus drug. *Clin Infec Diseases* **30**: 193-197

Lu KP, Means AR (1993) Regulation of the cell cycle by calcium and calmodulin. *Endocr Rev* **14**: 40-58

Lucas ALC, Lemons JE (1992) Biodegradation of restorative metallic systems. *Adv Dent Res* **6**: 32

Lumbikanonda N, Sammons R (2001) Bone cell attachment to dental implants of different surface characteristics. *Int J Oral Maxillofac Implants* **16**: 627-636

Mackie EJ (2003) Osteoblasts: novel roles in orchestration of skeletal architecture. *Int J Biochem Cell Biol* **35**: 1301-1305

MacNeil RL, Berry J, D'Errico J, Strayhorn C, Piotrowski B, Somerman MJ (1995) Role of two mineral-associated adhesion molecules, osteopontin and bone sialoprotein, during cementogenesis. *Connect Tissue Res* **33**: 1-7

Maeztu MA, Alava JI, Gay-Escoda C (2003) Ion implantation: surface treatment for improving the bone integration of titanium and Ti-Al-4V dental implants. *Clin Oral Implants Res* **14**: 57-62

Maitz MF, Pham MT, Matz W, Reuther H, Steiner G (2002a) Promoted calcium-phosphate precipitation from solution on titanium for improved biocompatibility by ion-implantation. *Surf Coat Technol* **158-159**: 151-156

Maitz MF, Pham MT, Matz W, Reuther H, Steiner G, Richter E (2002b) Ion beam treatment of titanium surfaces for enhancing deposition of hydroxyapatite from solution. *Biomol Eng* **19**: 269-272

Malaval L, Modrowski D, Gupta AK, Aubin JE (1994) Cellular expression of bone-related proteins during the in vitro osteogenesis in rat bone marrow stromal cell cultures. *J Cell Physiol* **158**: 555-572

Mante M, Daniels B, Golden E, Diefenderfer D, Reilly G, Leboy PS (2003) Attachment of human marrow stromal cells to titanium surfaces. *J Oral Implantol* **29**: 66-72

Maroothynaden J, Hench LL (2001) Bioglass (R) stimulation of embryonic long-bones in altered loading environments. *J Gravit Physiol* **8**: 79-80

Martin JY, Schwartz Z, Hummert TW, Schraub DM, Simpson J, Lankford J, Jr., Dean DD, Cochran DL, Boyan BD (1995) Effect of titanium surface roughness on proliferation, differentiation, and protein synthesis of human osteoblast-like cells (MG63). *J Biomed Mater Res* **29**: 389-401

Martin JY, Dean DD, Cochran DL, Simpson J, Boyan BD, Schwartz Z (1996) Proliferation, differentiation, and protein synthesis of human osteoblast-like cells (MG-63) cultured on previously used titanium surfaces. *Clin Oral Implants Res* **7**: 27-37

Massaro C, Baker MA, Cosentino F, Ramires PA, Klose S, Milella E (2001) Surface and biological evaluation of hydroxyapatite-based coatings on titanium deposited by different techniques. *J Biomed Mater Res* **58**: 651-657

Massas R, Pitaru S, Weinreb MM (1993) The effects of titanium and hydroxyapatite on osteoblastic expression and proliferation in rat parietal bone cultures. *J Dent Res* **72**: 1005-1008

Masuda T, Salvi GE, Offenbacher S, Felton DA, Cooper LF (1997) Cell and matrix reactions at titanium implants in surgically prepared rat tibiae. *Int J Oral Maxillofac Implants* **12**: 472-485

Maurer-Schultze B, Siebert M, Bassukas ID (1988) An in vivo study on the synchronizing effect of hydroxyurea. *Exp Cell Res* **174**: 230-243

McKee, M. D. and Nanci, A (1996) Osteopontin at mineralized tissue interfaces in bone, teeth and osseointegrated implants: ultrastructural distribution and

implications for mineralized tissue formation, turnover, and repair. *Microsc Res Tech* **33[2]**:141-164.

Means AR (1994) Calcium, calmodulin and cell cycle regulation. *FEBS Lett* **347**: 1-4

Meng X, Kwon TY, Yang Y, Ong JL, Kim KH (2005) Effects of applied voltages on hydroxyapatite coating of titanium by electrophoretic deposition. *J Biomed Mater Res B Appl Biomater* [Epub ahead of print]

Merli M, Benassi MS, Gamberi G, Ragazzini P, Sollazzo MR, Molendini L, Magagnoli G, Ferrari C, Maltarello MC, Picci P (1999) Expression of G1 phase regulators in MG-63 osteosarcoma cell line. *Int J Oncol* **14**: 1117-1121

Miyamoto S, Teramoto H, Coso OA (1995) Integrin function: molecular hierarchies of cytoskeletal and signalling molecules. *J Cell Biol* **131**: 791-805

Miyazono K (1999) Signal transduction by bone morphogenetic protein receptors: functional roles of Smad proteins. *Bone* **25**: 91-93

Mohan S, Baylink DJ (1991) Bone growth factors. *Clin Orthop Relat Res* 30-48

Montanero L, Arciola CR, Campoccia D, Cervellati M (2002) In vitro effects of MG63 osteoblast-like cells following contact with two roughness-differing fluorohydroxyapatite-coated titanium alloys. *Biomaterials* **23**: 3651-3659

Mosmann T (1983) Rapid colorimetric assay for cellular growth and survival: application to proliferation and cytotoxicity assays. *J Immunol Methods* **65**: 55-63

Mrksich M, Chen CS, Xia Y, Dike LE, Ingber DE, Whitesides GM (1996) Controlling cell attachment on contoured surfaces with self-assembled monolayers of alkanethiolates on gold. *Proc Natl Acad Sci U S A* **93**: 10775-10778

Mucha A, Braun M (1992) Requisite parameters for optimal wear performance of nitrogen-implanted titanium and Ti6Al$_4$V. *Surf Coat Technol* **50**: 135-139

Mujoomdar M, Bennett A, Hoskin D, Blay J (2004) Adenosine stimulation of proliferation of breast carcinoma cell lines: evaluation of the [^{3}H] thymidine assay system and modulatory effects of the cellular microenvironment in vitro. *J Cell Physiol* **201**: 429-438

Mundy GR (1995) Local control of bone formation by osteoblasts. *Clin Orthop Relat Res* 19-26

Muriel MP, Bonaventure J, Stanescu R, Maroteaux P, Guenet JL, Stanescu V (1991) Morphological and biochemical studies of a mouse mutant (fro/fro) with bone fragility. *Bone* **12**: 241-248

Murray A, Hunt T (1993) *The cell cycle an introduction*. W.H.Freeman and Company

Murray AW (2004) Recycling the cell cycle: cyclins revisited. *Cell* **116**: 221-234

Mustafa K, Wroblewski J, Hultenby K, Lopez BS, Arvidson K (2000) Effects of titanium surfaces blasted with TiO2 particles on the initial attachment of cells derived from human mandibular bone. A scanning electron microscopic and histomorphometric analysis. *Clin Oral Implants Res* **11**: 116-128

Mustafa K, Wennerberg A, Wroblewski J, Hultenby K, Lopez BS, Arvidson K (2001) Determining optimal surface roughness of TiO(2) blasted titanium implant material for attachment, proliferation and differentiation of cells derived from human mandibular alveolar bone. *Clin Oral Implants Res* **12**: 515-525

Nishiguchi S, Kato H, Fujita H, Kim HM, Miyaji F, Kokubo T, Nakamura T (1999) Enhancement of bone-bonding strengths of titanium alloy implants by alkali and heat treatments. *J Biomed Mater Res* **48**: 689-696

Nishimura N, Kawai T (1998) Effect of microstructure of titanium surface on the behaviour of osteogenic cell line MC3T3-E1. *J Mater Sci Mater Med* **9**: 99-102

Nohe A, Keating E, Knaus P, Petersen NO (2004) Signal transduction of bone morphogenetic protein receptors. *Cell Signal* **16**: 291-299

Norbury C, Nurse P (1992) Animal cell cycles and their control. *Annu Rev Biochem* **61**: 441-470

Nylander S, Kalies I (1999) Brefeldin A, but not monensin, completely blocks CD69 expression on mouse lymphocytes: efficacy of inhibitors of protein secretion in protocols for intracellular cytokine staining by flow cytometry. *J Immunol Methods* **224**: 69-76

Oh IH, Nomura N, Chiba A, Murayama Y, Masahashi N, Lee BT, Hanada S (2005) Microstructures and bond strengths of plasma-sprayed hydroxyapatite coatings on porous titanium substrates. *J Mater Sci Mater Med* **16**: 635-640

Ohtsuki C, Iida H, Hayakawa S, Osaka A (1997) Bioactivity of titanium treated with hydrogen peroxide solutions containing metal chlorides. *J Biomed Mater Res* **35**: 39-47

Ojok L, Kaeufer-Weiss I, Weiss E (2001) Bone marrow response to acute and chronic Trypanosoma congolense infection in multimammate rats (Mastomys coucha). *J Comp Pathol* **124**: 149-158

Okabe T, Hero H (1995) The use of titanium in dentistry. *Cell Mater* **5**: 211-230

Okamura A, Yazawa S, Nishimura T, Tanaka S, Takai I, Kudo S, Asao T, Kuwano H, Matta KL, Akamatsu S, Kochibe N (2000) A new method for assaying adhesion of cancer cells to the greater omentum and its application for evaluating anti-adhesion activities of chemically synthesized oligosaccharides. *Clin Exp Metastasis* **18**: 37-43

Okumara A, Goto M, Goto T, Yoshinari M, Masuko S, Katsuki T, Tanaka T (2001) Substrate affects the initial attachment and subsequent behaviour of human osteoblastic cells (Saos-2). *Biomaterials* **22**: 2263-2271

Ong JL, Prince CW, Raikar GN, Lucas LC (1996) Effect of surface topography of titanium on surface chemistry and cellular response. *Implant Dent* **5**: 83-88

Ong JL, Chan D (2000) Hydroxyapatite and their use as coatings in dental implants: a review. *Crit Rev Biomed Eng* **28**: 667A-707A

Oreffo ROC, Triffitt JT (1999) *In vitro* and *in vivo* methods to determine the interactions of osteogenic cells with biomaterials. *J Mater Sci Mater Med* **10**: 607-611

Ormerod MJ (2000) *Flow cytometry; A practical approach*. Oxford University Press

Pagano M (1995) *Cell Cycle - Materials and Methods*. Springer

Pan J, Liao H, Leygraf C, Thierry D, Li J (1998) Variation of oxide films on titanium induced by osteoblast-like cell culture and the influence of an H2O2 pretreatment. *J Biomed Mater Res* **40**: 244-256

Peraire C, Arias JL, Bernal D, Pou J, Leon B, Arano A, Roth W (2006) Biological stability and osteoconductivity in rabbit tibia of pulsed laser deposited hydroxylapatite coatings. *J Biomed Mater Res A*

Petty W (1979) Influence of methyl methacrylate on quantitative gel diffusion assay of immunoglobulins. *J Biomed Mater Res* **13**: 645-656

Pham MT, Maitz MF, Matz W, Reuther H, Richter E, Steiner G (2000a) Promoted hydroxyapatite nucleation on titanium ion-implanted with sodium. *Thin Solid Films* **379**: 50-56

Pham MT, Matz W, Reuther H, Richter E, Steiner G, Oswald S (2000b) Ion beam sensitizing of titanium surfaces to hydroxyapatite formation. *Surf Coat Technol* **128-129**: 313-319

Piattelli A, Trisi P, Passi P, Piattelli M, Cordioli GP (1994) Histochemical and confocal laser scanning microscopy study of the bone-titanium interface: an experimental study in rabbits. *Biomaterials* **15**: 194-200

Postiglione L, Di DG, Ramaglia L, di Lauro AE, Di MF, Montagnani S (2004) Different titanium surfaces modulate the bone phenotype of SaOS-2 osteoblast-like cells. *Eur J Histochem* **48**: 213-222

Prigent H, Pellen-Mussi P, Cathelineau G, Bonnaure-Mallet M (1998) Evaluation of the biocompatibility of titanium-tantalum alloy versus titanium. *J Biomed Mater Res* **39**: 200-206

Puleo DA, Bizios R (1992) Formation of focal contacts by osteoblasts cultured on orthopedic biomaterials. *J Biomed Mater Res* **26**: 291-301

Puleo DA, Preston KE, Shaffer JB, Bizios R (1993) Examination of osteoblast-orthopaedic biomaterial interactions using molecular techniques. *Biomaterials* **14**: 111-114

Puleo DA, Nanci A (1999) Understanding and controlling the bone-implant interface. *Biomaterials* **20**: 2311-2321

Puleo DA, Kissling RA, Sheu MS (2002) A technique to immobilize bioactive proteins, including bone morphogenetic protein-4 (BMP-4), on titanium alloy. *Biomaterials* **23**: 2079-2087

Qin C, Baba O, Butler WT (2004) Post-translational modifications of sibling proteins and their roles in osteogenesis and dentinogenesis. *Crit Rev Oral Biol Med* **15**: 126-136

Quadroni M, L'Hostis EL, Corti C, Myagkikh I, Durussel I, Cox J, James P, Carafoli E (1998) Phosphorylation of calmodulin alters its potency as an activator of target enzymes. *Biochem* **37**: 6523-6532

Rieder CL, Palazzo RE (1992) Colcemid and the mitotic cycle. *J Cell Sci* **102**: 387-392

Radbruch A. (2000) *Flow cytometry and cell sorting.* Springer

Rao S, Ushida T, Tateishi T, Okazaki Y, Asao S (1996) Effect of Ti, Al, and V ions on the relative growth rate of fibroblasts (L929) and osteoblasts (MC3T3-E1) cells. *Biomed Mater Eng* **6**: 79-86

Ratner BD, Hoffmen AS, Schoen FJ, Lemons JE (1996) *Biomaterials Science: An Introduction to Materials in Medicine.* Academic Press

Ratner BD, Hoffmen AS, Schoen FJ, Lemons JE (2004) *Biomaterials science; an introduction to materials in medicine.* Elsevier Academic Press

Riccardi D (2000) Calcium ions as extracellular, first messengers. *Z Kardiol* **89 Suppl 2**: 9-14

Riccardi D, Gamba G (1999) The many roles of the calcium-sensing receptor in health and disease. *Arch Med Res* **30**: 436-448

Rieu J, Pichat A, Rabbe LM, Rambert A, Chabrol C, Robelet M (1991) Ion implantation effects on friction and wear of joint prosthesis materials. *Biomaterials* **12**: 139-143

Roach HI (1994) Why does bone matrix contain non-collagenous proteins? The possible roles of osteocalcin, osteonectin, osteopontin and bone sialoprotein in bone mineralisation and resorption. *Cell Biol Int* **18**: 617-628

Rodan, G. A. and Noda, M (1991) Gene expression in osteoblastic cells. Crit Rev.*Eukaryot.Gene Expr* **1**: 85-98.

Rohanizadeh R, LeGeros RZ, Harsono M, Bendavid A (2005) Adherent apatite coating on titanium substrate using chemical deposition. *J Biomed Mater Res A* **72**: 428-438

Roovers K, Davey G, Zhu X, Bottazzi ME, Assoian RK (1999) Alpha5beta1 integrin controls cyclin D1 expression by sustaining mitogen-activated protein kinase activity in growth factor-treated cells. *Mol Biol Cell* **10**: 3197-3204

Rosa AL, Beloti MM (2003) Effect of cpTi surface roughness on human bone marrow cell attachment, proliferation, and differentiation. *Braz Dent J* **14**: 16-21

Rosenthal ET, Hunt T, Ruderman JV (1980) Selective translation of mRNA controls the pattern of protein synthesis during early development of the surf clam, Spisula solidissima. *Cell* **20**: 487-494

Ruhling A, Hellweg A, Kocher T, Plagmann HC (2001) Removal of HA and TPS implant coatings and fibroblast attachment on exposed surfaces. *Clin Oral Implants Res* **12**: 301-308

Ryhänen S, Jääskeläinen T, Mahonen A, Mäenpää PH (2003) Inhibition of MG-63 cell cycle progression by synthetic vitamin D_3 analogs mediated by p27, Cdk2, cyclin E, and the retinoblastoma protein. *Biochem Pharmacol* **66**: 495-504

Ryssel, Ruge I (1986) *Ion-implantation*. John Wiley and Sons

Salih V, Knowles JC, O'Hare MJ, Olsen I (2001) Retroviral transduction of alveolar bone cells with a temperature-sensitive SV40 large T antigen. *Cell Tissue Res* **304**: 371-376

Satsangi A, Satsangi N, Glover R, Satsangi RK, Ong JL (2003) Osteoblast response to phospholipid modified titanium surface. *Biomaterials* **24**: 4585-4589

Schaffner P, Dard MM (2003) Structure and function of RGD peptides involved in bone biology. *Cell Mol Life Sci* **60**: 119-132

Scheffold A, Kern F (2000) Recent developments in flow cytometry. *J Clin Immunol* **20**: 400-407

Scheidbach H, Tannapfel A, Schmidt U, Lippert H, Kockerling F (2004) Influence of titanium coating on the biocompatibility of a heavyweight polypropylene mesh. An animal experimental model. *Eur Surg Res* **36**: 313-317

Scherer A, Graff JM (2000) Calmodulin differentially modulates Smad1 and Smad2 signaling. *J Biol Chem* **275**: 41430-41438

Schneider GB, Burridge K (1994) Formation of focal adhesions by osteoblasts adhering to different substrata. *Exp Cell R* **214**: 264-269

Schneider GB, Zaharias R, Stanford C (2001) Osteoblast integrin adhesion and signaling regulate mineralization. *J Dent Res* **80**: 1540-1544

Schneider GB, Perinpanayagam H, Clegg M, Zaharias R, Seabold D, Keller J, Stanford C (2003) Implant surface roughness affects osteoblast gene expression. *J Dent Res* **82**: 372-376

Schwartz Z, Martin JY, Dean DD, Simpson J, Cochran DL, Boyan BD (1996) Effect of titanium surface roughness on chondrocyte proliferation, matrix production, and differentiation depends on the state of cell maturation. *J Biomed Mater Res* **30**: 145-155

Schwartz Z, Kieswetter K, Dean DD, Boyan BD (1997) Underlying mechanisms at the bone-surface interface during regeneration. *J Periodontal Res* **32**: 166-171

Schwartz Z, Lohmann CH, Oefinger J, Bonewald LF, Dean DD, Boyan BD (1999) Implant surface characteristics modulate differentiation behavior of cells in the osteoblastic lineage. *Adv Dent Res* **13**: 38-48

Senger DR, Wirth DF, Hynes RO (1979) Transformmed mammalian cells secrete specific proteins and phosphoprotein. *Cell* **16**: 885-893

Shah AK, Sinha RK, Hickok NJ, Tuan RS (1999a) High-resolution morphometric analysis of human osteoblastic cell adhesion on clinically relevant orthopedic alloys. *Bone* **24**: 499-506

Shah AK, Lazatin J, Sinha RK, Lennox T, Hickok NJ, Tuan RS (1999b) Mechanism of BMP-2 stimulated adhesion of osteoblastic cells to titanium alloy. *Biol Cell* **91**: 131-142

Sheppard CJR, Shotton DM (1997) *Confocal laser scanning microscopy*. Bios Scientific Publishers

Sinha RK, Shah SA, Tuan RS (1991) Cell spreading and attachment of human osteoblasts to metallic substrates. *J Cell Biol* **115**:

Sinha RK, Morris F, Shah SA, Tuan RS (1994) Surface composition of orthopaedic implant metals regulates cell attachment, spreading, and cytoskeletal organization of primary human osteoblasts in vitro. *Clin Orthop* 258-272

Sinha RK, Tuan RS (1996) Regulation of human osteoblast integrin expression by orthopedic implant materials. *Bone* **18**: 451-457

Skalak R, Brånemark PI (1994) Definition of osseointegration. In *Osseointegration in skeletal reconstruction and joint replacement*, Brånemark PI, Rydevik BL, Skalak R (eds) Quintessence Publishing Co, Inc

Soboyejo WO, Nemetski B, Allameh S, Marcantonio N, Mercer C, Ricci J (2002) Interactions between MC3T3-E1 cells and textured Ti-6Al-4V surfaces. *J Biomed Mater Res* **62**: 56-72

Sodek J, Ganss B, McKee MD (2000) Osteopontin. *Crit Rev Oral Biol Med* **11**: 279-303

Stanford CM, Keller JC, Solurish M (1994) Bone cell expression on titanium surfaces is altered by sterilization treatments. *J Dent Res* **73**: 1061-1071

Suikkanen S, Antila M, Jaatinen A, Vihinen-Ranta M, Vuento M (2003) Release of canine parvovirus from endocytic vesicles. *Virology* **316**: 267-280

Sukenik CN, Balachander N, Culp LA, Lewandowska K, Merritt K (1990) Modulation of cell adhesion by modification of titanium surfaces with covalently attached self-assembled monolayers. *J Biomed Mater Res* **24**: 1307-1323

Sul YT, Johansson CB, Jeong Y, Roser K, Wennerberg A, Albrektsson T (2001) Oxidized implants and their influence on the bone response. *J Mater Sci Mater Med* **12**: 1025-1031

Sumner H, Abraham D, Bou-Gharios G, Plater-Zyberk C, Olsen I (1991) Simultaneous measurement of cell surface and intracellular antigens by multiple flow cytometry. *Immunol Meth* **136**: 259-267

Sundgren JE, Bodo P, Lundstrom I (1986) Auger electron spectroscopic studies of the interface between human tissue and implants of titanium and stainless steel. *J Colloid Interface Sci* **110**: 9-20

Suzawa M, Takeuchi Y, Fukumoto S, Kato S, Ueno N, Miyazono K, Matsumoto T, Fujita T (1999) Extracellular matrix-associated bone morphogenetic proteins are essential for differentiation of murine osteoblastic cells in vitro. *Endocrinology* **140**: 2125-2133

Suzuki, Y, Kusakabe M, Kaibara M, Iwaki M, Sasabe H, and Nishisaka H (1994) Cell adhesion control by ion-implantation into extra-cellular matrix. *Nucl Instr and Meth in Phys Res* **B91**: 588-592.

Swart KM, Keller JC, Wightman JP, Draughn RA, Stanford CM (1992) Short-term plasma-cleaning treatments enhance *in vitro* osteoblast attachment to titanium. *J Oral Implantol* **18**: 130-137

Sze (1981) *Physics of semiconductor devices.* John Wiley and sons

Takeuchi K, Saruwatari L, Nakamura HK, Yang JM, Ogawa T (2005) Enhanced intrinsic biomechanical properties of osteoblastic mineralized tissue on roughened titanium surface. *J Biomed Mater Res A* **72A**: 296-305

Takuwa N, Zhou W, Takuwa Y (1995) Calcium, calmodulin and cell cycle progression. *Cell Signal* **7**: 93-104

Tangvall P, Lundström L (1992) Physico-chemical considerations of titanium as a biomaterial. *Clin Mater* **9**: 115-134

Ten DP, Korchynskyi O, Valdimarsdottir G, Goumans MJ (2003) Controlling cell fate by bone morphogenetic protein receptors. *Mol Cell Endocrinol* **211**: 105-113

Thompson GJ, Puleo DA (1996) Ti-6Al-4V ion solution inhibition of osteogenic cell phenotype as a function of differentiation timecourse *in vitro*. *Biomaterials* **17**: 1949-1954

Tsyganov I, Weiser E, Matz W, Mücklich A, Reuther H, Pham MT, Richter E (2000) Phase formation in aluminium implanted titanium and the correlated modification of mechanical and corrosive properties. *Thin Solid Films* **376**: 188-197

Ungerbock A, Rahn B (1994) Methods to characterise the surface roughness of metallic implants. *J Mater Sci Mater Med* **5**: 434-440

Van Kooten TG, Klein a CL, Kirkpatrick CJ (2000) Cell-cycle control in cell-biomaterial interactions: expression of P53 and Ki-67 in human umbilical vein endolthelial cells in direct contact and extract testing of biomaterials. *J Biomed Mater Res* **52**: 199-209

Varner JA, Emerson DA, Juliano RL (1995) Integrin alpha 5 beta 1 expression negatively regulates cell growth: reversal by attachment to fibronectin. *Mol Biol Cell* **6**: 725-740

Vogel V, Baneyx G (2003) The tissue engineeting puzzle: a molecular perspective. *Annu Rev Biomed Eng* **5**: 441-463

Wen HB, Wolke JG, de W, Jr., Liu Q, Cui FZ, de GK (1997) Fast precipitation of calcium phosphate layers on titanium induced by simple chemical treatments. *Biomaterials* **18**: 1471-1478

Weston GD, Moule AJ, Bartold PM (1999) A scanning electron microscopic evaluation of root surfaces and the gutta-percha interface following root-end resection in vitro. *Int Endod J* **32**: 450-458

White PA, Patel M, Nair S, Ashmore J, Galgut P, Wilson M, Henderson B, Olsen I (1998) Control of the human cell cycle by a bacterial protein, gapstatin. *Eur J Cell Biol* **77**: 228-238

Whitesides GM, Ostuni E, Takayama S, Jiang X, Ingber DE (2001) Soft lithography in biology and biochemistry. *Annu Rev Biomed Eng* **3**: 335-373

Wieser E, Tsyganov I, Matz W, Reuther H, Oswald S, Pham T, Richter E (1999) Modification of titanium by ion-implantation of calcium and / or phosphorous. *Surf Coat Tech* **111**: 103-109

Williams JM, Buchanan RA (1985) Ion-implantation of surgical Ti-6A-l4V alloy. *Mater Sci Eng* **69**: 237-246

Wingate H, Bedrosian I, Akli S, Keyomarsi K (2003) The low molecular weight (LMW) isoforms of cyclin E deregulate the cell cycle of mammary epithelial cells. *Cell Cycle* **2**: 461-466

Xu RH, Lechleider RJ, Shih HM, Hao CF, Sredni D, Roberts AB, Kung H (1999) Functional analysis of human Smad1: role of the amino-terminal domain. *Biochem Biophys Res Commun* **258**: 366-373

Xynos ID, Edgar AJ, Buttery LD, Hench LL, Polak JM (2000) Ionic products of bioactive glass dissolution increase proliferation of human osteoblasts and

induce insulin-like growth factor II mRNA expression and protein synthesis. *Biochem Biophys Res Commun* **276**: 461-465

Yamaguchi T, Chattopadhyay N, Kifor O, Butters RR, Jr., Sugimoto T, Brown EM (1998a) Mouse osteoblastic cell line (MC3T3-E1) expresses extracellular calcium (Ca2+o)-sensing receptor and its agonists stimulate chemotaxis and proliferation of MC3T3-E1 cells. *J Bone Miner Res* **13**: 1530-1538

Yamaguchi T, Kifor O, Chattopadhyay N, Brown EM (1998b) Expression of extracellular calcium (Ca2 + o)-sensing receptor in the clonal osteoblast-like cell lines, UMR-106 and SAOS-2. *Biochem Biophys Res Commun* **243**: 753-757

Yang Y, Tian J, Deng L, Ong JL (2002) Morphological behavior of osteoblast-like cells on surface-modified titanium in vitro. *Biomaterials* **23**: 1383-1389

Yang Y, Cavin R, Ong JL (2003) Protein adsorption on titanium surfaces and their effect on osteoblast attachment. *J Biomed Mater Res A* **67**: 344-349

Yoshikawa H, Nakase T, Myoui A, Ueda T (2004) Bone morphogenetic proteins in bone tumors. *J Orthop Sci* **9**: 334-340

Yoshinari M, Oda Y, Kato T, Okuda K, Hirayama A (2000) Influence of surface modifications to titanium on oral bacterial adhesion in vitro. *J Biomed Mater Res* **52**: 388-394

Yoshinari M, Oda Y, Kato T, Okuda K (2001) Influence of surface modifications to titanium on antibacterial activity in vitro. *Biomaterials* **22**: 2043-2048

Yu SR, Zhang XP, He ZM, Liu YH, Liu ZH (2004) Effects of Ce on the short-term biocompatibility of Ti-Fe-Mo-Mn-Nb-Zr alloy for dental materials. *J Mater Sci Mater Med* **15**: 687-691

Zarb GA. and Albrektsson T (1998) Consensus report: Towards optimized treatment outcomes for dental implants. *J.Prosthet.Dent* **80**: 641

Zhu X, Ohtsubo M, Bohmer RM, Roberts JM, Assoian RK (1996) Adhesion-dependent cell cycle progression linked to the expression of cyclin D1, activation of cyclin E-cdk2, and phosphorylation of the retinoblastoma protein. *J Cell Biol* **133**: 391-403

Ziegler JF (1988) *Ion implantation; science and technology*. Academic Press

Zinger O, Anselme K, Denzer A, Habersetzer P, Wieland M, Jeanfils J, Hardouin P, Landolt D (2004) Time-dependent morphology and adhesion of osteoblastic cells on titanium model surfaces featuring scale-resolved topography. *Biomaterials* **25**: 2695-2711

Zreiqat H, Howlett CR (1999) Titanium substrata composition influences osteoblastic phenotype: In vitro study. *J Biomed Mater Res* **47**: 360-366

Zreiqat H, Howlett CR, Zannettino A, Evans P, Schulze-Tanzil G, Knabe C, Shakibaei M (2002) Mechanisms of magnesium-stimulated adhesion of osteoblastic cells to commonly used orthopaedic implants. *J Biomed Mater Res* **62**: 175-184

Zreiqat H, Akin FA, Howlett CR, Markovic B, Haynes D, Lateef S, Hanley L (2003) Differentiation of human bone-derived cells grown on GRGDSP-peptide bound titanium surfaces. *J Biomed Mater Res* **64A**: 105-113

Zreiqat H, Valenzuela SM, Nissan BB, Roest R, Knabe C, Radlanski RJ, Renz H, Evans PJ (2005) The effect of surface chemistry modification of titanium alloy on signalling pathways in human osteoblasts. *Biomaterials* **26(36)**: 7579-7586

Appendix A

Surface Characterisation of Titanium and Ion Implanted Titanium Samples

(Written by Dr. F. H. Jones)

Surface chemistry has been assessed in some detail using X-ray photoelectron spectroscopy (XPS) and secondary ion mass spectrometry (SIMS), although this analysis has been limited to high dose samples ($\geq 1\times10^{17}$ ions cm^{-2}). Surface topography was explored qualitatively using SEM and quantitatively using white light interferometry. The latter studies were carried out on a very limited number of samples. The experiments were carried out by L. Shinawi and F.H. Jones and the results given in the first section below are mostly limited to those which had been obtained at the time of completion of the biological studies detailed in this thesis. The major points have been summarised here by F.H. Jones.

Polished cp Ti

Topography

To the naked eye, the polished Ti surfaces were smooth, shiny and silver coloured. They were easily scratched and had to be handled with care. SEM images indicated that the surfaces were mostly smooth, but not fully uniform, showing some pits and grooves attributable to the polishing process. Surface roughness, measured on six randomly selected samples using white light interferometry gave a roughness average value, R_a = 0.04 ±0.01 μm and a root mean square roughness R_q = 0.06 ±0.02 μm (Nayab *et al.*, 2003; Appendix B), in broad agreement with values in the literature measured using a similar technique [Chauvy *et al.*, 1998; Yoshinari *et al.*, 2000].

Chemistry

X-ray photoelectron spectroscopy confirmed that the main elements present at the surface were titanium and oxygen (Shinawi, 2003; Nayab *et al.*, 2003). The Ti 2p spectrum showed the typical peak shape for a metallic Ti substrate covered by a natural oxide layer, with an estimated thickness of ~50-70Å (Lausmaa *et al.*, 1990; Sodhi *et al.*, 1991; Lausmaa, 1996; McCafferty and Wightman, 1999). The oxide largely contained Ti in the 4+ oxidation state, although intensity due to Ti^{3+} and probably also Ti^{2+} was also apparent. The major contaminant was found to be adventitious carbon; the C1s spectrum was dominated by a hydrocarbon-like component, but also

contained –C-OH and –C-OOH type features. The O1s peak featured the expected O^{2-} component, but also contained components due to hydroxide, water and adsorbed organic species. Both carbon and oxygen levels were found to be widely variable, with C/Ti ratios ranging from 1.02 to 3.19 and O/Ti ratios from 2.82 – 6.43, which are similar to values which appear in the literature for Ti implants (Sutherland *et al.*, 1993; Placko *et al.*, 2000). The variability in the amount of adsorbed carbon contamination and surface hydroxylation depended strongly on the form and duration of storage of the samples in agreement with Lausmaa (Lausmaa, 1996). Samples washed thoroughly with appropriate solvents, stored in aluminium foil and analysed within hours of cleaning were found to have C/Ti ratios as low as 0.4 (unpublished results). Ca contamination was also found on some samples, in agreement with reports in the literature (Lausmaa *et al.*, 1990; Sutherland *et al.*, 1993). Usually, levels were found to be less than Ca/Ti = 0.05, but on at least one occasion Ca/Ti = 0.13 was observed. Another prevalent contaminant was zinc. One major source of this was found to be cling film, but it was clear that there was another source which has not yet been identified, most probably the water source or contaminated glassware during washing. Surfaces also generally contained small amounts of nitrogen and sometimes also silicon, probably residual from the polishing process. No K or Ar contaminants were detected on the surface.

The XPS technique is limited to probing the near surface region of solid materials, to a depth limit of around 100 - 150 Å at the photon energy used in this work. In order to probe deeper into the Ti, secondary ion mass spectrometry was employed in dynamic (i.e. depth profiling) mode. In this mode, SIMS is not surface sensitive, since the first few Å of the surface (corresponding to the oxide layer) are sputtered off during the equilibration period. An O_2^+ primary ion beam was used in order to minimise artefacts arising from the interface between the Ti oxide overlayer and the underlying Ti. The crater depth was used to calculate an approximate sputter rate (~0.44 $\mu m\ h^{-1}$), thus enabling tracking of Ti^+ (m/z = 48), K^+ (m/z = 39) and Ca^+ (m/z = 40) secondary ions as a function of depth. The depth distribution for cp Ti was, as expected, dominated by the $^{48}Ti^+$ signal, although a very small trace of $^{40}Ca^+$ was also apparent at the immediate surface, again indicating the

presence of some minor calcium contamination on these surfaces. This is in agreement with SIMS studies in the literature (Lausmaa *et al.*, 1990). No significant signal was observed for $^{39}K^+$, nor for $^{12}C^+$, $^{28}Si^+$ nor $^{31}P^+$ secondary ions. SIMS cannot be used to analyse Ar (mass 40) due to its inert nature, which results in an extremely low secondary ion yield; 99.999% of sputtered Ar will be in the form of neutral particles (Shinawi, 2003).

Ion implanted Ti

Topography

Ion implantation did not result in any clear change in sample appearance, either by eye or in SEM images. Since implantation involves ion bombardment and sputtering, it is possibly that the process may affect surface topography. However, roughness measurements using white light interferometry for 6 randomly selected samples of each ion type (dose 1×10^{17} ions cm^{-2}) indicated no significant difference in R_a and R_q values for ion implanted Ti compared to cp Ti (Nayab *et al.*, 2003; Appendix B). It should be noted that this does not mean that the implantation process has no effect on topography at all, but rather that any effect is too small to be measured in comparison with the inherent roughness of the polished Ti surface.

Chemistry

Computer simulations (carried out by Dr T.J. Tate at Imperial College London) and dynamic SIMS were used to assess the distribution of the implanted ions in the Ti substrates, while XPS was used to assess the nature of the implanted surface.

Simulations (PROFILE CODE and SRIM) were used to predict the ion ranges and implantation profiles in the Ti targets and to assess the degree of disturbance to the host Ti lattice, estimated by the parameter known as the displacements per atom (dpa). For all the implanted ions, the predicted dpa was greater than or equal to 1 over the range from the surface to a depth of >35nm at doses $\geq1\times10^{15}$ ions cm^{-2}, indicating that all the implanted samples were likely to have similar amounts of damage. The simulations also indicated that the native titanium oxide layer should be fully sputtered off the surface at the implantation doses used in this work. Implantation occurs into

the bare Ti substrate, resulting in radiation damage and amorphisation of the surface that does not appear to affect surface roughness to any great extent (Nayab *et al.*, 2003).

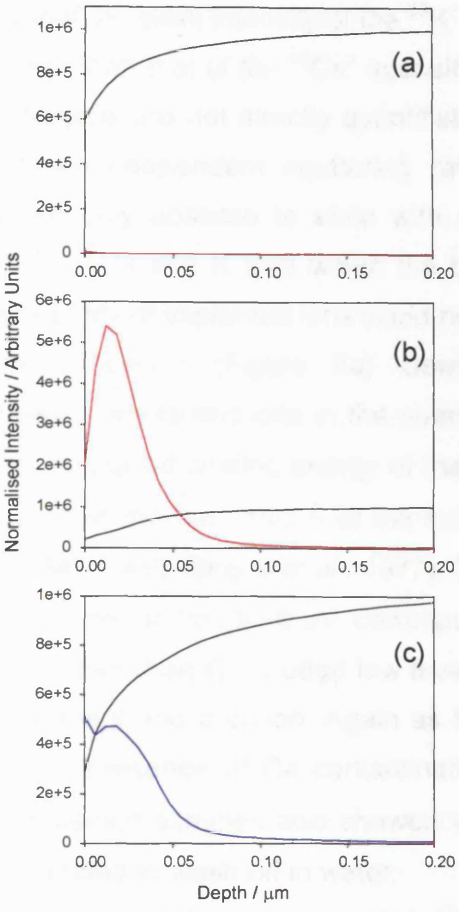

Figure 1: SIMS depth profiles showing the distribution of $^{48}Ti^{+}$,(black lines), $^{40}Ca^{+}$ (red lines) and $^{39}K^{+}$ (blue lines) in (a) non-implanted cp Ti, (b) Ca-Ti, ion dose 1×10^{17} ions cm^{-2} and (c) K-Ti, ion dose 1×10^{17} ions cm^{-2}. Adapted from Shinawi, 2003.

Dynamic SIMS depth profiles (Figure 1) largely reflected the computer simulated depth profiles for Ca-Ti and K-Ti (1×10^{17} ions cm^{-2}). The maximum intensity of $^{40}Ca^{+}$ secondary ions occurred at a depth of ~200Å and the intensity approached zero between ~1000 and 1500 Å. The $^{39}K^{+}$ secondary ion profile also showed a maximum at ~200 Å depth, but additionally displayed an intensity maximum at the immediate surface of the modified Ti. This increase is not fully understood, but may involve some preferential segregation of K^{+} ions during surface re-oxidation. Alternatively it

may be due to naturally occurring K-contamination at the surface. The near surface region, while rich in implanted ions, corresponded in both cases to a Ti depleted region indicating that the compounds formed contain reduced levels of Ti.

It should be noted that the peak intensity of the $^{39}K^+$ signal was around an order of magnitude lower than that of the $^{40}Ca^+$ intensity. Unfortunately, in SIMS, elemental concentrations are not directly quantifiable from secondary ion intensities due to sample-dependent sputtering rates and ionisation probabilities. It is therefore only possible to state with certainty that from SIMS the distributions of the Ca and K ions within the bulk of the Ti were largely as expected; the quantity of implanted ions could not be fully verified.

X-ray photoelectron spectra (Figure 2a) clearly confirmed the presence of the three types of implanted ions in the outermost region of the modified Ti surfaces. The measured binding energy of the $Ca2p_{3/2}$ peak was 347.2 eV, indicating that Ca in the top ~100 Å of the surface is present as Ca^{2+} and not metallic Ca (345.7 eV) (Briggs *et al.,* 1977). The binding energy of the $K2p_{3/2}$ peak was measured to be 293.9 eV, corresponding to K^+. As for cp Ti, typical contaminants other than C included low levels of Si, N and Zn, depending on storage treatment and duration. Again as for cp Ti, both K-Ti and Ar-Ti often showed the presence of Ca contamination at levels up to Ca/Ti $\approx$ 0.08. Some Ca implanted samples also showed very small amounts of F^- contamination which tended to wash off in water.

The concentration of implanted ions present in the surface was confirmed to be around that expected from the implantation process for the Ca-Ti and K-Ti samples (Ca/Ti = 0.24 - 0.47, K/Ti = 0.34 - 0.54). There was some variation in Ca/Ti and K/Ti ratios even within implantation runs, which may be related to the storage time and conditions prior to analysis. It should be noted that XPS is, at best, a semi-quantitative technique. Elemental concentrations are calculated from the intensities of the photoelectron peaks which depend on a large number of parameters, including the depth distribution of the element within the material. One of the most important parameters is the atomic sensitivity factor, which is essentially a measure of the probability that the electronic transition responsible for the generation of a particular XPS peak will take place. This is material dependent, and although

tables of empirical (Wagner *et al.*, 1981) and theoretical (Schofield, 1976) sensitivity factors are available; the values will not necessarily result in accurate atomic concentrations. The values used in the current work were those of Wagner *et al.* (1981). Another important consideration is the selection of the start and finish points of the peak under consideration and the type of background used to remove contributions to the intensity arising from secondary electrons. In this case, a linear background was used and, for both the Ti 2p and Ca 2p peaks, the shake up satellites to high binding energy of the main photoemission peaks were ***not*** included in the peak area measurement.

The measured Ar/Ti ratios were found to be around a tenth of the Ca/Ti and K/Ti ratios (0.03 - 0.05). One possibility is that the inert nature of Ar allows the highly energetic implanted ions to penetrate into the Ti bulk without being trapped in lattice positions or interstitially, so that the majority exist at a depth beyond the detection limit of XPS. Alternatively, they may have sufficient energy to escape from the surface altogether following implantation.

The Ti2p spectra (Figure 2b) indicated that the sputtered Ti surface is re-oxidised following removal from the ion implanter and solvent cleaning. The spectra remained dominated by Ti^{4+} peaks. However, well defined peaks due to the underlying Ti^{0} metal were not observed, probably indicating an overall increase in the thickness of the oxide layer. Instead, broad features were seen to low binding energy of the Ti^{4+} $2p_{3/2}$ peak, the overall shape of which depended on the type of implanted ion. These features almost certainly contained some contribution from titanium carbide species, but there was also evidence for the presence of Ti suboxides (Ti^{2+} and Ti^{3+}). Such species might be formed at the metal – metal oxide interface by recoil implantation, or simply during the re-oxidation process, since they are known to form at the interface in the early stages of oxidation of clean Ti (Lu *al.*, 2000). Notably, recent experiments in which samples were analysed as soon as possible following implantation, avoiding any exposure to solvents, showed a prominent low binding energy peak which had a considerably higher relative intensity than the Ti^{0} $2p_{3/2}$ peak of cp Ti. This was attributed to high levels of carbide (see below), coupled with lower surface contamination

and oxidation of these surfaces. Surface oxidation may be accelerated by exposure to solvents and water (unpublished results).

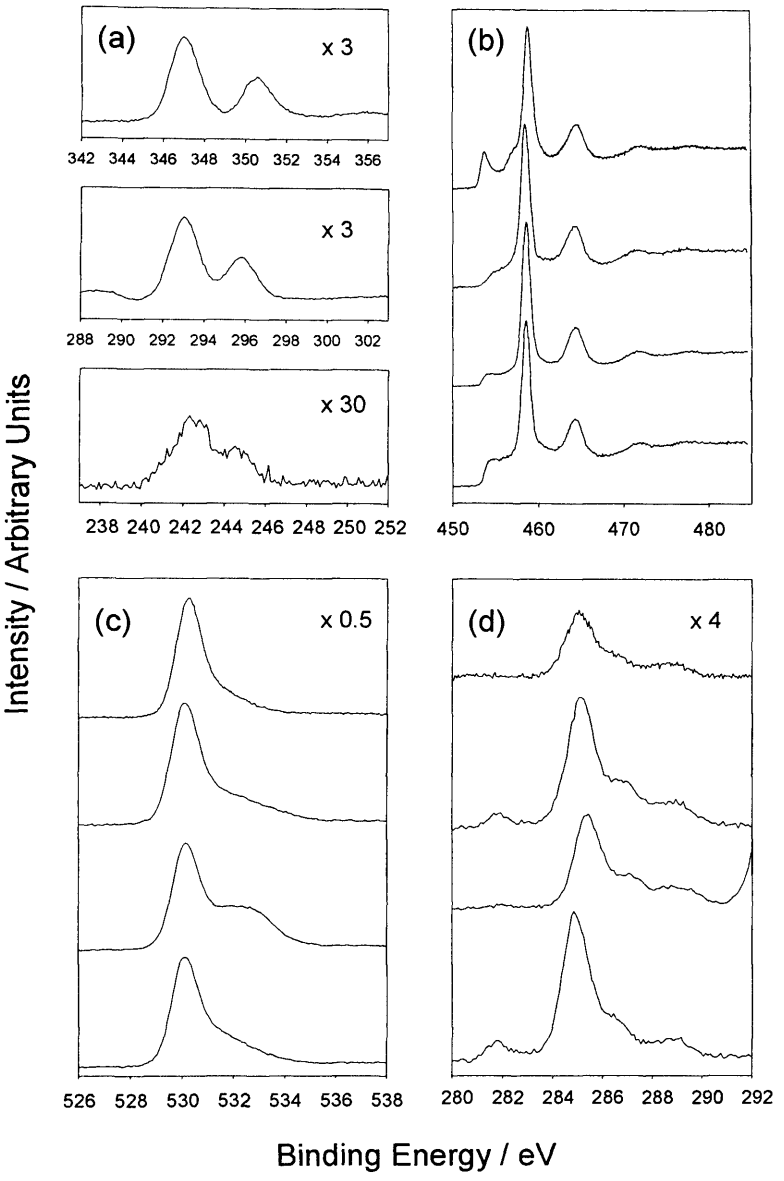

Figure 2: Core level X-ray photoelectron spectra from (from top to bottom) non-implanted Ti, Ca-Ti ($1x10^{17}$ ions cm^{-2}), K-Ti ($1x10^{17}$ ions cm^{-2}) and Ar-Ti ($2x10^{17}$ ions cm^{-2})
(a) The implanted ion regions, Ca2p, K2p and Ar2p (note the absence of a spectrum from non-implanted Ti); (b) the Ti2p region; (c) the O1s region and (d) the C1s region. As presented in Nayab *et al.*, 2003, Copyright 2003, Kluwer Academic Publishers.

O1s and C1s spectra were also examined (Figures 2c and d respectively). The most important difference between the C1s spectra from

implanted and non-implanted surfaces was the presence of a carbide peak on all implanted Ti samples. Evidence suggests that carbide is primarily located at the Ti / oxide interface, possibly arising from recoil implantation of carbon, or from direct reaction of C-containing species with the reactive bare Ti surface prior to or during re-oxidation following sputtering. Aside from the presence of carbide, in general, Ca-Ti and K-Ti surfaces showed increased levels of carbon contamination and the O1s region was generally found to have a greater contribution from O in OH, H_2O and organic species at the surface. Ar-Ti samples, on the other hand, were generally found to have C1s and O1s spectra more similar in appearance to cp Ti. However, the recent solvent-free experiments showed *no* change in C/Ti levels and a *decrease* in O/Ti ratios, although the percentage of the O1s peak attributed to O in species other than O^{2-} had increased slightly. In the current studies, therefore, it is probable that the majority of C contamination and hydroxylation is at the immediate surface and results from post-implantation storage and handling. This is of some interest, since surface hydroxylation may result in favourable biological interactions as hydroxyl groups have been proposed as nucleation sites for hydroxyapatite formation (Li *et al.*, 1997). The active Ca-Ti and K-Ti surfaces may react more rapidly with O resulting in thicker oxide formation and/or surface hydroxylation than the more inert Ar/Ti surface.

Reactivity

Further experiments have examined the reactivity of the ion implanted surfaces. XPS studies showed that the Ca/Ti and K/T ratios at the surface are significantly reduced on immersion in water, K/Ti more so than Ca/Ti. After 24 h immersion in deionised water at 37°C, the Ca/Ti ratio was reduced to around a third of its original value, while the K/Ti ratio was reduced to less than a fifth of its original value (Shinawi, 2003). At the same time, the surface of the Ca-Ti samples turned a deep blue colour. This effect is usually associated with a thickening of the oxide layer which results in constructive interference of light reflected from the air-oxide and oxide-metal interfaces at certain wavelengths. Formation of a titanium oxide layer depleted in

implanted ions at the surface of the samples could account for the reduction in Ca/Ti and K/Ti ratios. However, the XP spectra of the Ti2p core level peaks did not appear to reveal any difference in surface oxide thickness before and after immersion (see below). It was therefore considered most likely that ions were released into solution. Dynamic SIMS indicated that the ion release was from the uppermost layers of the surface, although some implanted ions were retained within the samples (Figure 3).

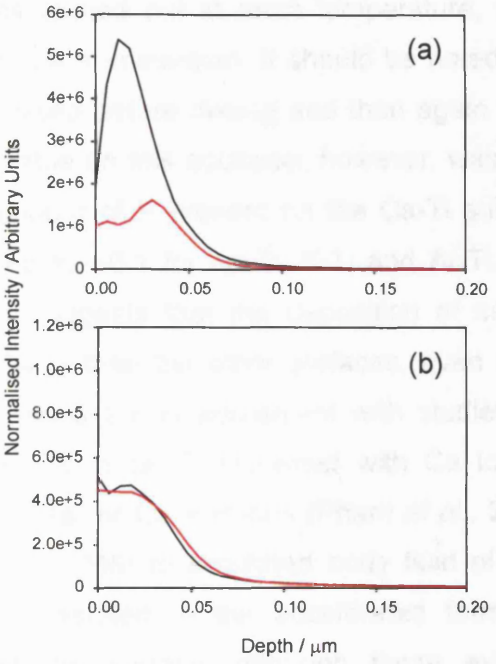

Figure 3: SIMS depth profiles showing the distribution of (a) $^{40}Ca^{+}$ in Ca-Ti, ion dose 1×10^{17} ions cm^{-2} and (b) $^{39}K^{+}$ in K-Ti, ion dose 1×10^{17} ions cm^{-2} before (black lines) and after (red lines) immersion in water at 37°C. Adapted from Shinawi, 2003.

The level of implanted ions (Ca^{2+} and K^{+}) at the surface was also found to be reduced by nitric acid treatment, such as that which might be used to "passivate" the surface prior to clinical application. In this case, the reduction in implanted ion concentration was accompanied by an apparent thinning of the surface oxide layer which was not seen on exposure to water alone (Shinawi, 2003). These results are broadly in agreement with previous studies which examined microdissolution of calcium ions from ion implanted titanium into nitric acid and buffer solutions (Hanawa *et al.*, 1996a and 1996b).

Studies have also been carried out to examine the effects of immersion of ion implanted Ti in simulated body fluids (Shinawi, 2003), in particular Hank's Balanced Salt Solution (HBSS). Results were highly dependent on experimental protocol. When immersion was carried out for 24 h at 37°C with a water rinse immediately following immersion, XPS indicated the deposition at the surface of a calcium and phosphorous containing layer of sufficient thickness to obscure the Ti 2p signal on all four surfaces (cp Ti, Ca-Ti, K-Ti and Ar-Ti). The Ca/P ratio on all four surfaces was ~1.3. When a similar experiment was carried out at room temperature, the underlying Ti was not obscured after 24 h immersion. It should be noted in this case that the samples were analysed before rinsing and then again following a water rinse. What was noticeable on this occasion, however, was that there was a significantly greater amount of P present on the Ca-Ti surface, with a P/Ti ratio of ~ 0.6 compared to ~0.1 for cp Ti, K-Ti and Ar-Ti. This fell to ~0.4 following rinsing. This suggests that the deposition of calcium phosphate species is faster on Ca-Ti than the other surfaces, even at relatively short time periods. These results are in agreement with studies in the literature which showed that exposure of Ti implanted with Ca ions (Pham *et al.*, 2000a; Krupa *et al.*, 2001a) or Ca + P ions (Pham *et al.*, 2000a and 2000b; Krupa *et al.*, 2001b and 2005) to simulated body fluid of the Kokubo type (Kokubo *et al.*, 1990) resulted in the accelerated formation of calcium phosphate phases at the surface, although these experiments mainly examined prolonged exposure. Interestingly, Na implantation of Ti resulted in a similar acceleration (Pham *et al.*, 2000c, 2000d, 2001 and 2002; Maitz *et al*, 2002a and 2002b). This suggests that a similar response might be expected for K-Ti in the current work. This was not observed.

Recent experiments

Very recent experiments have been carried out by R. Mihoc, D. Armitage and F.H. Jones (in preparation for publication). These provide some additional information about the processes occurring at the Ca ion-implanted

surfaces and are included here for completeness, again summarised by F.H. Jones.

XPS depth profiling

Depth profiling experiments have been carried out by using X-ray photoelectron spectroscopy following surface etching with an Ar^+ ion beam. Ca-Ti samples (1×10^{17} ions cm^{-2}) implanted in the same way to those used in the biological experiments were found to have a Ca distribution similar in shape to that predicted by the computer simulations and observed using SIMS, confirming the sub-surface maximum in Ca concentration (Figure 4). The presence of carbide, with a sub-surface maximum concentration, was also confirmed. Following immersion in water (18 h, room temperature), XPS profiling as a function of Ar^+ etching showed a significant drop in the Ca concentration both at the surface and deeper into the Ca-Ti samples. At the same time, beyond a certain depth, the Ti was found to be highly oxidised, with XPS profiles showing O/Ti ratios approaching those at the immediate surface.

The presence and location of the carbide species below the Ti surface was largely unaffected by immersion. Together with the fact that the surface Ti2p spectra showed only minimal changes following immersion, this suggests that the majority of oxidation occurs beneath the level of the carbide species. Samples implanted with "control" ions including $^{40}Ar^+$, $^{18}O_2^+$ and $^{65}Ti^+$ showed no such behaviour on immersion, although Ar-Ti and Ti-Ti samples showed the presence of carbide. It is therefore tentatively suggested that the presence of Ca ions compromises the passive nature of the Ti surface oxide, allowing oxygen diffusion into the Ti bulk. This effect is likely to be responsible for the characteristic deep blue colour observed on the majority of water immersed Ca-Ti samples.

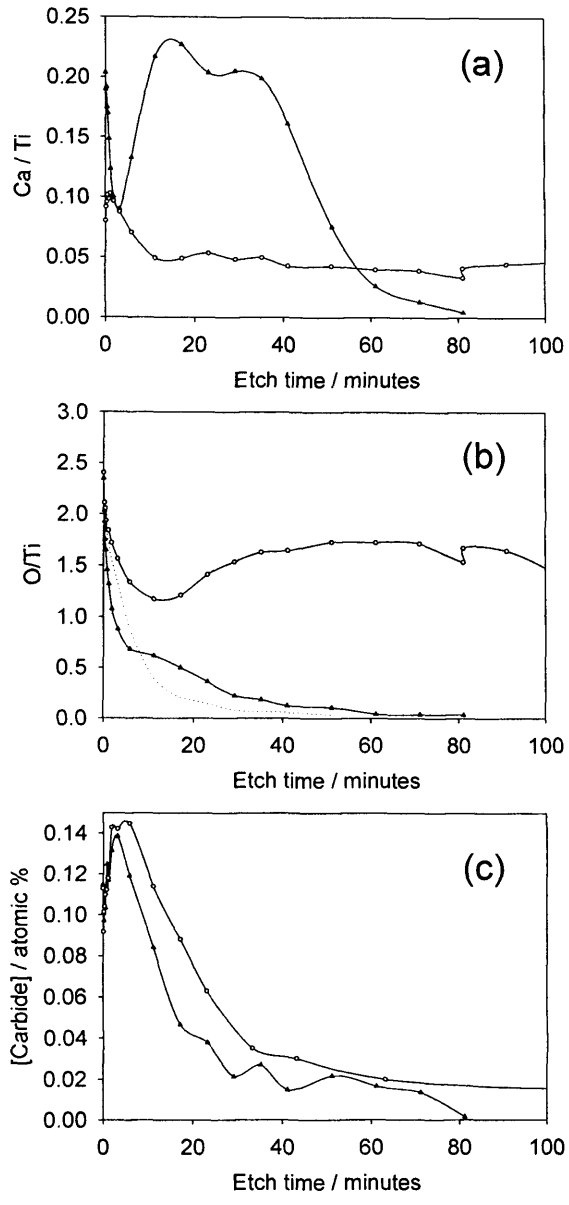

Figure 4: Composition profiles showing (a) Ca/Ti elemental ratios, (b) O/Ti elemental ratios and (c) carbide concentrations as a function of Ar etch time measured using XPS. Solid triangles indicate the as-implanted Ca-Ti samples, while the open circles are from Ca-Ti samples following 18 h immersion in ultrapure water. The dotted line in (b) is from a cp Ti control sample.

K-Ti samples were also examined using this technique. Unexpectedly, it was found that despite high levels of K at the surface, K-concentrations further into the bulk of the Ti were not comparable to Ca concentrations in the Ca-Ti samples. After ~17 min etching (at which point the Ca/Ti ratio in Ca-Ti

maximised at ~0.23) the K/Ti ratio was measured to be ~0.04. Although these samples were prepared subsequently to those used in the biological experiments, it is probable, particularly given the relatively low intensity of $^{39}K^{+}$ secondary ions in the SIMS distributions, that the earlier samples also contained much lower K levels in the bulk than expected, despite containing the expected levels of K at the surface. It therefore appears that ion implantation of K does ***not*** result in the bulk concentrations of K expected from the simulations. The reason for this is not understood at present, but is potentially due to the extremely high reactivity of potassium. Following implantation and removal into the atmosphere, implanted K may be lost through reaction with oxygen at the same time as the Ti surface is oxidised. This might explain the differences in reactivity mentioned above.

Ion Chromatography

In a separate series of studies, calcium ion release into water was confirmed using ion chromatography. After 2 min immersion at 37°C in 1 ml ultrapure water; Ca ion concentrations of 0.13 (± 0.09) ppm were detected, compared to control values of 0.07 (± 0.07), tending to indicate that ion release was occurring. After 4 h immersion, the Ca concentration had increased to 1.27 (± 0.18) ppm, and this level did not show a statistically significant increase on further immersion. It should be noted that the levels of calcium detected were very much lower than the levels present in simulated biofluids such as Hank's balanced salt solution (66 ppm [1]) and complete medium (95 ppm [2]).

XPS confirmed the ion release. After immersion for 2 min, the Ca/Ti ratio at the surface fell from 0.18 (± 0.01) to 0.09 (± 0.01) (NB, the peak areas in this case were measured following Shirley background subtraction and including the high binding energy shake-up peaks, hence the difference from the values quoted previous). Immersion for 4 h gave a very similar Ca/Ti ratio of 0.08 (± 0.01) which remained unchanged after immersion for 168 h (1 week). It should be noted that, in this and certain repeat experiments, not all immersed samples turned a uniform blue colour; several went "patchy" blue while some actually remained largely silver. The surface XP spectra from the

blue and silver regions were largely identical, but depth profiles indicated that only the samples that went blue had decreased Ca and increased O concentrations in the "bulk". Closer examination of ion chromatography results indicated that, in general, the more blue colouration on the sample surface, the higher the Ca concentration detected in solution. The reason for this variability between (and even within) samples remains unclear, but may be related to inhomogeneity in the integrity of the surface oxide layer formed following implantation.

References

Chauvy PF, Madore C, and Landolt D (1998) Variable length scale analysis of surface topography: characterization of titanium surfaces for biomedical applications. *Surface and Coatings Technology* **110**: 48-56.

Hanawa T, Asami K and Asaoka K (1996a) AES studies on the dissolution of surface oxide from calcium-ion-implanted titanium in nitric acid and buffer solutions. *Corrosion Science*, **38**(11): 2061-2067.

Hanawa T, Asami K and Asaoka K (1996b) Microdissolution of calcium ions from calcium-ion-implanted titanium. *Corrosion Science* **38**(9): 1579-1594.

Kokubo T, Kushitani H, Sakka S, Kitsugi T and Yamamuro TJ (1990) Solutions able to reproduce *in-vivo* surface-structure changes in bioactive glass-ceramic A-W3. *Biomedical Materials Research* **24**: 721-734.

Krupa D, Baszkiewicz J, Kozubowski JA, Barcz A, Sobczak JW, Biliński A, Lewandowska-Szumieł M and Rajchel B (2001a) Effect of calcium-ion implantation on the corrosion resistance and biocompatibility of titanium. *Biomaterial*, **22**(15): 2139-2151.

Krupa D, Baszkiewicz J, Kozubowski J, Barcz A, Sobczak J, Biliński A, and Rajchel B (2001b) The influence of calcium and/or phosphorus ion implantation on the structure and corrosion resistance of titanium. *Vacuum* **63**(4): 715-719.

Krupa D, Baszkiewicz J, Kozubowski JA, Barcz A, Sobczak JW, Biliński A, Lewandowska-Szumieł M and Rajchel B (2005) Effect of dual ion implantation of calcium and phosphorus on the properties of titanium. *Biomaterials* **26:** 2847-2856.

Lausmaa J, Kasemo B and Mattsson (1990) Surface spectroscopic characterization of titanium implant materials. *Applied Surface Science* **44**: 133-146.

Lausmaa J (1996) Surface spectroscopic characterization of titanium implant materials. *Journal of Electron Spectroscopy and Related Phenomena* **81:** 343-361.

Lu G, Bernasek SL and Schwartz, J (2000) Oxidation of a polycrystalline titanium surface by oxygen and water. *Surface Science* **458:** 80-90.

Maitz MF, Pham MT, Matz W, Reuther H Steiner G and Richter E (2002a) Ion beam treatment of titanium surfaces for enhancing deposition of hydroxyapatite from solution. *Biomolecular Engineering* **19**(2-6): 269-272.

Maitz MF, Pham MT, Matz W, Reuther H and Steiner G (2002b) Promoted calcium-phosphate precipitation from solution on titanium for improved biocompatibility by ion implantation. *Surface and Coatings Technology* **158**: 151-156.

McCafferty E and Wightman JP (1999) An X-ray photoelectron spectroscopy sputter profile study of the native air-formed oxide film on titanium. *Applied Surface Science* **143:** 92-100.

Nayab SN, Shinawi L, Hobkirk J, Tate TJ, Jones FH and Olsen I (2003) Adhesion of bone cells to ion-implanted titanium. *Journal of Materials Science: Materials in Medicine* **14**: 991-997.

Pham MT, Matz W, Reuther H, Richter E, Steiner G and Oswald S (2000a), Surface sensitivity of ion implanted titanium to hydroxyapatite formation. *Journal of Materials Science Letters* **19**(5): 443-445.

Pham MT, Matz W, Reuther H, Richter E, Steiner G, and Oswald S (2000b), Ion beam sensitizing of titanium surfaces to hydroxyapatite formation. *Surface and Coatings Technology* **128**: 313-319.

Pham MT, Maitz MF, Matz W, Reuther H, Richter E and Steiner G (2000c), Promoted hydroxyapatite nucleation on titanium ion-implanted with sodium. *Thin Solid Films* **379**(1-2): 50-56.

Pham MT, Matz W, Reuther H, Richter E and Steiner G (2000d) Hydroxyapatite nucleation on Na ion implanted Ti surfaces. *Journal of Materials Science Letters*, **19**(12): 1029-1031.

Pham MT, Maitz MF, Grambole D, Herrmann F, Reuther H and Richter E (2001) Surface stimuli to precipitating hydroxyapatite on titanium. *Journal of Materials Science Letters* **20**(4): 295-296.

Pham MT, Matz W, Grambole D, Herrmann F, Reuther H, Richter E and Steiner G (2002) Solution deposition of hydroxyapatite on titanium pretreated with a sodium ion implantation. *Journal of Biomedical Materials Research* **59**(4): 716-724.

Placko HE, Mishra S, Weimer JJ and Lucas LC (2000), Surface characterization of titanium-based implant materials. *International Journal of Oral and Maxillofacial Implants* **15:** 355-363.

PROFILE CODE Implant Sciences Co. Mass. USA

Scofield JH (1976) Hartree-Slater subshell photoionisation cross-scetions at 1254 and 1487eV. *Journal of Electron Spectrosccopy and Related Phenomena* **8:** 129-137.

Shinawi L 2003 PhD Thesis, "Ion implantation as a route to enhancing osseointegration on modified titanium surfaces". University College London.

Sodhi RNS, Weninger A, Davies JE and Screenivas K (1991), X-ray photoelectron spectroscopic comparison of sputtered Ti, Ti6Al4V and passivated bulk metals for use in cell culture techniques. *Journal of Vacuum Science and Technology A* **9**: 1329-1333.

SRIM 2000 J. F. Ziegler IBM-Research NY, USA

Sutherland DS, Forshaw PD, Allen GC, Brown IT and Williams KR (1993), Surface analysis of titanium implants. *Biomaterials* **14**(12): 893-899.

Wagner CD, Davis LE, Zeller MV, Taylor JA, Raymond RH and Gale LH (1981) Empirical atomic sensitivity factors for quantitative analysis by electron spectroscopy for chemical analysis. *Surface and Interface Analysis* **3**: 211-225.

Yoshinari M, Oda Y, Kato T, Okuda K and Hirayama A (2000), Influence of surface modification to titanium on oral bacterial adhesion *in vitro*". Journal of Biomedical Material Research **52:** 388-394.

Appendix B